1-30-2013

Transport theoretical studies of some microscopic and macroscopic systems

Alden Astwood

Alden M. Astwood

Candidate

Physics and Astronomy

Department

This dissertation is approved, and it is acceptable in quality and form for publication:

Approved by the Dissertation Committee:

V. M. Kenkre , Chairperson

David H. Dunlap

Helen Wearing

Rouzbeh Allahverdi

Transport Theoretical Studies of Some Microscopic and Macroscopic Systems

by

Alden Matthew Astwood

B.S., Texas Tech University, 2008

DISSERTATION

Submitted in Partial Fulfillment of the
Requirements for the Degree of

Doctor of Philosophy,
Physics

The University of New Mexico

Albuquerque, New Mexico

December, 2012

Dedication

To my parents.

Acknowledgments

I would like to express my great appreciation to my advisor Professor V. M. Kenkre for much guidance and support during my time at the University of New Mexico. It was a great pleasure to be his student, and I am extremely grateful for all his teachings and advice.

Advice and suggestions given by my collaborator Michael Raghib were a great help during the writing of this thesis.

I would also like to offer thanks to my other teachers in the Department of Physics and Astronomy at UNM, especially Profs. David Dunlap, Rouzbeh Allahverdi, Kevin Cahill, and Daniel Finley, for excellent and challenging courses.

It was a great benefit to be a part of the Consortium of the Americas for Interdisciplinary Science. I thank its members and visitors for many interesting discussions.

Finally, I would like to thank my family, especially my parents, for their support and encouragement during the preparation of this thesis.

This work was supported in part by the Air Force Research Laboratory at Kirtland Air Force Base, and by the Department of Energy at Los Alamos National Laboratory.

Transport Theoretical Studies of Some Microscopic and Macroscopic Systems

by

Alden Matthew Astwood

B.S., Texas Tech University, 2008

Ph.D., Physics, University of New Mexico, 2012

Abstract

This dissertation is a report on theoretical transport studies of two systems of vastly different sizes. The first topic is electronic motion in quantum wires. In recent years, it has become possible to fabricate wires that are so small that quantum effects become important. The conduction properties of these wires are quite different than those of macroscopic wires. In this dissertation, we seek to understand scattering effects in quantum wires in a simple way. Some of the existing formalisms for studying transport in quantum wires are reviewed, and one such formalism is applied to calculate conductance in some simple systems. The second topic concerns animals which move in groups, such as flocking birds or schooling fish. Exact analytic calculations of the transport properties of such systems are very difficult because a flock is a system that is far from equilibrium and consists of many interacting particles. We introduce two simplified models of flocking which are amenable to analytic study. The first model consists of a set of overdamped Brownian particles that interact via spring forces. The exact solution for the probability distribution is calculated, and equations of motion for continuous coarse-grained quantities, such as the density, are obtained from the full solution. The second model consists of particles which move in one dimension

at constant speed, but which change their directions at random. The flipping rates are constructed in such a way that particles tend to align their directions with each other. The model is solved exactly for one and two particles, the first two moments are obtained, and equations of motion for continuous coarse-grained quantities are written. The model cannot be solved exactly for many particles, but the first and second moments are calculated. Finally, two additional topics are briefly discussed. The first is transport in disordered lattices, and the second is a static magnetic model of flocking.

Contents

List of Figures

Chapter 1

Introduction

In our everyday lives we encounter many objects, both large and small, that move from one place to another. Several tools have been developed over the years in transport theory, the branch of statistical physics dealing with entities in motion, which are useful for modeling such objects.

This thesis is in two parts. In the first part we study the motion of very small objects: electrons moving in tiny wires with sizes on the order of hundreds of nanometers to microns. In the second part, we look at much larger objects: animals, such as birds or fish, moving together in groups.

One way to model electronic motion in solids is to simply treat the electrons and ions as point particles and apply kinetic theory to calculate the desired transport properties. This is the basis of the Drude-Sommerfeld theory described in many textbooks on solid state physics (for example ref. [1]). In such a theory, the heavier ions are assumed to be stationary, and the electrons move in straight lines according to Newton's laws until they collide with an ion and scatter. Long range electron-electron interactions and electron-ion interactions are ignored, and collisions happen instantaneously with a constant probability per unit time.

In this simple picture, the current density $\mathbf{J}$ in the solid is directly proportional to the applied electric field $\mathbf{E}$,

$$\mathbf{J} = \sigma \mathbf{E} \tag{1.1}$$

where the proportionality constant σ is called the *conductivity*. This relation is simply Ohm's law, which can be written in terms of the total current I and the voltage difference V across the conductor as

$$I = GV. \tag{1.2}$$

The proportionality constant G is called the *conductance* and for a three-dimensional conductor is related to the conductivity by

$$G = \frac{\sigma A}{L} \tag{1.3}$$

where A is the cross-sectional area of the conductor and L is its length. In the Drude-Sommerfeld model, the conductance σ is independent of the dimensions of the conductor, but the conductivity G is not.

Although the largely classical Drude-Sommerfeld theory has been relatively successful in qualitatively describing some of the observed properties of macroscopic solids, in the past few decades it has become possible to fabricate devices which are so small that the crude form of the theory must be abandoned in favor of more sophisticated quantum mechanical models.

Quantum mechanics tells us that electrons and ions are certainly not point particles with definite position and momentum; they must instead be described by a wavefunction. In macroscopic conductors, electrons scatter many times, and after they have traveled a distance which is small compared to the size of the conductor any information about the phase of their wavefunctions is destroyed and interference effects are washed out. This is not the case in small high mobility conductors where electrons are only scattered a few times, or not at all, as they move through the

device. The conductance in very small systems with low scattering can therefore be quite different than in macroscopic systems. For example, in a ballistic conductor (i.e. a conductor in which the electrons move without being scattered at all), the conductance G is *not* proportional to the width of the device, as it is in the classical expression (1.3). Instead, as the width of a ballistic conductor is increased the conductance can remain constant, then suddenly jump to a higher value. This behavior, called conductance quantization, has been observed experimentally (see refs. [2–4]) and is well understood in terms of current quantum theories of transport.

This effect can be seen in devices called *heterostructures*, which consist of two different materials, such as GaAs and GaAlAs, in contact with each other. If the two materials have different electrochemical potentials, when the two materials are put in contact with each other, in order to equalize the electrochemical potential, electrons spill over and the bands "bend" at the interface. In some cases, the conduction band edge on one side of the interface can dip below the electrochemical potential, resulting in the formation of a high mobility two-dimensional electron gas at the interface. The device can be made into a field-effect transistor by etching a gate onto the structure. The effective width of the conductor, and thus its conductance, can then be varied by changing the gate voltage.

A topic of present interest in the literature is when the electronic motion is neither completely ballistic nor completely classical. The subject of Chapter 2 is a review of some of the existing formalisms developed by various authors for studying quantum transport, and the origin of conductance quantization in ballistic conductors will be addressed. In Chapter 3, one of these formalisms, the Landauer-Büttiker transmission theory, will be applied to some simple one-dimensional systems with scattering.

The second part of this thesis concerns motion on a much larger scale. It is often advantageous for biological organisms to move together in cohesive groups. This is termed flocking or collective motion and occurs in many different kinds of biological systems such as the motion of bacteria [5–10], flocking of birds [11–15], schooling of

fish and other marine life [16–19], insect motion [20, 21], and even human behavior [22, 23].

The problem of collective motion presents several interesting challenges from a theoretical perspective. A flock is a non-equilibrium system consisting of a large, but finite, number of objects which can interact in complicated ways. Furthermore, since the constituents of flock are biological organisms, they can sometimes move in ways which are difficult to predict. These challenges can make analytic calculations of the transport properties quite difficult.

One method of avoiding the difficulties of analytic calculations is to simply perform numerical simulations. Typically, one begins with a model of individual behavior (i.e. a description of how each member of the flock moves and interacts with others), simulates this behavior on a computer, and looks at the results. The quantities of interest are usually coarse-grained quantities such as the average position and velocity of the whole flock, its size, its angular momentum, and whether or not there is a phase transition from coherent to incoherent motion. One disadvantage of this approach is that if the parameters of the individual-level model (such as interaction strength between individuals or amount of noise) are changed, the simulation must be run again.

An example of an individual-level model is the one devised by Mikhailov and Zanette [24]. In this model, the members of the flock are taken to be point particles which move in one dimension. Biological entities like birds and fish are able to propel themselves, so in this model each particle is subject to a force which drives its speed to a constant, nonzero value. The particles interact simply via spring forces which pull all particles toward all others. Finally, a stochastic force is added to account for random perturbations. The equation of motion for the evolution of the position of the mth particle is

$$\ddot{x}_m + (\dot{x}_m^2 - 1)\dot{x}_m + \frac{a}{N}\sum_n (x_m - x_n) = \Gamma_m(t). \tag{1.4}$$

The first term is the acceleration of the particle, the second term is the self-propulsion force, the third term is the interaction forces, and $\Gamma_m(t)$ is the stochastic force. This model is relatively simple, but the presence of nonlinearity in self-propulsion term makes an exact analysis impossible.

The aim in this thesis is to construct two highly simplified models of collective motion, and use tools from statistical physics to calculate analytically their transport properties. The subject of Chapter 4 is a model of collective motion with a centering interaction, and the subject of Chapter 5 is a model of collective motion with an alignment interaction. The precise meaning of the terms centering and alignment will be made clear in Chapter 4.

In Chapter 6, two final topics will be briefly discussed, followed by some closing remarks. The first of these topics is motion in disordered lattices, and the second is a magnetic model of flocking with focus on static analysis.

Chapter 2

Review of Some Existing Formalisms of Quantum Transport

2.1 Introduction

In this chapter several existing formalisms which have been used in the literature to study electronic quantum transport will be reviewed, beginning with the transmission formalism developed by Landauer [25–27] and others [28–30] (for a textbook introduction to the subject, see ref. [31]). Landauer's first paper on the subject was published in 1957, but the connection between transmission and conductance was not well understood until further publications in the 1970s and 1980s. Here we will first show the derivation of the well known expressions for the current in one-dimensional (1D) and quasi-1D ballistic conductors and obtain the relationship between conductance and transmission for a 1D conductor with elastic scattering. We then show how the transmission can be calculated from the single-particle Green's function and explain the connection to the non-equilibrium Green's function formalism.

Next we will discuss a formalism based on quantum quasi-distribution functions known as *Wigner functions* [32], emphasizing their similarity to classical distribution

functions. Although Wigner first introduced the functions in 1932, it was not until the 1980s that authors began to apply Wigner functions to study quantum transport in mesoscopic devices [33–37]. Here we will provide a brief description of Wigner functions and their properties. Next, we calculate the conductance of a quasi-1D ballistic conductor from the Wigner function and show the conductance obtained in this fashion is equivalent to the Landauer result.

Thirdly, we review an approach for studying current flow of arbitrary degree of coherence in scanning tunneling microscopes developed by Kenkre, Biscarini, and Bustamante in the 1990s [38–43]. The basic formulas for the current will be derived here, and it will be shown how partially coherent motion can be modeled with a generalized Master equation.

Finally, we briefly discuss an approach developed by Lyo and Huang in the early 2000s which uses a formal solution to the Boltzmann equation for studying different kinds of scattering [44–47].

2.2 Transmission Formalism

One intuitively expects the resistance of a device to depend on the ease with which carriers may pass through the device. If it is difficult to move a carrier through the device, for example due to the presence of scatterers, it is reasonable to expect a higher resistance than if there were no scattering. For a device in which carriers are only scattered elastically, this idea can be made more precise by introducing a quantity called the *transmission function*. The transmission function $T(E)$ is defined as the probability that a carrier with energy E incident from one terminal will pass through the conductor and reach the other terminal. The transmission formalism developed by Landauer, Imry, and Büttiker and others indeed expresses the current, and thus the conductance, in a simple way in terms of the transmission function [25–30].

Several review articles [48–50] and books [29, 31, 51–53] are available on the subject. We will follow here mainly the standard development as in Datta [31]. First, a 1D conductor in which the charge carriers are not scattered at all will be considered. Surprisingly, the conductance $G = 1/R$ is found to be finite. It will be seen that this finite conductance is a result of the coupling to the contacts. The result is then generalized to a two-dimensional conductor in which the carriers are confined in the dimension perpendicular to current flow. Finally, formulae relating transmission to conductance will be obtained in the 1D case.

2.2.1 1D Ballistic Conductor

Consider now the 1D conductor in which carriers move ballistically (without scattering). The device must be connected to at least two reservoirs for current to flow through it. Suppose that one end of the device is connected to a source reservoir held at constant temperature T and electrochemical potential μ_S, and the other end is connected to a drain reservoir held at temperature T and electrochemical potential μ_D. We will take the source reservoir to be on the left of the device and the drain reservoir to be on right of the device. The difference in electrochemical potentials is related to the voltage difference ϕ by

$$\mu_S - \mu_D = q\phi \tag{2.1}$$

with q being the carrier charge. This difference in chemical potentials is responsible for the injection of carriers into the device from the source reservoir and the corresponding removal in the drain reservoir, causing a net flow of current. The conductor will never reach electrochemical equilibrium with either of the reservoirs, but arguments can be made about which states in the conductor are filled when a steady state is reached. It is generally assumed that a rightward moving carrier may exit into the drain reservoir without being reflected, and that similarly a leftward moving carrier may exit into the source reservoir without reflection (see ref. [31] for example for discussion). Under

this assumption, in the steady state, positive k (rightward moving) states must have originated in the source reservoir, and are thus distributed according to the Fermi function at chemical potential μ_S:

$$f_S(E) = \frac{1}{1 + e^{(E-\mu_S)/(kT)}}. \tag{2.2}$$

Similarly, in the steady state, all negative k (leftward moving) must have originated in the drain reservoir and are distributed according to the Fermi function at electrochemical potential μ_D,

$$f_D(E) = \frac{1}{1 + e^{(E-\mu_S)/(kT)}}. \tag{2.3}$$

Knowing the steady state distribution of states in the conductor, the current may now be calculated. The current carried by a single state with wavenumber k is two (for spin) times the carrier charge q times the probability current $j(k)$ carried by the state:

$$i(k) = 2qj(k). \tag{2.4}$$

The total current in the conductor is then the current carried by each k state times the probability that the state is occupied, multiplied by the k-space density of states $\rho_k(k)$ and integrated over all k. There is no phase relationship between the carriers originating in the source reservoir and carriers originating in the drain reservoir so that leftward and rightward moving waves do not interfere with each other. This allows us to simply add up the currents from the leftward and rightward moving carriers. The total current carried by the positive k states is

$$I_+ = \int_0^\infty i(k) f_S(E(k)) \rho_k(k) dk = 2q \int_0^\infty j(k) f_S(E(k)) \rho_k(k) dk \tag{2.5}$$

with $E(k)$ being the energy of a state with wavenumber k. Similarly, the current carried by the negative k states is

$$I_- = -\int_0^\infty i(k) f_D(E(k)) \rho_k(k) dk = -2q \int_0^\infty j(k) f_D(E(k)) \rho_k(k) dk \tag{2.6}$$

with a minus sign since the carriers are moving to the left. The net current is then

$$I = 2q \int_0^\infty j(k)[f_S(E(k)) - f_D(E(k))]\rho_k(k)dk. \tag{2.7}$$

Let us now calculate the probability current $j(k)$ and k-space density of states a 1D conductor. Instead of writing a Hamiltonian which explicitly includes a potential due to interaction of the carriers with atoms in the lattice, we will take simply a 1D effective mass Hamiltonian which treats the carriers as free particles,

$$H = \mathcal{E}_0 + \frac{p^2}{2m^*} \tag{2.8}$$

with $\mathcal{E}_0$ being the energy at the bottom of the band. The mass m^* is not the carrier mass; it is an effective mass which is related to the curvature at the bottom of the band. In typical solids the band will not be parabolic, but this can still be used as an approximation near the bottom of the band (i.e. when k is small).

The eigenfunctions of the effective mass Hamiltonian are

$$\psi_n(x) = \frac{e^{ik_m x}}{\sqrt{L}} \tag{2.9}$$

where

$$k_n \equiv \frac{2\pi m}{L} \tag{2.10}$$

and with L being the length of the conductor and m being any integer. The corresponding energy eigenvalues are

$$E(k_m) = \mathcal{E}_0 + \frac{\hbar^2 k_m^2}{2m^*} = \mathcal{E}_0 + \frac{\hbar^2 (2\pi m)^2}{2m^* L^2}. \tag{2.11}$$

The probability current is given by [54]

$$j(k_m) = \frac{\hbar}{2m^* i}\left(\psi_m^* \frac{\partial \psi_m}{\partial x} - \psi_m \frac{\partial \psi_m^*}{\partial x}\right) = \frac{\hbar k_m}{m^* L}. \tag{2.12}$$

In the limit as L becomes large, the discrete set of k states becomes a continuum, and sums over states m can be converted to integrals over k via the usual prescription

$$\sum_m \to \frac{L}{2\pi} \int dk \tag{2.13}$$

so the k-space density of states is

$$\rho_k(k) = \frac{L}{2\pi}. \tag{2.14}$$

Using these, the current becomes

$$I = 2q\frac{L}{2\pi}\frac{\hbar}{m^* L}\int_0^\infty [f_S(E(k)) - f_D(E(k))]kdk. \tag{2.15}$$

This can be converted to an integral over energy using

$$\frac{dE}{dk} = \frac{\hbar^2 k}{m^*}. \tag{2.16}$$

The current is finally

$$I = \frac{2q}{h}\int_{\mathcal{E}_0}^\infty [f_S(E) - f_D(E)]dE. \tag{2.17}$$

In deriving this result, we have used a parabolic effective mass band; however, similar calculations can be done for other systems. For example, if the conductor consists of a 1D tight binding chain the result is the same, except the upper bound of the energy integral becomes the upper band edge energy [53].

In the limit of zero temperature, the Fermi functions are step-like so states with energies below the electrochemical potential are filled and states with energies above μ are empty. Thus, if the electrochemical potentials μ_S and μ_D are below the energy at the bottom of the band $\mathcal{E}_0$, then the reservoirs are unable to inject any electrons into the conductor, and no current flows. If however the electrochemical potentials are greater than $\mathcal{E}_0$, then we have

$$I = \frac{2q}{h}(\mu_S - \mu_D) = \frac{2q^2}{h}\phi \tag{2.18}$$

and thus the conductance is

$$G \equiv \frac{I}{\phi} = \frac{2q^2}{h} \equiv G_0. \tag{2.19}$$

The quantity $G_0 \equiv 2q^2/h$ when q is taken to be the electron charge is sometimes known as the "quantum of conductance" for reasons which will soon become clear.

The numerical value of $1/G_0$ is approximately 12.9 kΩ and represents the minimum possible resistance for a 1D conductor.

It should also be noted that in this limit, only carriers with energies between μ_S and μ_D are responsible for current flow. Although leftward moving states are filled below μ_D, their current flow is exactly canceled by filled rightward moving states below μ_D.

Why is the resistance nonzero if the charge carriers move ballistically? A thorough discussion and explanation of this point may be found in the literature. Authors such as Imry [29] have pointed out that the resistance in fact depends on how the voltage difference ϕ is measured. If the voltage difference is measured between two different points *inside the conductor*, then it is found to be zero, and thus the resistance is also zero. However, the resistance is nonzero if the voltage difference is measured between two points in the source and drain reservoirs, as we have defined it to be. For this reason, this resistance is sometimes known as the "contact resistance" since it arises from coupling to the contacts. Although carriers may exit from the conductor into the reservoirs without scattering, the reverse is not likely true [31]. The source and drain reservoirs typically contain many more states than the conductor, and thus some carriers in the reservoirs must be reflected back rather than entering into the conductor, resulting in a finite resistance.

2.2.2 Mutli-Mode Ballistic Conductor

Next, consider a two-dimensional conductor in which carriers are confined in the direction perpendicular to current flow. Coordinates will be labeled x and y, with x measuring the coordinate along the direction of current flow and y being perpendicular to x. We take an effective mass Hamiltonian of the form

$$H = \frac{p_x^2}{2m^*} + \frac{p_y^2}{2m^*} + V(y) \tag{2.20}$$

where $V(y)$ is a potential which confines the carriers in the y direction. Again, we treat the carriers as free particles with an effective mass m^* rather than modeling the interaction with the atomic lattice explicitly. In devices such as field effect transistors, the strength of the confinement potential $V(y)$, and thus the effective width of the conductor, may be controlled through use of an electric field. The eigenfunctions are of the form

$$\psi_{m,n}(x,y) = \frac{e^{ik_m x}}{\sqrt{L}}\phi_n(y) \tag{2.21}$$

with again $k_m \equiv 2\pi m/L$ for integer m, and $\phi_n(y)$ being eigenfunctions of the y part of the Hamiltonian with eigenvalues $\mathcal{E}_n$,

$$\left[\frac{p_y^2}{2m^*} + V(y)\right]\phi_n(y) = \mathcal{E}_n\phi_n(y). \tag{2.22}$$

The corresponding eigenvalues for the total eigenfunctions $\psi_{m,n}$ are then

$$E(k_m, n) = \frac{\hbar^2 k_m^2}{2m^*} + \mathcal{E}_n. \tag{2.23}$$

The energy levels are illustrated in Figure 2.1. Rather than one single parabolic band, we now have one for each $\mathcal{E}_n$. These are sometimes known as "sub-bands", "channels", or "modes".

The preceding calculation for the 1D conductor may now be repeated for each mode. In the low temperature limit, every mode which is occupied contributes G_0 to the conductance, thus the total conductance becomes

$$G = \frac{2q^2}{h}M = G_0 M \tag{2.24}$$

where M is the integer number of occupied modes which participate in transport, i.e. the number of modes for which $\mathcal{E}_n$ is less that μ_D. The separation between the sub-band edges may be controlled by changing the strength of the confinement potential $V(y)$. If the source and drain electrochemical potentials are held constant, this then changes the number of occupied modes M. The observed conductance thus jumps in steps of $G_0 = 2q^2/h$. This is the origin of the term *quantum of conductance*.

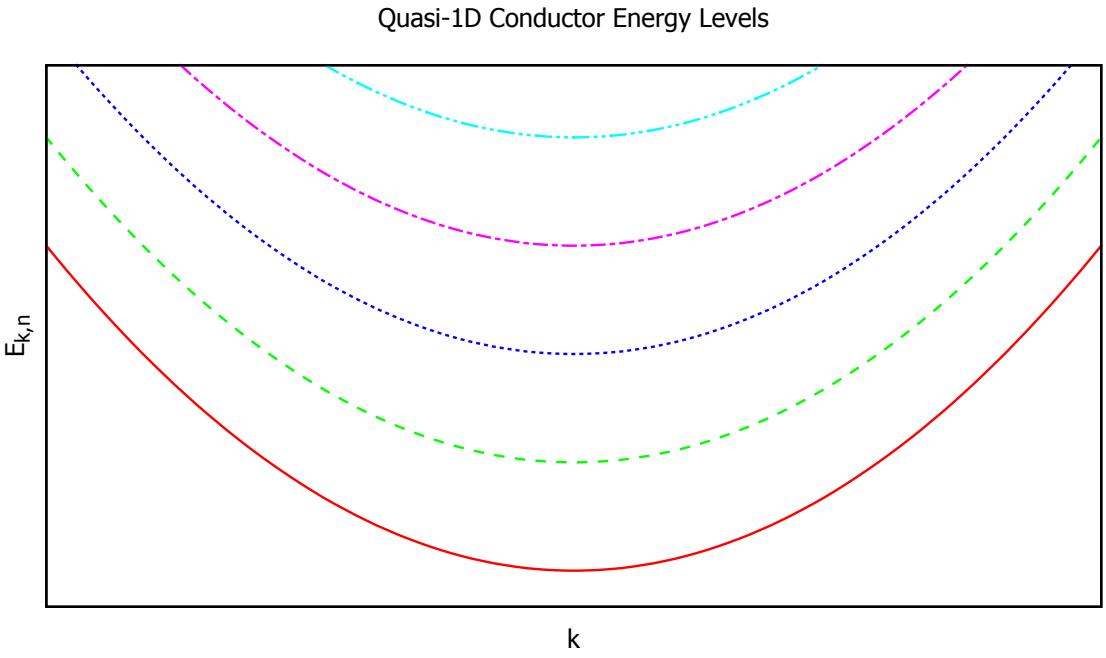

Figure 2.1: Example energy diagram for a quasi-1D conductor with multiple sub-bands. Each line represents a single sub-band.

The same effect can be achieved as the strength of an external magnetic field is varied. The mechanism for this is similar to the Shubnikov-de Haas effect [55]. In the presence of a sufficiently strong magnetic field, the electron levels become Landau levels with energies $\mathcal{E}_n = \hbar\omega_c\left(n + \frac{1}{2}\right)$ where ω_c is the cyclotron frequency. As the strength of the field is increased (or decreased), the separation between successive sub-bands increases (or decreases). If the chemical potential is held constant, this causes depletion (or filling) of modes.

This is not a true quantization (as in the case of charge quantization, for example) because the conductance may be less than $G_0 M$, for instance if there is scattering in the conductor. This "quantization" has been observed experimentally in split gate heterostructures [2–4].

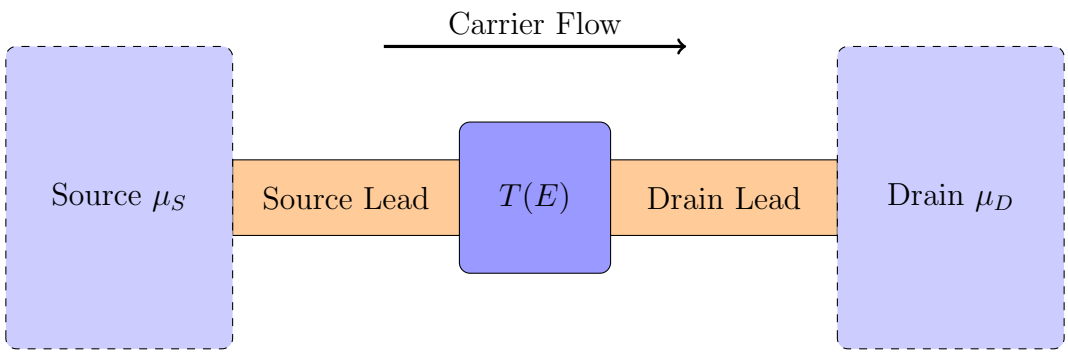

Figure 2.2: Illustration of a how current may be driven through an elastic scatterer. The scatterer with transmission function $T(E)$ is connected to two 1D ballistic source and drain leads. The leads are in turn connected to source and drain reservoirs held respectively at electrochemical potentials μ_S and μ_D.

2.2.3 Relation between Transmission and Conductance

We will now return to the 1D conductor in the presence of elastic scattering and determine the relationship between the conductance G and the transmission function $T(E)$. We follow here again the standard development as given in ref. [31]. The elastic scatterer is connected to two 1D ballistic leads, which in turn are connected to reservoirs so that a current may be passed through the device as in Figure 2.2. Charge carriers flow into the leads from source and drain reservoirs held at differing electrochemical potentials μ_S and μ_D. Again, carriers are allowed to exit from the leads into the source and drain without reflection.

In the source lead, there are:

- Rightward moving (positive k) carriers injected from the source reservoir
- Leftward moving (negative k) carriers which originated in the source reservoir and were reflected in the conductor
- Leftward moving (negative k) carriers which originated in the drain reservoir and were transmitted through the conductor

Assuming again that the k states from source and drain have random phases and thus do not interfere with each other, the total current in the source lead can be written as the sum of the currents due to incident, reflected, and transmitted beams. The total current carried in the incident beam I_I is then the current carried by each state k, times the distribution of incoming states from the source $f_S(E(k))$, times the k-space density of states $\rho_k(k)$ and integrated over all positive (rightward moving) k states:

$$I_I = 2q \int_0^\infty j(k) f_S(E(k)) \rho_k(k) dk \tag{2.25}$$

where f_S is again the Fermi function at electrochemical potential μ_S. Similarly, the current in the source lead due to the reflected beam is

$$I_R = -2q \int_0^\infty j(k) R(E(k)) f_S(E(k)) \rho_k(k) dk \tag{2.26}$$

with a negative sign since the carriers are traveling to the left, and with $R(E(k))$ being the probability that a carrier with energy $E(k)$ is reflected. The current in the source lead due to transmitted carriers originating in the drain is

$$I_D = -2q \int_0^\infty j(k) T(E(k)) f_D(E(k)) \rho_k(k) dk \tag{2.27}$$

with $f_D(E^k)$ being again the Fermi distribution at the drain electrochemical potential μ_D. Adding these, the total current in the source terminal is

$$I = I_I + I_R + I_D = 2q \int_0^\infty j(k) [f_S(E(k)) - f_D(E(k))] T(E(k)) \rho_k(k) dk \tag{2.28}$$

where we have used the fact that since the scattering is elastic $R(E(k)) + T(E(k)) = 1$ (i.e. the carrier must be either transmitted through the conductor or reflected back; it cannot be absorbed).

Using our earlier results for the probability current $j(k)$ and the k-space density of states $\rho_k(k)$, and changing integration variables to E, we have finally

$$I = \frac{2q}{h} \int_{\mathcal{E}_0}^\infty T(E) [f_S(E) - f_D(E)] dE. \tag{2.29}$$

In the limit of small bias, we can write

$$I = \frac{2q}{h}(\mu_S - \mu_D)\int_{\mathcal{E}_0}^{\infty} T(E)\left[-\frac{df_D}{dE}\right]dE \tag{2.30}$$

Additionally, in the limit of low temperature, $-dF_D/dE \approx \delta(E - \mu_D)$ and we have approximately

$$I = \frac{2q}{h}(\mu_S - \mu_D)T(\mu_D). \tag{2.31}$$

The conductance is then

$$G = \frac{I}{\phi} = \frac{2q^2}{h}T(\mu_D) = G_0 T(\mu_D). \tag{2.32}$$

This formula relating the conductance to the transmission function is the simplest version of what is known as the *Landauer formula* [26]. As expected, a higher transmission means a higher conductance, with the ballistic result being recovered in the limiting case $T = 1$.

In the case where there are multiple sub-bands, such as the two-dimensional conductor discussed earlier, then the generalized version of the Landauer formula (when potential difference is measured between the reservoirs) is

$$G = G_0 \mathrm{Tr}(tt^\dagger) \tag{2.33}$$

where t is the matrix of transmission amplitudes.

More generalizations may be displayed, in particular there is a formula for multiple terminals derived in ref. [28]. Phase breaking scattering processes can then be incorporated into the theory by introducing a "scattering" terminal which removes electrons and reinjects them with different energies. The transmission formalism has been successfully applied in the literature to understand conductance in mesoscopic semiconductors. In the following chapter, the transmission formalism will be applied to calculate the conductance for various kinds of elastic scatterers.

2.2.4 Transmission and the Green's Function

So far we have not yet discussed how the transmission function $T(E)$ can be calculated. One simple method, oft found in quantum mechanics textbooks (see ref. [54]), is to take an incoming wave of the form e^{ikx} to the left of the scatterer, a reflected wave re^{-ikx} to the left of the scatterer, and a transmitted wave te^{ikx} to the right of the scatterer. The amplitudes r and t are then calculated by matching the wavefunction at the boundaries of the scatterer so that the Schrödinger equation is everywhere satisfied. If the group velocities are the same on either side of the scatterer, the transmission and reflection functions are $R = |r|^2$ and $T = |t|^2$.

In certain cases, it may be more convenient to calculate the transmission function from the single-particle Green's function. The Green's function is defined as [56]

$$G(E) \equiv \frac{1}{E - H}. \tag{2.34}$$

It can be shown that only the part of the Green's function for the conductor subsystem (i.e. the elements $\langle m|G(E)|n\rangle$ where $|m\rangle, |n\rangle$ are conductor states) is needed to calculate the transmission function. The effect of the coupling to reservoirs may be incorporated into the conductor Green's function by introducing a complex energy dependent function $\Sigma(E)$ known as the self energy. This may be done as follows [56]. Suppose for now that only one contact is connected to the conductor. Dividing the Hilbert space into conductor and reservoir subspaces and writing the total Hamiltonian for the total system as a block matrix gives

$$H = \begin{pmatrix} H_R & \tau^\dagger \\ \tau & H_c \end{pmatrix} \tag{2.35}$$

where H_R and H_c are respectively the Hamiltonians for the isolated reservoir and conductor and τ represents the coupling between reservoir and conductor. The Green's function obeys $(E - H)G = 1$, so as block matrices,

$$\begin{pmatrix} E - H_R & -\tau^\dagger \\ -\tau & E - H_c \end{pmatrix} \begin{pmatrix} G_{RR} & G_{Rc} \\ G_{cR} & G_{cc} \end{pmatrix} = \begin{pmatrix} 1 & 0 \\ 0 & 1 \end{pmatrix}. \tag{2.36}$$

Multiplying the two block matrices on the left hand side,

$$(E - H_R)G_{RR} + \tau^\dagger G_{cR} = 1 \tag{2.37}$$

$$(E - H_R)G_{Rc} + \tau^\dagger G_{cc} = 0 \tag{2.38}$$

$$\tau G_{RR} + (E - H_c)G_{cR} = 0 \tag{2.39}$$

$$\tau G_{Rc} + (E - H_c)G_{cc} = 1 \tag{2.40}$$

If we are only interested in the part of the Green's function for the conductor subspace, G_{cc}, we can combine the second equation with the fourth equation to write

$$G_{cc}(E) = \frac{1}{E - H_c - \Sigma(E)} \tag{2.41}$$

with the self energy $\Sigma(E)$ given by[1]

$$\Sigma(E) = \tau G_R \tau^\dagger \tag{2.42}$$

where G_R is the Green's function for the isolated reservoir, $G_R = [E - H_R]^{-1}$. In the case where multiple terminals are connected, it may be shown that the resulting self energies add, provided that the leads do not interact with each other.

The transmission function $T(E)$ may be expressed in terms of the conductor Green's function, even when there are multiple terminals and multiple channels per lead. The details of the derivation may be found in textbooks such as [31, 56]. For the special case of two terminals, the result is

$$T(E) = \mathrm{Tr}\{\Gamma_S G \Gamma_D G^\dagger\} \tag{2.43}$$

where the trace runs over conductor states and the quantities Γ are related to the self energies by

$$\Gamma(E) \equiv i[\Sigma(E) - \Sigma^\dagger(E)]. \tag{2.44}$$

[1]When H has a continuous spectrum, G has a branch cut along the real axis and must therefore be defined through a limiting process. In these expressions, $G(E)$ should be taken to mean $G^+(E) \equiv \lim_{\eta \to 0^+} G(E + i\eta)$ [56].

This is sometimes known as the Fisher-Lee relation [57].

In addition to providing another way to calculate the transmission function, this relation also connects the transmission theory to the non-equilibrium Green's function (NEGF) formalism. The NEGF approach, developed by Keldysh [58], Kadanoff and Baym [59], and others, is completely equivalent to the transmission theory when the motion is coherent. However, rather than incorporating incoherent scattering effects phenomenologically as in the Landauer-Büttiker theory, scattering can be modeled microscopically. Scattering is introduced into the Green's function through additional self energy terms Σ. As the Green's function depends on the self energies, these self energy terms typically will depend on the Green's function itself. This necessitates an iterative procedure whereby a self-consistent solution can be arrived at.

2.3 Wigner Function Approach

Although the transmission theory and the NEGF formalism have been successfully used in the literature, they are quite different from the classical theory of conductance based on the kinetic Boltzmann equation. Some authors have used so called *Wigner functions* to study quantum transport because of certain similarities to classical transport theory. A Wigner function, first introduced by Eugene Wigner in 1932 [32], like the classical probability distribution, is a quantity defined on phase space, yet it completely describes the quantum state of the system. It obeys an equation of motion which is similar to the semi-classical Boltzmann transport equation, and observables are calculated in a similar manner.

Many review and tutorial articles are available in the literature, see refs. [60–64] and references therein. We follow here a similar development as in ref. [64].

In classical transport theory, the state of a system can be described by a distribution function $f(\mathbf{x}, \mathbf{p}, t)$ defined on phase space which describes the density of particles

with position $\mathbf{x}$ and momentum $\mathbf{p}$ at time t. The time evolution of the distribution function f is governed by the Boltzmann equation [65],

$$\frac{\partial f}{\partial t} + \frac{\mathbf{p}}{m} \cdot \nabla_{\mathbf{r}} f + \mathbf{F} \cdot \nabla_{\mathbf{p}} f = \left(\frac{\partial f}{\partial t} \right)_{\text{coll}} \tag{2.45}$$

where the term on the right hand side accounts for the change in the distribution function due to collisions. To find the expectation value of an observable quantity $O(\mathbf{x}, \mathbf{p})$, the distribution function is multiplied by the observable and integrated over all phase space,

$$\langle O \rangle = \int \int O(\mathbf{x}, \mathbf{p}) f(\mathbf{x}, \mathbf{p}, t) d\mathbf{x} d\mathbf{p}. \tag{2.46}$$

In a quantum system, because of the uncertainty principle, the momentum and position of a particle cannot be simultaneously specified, and the semi-classical distribution function f cannot be used. Instead, for a quantum mechanical system in a statistical mixture of states, the density operator ρ is used to describe the complete state of the system. The density operator may be defined as (see any standard quantum mechanics textbook, e.g. [54])

$$\rho = \sum_m p_m |\psi_m\rangle\langle\psi_m| \tag{2.47}$$

where p_m is the statistical weight to find the system in state $|\psi_m\rangle$. In the Schrödinger picture, states evolve as

$$|\psi(t)\rangle = e^{-iHt/\hbar} |\psi(0)\rangle, \tag{2.48}$$

so the density matrix evolves as

$$\rho(t) = \sum_m p_m e^{-iHt/\hbar} |\psi_m(0)\rangle\langle\psi_m(0)| e^{+iHt/\hbar}. \tag{2.49}$$

Taking a time derivative, we have

$$\frac{\partial \rho}{\partial t} = \sum_m p_m \left(\frac{H}{i\hbar} |\psi_m(t)\rangle\langle\psi_m(t)| - |\psi_m(t)\rangle\langle\psi_m(t)| \frac{H}{i\hbar} \right). \tag{2.50}$$

The density operator thus obeys

$$\frac{\partial \rho}{\partial t} = \frac{1}{i\hbar}[H, \rho]. \tag{2.51}$$

This is the quantum mechanical analogue of the Liouville equation and is known as the von Neumann equation or Liouville-von Neumann equation.

For a system in a pure quantum mechanical state $|\psi\rangle$, the expectation value of an observable O is given by $\langle O\rangle = \langle\psi|O|\psi\rangle$. When in a statistical mixture of states, the expectation value is averaged over possible states, weighted by the statistical probability to be in each state,

$$\langle O\rangle = \sum_m p_m \langle\psi_m|O|\psi_m\rangle. \tag{2.52}$$

Inserting a complete set of states, (assuming the $|\psi_m\rangle$ are normalized so that $\langle\psi_m|\psi_n\rangle = \delta_{mn}$), we have

$$\langle O\rangle = \sum_{n,m} p_m \langle\psi_m|O|\psi_n\rangle\langle\psi_n|\psi_m\rangle = \sum_{n,m} p_n \langle\psi_m|O|\psi_n\rangle\langle\psi_n|\psi_m\rangle \tag{2.53}$$

where p_n has been substituted for p_m, which is valid since the only nonzero terms in the double sum have $m = n$. Using the definition for the density operator, this is just

$$\langle O\rangle = \sum_m \langle\psi_m|O\rho|\psi_m\rangle \equiv \mathrm{Tr}\{O\rho\} \tag{2.54}$$

where Tr denotes the trace.

The statements made thus far apply in any representation. If we have a set of position states, $|\mathbf{x}\rangle$, such that

$$\langle\mathbf{x}|\mathbf{x}'\rangle = \delta(\mathbf{x} - \mathbf{x}') \tag{2.55}$$

and for any state $|\psi(t)\rangle$,

$$\langle\mathbf{x}|\psi(t)\rangle = \psi(\mathbf{x}, t), \tag{2.56}$$

the density operator may then be defined as a function of two position variables (and time) via

$$\rho(\mathbf{x},\mathbf{x}',t) \equiv \langle \mathbf{x}'|\rho|\mathbf{x}\rangle = \sum_m p_m \psi_m^*(\mathbf{x},t)\psi_m(\mathbf{x}',t). \tag{2.57}$$

The Wigner function in d dimensions is defined by changing to mean and relative coordinates, and Fourier transforming on the relative coordinate,

$$W(\mathbf{x},\mathbf{p},t) \equiv \frac{1}{(\pi\hbar)^d}\int \rho(\mathbf{x}+\mathbf{y},\mathbf{x}-\mathbf{y},t)e^{2i(\mathbf{p}\cdot\mathbf{y})/\hbar}d^d\mathbf{y}. \tag{2.58}$$

To derive the evolution equation for the Wigner function, the von Neumann equation in the position representation will first be written and then transformed to obtain the evolution equation for the Wigner function. Using equation (2.57), the von Neumann equation becomes

$$i\hbar\frac{\partial}{\partial t}\rho(\mathbf{x},\mathbf{x}',t) = \sum_m p_m\left[i\hbar\psi_m(\mathbf{x}',t)\frac{\partial}{\partial t}\psi_m^*(\mathbf{x},t) + i\hbar\psi_m^*(\mathbf{x},t)\frac{\partial}{\partial t}\psi_m(\mathbf{x}',t)\right]. \tag{2.59}$$

For a Hamiltonian of the form $H = \mathbf{p}^2/(2m) + V(\mathbf{x})$, the Schrödinger equation and its complex conjugate can be used to rewrite this as

$$\begin{aligned} i\hbar\frac{\partial}{\partial t}\rho(\mathbf{x},\mathbf{x}',t) = \sum_m p_m\Bigg[&\left(\frac{\hbar^2}{2m}\nabla_{\mathbf{x}}^2 - V(\mathbf{x})\right) \\ &+ \left(\frac{-\hbar^2}{2m}\nabla_{\mathbf{x}'}^2 + V(\mathbf{x}')\right)\Bigg]\psi_m^*(\mathbf{x},t)\psi_m(\mathbf{x}',t). \end{aligned} \tag{2.60}$$

Again using equation (2.57), the von Neumann equation in the position representation is

$$i\hbar\frac{\partial}{\partial t}\rho(\mathbf{x},\mathbf{x}',t) = \left[-\frac{\hbar^2}{2m}\nabla_{\mathbf{x}'}^2 + \frac{\hbar^2}{2m}\nabla_{\mathbf{x}}^2 + V(\mathbf{x}') - V(\mathbf{x})\right]\rho(\mathbf{x},\mathbf{x}',t). \tag{2.61}$$

Changing to centered and relative coordinates, this is

$$\begin{aligned} i\hbar\frac{\partial}{\partial t}\rho(\mathbf{x}+\mathbf{y},\mathbf{x}-\mathbf{y},t) = \Bigg[&\frac{\hbar^2}{2m}\nabla_{\mathbf{x}}\cdot\nabla_{\mathbf{y}} + V(\mathbf{x}-\mathbf{y}) \\ &- V(\mathbf{x}+\mathbf{y})\Bigg]\rho(\mathbf{x}+\mathbf{y},\mathbf{x}-\mathbf{y},t) \end{aligned} \tag{2.62}$$

Fourier transforming, integrating the first term by parts and using the convolution theorem for the second term, the evolution of the Wigner function is finally given by

$$\frac{\partial W}{\partial t} = -\frac{\mathbf{p}}{m} \cdot \nabla_{\mathbf{x}} W(\mathbf{x}, \mathbf{p}, t) + \int \chi(\mathbf{x}, \mathbf{p} - \mathbf{p}') W(\mathbf{x}, \mathbf{p}', t) d^d\mathbf{p}' \tag{2.63}$$

with χ given by

$$\chi(\mathbf{x}, \mathbf{p}) \equiv \frac{1}{i\hbar} \frac{1}{(\pi\hbar)^d} \int [V(\mathbf{x} - \mathbf{y}) - V(\mathbf{x} + \mathbf{y})] e^{2i\mathbf{p}\cdot\mathbf{y}/\hbar} d^d\mathbf{y}. \tag{2.64}$$

This equation, known sometimes as Moyal's evolution equation [66], is superficially similar to the Boltzmann equation (2.45), except now with a term which is nonlocal in momentum space. Again, since all transforms are invertible, this is completely equivalent to the fully quantum von Neumann equation, thus this equation completely describes the evolution of the quantum system. Additional terms may be added to account for incoherent scattering effects.

Next, it will be shown how the expectation value of any observable can be calculated. Starting from (2.54), and taking the trace over position states,

$$\langle O \rangle = \mathrm{Tr}\{O\rho\} = \int \langle \mathbf{x}|O\rho|\mathbf{x}\rangle d^d\mathbf{x}. \tag{2.65}$$

Inserting a complete set of position states,

$$\langle O \rangle = \int \int \langle \mathbf{x}|O|\mathbf{x}'\rangle \langle \mathbf{x}'|\rho|\mathbf{x}\rangle d^d\mathbf{x} d^d\mathbf{x}'. \tag{2.66}$$

Next, changing to centered and relative coordinates,

$$\langle O \rangle = 2^d \int \int \langle \mathbf{x} + \mathbf{y}|O|\mathbf{x} - \mathbf{y}\rangle \langle \mathbf{x} - \mathbf{y}|\rho|\mathbf{x} + \mathbf{y}\rangle d^d\mathbf{x} d^d\mathbf{y}. \tag{2.67}$$

Using the properties of Fourier transforms, this can be rewritten as

$$\langle O \rangle = \int \int \tilde{O}(\mathbf{x}, \mathbf{p}) W(\mathbf{x}, \mathbf{p}, t) d^d\mathbf{x} d^d\mathbf{p} \tag{2.68}$$

where $\tilde{O}$ is said to be the Wigner-Weyl transform of the operator O, defined by

$$\tilde{O}(\mathbf{x}, \mathbf{p}) \equiv 2^d \int \langle \mathbf{x} - \mathbf{y}|O|\mathbf{x} + \mathbf{y}\rangle e^{2i\mathbf{p}\cdot\mathbf{y}/\hbar} d^d\mathbf{y}. \tag{2.69}$$

Equation (2.68) is analogous to the classical expression (2.46) used for calculating observables.

To apply the Wigner function formalism to quantum transport, one must solve equation (2.63) subject to appropriate boundary conditions. In [51] the problems of specifying the correct boundary conditions are discussed, and it is suggested that an appropriate method is to extend the domain of the problem far from the source of quantum effects (i.e. into the reservoirs) so that a semi-classical distribution may be used at the boundaries. In the literature, the Wigner function formalism has been successfully applied by a few authors to simple systems, such as the 1D resonant tunneling diode (RTD), in particular see [33–37].

Next, the equivalence of the Landauer transmission theory and the Wigner function theory for the two-dimensional ballistic conductor discussed earlier will be demonstrated. Instead of solving (2.63) directly, the steady-state Wigner function can be found from the steady-state density matrix. Knowing the Wigner function, the current can then be calculated using (2.68). The result is equivalent to the Landauer result.

Starting with the same effective mass Hamiltonian,

$$H = \frac{p_x^2}{2m^*} + \frac{p_y^2}{2m^*} + V(y) \tag{2.70}$$

recall that the rightward moving k states are filled according to the source distribution function, and leftward moving k states are filled according to the drain distribution function. The steady state density matrix in the position representation is then

$$\begin{aligned}\rho(\mathbf{x},\mathbf{x}') = \frac{1}{2\pi}\sum_n \int_0^\infty f_S(\mathcal{E}_{k_x,n})\phi_n^*(y)\phi_n(y')e^{-ik_x(x-x')}dk_x \\ + \frac{1}{2\pi}\sum_n \int_{-\infty}^0 f_D(\mathcal{E}_{k_x,n})\phi_n^*(y)\phi_n(y')e^{-ik_x(x-x')}dk_x\end{aligned} \tag{2.71}$$

with $\mathcal{E}_{k_x,n} = \hbar^2k^2/(2m^*) + \mathcal{E}_n$ being the energy eigenvalue associated with a state

$$\psi_{k_x,n}(x,y) = \frac{e^{ikx}}{\sqrt{L}}\phi_n(y) \tag{2.72}$$

with $\phi_n(y)$ an eigenfunction of the y part of the Hamiltonian with eigenvalue $\mathcal{E}_n$. Changing coordinates, this becomes

$$\rho(\mathbf{x}+\mathbf{u},\mathbf{x}-\mathbf{u}) = \frac{1}{2\pi}\sum_n \int_0^\infty f_S(\mathcal{E}_{k_x,n})\phi_n^*(y+u_y)\phi_n(y-u_y)e^{-2ik_x u_x}dk_x + \frac{1}{2\pi}\sum_n \int_{-\infty}^0 f_D(\mathcal{E}_{k_x,n})\phi_n^*(y+u_y)\phi_n(y-u_y)e^{-2ik_x u_x}dk_x. \tag{2.73}$$

Fourier transforming, the Wigner function in the steady state is

$$W(\mathbf{x},\mathbf{p}) = \frac{1}{h}\sum_n \left[f_S(\mathcal{E}_{p_x/\hbar,n})\Theta(p_x) + f_D(\mathcal{E}_{p_x/\hbar,n})\Theta(-p_x)\right] W_n(y,p_y) \tag{2.74}$$

where Θ is the Heaviside step function and W_n is the Wigner function associated with the nth eigenfunction of the y Hamiltonian $\phi_n(y)$,

$$W_n(y,p_y) \equiv \frac{1}{\pi\hbar}\int \phi_n^*(y+u_y)\phi_n(y-u_y)e^{2ip_y u_y/\hbar}du_y. \tag{2.75}$$

The current operator is

$$I = \frac{2q}{m^* L}p_x, \tag{2.76}$$

and its Wigner-Weyl transform is

$$\tilde{I}(\mathbf{x},\mathbf{p}) = h\delta(p_y)\frac{2q}{m^* L}p_x. \tag{2.77}$$

We then have for the current

$$\langle I\rangle = \frac{2q}{m^* h}\sum_n \int_0^\infty [f_S(\mathcal{E}_{p_x,n}) - f_D(\mathcal{E}_{p_x,n})]p_x dp_x. \tag{2.78}$$

Converting to an integral over energy gives

$$\langle I\rangle = \frac{2q}{h}\sum_n \int_{\mathcal{E}_n}^\infty [f_S(\mathcal{E}) - f_D(\mathcal{E})]d\mathcal{E}. \tag{2.79}$$

In the low temperature, low bias limit, this reduces to the Landauer result,

$$\langle I\rangle = \frac{2q}{h}(\mu_S - \mu_D)M. \tag{2.80}$$

Although the current depends only on the number of occupied sub-bands at a particular energy, not the specific form of the y part of the Wigner function, we display here the Wigner functions $W_n(y, p_y)$ for the two most commonly used types of confinement: square well and harmonic.

2.3.1 Wigner Functions for Infinite Square Well Confinement

For the infinite square well the potential is

$$V(y) = \begin{cases} 0 & \text{if } 0 < y < L_y \\ \infty & \text{otherwise} \end{cases} \tag{2.81}$$

and the eigenfunctions are

$$\phi_n(y) = \begin{cases} \sqrt{\frac{2}{L_y}} \sin\left(\frac{n\pi}{L_y} y\right) & \text{if } 0 < y < L_y \\ 0 & \text{otherwise} \end{cases} \tag{2.82}$$

with energies

$$\mathcal{E}_n = \frac{\hbar^2 \pi^2}{2m^* L_y^2} n^2. \tag{2.83}$$

The associated Wigner functions are [67]

$$W_n(y, p_y) = \left(\frac{2}{\pi \hbar L_y}\right) \left\{ \frac{\sin[2(p_y/\hbar - n\pi/L_y)y]}{4(p_y/\hbar - n\pi/L_y)} + \frac{\sin[2(p_y/\hbar + n\pi/L_y)y]}{4(p_y/\hbar + n\pi/L_y)} - \cos\left(\frac{2n\pi y}{L_y}\right) \frac{\sin(2p_y y/\hbar)}{(2p_y/\hbar)} \right\} \tag{2.84}$$

for $y < L_y/2$ and $W_n(y, p_y) = W_n(L_y - y, p_y)$ for $y > L_y/2$. The functions $W_n(y, p_y)$ are plotted for $n = 1$ through $n = 4$ in Figure (2.3).

2.3.2 Wigner Functions for Harmonic Confinement

For harmonic confinement, we have for the potential

$$V(y) = \frac{1}{2} m^* \omega^2 y^2 \tag{2.85}$$

and the eigenfunctions are [54]

$$\phi_n(y) = \left(\frac{m^*\omega}{\pi\hbar}\right)^{1/4} \frac{1}{\sqrt{2^n n!}} H_n\left(\sqrt{\frac{m^*\omega}{\hbar}}y\right) e^{-m\omega y^2/2\hbar^2} \tag{2.86}$$

where H_n is the nth Hermite polynomial. The energies are

$$\mathcal{E}_n = \left(n + \frac{1}{2}\right)\hbar\omega. \tag{2.87}$$

The corresponding Wigner functions are [61]

$$W_n(y, p_y) = \frac{2}{h}(-1)^n e^{-2H(y,p_y)/\hbar\omega} L_n\left(\frac{4H(y,p_y)}{\hbar\omega}\right) \tag{2.88}$$

where L_n is the nth Laguerre polynomial and

$$H(y, p_y) \equiv \frac{p_y^2}{2m^*} + \frac{1}{2}m^*\omega^2 y^2. \tag{2.89}$$

Explicitly, the first few are

$$W_0(y, p_y) = +\frac{2}{h}e^{-2H(y,p_y)/\hbar\omega}, \tag{2.90}$$

$$W_1(y, p_y) = -\frac{2}{h}e^{-2H(y,p_y)/\hbar\omega}\left[-\frac{4H(y,p_y)}{\hbar\omega} + 1\right], \tag{2.91}$$

$$W_2(y, p_y) = +\frac{2}{h}e^{-2H(y,p_y)/\hbar\omega}\left[\frac{1}{2}\left(\frac{4H(y,p_y)}{\hbar\omega}\right)^2 - 2\left(\frac{4H(y,p_y)}{\hbar\omega}\right) + 1\right]. \tag{2.92}$$

The functions $W_n(y, p_y)$ are plotted for $n = 0$ through $n = 3$ in Figure (2.4).

2.4 Kenkre, Biscarini, Bustamante Scanning Tunneling Microscope Formalism

Motivated by a desire to understand partially coherent transport in scanning tunneling microscope (STM) junctions in a simple fashion, Kenkre, Biscarini, and Bustamante formulated a theory of quantum transport using generalized Master equations

(GMEs) to study transport of with an arbitrary degree of coherence [38–43]. Scattering effects are not modeled microscopically; they are instead introduced phenomenologically through the use of stochastic Liouville equations (SLEs). One advantage of this approach is that one can make use of several exact solutions to SLEs that have already been published in the literature (see for example refs. [68–70]).

2.4.1 Derivation of Formulae for Calculating Current

The current will be calculated here for the simplest case, following the same procedure as described in detail in ref. [41], but relaxing the assumption that there is no transient net buildup of charge in the conductor. Suppose we have a conductor which consists of a discrete set of states with labels m. When the conductor is isolated (not connected to any contacts), suppose that the probabilities obey a generalized Master equation (GME), i.e.

$$\frac{\partial P_m}{\partial t} = -\sum_n \int_0^t A_{mn}(t-t')P_n(t')dt'. \tag{2.93}$$

Later in this section, it will be shown how a GME may be used to model coherent (quantum mechanical) motion, incoherent (classical) motion, and partially coherent motion.

Next, suppose that only a single state $m = S$ is connected to a source reservoir and a single state $m = D$ is connected to a drain reservoir. The source and drain will be assumed to be held at equal temperatures, but differing electrochemical potentials μ_S and μ_D. This results in a flow of probability into the source state at a rate which will be denoted $R_S(t)$, and a removal of probability from drain state at a rate $R_D(t)$. In the steady state, there should be no accumulation of charge, thus $R_S(t) = R_D(t)$ at long times. The steady state current is then the carrier charge q times the number of carriers n_c times the probability flux out of the conductor,

$$I(t) = qn_cR_D(t) = qn_cR_S(t). \tag{2.94}$$

When the conductor is connected to source and drain terminals, the generalized Master equation for the *open* system becomes

$$\frac{dP_m}{dt} = -\sum_n \int_0^t A_{mn}(t-t')P_n(t')dt' + \delta_{m,S}R_S(t) - \delta_{m,D}R_D(t). \tag{2.95}$$

Laplace transforming, this is

$$\epsilon\tilde{P}_m(\epsilon) - P_m(0) = -\sum_n \tilde{A}_{mn}(\epsilon)\tilde{P}_n(\epsilon) + \delta_{m,S}\tilde{R}_S(\epsilon) - \delta_{m,D}\tilde{R}_D(\epsilon) \tag{2.96}$$

where the Laplace transform of a function f is

$$\tilde{f}(\epsilon) \equiv \mathcal{L}_\epsilon\{f(t)\} \equiv \int_0^\infty f(t)e^{-\epsilon t}dt. \tag{2.97}$$

The solution is

$$\tilde{P}_m(\epsilon) = \tilde{\eta}_m(\epsilon) + \tilde{\Pi}_{mS}(\epsilon)\tilde{R}_S(\epsilon) - \tilde{\Pi}_{mD}(\epsilon)\tilde{R}_D(\epsilon) \tag{2.98}$$

where η_m is the solution to the Master equation for the isolated conductor,

$$\tilde{\eta}_m(\epsilon) = \sum_n \tilde{\Pi}_{mn}(\epsilon)P_n(0). \tag{2.99}$$

The Πs are the propagators of the isolated conductor, i.e. $\Pi_{mn}(t)$ is the probability of finding the particle at state m at time t given that it began at state n. The Laplace transformed propagators $\tilde{\Pi}_{mn}(\epsilon)$ are given in terms of the rates $\tilde{A}_{mn}(\epsilon)$ through the matrix equation

$$\tilde{\mathbf{\Pi}}(\epsilon) = [\epsilon\mathbf{I} + \tilde{\mathbf{A}}(\epsilon)]^{-1}. \tag{2.100}$$

To proceed, the form that the rates R_S and R_D should take must now be determined. The rates must depend on the probabilities in some way, since for example if the conductor were in equilibrium with only the source (or drain), then R_S (or R_D) should vanish. Ideally, this dependence on the probabilities should be linear. The interaction with the reservoir should attempt to drive the state connected to the

reservoir to its thermal value. Thus, it is reasonable to assume that the rates should take the simple form

$$R_S(t) = \frac{P_S^{\text{th}} - P_S(t)}{\tau_S}, \tag{2.101}$$

$$R_D(t) = -\frac{P_D^{\text{th}} - P_D(t)}{\tau_D}. \tag{2.102}$$

Here P_S^{th} is the probability to find a carrier at the source state S if the conductor were in equilibrium with the source reservoir alone. P_D^{th} is similarly defined; it is the probability to find a carrier at the drain state D if the conductor were in equilibrium with only the *drain* reservoir. τ_S and τ_D are constants with the dimensions of time which describe respectively the strength of the coupling to the source and drain reservoirs, with a smaller τ meaning a stronger coupling.

Returning to (2.98) and writing out explicitly the equations for $m = S$ and $m = D$ gives

$$\tilde{P}_S(\epsilon) = \tilde{\eta}_S(\epsilon) + \tilde{\Pi}_{SS}(\epsilon)\tilde{R}_S(\epsilon) - \tilde{\Pi}_{SD}(\epsilon)\tilde{R}_D(\epsilon), \tag{2.103}$$

$$\tilde{P}_D(\epsilon) = \tilde{\eta}_D(\epsilon) + \tilde{\Pi}_{DS}(\epsilon)\tilde{R}_S(\epsilon) - \tilde{\Pi}_{DD}(\epsilon)\tilde{R}_D(\epsilon). \tag{2.104}$$

Equations (2.101) and (2.102) may now be used to eliminate P_S and P_D in favor of R_S and R_D, giving

$$P_S^{\text{th}}/\epsilon - \tau_S\tilde{R}_S(\epsilon) = \tilde{\eta}_S(\epsilon) + \tilde{\Pi}_{SS}(\epsilon)\tilde{R}_S(\epsilon) - \tilde{\Pi}_{SD}(\epsilon)\tilde{R}_D(\epsilon), \tag{2.105}$$

$$P_D^{\text{th}}/\epsilon + \tau_D\tilde{R}_D(\epsilon) = \tilde{\eta}_D(\epsilon) + \tilde{\Pi}_{DS}(\epsilon)\tilde{R}_S(\epsilon) - \tilde{\Pi}_{DD}(\epsilon)\tilde{R}_D(\epsilon). \tag{2.106}$$

This is now a set of two coupled equations in two unknowns, the rates R_S and R_D, which we may be easily solved. After some rearrangement,

$$-(\tilde{\Pi}_{SS}(\epsilon) + \tau_S)\tilde{R}_S(\epsilon) + \tilde{\Pi}_{SD}(\epsilon)\tilde{R}_D(\epsilon) = [\tilde{\eta}_S(\epsilon) - P_S^{\text{th}}/\epsilon], \tag{2.107}$$

$$-\tilde{\Pi}_{DS}(\epsilon)\tilde{R}_S(\epsilon) + (\tilde{\Pi}_{DD}(\epsilon) + \tau_D)\tilde{R}_D(\epsilon) = [\tilde{\eta}_D(\epsilon) - P_D^{\text{th}}/\epsilon]. \tag{2.108}$$

Using Cramer's rule to solve this system gives the rates explicitly in the Laplace

domain,

$$\tilde{R}_S(\epsilon) = \frac{[\tilde{\eta}_D(\epsilon) - P_D^{\text{th}}/\epsilon][\tilde{\Pi}_{SD}(\epsilon)] - [\tilde{\eta}_S(\epsilon) - P_S^{\text{th}}/\epsilon][\tilde{\Pi}_{DD}(\epsilon) + \tau_D]}{[\tilde{\Pi}_{DD}(\epsilon) + \tau_D][\tilde{\Pi}_{SS}(\epsilon) + \tau_S] - \tilde{\Pi}_{SD}(\epsilon)\tilde{\Pi}_{DS}(\epsilon)}, \tag{2.109}$$

$$\tilde{R}_D(\epsilon) = \frac{[\tilde{\eta}_D(\epsilon) - P_D^{\text{th}}/\epsilon][\tilde{\Pi}_{SS}(\epsilon) + \tau_S] - [\tilde{\eta}_S(\epsilon) - P_S^{\text{th}}/\epsilon][\tilde{\Pi}_{DS}(\epsilon)]}{[\tilde{\Pi}_{DD}(\epsilon) + \tau_D][\tilde{\Pi}_{SS}(\epsilon) + \tau_S] - \tilde{\Pi}_{SD}(\epsilon)\tilde{\Pi}_{DS}(\epsilon)}. \tag{2.110}$$

The steady state current may now be obtained using the final value theorem for Laplace transforms,

$$\lim_{t\to\infty} f(t) = \lim_{\epsilon\to 0} \epsilon\tilde{f}(\epsilon). \tag{2.111}$$

For R_S we have

$$R_S(\infty) = \lim_{\epsilon\to 0} \frac{[\epsilon\tilde{\eta}_D(\epsilon) - P_D^{\text{th}}][\epsilon\tilde{\Pi}_{SD}(\epsilon)] - [\epsilon\tilde{\eta}_S(\epsilon) - P_S^{\text{th}}][\epsilon\tilde{\Pi}_{DD}(\epsilon) + \epsilon\tau_D]}{\epsilon[\tilde{\Pi}_{DD}(\epsilon) + \tau_D][\tilde{\Pi}_{SS}(\epsilon) + \tau_S] - \epsilon\tilde{\Pi}_{SD}(\epsilon)\tilde{\Pi}_{DS}(\epsilon)} \tag{2.112}$$

where we have multiplied top and bottom by ϵ.

If the conductor were isolated, we should expect it to reach the same final state regardless of whatever the initial condition is. Using the same notation as (ref), let $\eta_m^{\text{th}} = \lim_{t\to\infty} \eta_m(t) = \lim_{\epsilon\to 0} \epsilon\tilde{\eta}_m(\epsilon)$ be the probability to find a particle at state m at long times in the *isolated* conductor. We may then write

$$\lim_{\epsilon\to 0} \epsilon\tilde{\Pi}_{mn}(\epsilon) = \eta_m^{\text{th}}, \tag{2.113}$$

again since the final state is independent of initial condition. This should hold provided that any state m may be reached from any other state n (i.e. there are no states or sets of states which are totally cut off from the rest of the conductor). Using this, we have in the numerator

$$\begin{aligned}
&\lim_{\epsilon\to 0}[\epsilon\tilde{\eta}_D(\epsilon) - P_D^{\text{th}}][\epsilon\tilde{\Pi}_{SD}(\epsilon)] - [\epsilon\tilde{\eta}_S(\epsilon) - P_S^{\text{th}}][\epsilon\tilde{\Pi}_{DD}(\epsilon) + \epsilon\tau_D] \\
=&[\eta_D^{\text{th}} - P_D^{\text{th}}]\eta_S^{\text{th}} - [\eta_S^{\text{th}} - P_S^{\text{th}}]\eta_D^{\text{th}} \\
=&\eta_D^{\text{th}} P_S^{\text{th}} - \eta_S^{\text{th}} P_D^{\text{th}}
\end{aligned} \tag{2.114}$$

In the denominator we have

$$\begin{aligned}
&\lim_{\epsilon\to 0}\epsilon[\tilde{\Pi}_{DD}(\epsilon)+\tau_D][\tilde{\Pi}_{SS}(\epsilon)+\tau_S]-\epsilon\tilde{\Pi}_{SD}(\epsilon)\tilde{\Pi}_{DS}(\epsilon)\\
=&\lim_{\epsilon\to 0}\epsilon\tilde{\Pi}_{DD}(\epsilon)\tilde{\Pi}_{SS}(\epsilon)-\epsilon\tilde{\Pi}_{SD}(\epsilon)\tilde{\Pi}_{DS}(\epsilon)+\epsilon\tau_D\tilde{\Pi}_{SS}(\epsilon)+\epsilon\tau_S\tilde{\Pi}_{DD}(\epsilon)+\epsilon\tau_D\tau_S\\
=&\lim_{\epsilon\to 0}\epsilon\tilde{\Pi}_{DD}(\epsilon)\tilde{\Pi}_{SS}(\epsilon)-\epsilon\tilde{\Pi}_{SD}(\epsilon)\tilde{\Pi}_{DS}(\epsilon)+\tau_D\eta_S^{\rm th}+\tau_S\eta_D^{\rm th}. \qquad (2.115)
\end{aligned}$$

We must proceed with care here since the Laplace transformed propagators have poles at the origin in the complex ϵ plane, as a consequence of probability conservation in the isolated conductor. However, due to the preceding argument, we know that the residue of $\tilde{\Pi}_{mn}$ at zero is just the thermal value $\eta_m^{\rm th}$. Thus writing $\tilde{\Pi}_{DD}$ as

$$\tilde{\Pi}_{DD}(\epsilon)=[\tilde{\Pi}_{DD}(\epsilon)-\eta_D^{\rm th}/\epsilon]+\eta_D^{\rm th}/\epsilon \qquad (2.116)$$

and similarly for $\tilde{\Pi}_{SS}$, gives

$$\begin{aligned}
\epsilon\tilde{\Pi}_{DD}(\epsilon)\tilde{\Pi}_{SS}(\epsilon)=&\,\epsilon[\tilde{\Pi}_{DD}(\epsilon)-\eta_D^{\rm th}/\epsilon][\tilde{\Pi}_{SS}(\epsilon)-\eta_S^{\rm th}/\epsilon]+\eta_D^{\rm th}[\tilde{\Pi}_{SS}(\epsilon)-\eta_S^{\rm th}/\epsilon]\\
&+\eta_S^{\rm th}[\tilde{\Pi}_{DD}(\epsilon)-\eta_D^{\rm th}/\epsilon]+\eta_D^{\rm th}\eta_S^{\rm th}/\epsilon. \qquad (2.117)
\end{aligned}$$

Similarly, we have also

$$\begin{aligned}
\epsilon\tilde{\Pi}_{DS}(\epsilon)\tilde{\Pi}_{SD}(\epsilon)=&\,\epsilon[\tilde{\Pi}_{DS}(\epsilon)-\eta_D^{\rm th}/\epsilon][\tilde{\Pi}_{SD}(\epsilon)-\eta_S^{\rm th}/\epsilon]+\eta_D^{\rm th}[\tilde{\Pi}_{SD}(\epsilon)-\eta_S^{\rm th}/\epsilon]\\
&+\eta_S^{\rm th}[\tilde{\Pi}_{DS}(\epsilon)-\eta_D^{\rm th}/\epsilon]+\eta_D^{\rm th}\eta_S^{\rm th}/\epsilon. \qquad (2.118)
\end{aligned}$$

Subtracting the two yields

$$\begin{aligned}
\epsilon\tilde{\Pi}_{DD}(\epsilon)\tilde{\Pi}_{SS}(\epsilon)-\epsilon\tilde{\Pi}_{DS}(\epsilon)\tilde{\Pi}_{SD}(\epsilon)=&\,\epsilon[\tilde{\Pi}_{DD}(\epsilon)-\eta_D^{\rm th}/\epsilon][\tilde{\Pi}_{SS}(\epsilon)-\eta_S^{\rm th}/\epsilon]\\
&-\epsilon[\tilde{\Pi}_{DS}(\epsilon)-\eta_D^{\rm th}/\epsilon][\tilde{\Pi}_{SD}(\epsilon)-\eta_S^{\rm th}/\epsilon]+\eta_D^{\rm th}[\tilde{\Pi}_{SS}(\epsilon)-\tilde{\Pi}_{SD}(\epsilon)]\\
&+\eta_S^{\rm th}[\tilde{\Pi}_{DD}(\epsilon)-\tilde{\Pi}_{DS}(\epsilon)]. \qquad (2.119)
\end{aligned}$$

The limit $\epsilon\to 0$ may now be taken. The first term (and similarly the second term) on the right hand side vanishes in the limit since neither $\tilde{\Pi}_{DD}(\epsilon)-\eta_D^{\rm th}/\epsilon$ nor $\tilde{\Pi}_{DD}(\epsilon)-\eta_D^{\rm th}/\epsilon$ have poles at zero (we have subtracted them out). The third and fourth terms may appear infinite since the $\tilde{\Pi}$'s have poles at zero; however, $\tilde{\Pi}_{SS}$ and $\tilde{\Pi}_{SD}$ have the same

residue at zero ($\eta_S^{\rm th}$), thus the difference is finite in the limit. Similarly, the fourth term also remains finite, and we have

$$\lim_{\epsilon\to 0}\epsilon[\tilde{\Pi}_{DD}(\epsilon)+\tau_D][\tilde{\Pi}_{SS}(\epsilon)+\tau_S]-\epsilon\tilde{\Pi}_{SD}(\epsilon)\tilde{\Pi}_{DS}(\epsilon)$$
$$=\eta_D^{\rm th}[\tilde{\Pi}_{SS}(0)-\tilde{\Pi}_{SD}(0)+\tau_S]+\eta_S^{\rm th}[\tilde{\Pi}_{DD}(0)-\tilde{\Pi}_{DS}(0)+\tau_D]. \tag{2.120}$$

Finally, we have for the steady state rate

$$R_S(\infty)=\frac{\eta_D^{\rm th}P_S^{\rm th}-\eta_S^{\rm th}P_D^{\rm th}}{\eta_D^{\rm th}[\tilde{\Pi}_{SS}(0)-\tilde{\Pi}_{SD}(0)+\tau_S]+\eta_S^{\rm th}[\tilde{\Pi}_{DD}(0)-\tilde{\Pi}_{DS}(0)+\tau_D]}. \tag{2.121}$$

A similar calculation for R_D shows that indeed in the steady state $R_D = R_S$, as expected. The differences of propagators in the denominator may also be rewritten in terms of time integrals using the fact that from the definition of the Laplace transform

$$\tilde{f}(0)=\int_0^\infty f(t)dt. \tag{2.122}$$

The result (2.121) differs slightly from the result obtained by Kenkre, Biscarini, and Bustamante in ref. [41] due to the face that here it was not assumed that $R_S(t) = R_D(t)$ for all times. In situations where the source and drain are coupled not to a single state each, but to multiple states, Kenkre, Biscarini, and Bustamante also obtain approximate expressions in terms of averages of probability propagators. Details may be found in ref. [41].

Although this approach may be used for incoherent or partially coherent motion, we found that it does not reproduce the Landauer result in the fully coherent limit. The reason appears to be the fact that level broadening of the conductor states due to the coupling to the contacts has not been included in the STM theory. Such a possibility is pointed out in ref. [53]. We follow closely that argument in the following.

Consider a conductor which consists only of a single state with energy $\mathcal{E}_0$. This single state is connected to both the source and drain reservoirs. The Master equation for the evolution of the probability P to find an electron in the conductor is then

$$\frac{dP}{dt}=\frac{P_S^{\rm th}-P}{\tau}+\frac{P_D^{\rm th}-P}{\tau} \tag{2.123}$$

where for simplicity, the time constants have been set equal, $\tau_S = \tau_D = \tau$. In the steady state, the probability to find an electron in the conductor is simply the average of the source and drain thermal probabilities,

$$P = \frac{P_S^{\rm th} + P_D^{\rm th}}{2}, \tag{2.124}$$

and the rate at which probability flows out of (and into) the conductor is

$$R_D = R_S = \frac{P_S^{\rm th} - P_D^{\rm th}}{2\tau}. \tag{2.125}$$

From this expression, is appears that an arbitrarily large amount of current could be passed through the device; however, we have seen earlier that there is a maximum amount of current that may be passed through a 1D conductor, $I_{\rm max} = VG_0$.

To see how level broadening can decrease the amount of current that can be passed through the device, consider the zero temperature limit. In this case $P_S^{\rm th}$ is zero if the energy of the conductor state $\mathcal{E}_0$ is above the source chemical potential μ_S and one if $\mathcal{E}_0$ is below μ_S. Similarly $P_D^{\rm th}$ is zero for $\mathcal{E}_0 > \mu_D$ and one if $\mathcal{E}_0 < \mu_D$. Thus if $\mathcal{E}_0$ is below both the source and drain chemical potentials, both reservoirs try to inject electrons into the conductor, and no net current flows. Similarly, if $\mathcal{E}_0$ is larger than both source and drain potentials, then no current flows since neither reservoir has electrons with high enough energies to enter into the conductor.

Is is only when the energy of the conductor state is *between* source and drain potentials, $\mu_D < \mathcal{E}_0 < \mu_S$, that net current flows. However, the stronger the conductor is coupled to the contacts, the broader its energy level becomes, part of which leaks out from between μ_D and μ_S, thus decreasing the amount of current that flows.

This problem also arises in other coherent conductors (this is discussed briefly for a two site conductor in ref. [39]) where the current is proportional to $1/\tau$. Although broadening effects can be incorporated into the one level conductor, it remains unclear, at least to us at the moment, how they can be included in a Master equation approach with many sites or energy levels. This remains an issue in the STM formalism for perfectly coherent motion; however, in the presence of sufficiently strong

scattering or phase breaking processes, the contribution to the resistance due to the coupling to the contacts is typically small and the formulae would become valid.

2.4.2 Generalized Master Equation for Modeling Partially Coherent Motion

We will now discuss briefly how a generalized Master equation can be used to model coherent and partially coherent motion following the analyses of Kenkre [68, 71, 72]. We will begin with a discussion of stochastic Liouville equations (SLEs) and show [73] how they can be converted into generalized Master equations via a projection technique.

As discussed earlier, the state of a quantum system is described by the density matrix ρ, which obeys the quantum version of the Liouville equation, the von Neumann equation,

$$i\hbar\frac{\partial\rho}{\partial t} = [H, \rho]. \tag{2.126}$$

The diagonal elements $\rho_{mm} \equiv \langle m|\rho|m\rangle$ represent the probabilities to find the system in a state $|m\rangle$. The off diagonal elements of the density matrix ρ_{mn} arise when the system is in a quantum superposition of states and are related to the relative phases. To illustrate this, consider a two state system consisting of states $|1\rangle$ and $|2\rangle$.

If an ensemble is prepared in such a way that each member has statistical probability 1/2 to be in state $|1\rangle$ and probability 1/2 to be in state $|2\rangle$, then the density matrix is

$$\rho = \frac{1}{2}|1\rangle\langle 1| + \frac{1}{2}|2\rangle\langle 2| \tag{2.127}$$

If however, the ensemble is prepared so that each member has probability one to be in a quantum superposition of states $|1\rangle$ and $|2\rangle$ given by

$$|+\rangle = \frac{|1\rangle + |2\rangle}{\sqrt{2}}, \tag{2.128}$$

then the resulting density matrix is

$$\rho = \frac{1}{2}|1\rangle\langle 1| + \frac{1}{2}|1\rangle\langle 2| + \frac{1}{2}|2\rangle\langle 1| + \frac{1}{2}|2\rangle\langle 2|. \tag{2.129}$$

The diagonal elements are the same, so an observer measuring in the $|1\rangle, |2\rangle$ basis measures $|1\rangle$ with probability 1/2 and $|2\rangle$ with probability 1/2. The difference here is that an observer measuring $|+\rangle$ will find it with probability 1 in this case, but only with probability 1/2 in the previous case.

When the system is put in interaction with a bath or incoherent scattering is introduced, we should expect the system to evolve toward a classical statistical mixture of states in which the density matrix is diagonal in the energy basis. Thus, one may approximate the interaction with a reservoir in a simple way by adding to the von Neumann equation a term which causes the off diagonal elements of the density matrix to decay, such as [68]

$$i\hbar\frac{\partial \rho_{mn}}{\partial t} = [H, \rho]_{mn} - i\hbar\alpha(1 - \delta_{mn})\rho_{mn} \tag{2.130}$$

with α being a constant representing the strength of the incoherence, $\alpha = 0$ meaning that the motion is perfectly coherent and $\alpha \to \infty$ meaning totally incoherent, or classical motion. This is the simplest form of the stochastic Liouville equation. Although strictly speaking the off diagonal elements should only vanish in the energy representation, this simple approach may be used approximately in other representations such as when the $|m\rangle$s are tight binding states. More sophisticated SLEs exist, and may be found in the literature (see for example [68–70, 74, 75] and references therein).

We have seen how an SLE may be used to introduce incoherent scattering effects in a simple phenomenological way. Now let us look at how we can pass [73] from an SLE to a generalized Master equation to be used in the STM formalism described above, following the projection approach as described by Zwanzig and Nakajima [76–78]. First, define a Liouville superoperator $\mathcal{L}$ and write the evolution of the density matrix as

$$\frac{\partial \rho}{\partial t} = -i\mathcal{L}\rho \tag{2.131}$$

where the action of L on an operator is defined according to the von Neumann equation or SLE equation being used. For the simple SLE (2.130), $\mathcal{L}$ on an operator f is

$$(\mathcal{L}f)_{mn} = (\mathcal{L}_0 f)_{mn} + (\mathcal{L}_\alpha f)_{mn} = \frac{1}{\hbar}[H, f]_{mn} - i\alpha(1 - \delta_{mn})f_{mn} \tag{2.132}$$

where $\mathcal{L}_0$ and $\mathcal{L}_\alpha$ are superoperators which produce respectively the commutator and the off-diagonal part,

$$(\mathcal{L}_0 f)_{mn} \equiv \frac{1}{h}[H, f]_{mn}, \tag{2.133}$$

$$(\mathcal{L}_\alpha f)_{mn} \equiv -i\alpha(1 - \delta_{mn}). \tag{2.134}$$

Next, define a time independent, idempotent ($\mathcal{P}^2 = 1$) projection superoperator $\mathcal{P}$. Since we are interested in the evolution of the probabilities $P_m = \rho_{mm}$ (in a particular representation), an appropriate choice is a $\mathcal{P}$ which when acted on the density matrix projects away the off diagonal elements,

$$(\mathcal{P}\rho)_{mn} = \delta_{mn}\rho_{mn}. \tag{2.135}$$

We would like write an evolution equation for the projected part of the density matrix alone, $\mathcal{P}\rho$. To this end, we formally solve for the evolution of the remaining part, $(1 - \mathcal{P})\rho$. Applying $\mathcal{P}$ and $(1 - \mathcal{P})$ to (2.131) and writing $\rho = \mathcal{P}\rho + (1 - \mathcal{P})\rho$ gives

$$\frac{\partial}{\partial t}\mathcal{P}\rho = -i\mathcal{P}\mathcal{L}\mathcal{P}\rho - i\mathcal{P}\mathcal{L}(1 - \mathcal{P})\rho, \tag{2.136}$$

$$\frac{\partial}{\partial t}(1 - \mathcal{P})\rho = -i(1 - \mathcal{P})\mathcal{L}\mathcal{P}\rho - i(1 - \mathcal{P})\mathcal{L}(1 - \mathcal{P})\rho. \tag{2.137}$$

Solving the second equation formally for $(1 - \mathcal{P})\rho$, treating $\mathcal{P}\rho$ as an independent quantity gives

$$(1 - \mathcal{P})\rho(t) = e^{-i(1-\mathcal{P})\mathcal{L}t}(1 - \mathcal{P})\rho(0) - i\int_0^t e^{-i(1-\mathcal{P})\mathcal{L}(t-t')}(1 - \mathcal{P})\mathcal{L}\mathcal{P}\rho(t')dt'. \tag{2.138}$$

Inserting this into the first equation now gives an equation which depends on the projected part $\mathcal{P}\rho$ and only the initial condition of the non-projected part $(1-\mathcal{P})\rho(0)$,

$$\frac{\partial}{\partial t}\mathcal{P}\rho = -i\mathcal{P}\mathcal{L}\mathcal{P}\rho - \mathcal{P}\mathcal{L}\int_0^t e^{-i(1-\mathcal{P})\mathcal{L}(t-t')}(1-\mathcal{P})\mathcal{L}\mathcal{P}\rho(t')dt' + \mathcal{I}(t) \tag{2.139}$$

with the initial condition term given by

$$\mathcal{I}(t) \equiv -i\mathcal{P}\mathcal{L}(1-\mathcal{P})e^{-i(1-\mathcal{P})\mathcal{L}t}(1-\mathcal{P})\rho(0). \tag{2.140}$$

If the initial condition term vanishes or can otherwise be neglected, we have successfully obtained a closed generalized Master equation for the probabilities, as we set out to do. The generalized Master equation can be written in gain-loss form as

$$\frac{d}{dt}P_m(t) = \sum_n \int_0^t [\mathcal{W}_{mn}(t-t')P_n(t') - \mathcal{W}_{nm}(t-t')P_m(t')]dt' \tag{2.141}$$

where P_m is the probability to be in state m and the quantities $\mathcal{W}_{mn}(t-t')$ are known as the memories or memory functions since they connect the evolution of the system at time t with the state of the system at earlier times.

For the Liouville superoperator in equation (2.132), $\mathcal{L} = \mathcal{L}_0 + \mathcal{L}_\alpha$, Kenkre showed in ref. [73] that the total memory is simply the coherent memory function multiplied by a factor $e^{-\alpha t}$, i.e.

$$\mathcal{W}_{mn}(t) = e^{-\alpha t}\mathcal{W}^0_{mn}(t) \tag{2.142}$$

where $\mathcal{W}^0$ is the memory obtained from the coherent part $\mathcal{L}_0$ alone.

2.5 Lyo and Huang Boltzmann Equation Solution

Although the semi-classical distribution function does not contain information about the full quantum state of the system, a Boltzmann equation approach can may be useful to help understand the effects of scattering in quantum devices. In particular, Lyo and Huang have applied a Boltzmann equation approach to study the effects of

different kinds of scattering in quantum wires [44–47]. Their approach, as described in more detail in [44] and [45] is to begin with a Boltzmann equation,

$$v_j + \frac{2\pi}{\hbar}\sum_{j'}|V_{j,j'}|^2(g_{j'} - g_j)\delta(\mathcal{E}_j - \mathcal{E}'_j) + P_j + Q_j = 0. \tag{2.143}$$

Here j is used to represent a set of quantum numbers. For instance, in the two-dimensional conductor an appropriate set of quantum numbers is the sub-band index n and the wave number in the direction of current flow, k_x. v_j represents the group velocity in the direction of current flow,

$$v_j = \frac{1}{\hbar}\frac{\partial \mathcal{E}_j}{\partial k}. \tag{2.144}$$

The quantities $V_{j,j'}$ represent matrix elements of the elastic scattering matrix. g_j is the non-equilibrium component of the distribution function, defined implicitly through

$$f_j = f_0(\mathcal{E}_j) + g_j[-f'_0(\mathcal{E}_j)]qE, \tag{2.145}$$

f_0 being the equilibrium distribution function. Additional terms may be added for electron-electron scattering and electron-phonon scattering. Implicit in writing this equation are the assumptions firstly that a Boltzmann equation is valid (i.e. that the off diagonal elements of the density matrix decay quickly) and secondly that the scattering is small so that Fermi Golden Rule transition rates may be used. A careful analysis of the particular system under consideration should be performed to determine the validity of these assumptions.

Lyo and Huang write the conductance in terms of the distribution function g,

$$G = \frac{2q^2}{hL}\int_0^\infty d\mathcal{E}[-f'_0(\mathcal{E})]\sum_\nu s_\nu g_\nu. \tag{2.146}$$

Here ν are the quantum numbers for which $\mathcal{E}_\nu = E$, and s_ν represents the sign of the velocity for a state with quantum numbers ν. Lyo and Huang refer to these points as "Fermi points".

Next, they formally solve the Boltzmann equation (2.143) and write

$$G = -\frac{2q^2}{hL}\int_0^\infty d\mathcal{E}[-f'_0(\mathcal{E})]\mathbf{s}^\dagger\mathbf{u}^{-1}\mathbf{s} \tag{2.147}$$

where $\mathbf{s}$ is a column vector whose elements s_ν give the sign of the velocity for a state with quantum numbers ν and $\mathbf{u}$ is defined from the scattering matrix elements by

$$u_{\nu,\nu'} \equiv \begin{cases} \frac{L}{\hbar^2}\frac{|V_{\nu,\nu'}|^2}{|v_\nu v_{\nu'}|} & \text{if } \nu \neq \nu' \\ -\sum_{\nu' \neq \nu} u_{\nu,\nu'} & \text{otherwise} \end{cases}. \tag{2.148}$$

One row and column are deleted from $\mathbf{u}$ to make the matrix nonsingular, but it is shown that the result does not depend on the removed part.

Lyo and Huang are then able to calculate the elements of the matrix $\mathbf{u}$ to study how different types of scattering affect the conductance. One interesting result in particular they have predicted in [44] is the behavior conductance as the strength of an applied magnetic field is strikingly different when scattering is present than when the motion is ballistic.

2.6 Remarks

In this chapter several formalisms of quantum transport have been reviewed, each with advantages and disadvantages, summarized here.

The Landauer-Büttiker theory is popular in the literature for analyzing quantum transport, but incoherent scattering is introduced only phenomenologically. The NEGF formalism is valid even for strong bias and incoherent scattering effects may be modeled from microscopic considerations, but it typically requires iterative numerical solution.

Wigner functions are desirable because of their similarity to classical distribution functions, but difficulties can arise when attempting to determine the correct boundary conditions in nontrivial systems. Furthermore, they obey an equation of motion which is nonlocal in momentum space which may be difficult to solve for certain potentials.

The STM theory of Kenkre, Biscarini, and Bustamante provides a simple way to study motion of any degree of coherence, but needs to be extended to include broadening effects before it can be connected to the Landauer theory when the motion is fully coherent.

The approach by Lyo and Huang using a Boltzmann equation, but the procedure of calculating the scattering matrix and its inverse can be computationally difficult. Furthermore, a careful analysis should be made to examine the validity of the approximations made.

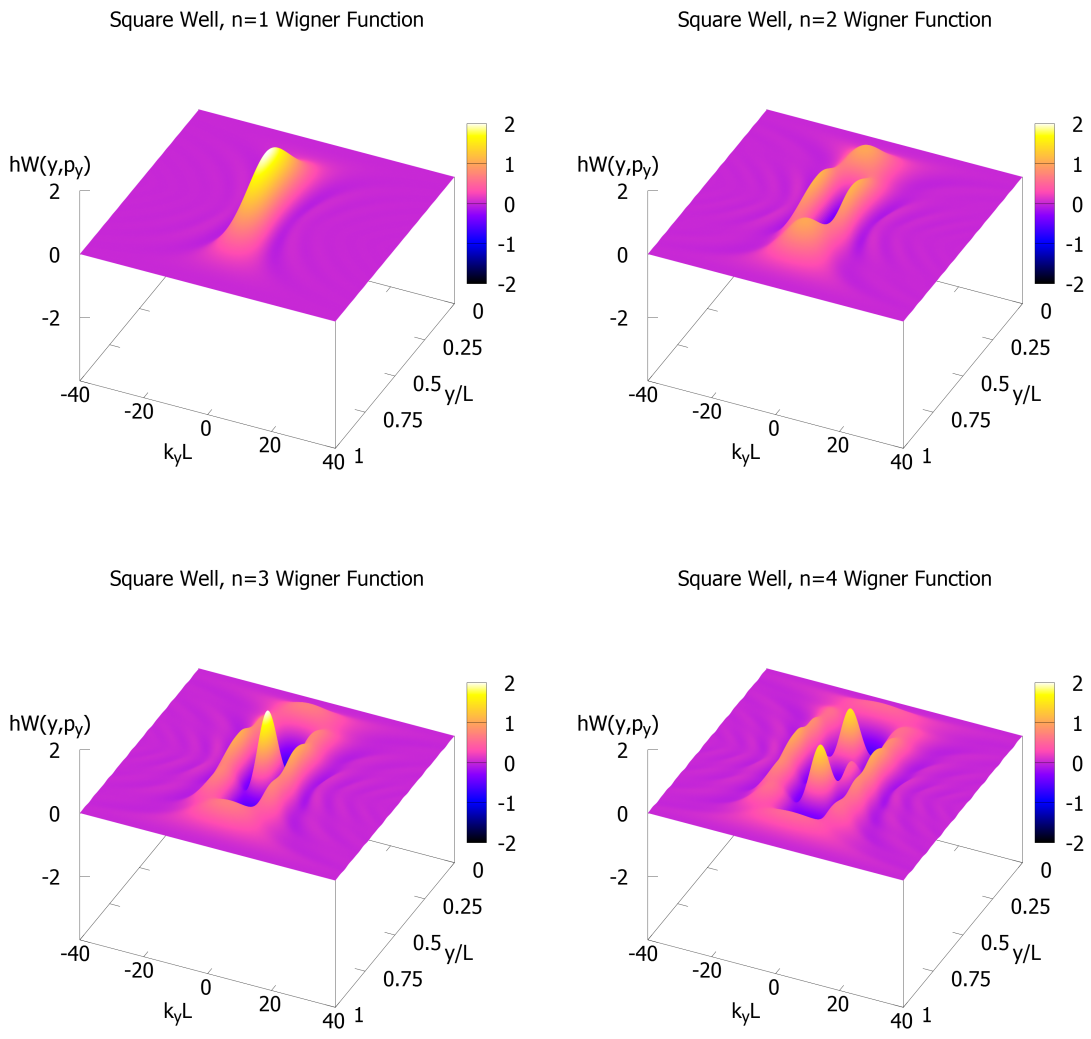

Figure 2.3: Wigner Functions for the first four eigenstates of the infinite square well.

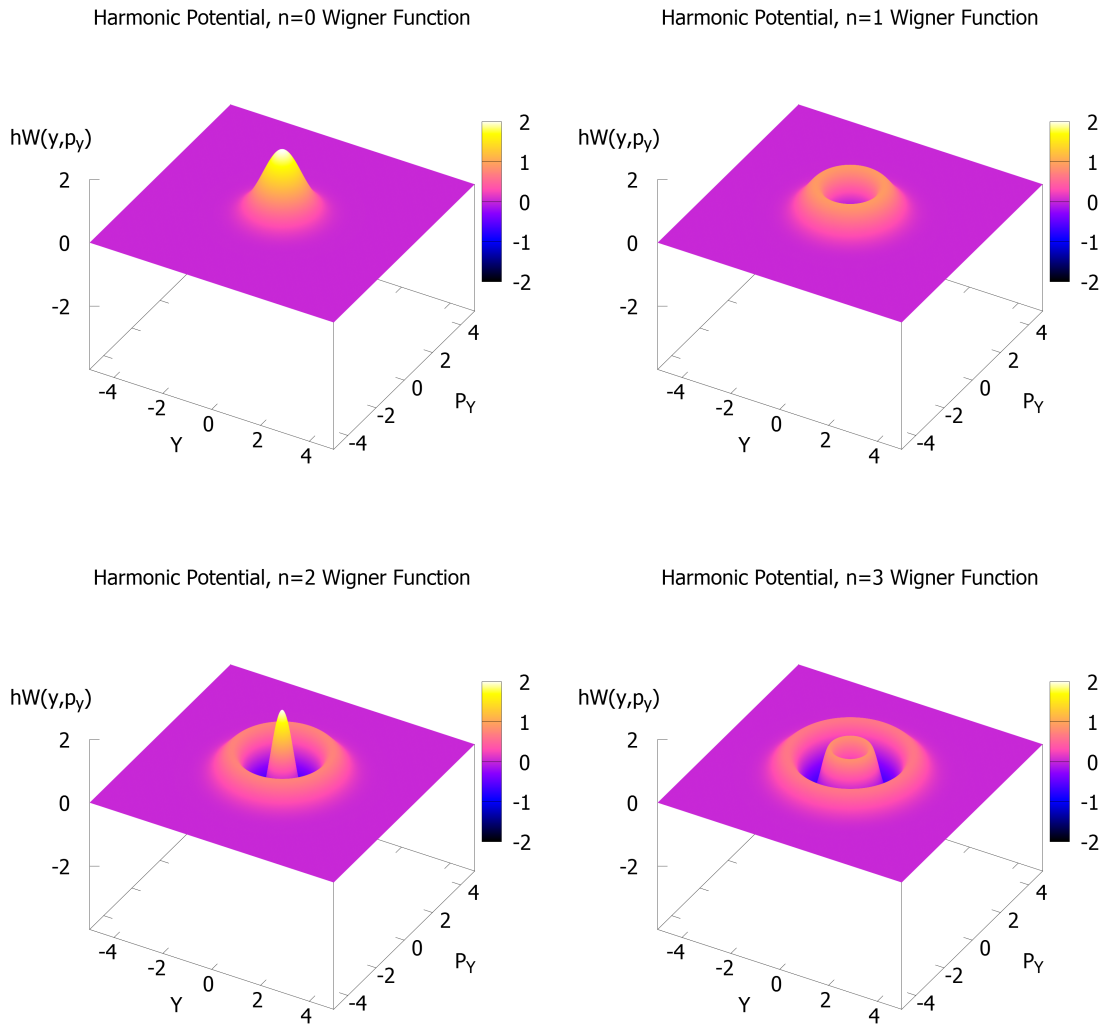

Figure 2.4: Wigner Functions for the first four eigenstates of the harmonic oscillator potential. The lower axes are the dimensionless quantities $Y \equiv \sqrt{\frac{m^*\omega}{\hbar}}x$ and $P_Y \equiv \sqrt{\frac{1}{m^*\hbar\omega}}p_y$.

Chapter 3

Application of the Transmission Formalism to Simple 1D Conductors

3.1 Introduction

In Chapter 2, it was shown that the conductance of an elastic scatterer is related to the transmission function $T(E)$ through the scatterer. In this chapter, the transmission function through several different kinds of conductors will be calculated. Two methods will be used for calculating the transmission function. Firstly, the "textbook" method of taking an incoming and reflected wave in one lead and a transmitted wave in the other and calculating the amplitudes by ensuring that the Schrödinger equation is everywhere satisfied will be applied (see ref. [54] for example). Secondly, the relation between Green's function and transmission function,

$$T(E) = \mathrm{Tr}\{\Gamma_S G \Gamma_D G^\dagger\} \tag{3.1}$$

will be used.

The first system to be considered is a conductor consisting of a single site. It will be coupled to two semi-infinite 1D ballistic tight binding leads which are in contact with reservoirs held at different electrochemical potentials. Although the result is well known in the literature, the transmission function $T(E)$ will be derived again here for purposes of comparison with more complicated systems and to demonstrate both methods of calculating the transmission function.

Next to be considered is a two-level system where both states are connected to both leads and there is no interaction between the two conductor states. It will be shown that when the two-levels are degenerate, the result is related to to the one-level conductor with a stronger coupling to the leads. The result is then extended to N degenerate levels, with each connected to both leads, and it is shown again that the result is related to the one-level result.

Another two-level system of a different configuration will then be analyzed. Only one of the two states is connected to the leads, but an interaction between the two conductor states is added.

Finally, a one-level system in interaction with a harmonic oscillator is examined. This could be looked at as a simplified model of electron-phonon interaction.

3.2 Single-Site Conductor

First, consider a conductor which consists only of a single lattice site. This problem has already been examined in the literature, see for example [79] or section 9.5 in [53].

The conductor will be coupled to two semi-infinite 1D tight binding chains, representing the leads. Let V be the magnitude of the matrix element connecting adjacent sites within the leads, and let the matrix element coupling the reservoirs to the conductor be ηV. Let the site energies of all the sites in the contacts to be zero and the

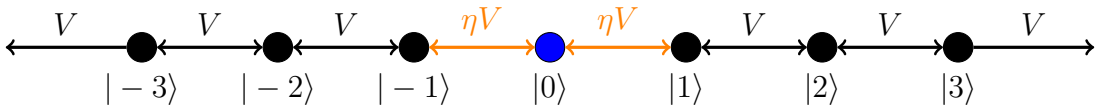

Figure 3.1: A conductor consisting of a single site (blue) connected to two semi-infinite tight binding leads (black). The strength of the coupling from the conductor to the leads ηV (orange) is allowed to differ from the intersite coupling within the leads V.

site energy of the conductor to be $\mathcal{E}_0$. The situation is illustrated in Figure (3.1).

Suppose that the tight binding states are labeled as $|m\rangle$ with m being the integer index of the site that the state is centered on. The conductor site will be labeled as $m = 0$, thus all sites with $m < 0$ belong to the left (source) lead, and all sites $m > 0$ belong to the right (drain) lead. The Hamiltonian for the total system can be decomposed as follows,

$$H = H_c + H_S + H_D + \tau_S + \tau_S^\dagger + \tau_D + \tau_D^\dagger. \tag{3.2}$$

Here H_c is the Hamiltonian for the isolated conductor,

$$H_c = \mathcal{E}_0 |0\rangle\langle 0|, \tag{3.3}$$

H_S and H_D are the Hamiltonians for the isolated left and right leads,

$$H_S = V \sum_{m<-1} [|m\rangle\langle m+1| + |m+1\rangle\langle m|], \tag{3.4}$$

$$H_D = V \sum_{m>1} [|m\rangle\langle m+1| + |m+1\rangle\langle m|], \tag{3.5}$$

and τ_S and τ_D are the couplings from conductor to the left and right leads,

$$\tau_S = \eta V |0\rangle\langle -1|, \tag{3.6}$$

$$\tau_D = \eta V |0\rangle\langle +1|. \tag{3.7}$$

3.2.1 Textbook Calculation of the Transmission Function

First, the transmission function $T(E)$ will be calculated in the traditional textbook way, by looking for eigenstates $|\psi^k\rangle$ of the total Hamiltonian H with wavenumber k which consist of an incoming and reflected wave to the left of the conductor and a transmitted wave to the right of the conductor. Defining ψ^k_m as the projection of $|\psi^k\rangle$ onto the state $|m\rangle$,

$$\psi^k_m \equiv \langle m|\psi^k\rangle, \tag{3.8}$$

to the left of the conductor, for $m < 0$, ψ^k_m is

$$\psi^k_m = e^{ikm} + re^{-ikm} \tag{3.9}$$

where r is the amplitude of the reflected wave, and to the right of the conductor ($m > 0$) is it

$$\psi^k_m = te^{-ikm} \tag{3.10}$$

with t being the amplitude of the transmitted wave. Away from the conductor, this is an eigenstate of the Hamiltonian with eigenvalue

$$E^k = 2V\cos k. \tag{3.11}$$

The values of the reflection and transmission amplitudes r and t as well as the wavefunction inside the conductor $\psi^k_0 = \langle 0|\psi^k\rangle$ which ensure that the Schrödinger equation is satisfied everywhere must now be determined.

The Schrödinger equation for the conductor and the two adjacent sites is

$$E^k\psi^k_{-1} = V\psi^k_{-2} + \eta V\psi^k_0, \tag{3.12}$$

$$E^k\psi^k_0 = \mathcal{E}_0\psi^k_0 + \eta V\psi^k_{-1} + \eta V\psi^k_1, \tag{3.13}$$

$$E^k\psi^k_1 = \eta V\psi^k_0 + V\psi^k_2. \tag{3.14}$$

Using equations (3.9) and (3.10) for ψ_m^k for the sites in the left and right leads, these three equations become

$$E^k(e^{-ik} + re^{ik}) = V(e^{-2ik} + re^{2ik}) + \eta V\psi_0^k, \tag{3.15}$$

$$E^k\psi_0^k = \mathcal{E}_0\psi_0^k + \eta V(e^{-ik} + re^{ik}) + \eta Vte^{ik}, \tag{3.16}$$

$$E^kte^{ik} = \eta V\psi_0^k + Vte^{2ik}. \tag{3.17}$$

The three unknowns (ψ_0^k, r, and t) must now be found which satisfy these three equations. Rearranging,

$$\eta V\psi_0^k = E^ke^{-ik} - Ve^{-2ik} + r(E^ke^{ik} - Ve^{2ik}), \tag{3.18}$$

$$(E^k - \mathcal{E}_0)\psi_0^k = \eta V(e^{-ik} + re^{ik}) + \eta Vte^{ik}, \tag{3.19}$$

$$\eta V\psi_0^k = t(E^ke^{ik} - Ve^{2ik}). \tag{3.20}$$

Combining the first and third equations, and solving for t,

$$t = r + \frac{E^ke^{-ik} - Ve^{-2ik}}{E^ke^{ik} - Ve^{2ik}} = r + 1 \tag{3.21}$$

where the second equality follows since $E^k = 2V\cos k$. Now using the second equation and eliminating r,

$$(E^k - \mathcal{E}_0)\psi_0 = \eta V[e^{-ik} + (t-1)e^{ik}] + \eta Vte^{ik} = -2i\eta V\sin k + 2t\eta Ve^{ik}. \tag{3.22}$$

Using again the third equation to eliminate ψ_0^k and solving for t finally gives

$$t = \frac{-2i\eta^2V^2\sin k}{(E^k - \mathcal{E}_0) - 2\eta^2Ve^{ik}}. \tag{3.23}$$

The transmission function is then

$$T(E^k) = |t|^2 = \frac{[2\eta^2V\sin k]^2}{[E^k - \mathcal{E}_0 - 2\eta^2V\cos k]^2 + [2\eta^2V\sin k]^2}. \tag{3.24}$$

The carrier velocity is given by [31]

$$v(E) = \frac{1}{\hbar}\frac{dE}{dk} = -2V\sin k \tag{3.25}$$

so the transmission function can now be written

$$T(E) = \frac{\eta^4[\hbar v(E)]^2}{[E(1-\eta^2) - \mathcal{E}_0]^2 + \eta^4[\hbar v(E)]^2}. \tag{3.26}$$

where $E^k = 2V\cos k$ has been used to completely eliminate k. The squared velocity as a function of energy is

$$[\hbar v(E)]^2 = 4V^2 \sin^2 k = 4V^2 - E^2. \tag{3.27}$$

3.2.2 Transmission from the Green's Function

Before the properties of (3.26) are examined further, the transmission function will now be obtained from the Green's function using equation (2.43),

$$T(E) = \mathrm{Tr}\{\Gamma_S G \Gamma_D G^\dagger\} \tag{3.28}$$

to illustrate the equivalence to the preceding method.

The first step in this process is to calculate the self energies which result from the coupling to the leads. The self energy for the source lead is

$$\Sigma_S = \tau_S G_S \tau_S^\dagger \tag{3.29}$$

where τ_S is the coupling between lead and channel and G_S is the (retarded) Green's function for the *isolated* lead,

$$G_S = [(E + i\eta)I - H_S]^{-1}.$$

The self energy is a matrix, but for this single-site system is is only a 1x1 matrix,

$$\Sigma_S(E) = \eta^2 V^2(\langle -1|G_S(E)|-1\rangle)|0\rangle\langle 0| \tag{3.30}$$

Since the coupling τ_S couples only the end of the reservoir chain to the conductor, only the self propagator for the site at the end of the chain, $\langle -1|G_S(E)|-1\rangle$ is needed.

This may be obtained easily from the Green's function for an infinite 1D tight binding chain by applying the method of images.

From Chapter 5 in ref. [56], the (retarded) Green's function for the 1D tight binding chain for E coinciding with the spectrum ($E < 2V$) is

$$G_0(l, m; E) = \frac{-i}{2V\sqrt{1-x^2}} \left(-x + i\sqrt{1-x^2}\right)^{|l-m|} \tag{3.31}$$

where

$$x \equiv \frac{E}{2V}. \tag{3.32}$$

Using the method of images, the self propagator for the site at the end of the chain is

$$\begin{aligned} \langle -1|G_S(E)|-1\rangle &= G_0(-1,-1;E) + G_0(-1,+1;E) \\ &= \frac{-i}{2V\sqrt{1-x^2}} \left[1 - \left(-x + i\sqrt{1-x^2}\right)^2\right] \\ &= \frac{-i}{2V\sqrt{1-x^2}} 2\left[(1-x^2) + ix\sqrt{1-x^2}\right]. \end{aligned} \tag{3.33}$$

Define ϕ between π and $+\pi$ so that

$$\cos\phi = x, \tag{3.34}$$

then this can be written more compactly as

$$\begin{aligned} \langle -1|G_S(E)|-1\rangle &= \frac{1}{V}\left[x - i\frac{1-x^2}{\sqrt{1-x^2}}\right] \\ &= \frac{1}{V}\left[\cos\phi - i\frac{\sin^2\phi}{\sqrt{\sin^2\phi}}\right] \\ &= \frac{1}{V} e^{-i|\phi|}. \end{aligned} \tag{3.35}$$

The self energy is finally

$$\Sigma_S(E) = \eta^2 V e^{-i|\phi|}. \tag{3.36}$$

A similar calculation for the drain lead shows that $\Sigma_D(E) = \Sigma_S(E) = \eta^2 V e^{-i|\phi|}$.

The matrices Γ_S and Γ_D may now be calculated. They are

$$\Gamma_S = \Gamma_D = i[\Sigma_D - \Sigma_D^\dagger] = 2\eta^2 V \sin|\phi|. \tag{3.37}$$

The next step is to write the Green's function for the channel subsystem. Since the conductor only consists of a single site this is easily done as it is only a 1x1 matrix:

$$\begin{aligned} G(E) &= [E - H - \Sigma_S - \Sigma_D]^{-1} \\ &= \frac{|0\rangle\langle 0|}{E - \mathcal{E}_0 - 2\eta^2 V e^{-i|\phi|}}. \end{aligned} \tag{3.38}$$

The energy dependent transmission function through the conductor is then

$$\begin{aligned} T(E) &= \mathrm{Tr}\{\Gamma_S G \Gamma_D G^\dagger\} \\ &= \frac{[2\eta^2 V \sin|\phi|]^2}{[E - \mathcal{E}_0 - 2\eta^2 V e^{-i|\phi|}][E - \mathcal{E}_0 - 2\eta^2 V e^{+i|\phi|}]} \\ &= \frac{[2\eta^2 V \sin|\phi|]^2}{[E - \mathcal{E}_0 - 2\eta^2 V \cos\phi]^2 + [2\eta^2 V \sin|\phi|]^2}. \end{aligned} \tag{3.39}$$

Using $2V\cos\phi = E$ and $\hbar v(E) = \frac{\partial E}{\partial k}$ the transmission function when E is inside the band is

$$T(E) = \frac{\eta^4[\hbar v(E)]^2}{[E(1-\eta^2) - \mathcal{E}_0]^2 + \eta^4[\hbar v(E)]^2} \tag{3.40}$$

(and zero outside the band). This is exactly the result obtained earlier through a different method.

3.2.3 Discussion of the One-Level Conductor

First consider the special case when the coupling from the leads to the conductor is equal to the intersite coupling within the leads, i.e. $\eta = 1$. In this case, the transmission function becomes

$$T(E) = |t|^2 = \frac{[\hbar v(E)]^2}{\mathcal{E}_0^2 + [\hbar v(E)]^2} \tag{3.41}$$

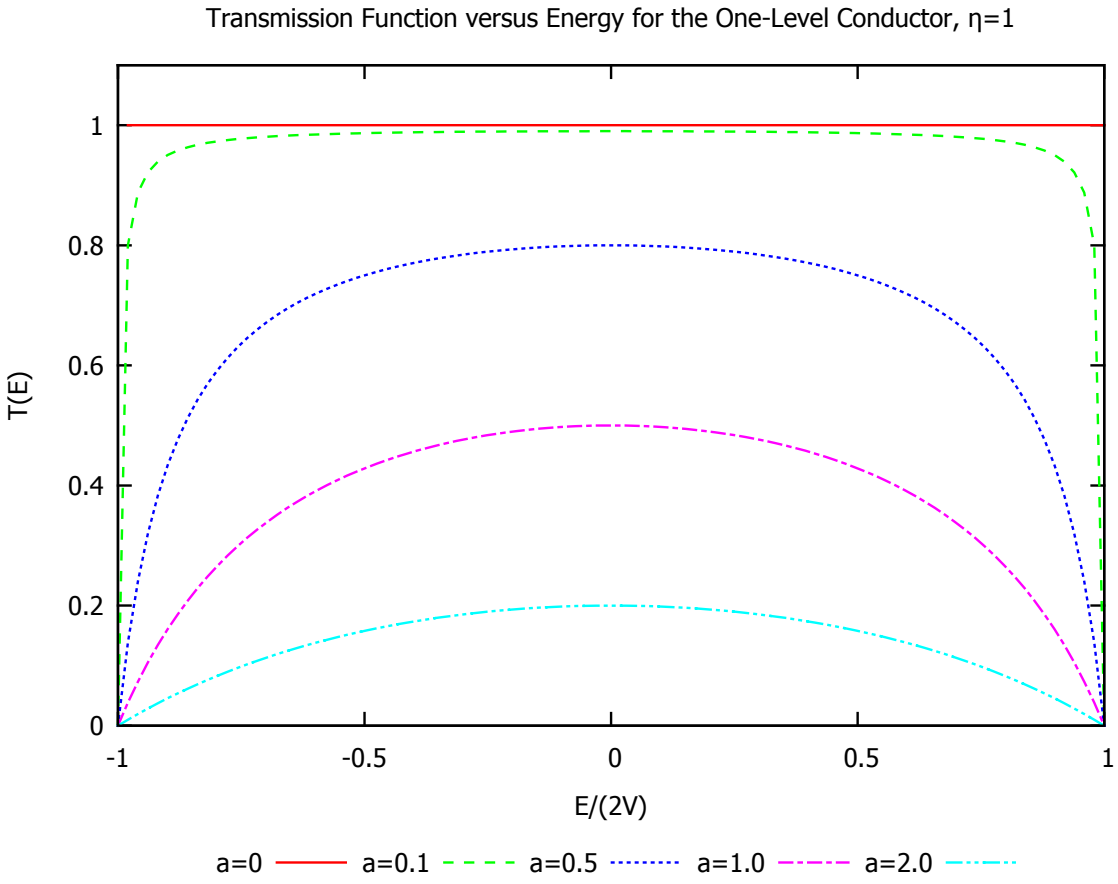

Figure 3.2: Transmission function versus energy for the one-level conductor with $\eta = 1$ for different values of $a \equiv \mathcal{E}_A/(2V)$.

If additionally the conductor site energy $\mathcal{E}_0$ vanishes, then it is easy to see that the incoming waves are not scattered at all and $T = 1$. As the magnitude of the site energy $|\mathcal{E}_0|$ is increased, the transmission function everywhere decreases. In particular, at the band edges $E = \pm 2V$, the velocity vanishes, so the transmission also goes to zero. The maximum transmission is at the center of the band $E = 0$, and its value is

$$T_{\max} = \frac{1}{1 + \frac{\mathcal{E}_0^2}{4V^2}}. \tag{3.42}$$

Furthermore, for this special case, $\eta = 1$, the transmission function is not sensitive to the sign of $\mathcal{E}_0$, and $T(E)$ is symmetric around $E = 0$. This is illustrated in Figure

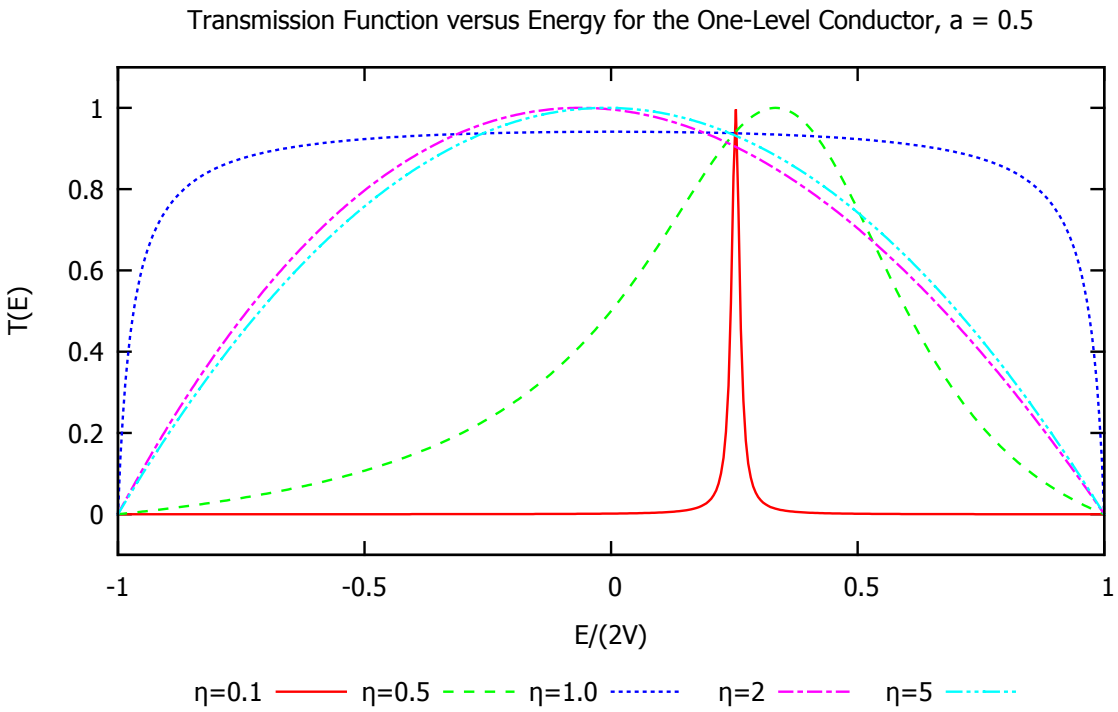

Figure 3.3: Transmission function versus energy for the one-level conductor with $a = \mathcal{E}_A/(2V) = 0.5$ for different coupling strengths η.

3.2.

If the coupling to the leads is strong (η large), then the transmission function is

$$T(E) = 1 - \frac{E^2}{4V^2} + O(1/\eta^2). \tag{3.43}$$

In this limit, the transmission function is parabolic, with $T = 1$ at the center of the band and again $T = 0$ at the edges, independent of the strength of $\mathcal{E}_0$.

In the general case, $T(E)$ still vanishes at the band edges, but it loses its symmetry around $E = 0$. If $\eta \neq 1$ and the value $\mathcal{E}_0/(1-\eta^2)$ is within the band, i.e.

$$|\mathcal{E}_0/(1-\eta^2)| < 2V, \tag{3.44}$$

maximum transmission occurs at that energy and is unity. Otherwise, maximum

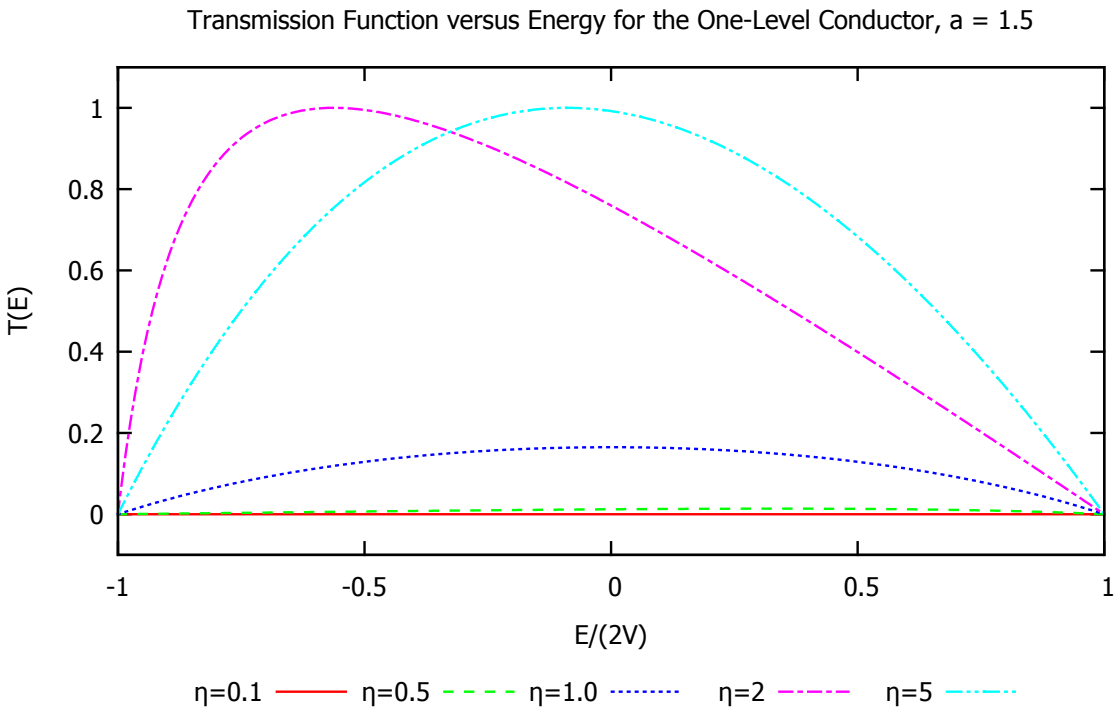

Figure 3.4: Transmission function versus energy for the one-level conductor with $a = \mathcal{E}_A/(2V) = 1.5$ for different coupling strengths η.

transmission occurs at

$$E = (1 - \eta^2)\frac{4V^2}{\mathcal{E}_0} \tag{3.45}$$

and is less than unity,

$$T_{\max} = \frac{\eta^4}{2\eta^2 - 1 + \frac{\mathcal{E}_0^2}{4V^2}}. \tag{3.46}$$

The transmission function versus energy for different values of η for constant $\mathcal{E}_A$ is displayed in Figures (3.3) and (3.4).

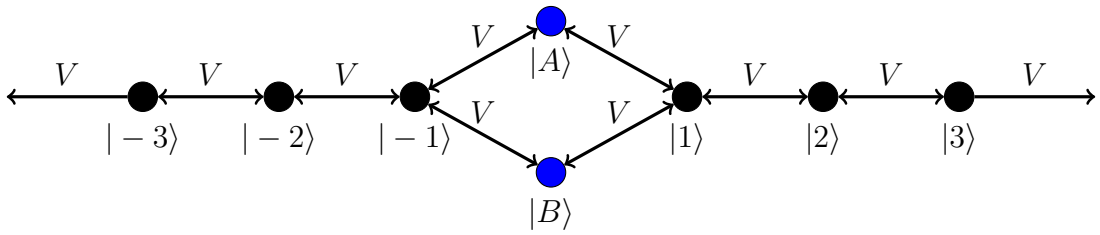

Figure 3.5: A conductor consisting of a two-levels (blue) connected to two semi-infinite tight binding leads (black).

3.3 Two-Level Systems

There are various different configurations of two-level conductors and different ways of connecting them to the leads. First, consider a two-level system with Hamiltonian

$$H = \mathcal{E}_A|A\rangle\langle A| + \mathcal{E}_B|B\rangle\langle B|$$

where $|A\rangle$ and $|B\rangle$ are the energy eigenstates of H and $\mathcal{E}_A$ and $\mathcal{E}_B$ their energies. There is no matrix element coupling the two states $|A\rangle$ and $|B\rangle$. Now suppose that both A and B are connected to both leads (the same 1D semi-infinite chains as before) with a coupling strength V which is the same as the intersite coupling V within the leads. This is illustrated in Figure (3.5).

3.3.1 Calculation of the Transmission

The transmission function will now be calculated using the Green's function method to illustrate its use for a system consisting of more than one state. Again, the first step is to calculate the self energies due to the coupling to the leads.

The coupling τ_S from the conductor to the source lead is

$$\tau_S = V(|A\rangle\langle -1| + |B\rangle\langle -1|) \tag{3.47}$$

where $|-1\rangle$ is the state on the end of the contact chain. Then the self energy is

$$\Sigma_S = \tau_S G_S \tau_S^\dagger \tag{3.48}$$

$$= V^2 \langle -1|G_S|-1\rangle (|A\rangle\langle A| + |A\rangle\langle B| + |B\rangle\langle A| + |B\rangle\langle B|). \tag{3.49}$$

The matrix element $\langle -1|G_S|-1\rangle$ was already calculated in the previous section, it is

$$\langle -1|G_S|-1\rangle = \frac{1}{V} e^{-i|\phi|} \tag{3.50}$$

where again $\cos\phi = E/(2V)$ and is between $-\pi$ and π. The self energy written as a matrix is then

$$\Sigma_s = V e^{-i|\phi|} \begin{pmatrix} 1 & 1 \\ 1 & 1 \end{pmatrix}. \tag{3.51}$$

A similar calculation for the drain lead yields $\Sigma_D = \Sigma_S$. The Γ matrices are

$$\Gamma_S = \Gamma_D = i(\Sigma_S - \Sigma_S^\dagger) = 2V \sin|\phi| \begin{pmatrix} 1 & 1 \\ 1 & 1 \end{pmatrix}. \tag{3.52}$$

The Green's function for the conductor subsystem is

$$\begin{aligned} G(E) &= [E - H - \Sigma_S - \Sigma_D]^{-1} \\ &= \left[\begin{pmatrix} E & 0 \\ 0 & E \end{pmatrix} - \begin{pmatrix} \mathcal{E}_A & 0 \\ 0 & \mathcal{E}_B \end{pmatrix} - 2Ve^{-i|\phi|} \begin{pmatrix} 1 & 1 \\ 1 & 1 \end{pmatrix} \right]^{-1} \\ &= \left[\begin{pmatrix} E - \mathcal{E}_A - 2Ve^{-i|\phi|} & -2Ve^{-i|\phi|} \\ -2Ve^{-i|\phi|} & E - \mathcal{E}_B - 2Ve^{-i|\phi|} \end{pmatrix} \right]^{-1}. \end{aligned} \tag{3.53}$$

The inverse on the right hand side may be easily calculated, and the result is

$$G(E) \begin{pmatrix} \frac{E-\mathcal{E}_B-2Ve^{-i|\phi|}}{(E-\mathcal{E}_A)(E-\mathcal{E}_B)-2Ve^{-i|\phi|}[2E-\mathcal{E}_A-\mathcal{E}_B]} & \frac{2Ve^{-i|\phi|}}{(E-\mathcal{E}_A)(E-\mathcal{E}_B)-2Ve^{-i|\phi|}[2E-\mathcal{E}_A-\mathcal{E}_B]} \\ \frac{2Ve^{-i|\phi|}}{(E-\mathcal{E}_A)(E-\mathcal{E}_B)-2Ve^{-i|\phi|}[2E-\mathcal{E}_A-\mathcal{E}_B]} & \frac{E-\mathcal{E}_A-2Ve^{-i|\phi|}}{(E-\mathcal{E}_A)(E-\mathcal{E}_B)-2Ve^{-i|\phi|}[2E-\mathcal{E}_A-\mathcal{E}_B]} \end{pmatrix}. \tag{3.54}$$

The transmission function may now be calculated. It is

$$\begin{aligned} T(E) &= \mathrm{Tr}\{\Gamma_S G \Gamma_D G^\dagger\} \\ &= \frac{[\hbar v(E)]^2}{\left(\frac{E^2-\mathcal{E}_A\mathcal{E}_B}{2E-\mathcal{E}_A-\mathcal{E}_B}\right)^2 + [\hbar v(E)]^2}. \end{aligned} \tag{3.55}$$

3.3.2 Discussion

Now let us examine the properties of equation (3.55). First, the following special cases will be considered:

- The two-levels are degenerate $\mathcal{E}_A = \mathcal{E}_B$.
- The two energies have the same magnitude, but opposite signs, $\mathcal{E}_A = -\mathcal{E}_B$.
- One of the energies is zero, $\mathcal{E}_B = 0$.

If the two sites are degenerate, $\mathcal{E}_A = \mathcal{E}_B = \mathcal{E}_0$, then the transmission function becomes

$$T(E) = \frac{[\hbar v(E)]^2}{\frac{(E+\mathcal{E}_0)^2}{4} + [\hbar v(E)]^2}. \tag{3.56}$$

This is exactly the same as for the one site conductor, equation (3.26), if η is set to $\sqrt{2}$ in that expression, and all the comments made about that system apply here also. The effect of adding a degenerate site with the same coupling is therefore equivalent to increasing the strength of the coupling for a one-level conductor.

Next, consider the special case where $\mathcal{E}_A = -\mathcal{E}_B$. The transmission function is

$$T(E) = \frac{[\hbar v(E)]^2}{\left(\frac{E^2+\mathcal{E}_A^2}{2E}\right)^2 + [\hbar v(E)]^2}. \tag{3.57}$$

The conductor is opaque ($T = 0$) at the center of the band (provided the energies are nonzero) as well as at the band edges, and the transmission function is symmetric around $E = 0$. The maximum transmission occurs at

$$E = \pm \frac{\mathcal{E}_A/2V}{\sqrt{2\left(\frac{\mathcal{E}_A}{2V}\right)^2 + 1}} \tag{3.58}$$

and has the value

$$T_{\max} = \frac{1}{1 + \left(\frac{\mathcal{E}_A}{2V}\right)^2 + \left(\frac{\mathcal{E}_A}{2V}\right)^4}. \tag{3.59}$$

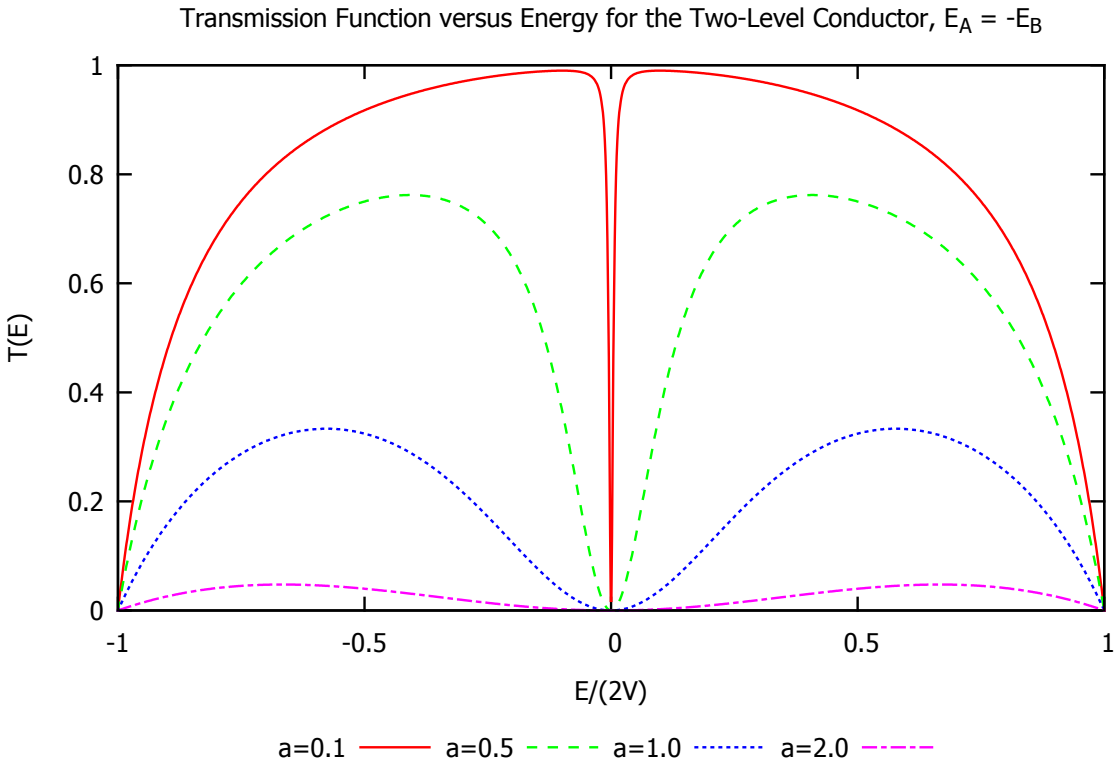

Figure 3.6: Transmission function versus energy for the two-level conductor described in Section 3.3 when $\mathcal{E}_A = -\mathcal{E}_B$ for different values of $a \equiv \mathcal{E}_A/(2V)$.

The maximum transmission is always less than one for $\mathcal{E}_A$ nonzero and decreases sharply as $\mathcal{E}_A$ is moved further outside of the band. This is illustrated in Figure (3.6).

Next, consider the case where one of the energies is zero. Since it does not matter which one, let $\mathcal{E}_B = 0$. The transmission function is then given by

$$T(E) = \frac{[\hbar v(E)]^2}{\left(\frac{E^2}{2E-\mathcal{E}_A}\right)^2 + [\hbar v(E)]^2}. \tag{3.60}$$

The conductor becomes transparent at the center of the band, $E = 0$, but the transmission function is no longer a symmetric function of energy. If $\mathcal{E}_A/2$ is within the band, then the conductor becomes opaque ($T = 0$) at $E = \mathcal{E}_A/2$. If $\mathcal{E}_A$ is moved far outside the band, then transmission function becomes nearly one everywhere inside the band. This is illustrated in Figure (3.7).

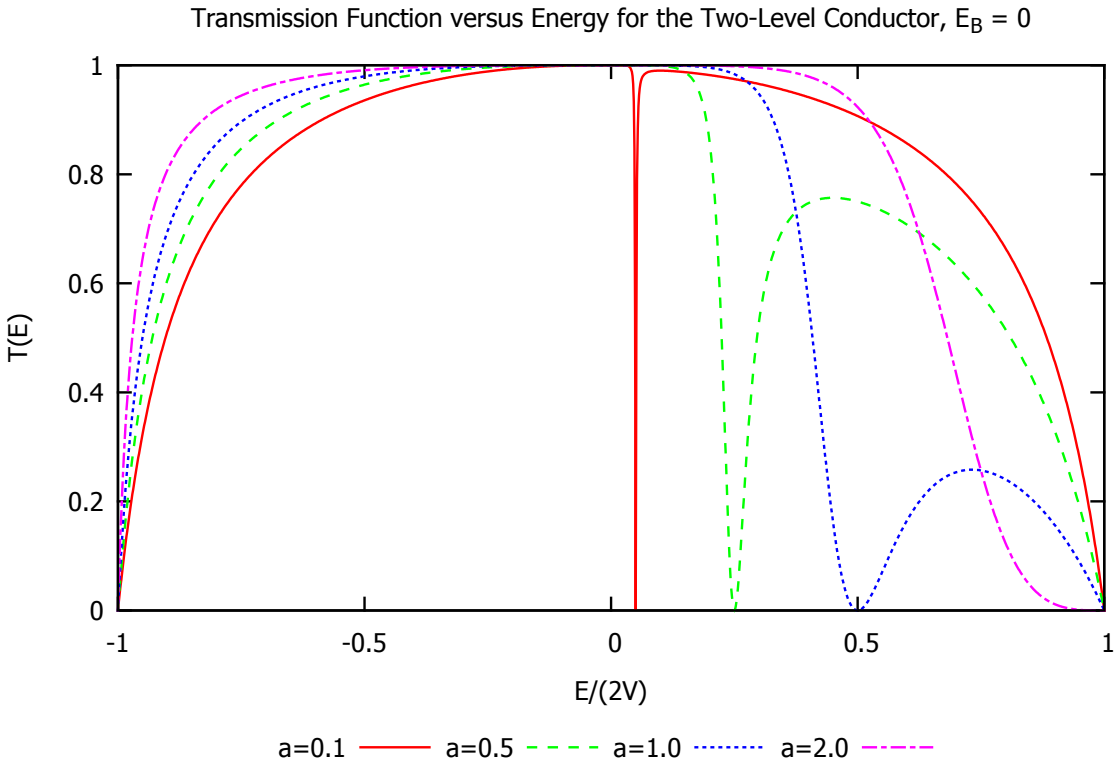

Figure 3.7: Transmission function versus energy for the two-level conductor described in Section 3.3 when $\mathcal{E}_B = 0$ for different values of $a \equiv \mathcal{E}_A/(2V)$.

Now some comments can be made about the general case. As with the one-level conductor, the transmission function vanishes at the band edges, $E = \pm 2V$. If $\mathcal{E}_A$ and $\mathcal{E}_B$ both have the same sign, and if $\sqrt{\mathcal{E}_A \mathcal{E}_B}$ is within the band, then the conductor becomes transparent at plus and minus the geometric mean of the site energies,

$$E = \pm\sqrt{\mathcal{E}_A \mathcal{E}_B}. \tag{3.61}$$

On the other hand, at the arithmetic mean of the site energies,

$$E = \frac{\mathcal{E}_A + \mathcal{E}_B}{2} \tag{3.62}$$

the conductor becomes opaque ($T = 0$), provided $\mathcal{E}_A \neq \mathcal{E}_B$. For certain values of $\mathcal{E}_A$ and $\mathcal{E}_B$, the arithmetic and geometric means are close to one another, causing

the conductance to dip (or rise) rapidly from one to zero (or zero to one). This is illustrated in Figure (3.8).

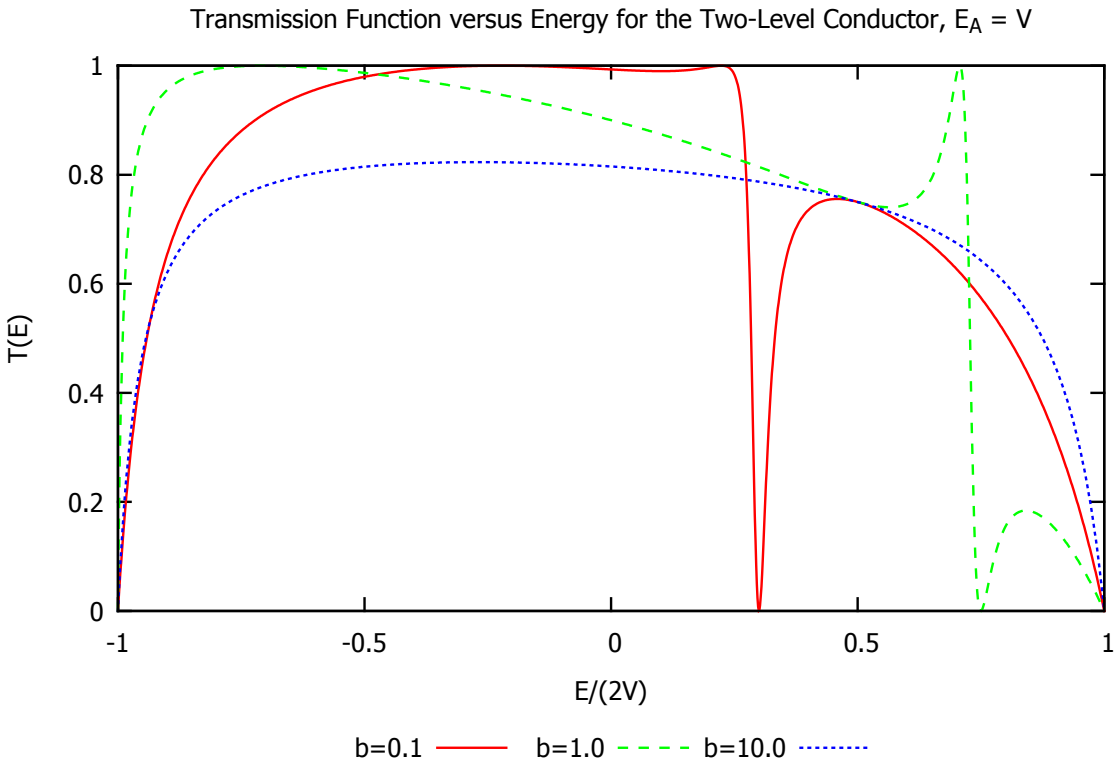

Figure 3.8: Transmission function versus energy for the two-level conductor described in Section 3.3 for different values of $b \equiv \mathcal{E}_B/(2V)$ for fixed $\mathcal{E}_A = V$.

3.4 N-Level Degenerate System

Now consider a conductor consisting of N degenerate levels at energy $\mathcal{E}_0$. Each level is coupled to the same semi-infinite contacts with a strength V. The states in the conductor will be labeled $|\phi_n\rangle$ for the nth degenerate level. The situation is illustrated in Figure (3.9) for $N = 4$.

It is simpler to perform this computation using the textbook way. Therefore, let

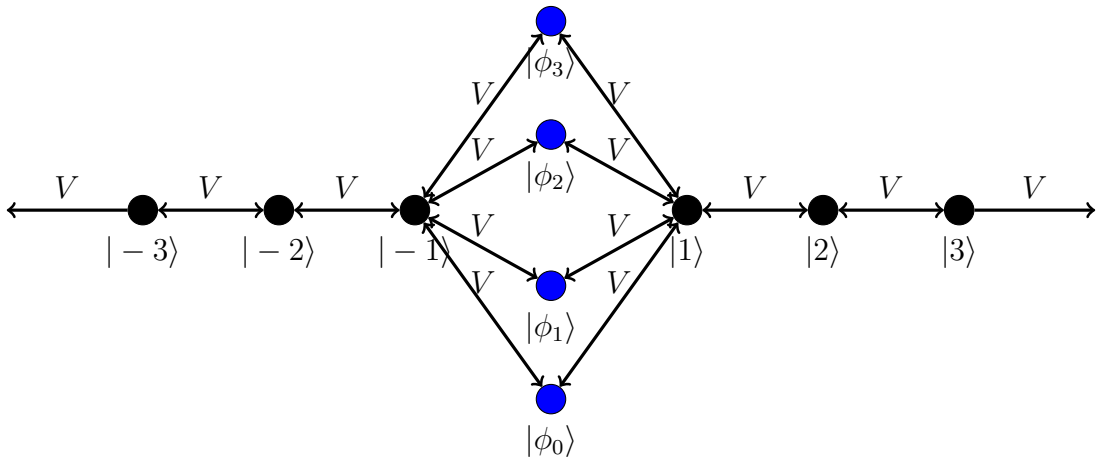

Figure 3.9: A conductor consisting of a 4 degenerate levels (blue), each of which are connected to two semi-infinite tight binding leads (black).

us take again an incoming and reflected wave to the left, and a transmitted wave to the right,

$$\psi_m^k = \begin{cases} e^{ikm} + re^{-ikm} & m < 0 \\ te^{-ikm} & m > 0 \end{cases}. \tag{3.63}$$

The reflection and transmission amplitudes $|r|$ and $|t|$, as well as the wavefunction inside the conductor $|\phi\rangle$ must now be determined so that the Schrödinger equation is everywhere satisfied. The Schrödinger equation for the conductor states and the two lead states to the left and right of the conductor is

$$E\psi_{-1} = V\left(\psi_{-2} + \sum_n c_n\right), \tag{3.64}$$

$$E\psi_{+1} = V\left(\psi_{+2} + \sum_n c_n\right), \tag{3.65}$$

$$Ec_n = \mathcal{E}_0 c_n + V(\psi_{-1} + \psi_{+1}), \tag{3.66}$$

where c_n is the amplitude of the wavefunction in the nth conductor state, $c_n \equiv \langle\phi_n|\phi\rangle$. From the third equation, all the amplitudes c_n must evidently be the same, i.e. $c_n = A$

for all n, and inserting this the Schrödinger equation becomes

$$E(e^{-ik} + re^{ik}) = V\left(e^{-2ik} + re^{2ik} + NA\right) \tag{3.67}$$

$$E(te^{ik}) = V\left(te^{2ik} + NA\right) \tag{3.68}$$

$$EA = \mathcal{E}_0 A + V(e^{-ik} + re^{ik} + te^{ik}). \tag{3.69}$$

Using the first two gives $t = r + 1$, and eliminating r from the third,

$$\begin{aligned}(E - \mathcal{E}_0)A &= V(e^{-ik} + te^{ik} - e^{ik} + te^{ik}) \\ &= V(-2i\sin k + 2te^{ik}).\end{aligned} \tag{3.70}$$

Combining this with the second equation to eliminate A,

$$(E - \mathcal{E}_0)tV = V^2 N(-2i\sin k + 2te^{ik}). \tag{3.71}$$

Finally, solving for the transmission amplitude t,

$$t = \frac{-2iNV\sin k}{E - \mathcal{E}_0 - 2NVe^{ik}} \tag{3.72}$$

so the transmission function is

$$T(E) = |t|^2 = \frac{[\hbar v(E)]^2}{\frac{[(1-N)E - \mathcal{E}_0]^2}{N^2} + [\hbar v(E)]^2}. \tag{3.73}$$

This is exactly equivalent to the transmission function obtained earlier for the one-level system under the replacement $\eta^2 = N$. Thus, adding degenerate levels has the same effect as increasing the strength of the coupling to the leads in a one-level system.

3.5 A Different Two-Level Conductor

Now consider again a two-level conductor, but suppose that only one of the states is coupled to the contacts, and add a coupling between the two states. Let the Hamiltonian for the isolated conductor be

$$H = \mathcal{E}_A|A\rangle\langle A| + \mathcal{E}_B|B\rangle\langle B| + V_{AB}\left(|B\rangle\langle A| + |A\rangle\langle B|\right), \tag{3.74}$$

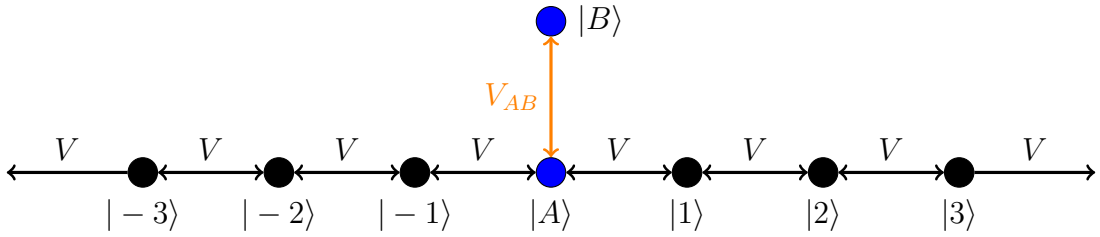

Figure 3.10: A conductor consisting of two states (blue). Only the $|A\rangle$ state is connected to the two semi-infinite tight binding leads (black). There is an interaction between the two conductor states of strength V_{AB}.

and let only the state $|A\rangle$ be coupled to the contacts. This is illustrated in Figure (3.10).

The Green's function method will be used to calculate the transmission function. The coupling matrices are

$$\tau_S = V\left(|A\rangle\langle -1|\right) \tag{3.75}$$

$$\tau_D = V\left(|A\rangle\langle +1|\right). \tag{3.76}$$

The self energies are then

$$\begin{aligned}\Sigma_S = \Sigma_D &= \tau_S G_S \tau_S^\dagger \\ &= V^2\langle -1|G_S|-1\rangle |A\rangle\langle A| \\ &= Ve^{-i|\phi|}|A\rangle\langle A|.\end{aligned} \tag{3.77}$$

where in going from the second to the third line the Green's function matrix element calculated earlier has been used. These may be written in matrix form as

$$\Sigma_S = \Sigma_D = Ve^{-i|\phi|}\begin{pmatrix}1 & 0\\ 0 & 0\end{pmatrix}. \tag{3.78}$$

The Γ matrices are

$$\Gamma_S = \Gamma_D = i(\Sigma - \Sigma^\dagger) = 2V\sin|\phi|\begin{pmatrix}1 & 0\\ 0 & 0\end{pmatrix}. \tag{3.79}$$

The Green's function inside the conductor is

$$\begin{aligned} G(E) &= [EI - H - \Sigma_S - \Sigma_D]^1 \\ &= \left[\begin{pmatrix} E & 0 \\ 0 & E \end{pmatrix} - \begin{pmatrix} \mathcal{E}_A & V_{AB} \\ V_{AB} & \mathcal{E}_B \end{pmatrix} - 2Ve^{-i|\phi|} \begin{pmatrix} 1 & 0 \\ 0 & 0 \end{pmatrix} \right]^{-1} \\ &= \frac{1}{(E-\mathcal{E}_A-2Ve^{-i|\phi|})(E-\mathcal{E}_B)-V_{AB}^2} \begin{pmatrix} E-\mathcal{E}_B & V_{AB} \\ V_{AB} & E-\mathcal{E}_A-2Ve^{-i|\phi|}. \end{pmatrix}. \end{aligned} \tag{3.80}$$

The transmission function is finally

$$T(E) = \mathrm{Tr}\{\Gamma G \Gamma G^\dagger\} = \frac{[\hbar v(E)]^2}{\left(\mathcal{E}_A + \frac{V_{AB}^2}{(E-\mathcal{E}_B)}\right)^2 + [\hbar v(E)]^2}.$$

It is worth pointing out that this calculation could have been done in a simpler way, by noting that the Green's function for the A subsystem (which is all that is needed when computing the trace since the leads are only coupled to A) is

$$G_A(E) = \frac{1}{E - \mathcal{E}_A - \Sigma_B - \Sigma_S - \Sigma_D} \tag{3.81}$$

where Σ_B is the self energy resulting from coupling to the $|B\rangle$ state,

$$\Sigma_B(E) = \frac{V_{AB}^2}{E - \mathcal{E}_B}. \tag{3.82}$$

Let us now discuss the properties of the transmission as a function of energy. Again, the transmission vanishes at the band edges, and it is not in general a symmetric function of energy. If $\mathcal{E}_B$ is within the band, the the conductor becomes opaque at $E = \mathcal{E}_B$. At

$$E = \mathcal{E}_B - \frac{V_{AB}^2}{\mathcal{E}_A}, \tag{3.83}$$

the conductor becomes transparent, provided this energy is within the band. As the magnitude of $\mathcal{E}_B$ becomes very large compared to V_{AB}, the transmission function approaches the single-site value, i.e. it behaves as if the site $|B\rangle$ were not there. This is illustrated in Figure (3.11).

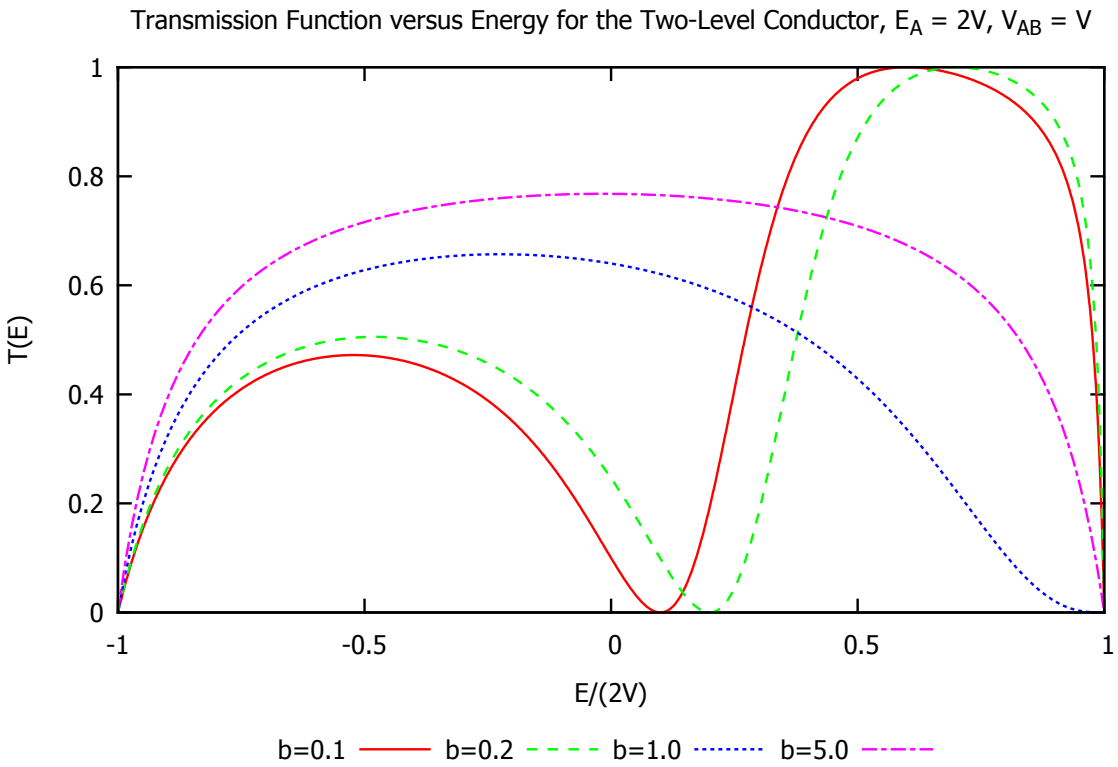

Figure 3.11: Transmission function versus energy for the two-level conductor described in Section 3.5 for different values of $b \equiv \mathcal{E}_B/(2V)$ for fixed $\mathcal{E}_A = V$ and $V_{AB} = V$.

3.6 Single-Site Conductor Coupled to Oscillator

Now consider a one-level conductor which is placed in interaction with a harmonic oscillator. This could be looked at as a highly simplified model of electron-phonon scattering. The total Hamiltonian exists in the product space of the electron and boson spaces, and consists of the following parts:

- Hamiltonians for the isolated source and drain leads.
- Coupling between leads and the conductor.
- Hamiltonian for the isolated conductor.

- Hamiltonian for the isolated oscillator.
- Interaction between conductor and oscillator.

The Hamiltonians for the isolated leads and the coupling between leads and conductor may be written in total as

$$H_{\text{leads}} = V \sum_{m=-\infty}^{\infty} (|m\rangle\langle m+1| + |m+1\rangle\langle m|) \otimes I_b \tag{3.84}$$

Here V is the intersite interaction energy in the leads as well as the coupling strength from leads to conductor. The states $|m\rangle$ are electronic states with $|0\rangle$ being the conductor state, and the operator I_b is the identity operator in the boson space. Next, the Hamiltonian for the isolated conductor is

$$H_{\text{conductor}} = \mathcal{E}_0 |0\rangle\langle 0| \otimes I_b \tag{3.85}$$

where $\mathcal{E}_0$ is the site energy of the conductor site relative to the site energies in the leads. The Hamiltonian for the isolated oscillator is

$$H_{\text{oscillator}} = I_e \otimes \hbar\omega \left(\frac{1}{2} I_b + b^\dagger b\right). \tag{3.86}$$

Here I_e is the identity operator in the electron space, ω is the frequency of the oscillator, and $b^\dagger$ and b are the raising and lowering operators in the oscillator space. Finally, let the interaction between oscillator and conductor to be

$$|0\rangle\langle 0| \otimes g\hbar\omega(b + b^\dagger) \tag{3.87}$$

where g is a dimensionless constant which determines the strength of the interaction. This type of interaction between conductor and oscillator changes the effective energy of the $|0\rangle$ state based on the position of the oscillator.

Putting everything together, the total Hamiltonian is

$$\begin{aligned} H = V \sum_{m=-\infty}^{\infty} (|m\rangle\langle m+1| + |m+1\rangle\langle m|) \otimes I_b + \mathcal{E}_0 |0\rangle\langle 0| \otimes I_b \\ + I_e \otimes \hbar\omega \left(\frac{1}{2} I_b + b^\dagger b\right) + |0\rangle\langle 0| \otimes g\hbar\omega(b + b^\dagger). \end{aligned} \tag{3.88}$$

If the temperature in source and drain reservoirs is low enough, the oscillator should be in its (non-shifted) ground state $|\phi_0\rangle$ before the electron passes through the junction, so for the incoming wave take

$$|\psi_i\rangle = \sum_{m<0} e^{ik_0 m}|m\rangle \otimes |\phi_0\rangle \tag{3.89}$$

where the energy of the incoming electron is $E_e = 2V\cos k_0$ and $|\phi_0\rangle$ is the ground state of the isolated oscillator. Because of the interaction, as the electron passes through the conductor it may create one or more excitations in the oscillator, so the reflected and transmitted waves must be of the form

$$\text{reflected wave: } |\psi_r\rangle = \sum_{m<0}\sum_n r_n e^{-ik_n m}|m\rangle \otimes |\phi_n\rangle, \tag{3.90}$$

$$\text{transmitted wave: } |\psi_t\rangle = \sum_{m>0}\sum_n t_n e^{-k_n m}|m\rangle \otimes |\phi_n\rangle. \tag{3.91}$$

where r_n and t_n are reflection and transmission amplitudes for modes with n bosons in the oscillator. The $|\phi_n\rangle$'s are n boson eigenstates of the non-shifted oscillator. Since the incoming wave only has enough energy to create a finite number of bosons, some of the k_n's will necessarily be complex, and part of the electron wavefunction will be exponentially localized around the conductor.

Enforcing $H|\psi\rangle = E|\psi\rangle$ with $|\psi\rangle$ consisting of the sum of incoming, reflected, and transmitted waves, it is possible to show that the k_n's are determined by

$$E_{\text{total}} = 2V\cos k_0 + \frac{\hbar\omega}{2} = 2V\cos k_n + \hbar\omega\left(n + \frac{1}{2}\right) \tag{3.92}$$

and the reflection and transmission amplitudes are

$$\delta_{n,0} + r_n = t_n = -2iV\sin k_0 \langle\phi_n|G(E)|\phi_0\rangle \tag{3.93}$$

and the Green's function G is

$$G(E) \equiv [E - H_0 - H_1 - 2\Sigma(E)]^{-1} \tag{3.94}$$

with

$$H_0 \equiv \epsilon_0 + \hbar\omega \left(b^\dagger b + \frac{1}{2} \right), \tag{3.95}$$

$$H_1 \equiv g\hbar\omega(b + b^\dagger), \tag{3.96}$$

$$\Sigma(E) \equiv V \sum_n e^{ik_n} |\phi_n\rangle\langle\phi_n|. \tag{3.97}$$

If we restrict ourselves to the special case $\hbar\omega > 4V$, then the incoming electron does not have enough energy to create a boson and keep propagating, so all k_n's for $n > 0$ will be complex, and the transmission function is only affected by t_0,

$$T = |t_0|^2 = [2V \sin k_0]^2 \langle\phi_0|G(E)|\phi_0\rangle\langle\phi_0|G^\dagger(E)|\phi_0\rangle. \tag{3.98}$$

Due to the difficulty in calculating $G(E)$ exactly, we have considered the limit of weak coupling g. Expanding equation (3.94), we have [56]

$$G = G_0 + G_0 H_1 G_0 + G_0 H_1 G_0 H_1 G_0 + ... \tag{3.99}$$

where

$$G_0(E) = [E - H_0 - 2\Sigma(E)]^{-1} = \sum_n \frac{|\phi_n\rangle\langle\phi_n|}{E - \epsilon_0 - \hbar\omega(n + 1/2) - 2Ve^{ik_n}}. \tag{3.100}$$

Using this approximation, the transmission when $\hbar\omega > 4V$ to order g^2 as a function of electron energy E_e is

$$T(E_e) \approx \frac{[\hbar v(E_e)]^2}{\mathcal{E}_0^2 + [\hbar v(E_e)]^2} + g^2 h(E_e) \tag{3.101}$$

where the correction term is

$$h(E_e) \equiv \frac{2\mathcal{E}_0 \hbar^2\omega^2\hbar^2 v^2(E_e)}{\left[\mathcal{E}_0^2 + \hbar^2 v^2(E_e)\right]^2 \left[\mathcal{E}_0 + \sqrt{\hbar^2\omega^2 - 2E_e\hbar\omega - \hbar^2 v^2(E_e)}\right]} \tag{3.102}$$

and with $v(E_e)$ again the velocity as a function of the electron energy, $[\hbar v(E_e)]^2 = 4V^2 - E_e^2$.

This correction term may be positive or negative depending on the sign of ϵ_0, and it is not symmetric around $E_e = 0$. Interestingly, $h(E_e)$ also vanishes if the site energy $\mathcal{E}_0$ is zero. The function $h(E_e)$ is plotted in figure (3.12).

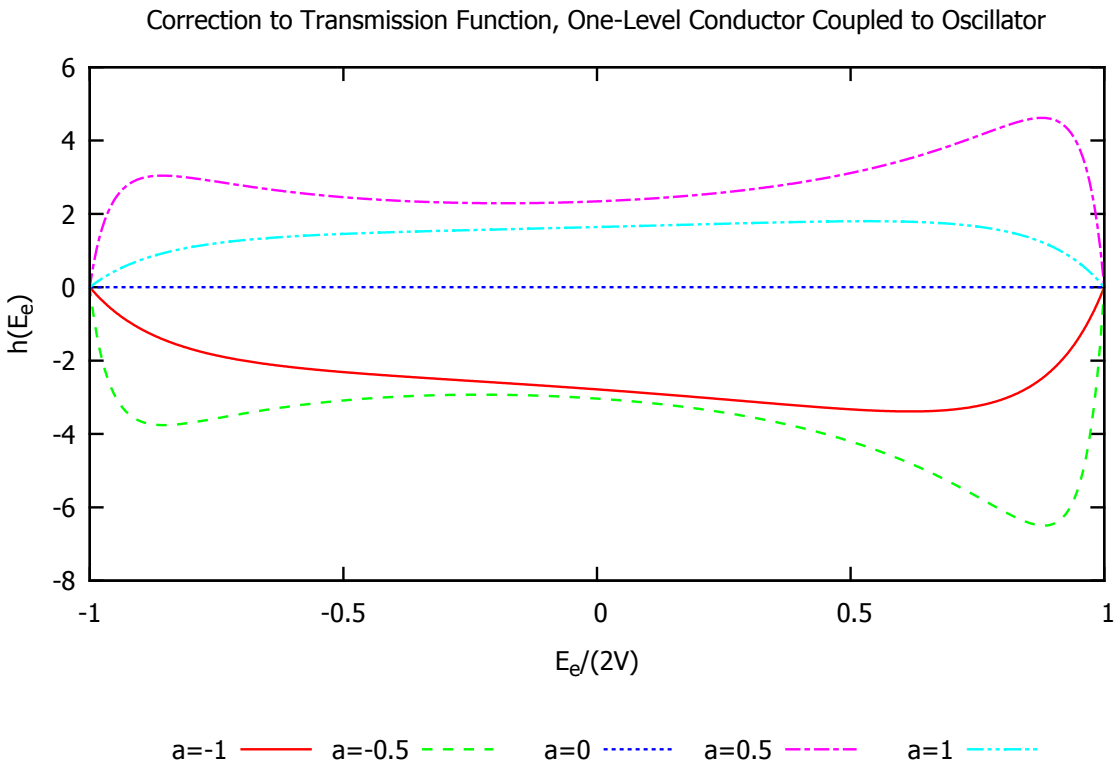

Figure 3.12: First order correction to the transmission for a one-level conductor coupled to a harmonic oscillator, with $\hbar\omega/(2V) = 4$ and for different values of $a \equiv \mathcal{E}_0/(2V)$.

3.7 Summary

In this chapter, we saw how the transmission varies as a function of energy for different kinds of conductors connected to 1D leads. For the conductor consisting of a single site, the known result was recovered using two different methods: the textbook scattering approach, and the Green's function method.

The transmission function was calculated for different configurations of two-level conductors, and it was shown that the transmission function depends on the how the leads are connected to the conductor.

For a conductor consisting of N degenerate levels at energy $\mathcal{E}_0$, each connected to the leads with interaction strength V, it was shown that the transmission is equivalent to a one-level system at the same energy $\mathcal{E}_0$ but with a stronger coupling strength $\sqrt{N}V$.

Finally, for a one-level conductor in interaction with an oscillator, although the problem could not be solved exactly, to lowest order it was found that the interaction can enhance or reduce the transmission function, depending on the sign of the site energy $\mathcal{E}_0$.

Chapter 4

Collective Motion of Macroscopic Objects: A Model with Centering

Several different approaches have been used in the literature for modeling the cooperative motion of various biological organisms. One approach is to explicitly model the motion of every member of the group by specifying how the positions and velocities of each individual evolve in time. One way to do this is to simply construct equations of motion for each individual's position and velocity. Such models are known as *Lagrangian* or *dynamical* models [10, 24, 80–82]. Other authors prefer to make time discrete in order to make it easier to perform computer simulations. In these discrete time models, at each time step a set of rules is used to determine the state of system in the next time step based on the current state of the system. These are typically known as *rule-based* models or cellular automata [17, 83–93].

Yet another approach is to construct equations of motion for continuous functions of space and time such as the density and velocity fields. This is a coarse-grained description since the motion of individual particles is *not* modeled explicitly. This is known as the *continuum* or *fluid dynamics* approach [94–100].

In the realm of collective motion, due to the difficulties inherent in studying sys-

tems of many interacting particles, very few authors have been able to analytically connect a description where each particle is modeled individually (a rule-based or dynamical model) to a coarse-grained continuum description. A notable exception is the 1999 paper by Czirók et al. [97] where approximate continuum equations of motion for the density and velocity fields are constructed from a rule-based model. Recently, some authors have used *hybrid* approaches to help bridge the gap between individual-level descriptions and continuum descriptions [101–109]. In such approaches, a model of individual behavior is chosen and numerical simulations are performed. Next, equations of motion are postulated for continuous coarse-grained quantities. The undetermined parameters in the equations of motion are then estimated from simulations. In particular, in a recent 2010 paper Raghib et al. [108] used an advection-diffusion equation with memory for the evolution of the center of mass distribution. An advection-diffusion equation with memory is a generalization of the advection-diffusion equation which is non-local in time in the sense that the evolution at time t depends on the state of the system at previous times. In one dimension, the advection-diffusion equation with memory has the form

$$\frac{\partial}{\partial t}P(x,t) = -\int_0^t \mathcal{V}(t-t')\frac{\partial}{\partial x}P(x,t')dt' + \int_0^t \mathcal{D}(t-t')\frac{\partial^2}{\partial x^2}P(x,t')dt'. \tag{4.1}$$

Raghib et al. postulate a form for the memory, and fit the unknown parameters using simulation of a rule-based model.

Although this procedure can produce coarse-grained equations of motion which fit well with simulation, it does not make clear why the memory has the particular form found. The presence of a memory at least should not be surprising. In Chapter 2 it was shown that for a quantity ρ which obeys

$$\frac{\partial \rho}{\partial t} = -i\mathcal{L}\rho \tag{4.2}$$

where $\mathcal{L}$ is a linear (super)operator, the Zwanzig-Nakajima projection approach [76–78] shows that the projected quantity $\mathcal{P}\rho$ naturally obeys a memory equation of the

form

$$\frac{\partial}{\partial t}\mathcal{P}\rho = -i\mathcal{P}\mathcal{L}\mathcal{P}\rho - \mathcal{P}\mathcal{L}\int_0^t e^{-i(1-\mathcal{P})\mathcal{L}(t-t')}(1-\mathcal{P})\mathcal{L}\mathcal{P}\rho(t')dt' + \mathcal{I}(t) \tag{4.3}$$

where $\mathcal{I}$ is a term which depends on initial conditions. This expression formally gives the memory in terms of the projection and evolution operators, but it is not very useful for practical calculations of the memory, since calculating the operator $e^{-i(1-\mathcal{P})\mathcal{L}t}$ can be difficult even for extremely simple systems [72].

In this chapter, we construct a simplified dynamical model of collective motion and obtain exact equations of motion for a few continuum quantities. We begin by writing stochastic differential equations of motion for the positions of each particle in the system. We then construct and solve the corresponding equation of motion for the probability distribution function using standard techniques. Next, we perform coarse-graining to find the evolution of continuous quantities such as the center of mass distribution function and the density.

For one particular coarse-grained quantity, the density, we find that even in this simple system an advection-diffusion equation with memory cannot completely capture the dynamics. The full dynamics are described via an evolution equation which is non-local in space as well as time.

4.1 Description of the Model

Models of collective motion typically consist of several ingredients. The majority of these ingredients can be classified as either self-propulsion, interaction, or noise. We will define each of these in turn.

Self-propulsion is the tendency for each individual to move at a particular speed. Self-propulsion can be incorporated into dynamical models by introducing a force which drives the speed of each particle to a given value. In rule based models, self-

propulsion is typically included simply by specifying that the particles move at a given constant speed and using a set of rules which only modifies the directions of the particles.

Collective motion is a result of interaction between individuals in a group. The most common kinds of interaction included in models of collective motion are:

- *Short Range Collision Avoidance*: The tendency for individuals to move away from each other if they are too close together.
- *Centering*: The tendency for individuals to move toward other nearby individuals.
- *Alignment*: The tendency for individuals to align their directions with the directions of nearby individuals.

Biological organisms can change speed or direction in apparently random ways. This is taken into account in models of collective motion through noise. Noise is typically included in dynamical models by introducing a stochastic force acting on the particles, or in rule-based models by randomly perturbing the direction of each particle at every time step.

Finally, one may also introduce a preferred direction. A group of organisms may have a preferred direction if, for example, a food source lies in that direction. One topic of interest in the literature is the idea of collective decision making [90, 92, 110, 111]. In the simplest approaches, the flock is divided into two groups: one group consisting of individuals which are "informed" and have a preferred direction, and the other group consisting of individuals which are "uninformed" and do not have any such preferred direction.

As an example of a model including some of these ingredients, the dynamical model of Mikhailov and Zanette [24] has self-propulsion, a centering interaction, and

noise. Their equation of motion for the position of the mth particle is

$$\ddot{x}_m + (\dot{x}_m^2 - 1)\dot{x}_m + \frac{a}{N}\sum_n (x_m - x_n) = \Gamma_m(t). \tag{4.4}$$

The first term on the left hand side is inertia, the second term is a self-propulsion force which drives the speed of the particle to -1 or $+1$, and the third term represents a centering interaction. The particular kind of centering interaction they have chosen is to simply couple all particles to all other particles with spring forces. Finally, the term on the right hand side, $\Gamma_m(t)$, represents a stochastic noise force, which they take to be delta-correlated white noise with a given strength. Although the model of Mikhailov and Zanette is relatively simple, the presence of the nonlinear self-propulsion term precludes exact analysis.

The simplified model of collective motion we construct and analyze in this chapter is similar to the model of Mikhailov and Zanette, but does not contain any self-propulsion. We do however allow for a preferred direction. Our simplified model thus consists of three ingredients: a centering interaction, noise, and a bias. The model can be solved exactly. The entire joint probability distribution as a function of time can be found and any observable dependent on the distribution can be calculated explicitly.

We begin with a description of the model and a discussion of the dynamics when there is no noise. Next, we find the evolution of the probability distribution when the dynamics are noisy. We then look at the evolution of coarse-grained quantities and write continuum equations of motion.

The model consists of N identical overdamped Brownian point particles in one dimension. As in the model by Mikhailov and Zanette, the centering interaction is introduced by coupling each particle to all others with spring forces of equal strengths. We take the springs to all have zero equilibrium length.

Next, we introduce a bias, i.e. a directional feature in the motion of the particles. Furthermore, to include the idea of informed and uninformed individuals, we allow

different particles to feel different strength biases.

The equation of motion for the position of the mth particle in the flock, x_m, is a Langevin equation,

$$\dot{x}_m = -\gamma \sum_n (x_m - x_n) + v_m + \Gamma_m(t) \tag{4.5}$$

where γ is a constant which determines the strength of the spring interactions and $\Gamma_m(t)$ is delta-correlated Gaussian white noise with

$$\langle \Gamma_m(t)\Gamma_n(t')\rangle = 2D_0\delta_{mn}\delta(t-t'). \tag{4.6}$$

The bias v_m depends on the particular particle m under consideration; some particles may feel a different bias than others. In the case where the group is divided only into informed and uninformed individuals, v_m only takes on two values: either zero (for uninformed individuals) or a constant v (for informed individuals).

4.2 Deterministic Dynamics

First, we consider the deterministic case, i.e. when there is no noise. The equations of motion become

$$\dot{x}_m = -\gamma \sum_n (x_m - x_n) + v_m. \tag{4.7}$$

One way of finding the solution is to decouple the equations of motion using a discrete Fourier transform. Here we first show that the all-to-all coupling can be viewed as a coupling to only the center of mass coordinate. We then solve for the center of mass position as a function of time, $\bar{x}(t)$, and substitute it into the equation of motion for x_m, which can then be integrated.

Define the center of mass position to be

$$\bar{x} \equiv \frac{1}{N}\sum_m x_m, \tag{4.8}$$

and rewrite the equations of motion as

$$\dot{x}_m = -N\gamma(x_m - \bar{x}) + v_m. \tag{4.9}$$

Written in this form, it is easy to see that the mth particle is only coupled to the center of mass position. The spring interactions exert no net force on the center of mass; it only affected by the bias. This can be seen explicitly by summing equation (4.9) over m, which gives

$$\dot{\bar{x}} = \bar{v} \tag{4.10}$$

where $\bar{v} \equiv \frac{1}{N}\sum_m v_m$ is the mean of the v_ms. The center of mass position as a function of time is then

$$\bar{x}(t) = \bar{x}(0) + \bar{v}t. \tag{4.11}$$

Substituting this into (4.9) gives an equation for x_m and t alone,

$$\dot{x}_m = -N\gamma(x_m - \bar{x}(0) - \bar{v}t) + v_m. \tag{4.12}$$

The solution to this equation is

$$x_m(t) = x_m(0)e^{-N\gamma t} + \bar{v}t + \left(\bar{x}(0) + \frac{v_m - \bar{v}}{N\gamma}\right)(1 - e^{-N\gamma t}). \tag{4.13}$$

When t is much less than $1/(N\gamma)$, the right hand side can be expanded in a Taylor series as

$$x_m(t) = x_m(0) + v_m t + (N\gamma t)[\bar{x}(0) - x_m(0)] + O(t^2). \tag{4.14}$$

At short times, the mth particle drifts at a velocity which is the sum of the bias it feels v_m and an amount which is proportional to its initial separation from the center of mass.

At times $t \gg 1/(N\gamma)$ the position becomes

$$x_m(t) \approx \bar{v}t + \bar{x}(0) + \frac{v_m - \bar{v}}{N\gamma}. \tag{4.15}$$

At long times, each particle drifts at a velocity $\bar{v}$ and is displaced from the center of mass by an amount which depends on the difference between the bias it feels v_m and the mean bias $\bar{v}$. For the special case when v_m is either zero (for uninformed individuals) or v (for informed individuals), the particles collect into two clusters. The informed birds cluster ahead of the center of mass at $x = \bar{x} + (1-a)v/(N\gamma)$ where a is the fraction of informed birds, and the uninformed birds cluster behind the center of mass at $x = \bar{x} - a/(N\gamma)$. The informed and uninformed birds are therefore separated from each other by a distance $v/(N\gamma)$.

4.3 Noisy Dynamics

We now add noise to the system. Although the Langevin equations (4.5) can be solved directly, it is simpler for the purposes of calculating observables to construct and solve the corresponding equation of motion for the evolution of the probability distribution function. We define the probability distribution function $W(x_1, ..., x_N, t)$ so that at time t the probability to find particle 1 in a small interval between x_1 and $x_1 + dx_1$, particle 2 between x_2 and $x_2 + dx_2$, et cetera is

$$W(x_1, ..., x_N, t)dx_1 \cdots dx_N. \tag{4.16}$$

The partial differential equation of motion for the distribution function W is known as a *Fokker-Planck equation* [112, 113]. The Fokker-Planck equation can be constructed from the Langevin equations (4.5) using standard techniques (see e.g. Chapter 4 in Risken [114] for a detailed discussion). For this system, the Fokker-Planck equation is

$$\frac{\partial W}{\partial t} = \gamma \sum_m \frac{\partial}{\partial x_m} \sum_n (x_m - x_n) W - \sum_m v_m \frac{\partial W}{\partial x_m} + D_0 \sum_m \frac{\partial^2 W}{\partial x_m^2}. \tag{4.17}$$

We proceed by first performing a coordinate transformation to a frame where the bias does not appear explicitly in the equations of motion. The transformed Fokker-

Planck equation can be solved with the standard techniques described in the book by Risken [114].

Motivated by the long time solution in the deterministic case, equation (4.15), define u_m to be

$$u_m \equiv x_m - \bar{v}t - \frac{v_m - \bar{v}}{N\gamma}. \tag{4.18}$$

In the deterministic case, each $u_m(t)$ at long times goes to a constant, $\bar{x}(0)$, independent of m. For the evolution of the u_ms we have

$$\dot{u}_m = \dot{x}_m - \bar{v} = -\gamma \sum_n \left(u_m + \frac{v_m}{N\gamma} - u_n - \frac{v_n}{N\gamma} \right) + v_m - \bar{v} + \Gamma_m(t). \tag{4.19}$$

Since the mean velocity is $\bar{v} = \frac{1}{N}\sum_n v_n$, this simplifies to

$$\dot{u}_m = -\gamma \sum_n (u_m - u_n) + \Gamma_m(t). \tag{4.20}$$

The equations of motion for the u_m variables do not explicitly contain any bias. The Fokker-Planck equation for evolution of the probability distribution function in terms of the new variables u_m may be obtained either by constructing it from the transformed Langevin equations, or by transforming the partial derivatives in the untransformed Fokker-Planck equation [114]. In either case, the result is

$$\frac{\partial W'}{\partial t} = \gamma \sum_m \frac{\partial}{\partial u_m} \sum_n (u_m - u_n) W' + D_0 \sum_m \frac{\partial^2}{\partial u_m^2} W'. \tag{4.21}$$

The prime is used here simply as a reminder that we have changed to a different coordinate frame.

Before we proceed to find the solution, let us first recall the single particle Orstein-Uhlenbeck process [115, 116], which is just an overdamped harmonic oscillator with noise,

$$\dot{x} = -\gamma x + \Gamma(t) \tag{4.22}$$

again where $\Gamma(t)$ is delta-correlated Gaussian white noise with $\langle \Gamma(t)\Gamma(t') \rangle = 2D_0\delta(t - t')$. The corresponding Fokker-Planck equation is

$$\frac{\partial W}{\partial t} = \gamma \frac{\partial}{\partial x}(xW) + D_0 \frac{\partial^2 W}{\partial x^2}. \tag{4.23}$$

The standard method of solving this is to Fourier transform and solve the resulting first order partial differential equation with the method of characteristics. The solution $G(x, x', t)$ subject to a delta function initial condition $G(x, x', 0) = \delta(x - x')$ is a Gaussian distribution [114],

$$G(x, x', t) = \sqrt{\frac{\gamma}{2\pi D_0(1 - e^{-2\gamma t})}} \exp\left[-\frac{\gamma(x - x'e^{-\gamma t})^2}{2D_0(1 - e^{-2\gamma t})} \right]. \tag{4.24}$$

At long times any information about the initial condition of the system is lost and the distribution is centered around $x = 0$ due to the spring force pulling the particle to the origin. The variance σ^2 at short times is $\sigma^2 = 2D_0 t$, like in an ordinary diffusive process, but at long times becomes constant because the spring force limits the distribution from spreading further.

The Ornstein-Uhlenbeck process can be generalized to higher dimensions. A stochastic process with linear drift and constant diffusion in any number of dimensions can be called an Ornstein-Uhlenbeck process. The most general form of the Fokker-Planck equation describing such a process is [114]

$$\frac{\partial W}{\partial t} = \sum_{ij} \alpha_{ij} \frac{\partial}{\partial x_i}(x_j W) + \sum_{ij} D_{ij} \frac{\partial^2 W}{\partial x_i \partial x_j}. \tag{4.25}$$

The system described by equation (4.21), in which all particles are coupled to all others with equal strengths, is indeed a particular special case of the multivariate Ornstein-Uhlenbeck process.

One method of solving equations of this form, as described by Wang and Uhlenbeck [116] is to transform to normal mode coordinates (i.e. transform to a basis in which the matrix $\boldsymbol{\alpha}$ is diagonal), then Fourier transform the Fokker-Planck equation and solve the resulting first order partial differential equation using the method of

characteristics. An equivalent method, described in section 6.5 of the book by Risken [114], is to first Fourier transform then, knowing that the solution must be a multivariate Gaussian distribution, work out the means and the covariance matrix so that equation (4.25) is satisfied.

Although both of these methods are able to produce exact solutions to equation (4.25), such general solutions are given in terms of eigenvalues and eigenvectors of the matrix $\boldsymbol{\alpha}$. To obtain the solution more explicitly for a particular special case, one must therefore specify the form of $\boldsymbol{\alpha}$ for the system and be able to diagonalize it. We apply here the method described by Risken [114] to find explicitly the Green's function for the special case described by equation (4.21).

We wish to find the Green's function for equation (4.21), i.e. the function $G'(\{u\},\{u'\},t)$[1] that obeys equation (4.21) subject to the initial condition

$$G'(\{u\},\{u'\},t) = \prod_m \delta(u_m - u'_m). \tag{4.26}$$

Next, define the Fourier transform of G' to be

$$\hat{G}'(\{k\},\{u'\},t) \equiv \int e^{-i(k_1u_1+\cdots+k_Nu_N)} G'(\{u\},\{u'\},t) d^Nu. \tag{4.27}$$

The Fourier transform of G' at $t = 0$ is simply

$$\hat{G}'(\{k\},\{u'\},0) = \exp\left(-i\sum_m k_m u'_m\right). \tag{4.28}$$

Next, Fourier transform equation (4.21) using integration by parts to obtain

$$\frac{\partial \hat{G}'}{\partial t} = -\sum_{m,n} \alpha_{mn} k_m \frac{\partial}{\partial k_n}\hat{G}' - D_0 \sum_m k_m^2 \hat{G}' \tag{4.29}$$

where the matrix $\boldsymbol{\alpha}$ has elements

$$\alpha_{mn} = \gamma(N\delta_{mn} - 1). \tag{4.30}$$

[1] As in Risken [114], we use the notation $f(\{x\})$ to mean the function f depends on every x_m, i.e. $G'(\{u\},\{u'\},t)$ is shorthand for $G'(u_1,...,u_N,u'_1,...,u'_N,t)$.

It can be shown [114] that the solution must be a Gaussian, therefore $\hat{G}'$ has the form

$$\hat{G}'(\{k\},\{u'\},t) = \exp\left[-i\sum_m k_m M_m(t) - \frac{1}{2}\sum_{m,n} k_m k_n \sigma_{mn}(t)\right] \tag{4.31}$$

where M_m and σ_{mn} are functions of time which must be chosen so that equation (4.29) is satisfied. Taking a derivative with respect to k_n, we have

$$\frac{\partial}{\partial k_n}\hat{G}'(\{k\},\{u'\},t) = \left[-i\sum_m k_m \dot{M}_m - \frac{1}{2}\sum_{m,n} k_m k_n \dot{\sigma}_{mn}\right]\hat{G}'(\{k\},\{u'\},t). \tag{4.32}$$

Substituting this into equation (4.29) and dividing by $\hat{G}'$ gives

$$\begin{aligned} &-i\sum_m k_m \dot{M}_m - \frac{1}{2}\sum_{m,n} k_m k_n \dot{\sigma}_{mn} = \\ &\quad -\sum_{m,n} \alpha_{mn} k_m \left[-iM_n - \frac{1}{2}\sum_l k_l(\sigma_{ln}+\sigma_{nl})\right] - D_0 k_m^2. \end{aligned} \tag{4.33}$$

Rearranging, this becomes

$$\begin{aligned} &i\sum_m k_m \left[\dot{M}_m + \sum_n \alpha_{mn} M_n\right] \\ &\quad = \sum_{m,n} k_m k_n \left[-\frac{\dot{\sigma}_{mn}}{2} - \sum_l \alpha_{ml}\frac{\sigma_{ln}+\sigma_{nl}}{2} + D_0\delta_{mn}\right]. \end{aligned} \tag{4.34}$$

For this to be true for any set of k_ms, M_n and σ_{mn} must be solutions to

$$\dot{M}_m = -\sum_n \alpha_{mn} M_n = -\gamma\sum_n [M_m - M_n], \tag{4.35}$$

$$\dot{\sigma}_{mn} = -\sum_l \alpha_{ml}(\sigma_{ln}+\sigma_{nl}) + D_0\delta_{mn}. \tag{4.36}$$

At time $t = 0$, the Green's function must reduce to equation (4.28), so the initial conditions for M_m and σ_{mn} are

$$M_m(0) = u'_m. \tag{4.37}$$

$$\sigma_{mn}(0) = 0. \tag{4.38}$$

The $M_m(t)$s are evidently solutions to the deterministic problem,

$$M_m(t) = \sum_n g_{mn}(t) u'_m \tag{4.39}$$

where g_{mn} is given by

$$g_{mn}(t) = \delta_{mn} e^{-N\gamma t} + \frac{1}{N}(1 - e^{-N\gamma t}). \tag{4.40}$$

The solution to the equation for the σ_{mn}s with initial condition $\sigma_{mn}(0) = 0$ is [114]

$$\sigma_{mn}(t) = \sum_{j,l} 2D_0 \delta_{jl} \int_0^t g_{mj}(t') g_{nl}(t') dt' = 2D_0 \sum_l \int_0^t g_{ml}(t') g_{ln}(t') dt' \tag{4.41}$$

Using the g_{mn} given above, this is

$$\sigma_{mn}(t) = 2D_0 \left[\delta_{mn} \frac{1 - e^{-2N\gamma t}}{2N\gamma} + \frac{1}{N} \left(t - \frac{1 - e^{-2N\gamma t}}{2N\gamma} \right) \right]. \tag{4.42}$$

The Fourier transform may be inverted to obtain the Green's function in real space. The Fourier inverse is

$$G'(\{u\}, \{u'\}, t) = \frac{1}{(2\pi)^N} \int \hat{G}'(\{k\}, \{u'\}, t) \exp(i\mathbf{k}^T \mathbf{u}) d^N k \tag{4.43}$$

where $\mathbf{k}$ and $\mathbf{u}$ are column vectors so that $\mathbf{k}^T\mathbf{u}$ means $\sum_m k_m u_m$. Plugging in equation (4.31), this becomes

$$G'(\{u\}, \{u'\}, t) = \frac{1}{(2\pi)^N} \int \exp\left(-i\mathbf{k}^T \mathbf{M} - \frac{1}{2} \mathbf{k}^T \boldsymbol{\sigma} \mathbf{k} \right) \exp(i\mathbf{k}^T \mathbf{u}) d^N k. \tag{4.44}$$

The integration can be done using the standard formula for multidimensional Gaussian integrals,

$$\int \exp\left(-\frac{1}{2} \mathbf{x}^T \mathbf{A} \mathbf{x} + \mathbf{B}^T \mathbf{x} \right) d^N x = \sqrt{\frac{(2\pi)^N}{\det \mathbf{A}}} \exp\left(\frac{1}{2} \mathbf{B}^T \mathbf{A}^{-1} \mathbf{B} \right). \tag{4.45}$$

Using this, we have for the Green's function in real space

$$G'(\{u\}, \{u'\}, t) = \frac{1}{\sqrt{(2\pi)^N \det \boldsymbol{\sigma}}} \exp\left(-\frac{1}{2} (\mathbf{u} - \mathbf{M})^T \boldsymbol{\sigma}^{-1} (\mathbf{u} - \mathbf{M}) \right). \tag{4.46}$$

The determinant and inverse of the matrix $\boldsymbol{\sigma}$ can be calculated explicitly for this system. The matrix $\boldsymbol{\sigma}$ can be written as

$$\boldsymbol{\sigma} = 2D_0 \left(\frac{1 - e^{-2N\gamma t}}{2N\gamma} \right) \mathbf{I}_N + 2D_0 \frac{1}{N} \left(t - \frac{1 - e^{-2N\gamma t}}{2N\gamma} \right) \mathbf{J}_N. \tag{4.47}$$

where $\mathbf{I}_N$ is the NxN identity matrix and $\mathbf{J}_N$ is an NxN matrix with each element equal to one, $(\mathbf{J}_N)_{mn} = 1$. Using the fact that $\det(c\mathbf{A}) = c^N \det \mathbf{A}$ for a constant c, we have

$$\det \boldsymbol{\sigma} = (2D_0)^N \left(\frac{1 - e^{-2N\gamma t}}{2N\gamma} \right)^N \det \left[\mathbf{I}_N + \frac{1}{N} \left(\frac{2N\gamma t}{(1 - e^{-2N\gamma t})} - 1 \right) \mathbf{J}_N \right]. \tag{4.48}$$

Next, consider determinants of the form

$$\det(\mathbf{I}_N + \alpha \mathbf{J}_N). \tag{4.49}$$

The determinant of a matrix may be written as a the product of its eigenvalues, while the trace of the matrix can be written as the sum of its eigenvalues. We can therefore write

$$\det(\mathbf{I}_N + \alpha \mathbf{J}_N) = e^{\mathrm{tr}[\ln(\mathbf{I}_N + \alpha \mathbf{J}_N)]} \tag{4.50}$$

where tr denotes the trace. Using the power series expansion for $\ln(1 + x)$, we have

$$\det(\mathbf{I}_N + \alpha \mathbf{J}_N) = \exp \left\{ \mathrm{tr} \left[- \sum_{n=1}^{\infty} \frac{(-1)^n (\alpha \mathbf{J}_N)^n}{n} \right] \right\}. \tag{4.51}$$

We have for the elements of $\mathbf{J}_N^2$

$$(\mathbf{J}_N^2)_{mn} = \sum_l (\mathbf{J}_N)_{ml} (\mathbf{J}_N)_{ln} = \sum_l 1 = N \tag{4.52}$$

therefore $\mathbf{J}_N^2 = N\mathbf{J}_N$. Then, by induction we have $\mathbf{J}_N^n = N^{n-1}\mathbf{J}_N$ for integer $n \geq 1$. Putting this in, we have

$$\det(\mathbf{I}_N + \alpha \mathbf{J}_N) = \exp \left\{ - \sum_{n=1}^{\infty} \frac{(-1)^n (\alpha N)^n}{n} \frac{\mathrm{tr}\, \mathbf{J}_N}{N} \right\}. \tag{4.53}$$

The trace of $\mathbf{J}_N$ is N, so

$$\det(\mathbf{I}_N + \alpha\mathbf{J}_N) = \exp\left\{-\sum_{n=1}^{\infty}\frac{(-1)^n(\alpha N)^n}{n}\right\} = \exp\left\{\ln(1+\alpha N)\right\}. \tag{4.54}$$

Using this identity, we have finally for the determinant of $\boldsymbol{\sigma}$,

$$\det\boldsymbol{\sigma} = (2D_0t)\left(2D_0\frac{(1-e^{-2N\gamma t})}{2N\gamma}\right)^{N-1}. \tag{4.55}$$

Next, we calculate the inverse of $\boldsymbol{\sigma}$. We have

$$\boldsymbol{\sigma}^{-1} = \frac{1}{2D_0\frac{1-e^{-2N\gamma t}}{2N\gamma}}\left[\mathbf{I}_N + \frac{1}{N}\left(\frac{2N\gamma t}{1-e^{-2N\gamma t}} - 1\right)\mathbf{J}_N\right]^{-1}. \tag{4.56}$$

Consider now inverses of the form $[\mathbf{I}_N + \alpha\mathbf{J}_N]^{-1}$. Expanding this in a power series gives

$$[\mathbf{I}_N + \alpha\mathbf{J}_N]^{-1} = \sum_{n=0}^{\infty}(-1)^n(\alpha\mathbf{J}_N)^n. \tag{4.57}$$

Using $\mathbf{J}_N^0 = \mathbf{I}_N$ and $\mathbf{J}_N^n = N^{n-1}\mathbf{J}_N$ for $n \geq 1$, this becomes

$$[\mathbf{I}_N + \alpha\mathbf{J}_N]^{-1} = \mathbf{I}_N + \frac{\mathbf{J}_N}{N}\sum_{n=1}^{\infty}(-1)^n(\alpha N)^n. \tag{4.58}$$

Summing the series gives

$$\begin{aligned}[\mathbf{I}_N + \alpha\mathbf{J}_N]^{-1} &= \mathbf{I}_N + \frac{\mathbf{J}_N}{N}\left[\sum_{n=0}^{\infty}(-1)^n(\alpha N)^n - 1\right] \\ &= \mathbf{I}_N + \frac{\mathbf{J}_N}{N}\left[\frac{-\alpha N}{1+\alpha N}\right].\end{aligned} \tag{4.59}$$

Using this to compute the inverse of $\boldsymbol{\sigma}$ gives finally

$$\boldsymbol{\sigma}^{-1} = \frac{2N\gamma}{2D_0(1-e^{-2N\gamma t})}\left(\mathbf{I}_N - \frac{\mathbf{J}_N}{N}\right) + \frac{\mathbf{J}_N}{2ND_0t}. \tag{4.60}$$

Inserting $M_m(t) = u'_m e^{-N\gamma t} + \bar{u}'(1-e^{-N\gamma t})$ where $\bar{u}' \equiv \frac{1}{N}\sum_m u'_m$ and the results for

$\det \boldsymbol{\sigma}$ and $\boldsymbol{\sigma}^{-1}$ into equation (4.46), the Green's function in real (u_m) space is finally

$$G'(\{u\},\{u'\},t) = \frac{1}{\sqrt{4\pi D_0 t \left(2\pi D_0 \frac{1-e^{-2N\gamma t}}{N\gamma}\right)^{N-1}}}$$
$$\cdot \exp\left\{ -\frac{N\gamma}{2D_0(1-e^{-2N\gamma t})} \sum_m \left[u_m - u'_m e^{-N\gamma t} - \bar{u}'(1-e^{-N\gamma t})\right]^2 \right.$$
$$\left. - \left(\frac{1}{4D_0 t} - \frac{N\gamma}{2D_0(1-e^{-2N\gamma t})}\right) \frac{1}{N} \left(\sum_m u_m - u'_m e^{-N\gamma t} - \bar{u}'(1-e^{-N\gamma t})\right)^2 \right\}. \tag{4.61}$$

Since the Jacobian matrix of the transformation from x_m variables to u_m variables has unit determinant, the Green's function back in x_m coordinates may be found now simply by substituting back

$$u_m = x_m - \bar{v}t - \frac{v_m - \bar{v}}{N\gamma}. \tag{4.62}$$

Although the general expression (4.46) for the real space Green's function for a multivariate Ornstein-Uhlenbeck process in terms of the covariance matrix $\boldsymbol{\sigma}$ and the vector $\mathbf{M}$ can be found in earlier literature (see page 156 in ref. [114]), the author does not know of any published work containing the explicit expressions for $\det \boldsymbol{\sigma}$, $\boldsymbol{\sigma}^{-1}$, and the real space Green's function, equations (4.55), (4.60), and (4.61), for the particular system described here.

Now that the Green's function is known, for any given initial condition $W(\{x\},0)$ the probability distribution as a function of time can be determined from

$$W(\{x\},t) = \int G(\{x\},\{x'\},t) W(\{x'\},t) d^N x, \tag{4.63}$$

and the average of any observable O can be calculated from

$$\langle O \rangle = \int O(\{x\}) W(\{x\},t) d^N x. \tag{4.64}$$

To gain a better understanding of noisy dynamics, let us now look at two coarse-grained quantities: the center of mass distribution function and the single particle distribution functions.

The center of mass distribution function $P(\bar{x},t)$ we define so that the probability to find the center of mass $\bar{x} \equiv \frac{1}{N}\sum_m x_m$ in a small interval between $\bar{x}$ and $\bar{x}+d\bar{x}$ at time t is $P(\bar{x},t)d\bar{x}$.

We can determine the evolution of the center of mass distribution function easily by returning to the Langevin equations. Summing equation (4.5) on m, and dividing by $1/N$, we have

$$\dot{\bar{x}} = \bar{v} + \bar{\Gamma}(t) \tag{4.65}$$

where $\bar{\Gamma}(t) \equiv \frac{1}{N}\sum_m \Gamma_m(t)$. Since $\langle \bar{\Gamma}(t)\bar{\Gamma}(t')\rangle = \frac{2D_0}{N}\delta(t-t')$, the center of mass distribution obeys simply an advection diffusion equation,

$$\frac{\partial}{\partial t}P(\bar{x},t) = -\bar{v}\frac{\partial}{\partial \bar{x}}P(\bar{x},t) + \frac{D_0}{N}\frac{\partial^2}{\partial \bar{x}^2}P(\bar{x},t). \tag{4.66}$$

For a delta function initial condition, the distribution as a function of time is a Gaussian centered at $\bar{x} = \bar{x}' + \bar{v}t$ with a variance which increases proportional to time, $\sigma^2 = 2D_0 t/N$.

Next, consider the single particle distribution functions $P_m^{(1)}(x,t)$. We define these so that $P_m^{(1)}(x,t)dx_m$ is the probability to find the mth particle in a small interval between x_m and $x_m + dx_m$ at time t, regardless of where any of the other particles are found. These can be obtained from the full distribution function by integrating out all variables except for one,

$$P_m^{(1)}(x,t) = \int \delta(x-x_m)W(\{x\},t)d^N x. \tag{4.67}$$

We will calculate now the single particle distribution functions for a delta function initial condition. Instead of performing a difficult integral on equation (4.61), it is simpler to return to the Fourier transformed expression, set every k_n except k_m to zero, then invert the remaining transform. This works because the Fourier transform of a function f at $k=0$ is simply its integral,

$$\hat{f}(k=0) = \int_{-\infty}^{\infty} f(x)dx. \tag{4.68}$$

Furthermore, we can use the expressions in u_m coordinates and change back to x_m coordinates at the end since each u_m is related to each x_m by only a translation. Using equation (4.31) and setting all but one k_m to zero, we have

$$\hat{P}_m'^{(1)} = \exp\left(-ik_m M_m - \frac{1}{2}k_m^2 \sigma_{mm}\right). \tag{4.69}$$

(with a prime to remind us that we are still in u_m coordinates). Inverting the Fourier transform gives

$$P_m'^{(1)} = \frac{1}{\sqrt{2\sigma_{mm}}} \exp\left(-\frac{(u_m - M_m)^2}{2\sigma_{mm}}\right). \tag{4.70}$$

Finally, inserting the values calculated earlier for M_m and σ_{mm} and changing back to x_m coordinates, the single particle distribution function for the mth particle is

$$P_m^{(1)}(x,t) = \frac{\exp\left(\frac{-[x_m - x_m' e^{-N\gamma t} - \bar{x}'(1-e^{-N\gamma t}) - v_m\tau - \bar{v}(t-\tau)]^2}{2S(t)}\right)}{\sqrt{2\pi S(t)}} \tag{4.71}$$

where we have defined the variance $S(t)$ to be

$$S(t) \equiv 2D_0\left[\frac{t}{N} + (1 - 1/N)\frac{1 - e^{-2N\gamma t}}{2N\gamma}\right] \tag{4.72}$$

and τ has units of time and is related to t by

$$\tau \equiv \frac{1 - e^{-N\gamma t}}{N\gamma}. \tag{4.73}$$

Our expression (4.71) for the single particle distribution function for this particular system, which follows from the known result (4.31) by inserting the $\mathbf{M}$ and $\boldsymbol{\sigma}$ calculated here, is apparently a new result.

At short times $\tau \approx t$, but at long times τ goes to a constant, $1/(N\gamma)$. The distribution is again a Gaussian, centered at the position where the particle would be deterministically, $x_m = x_m' e^{-N\gamma t} + \bar{x}'(1 - e^{-N\gamma t}) + v_m\tau + \bar{v}(t - \tau)$. At short times, the variance is

$$S(t) \approx 2D_0 t, \tag{4.74}$$

which is characteristic of diffusive motion with an effective diffusion constant D_0. At long times; however, the variance becomes

$$S(t) \approx \frac{2D_0 t}{N} + \text{constant} \tag{4.75}$$

so the effective diffusion constant at long times is reduced to D_0/N. This is due to the fact that the internal spring coordinates have stopped spreading (as in the 1D Orstein-Uhlenbeck process), but the center of mass is still diffusing with effective diffusion constant D_0/N.

4.4 A Mean Field Approach in the Presence of Noise

We will now rederive our results for the center of mass and single particle distribution functions in a different manner. In our calculation of the deterministic dynamics we already showed that we could view each particle as being coupled only to the center of mass. Instead of solving the full N particle problem, we now treat the group as an effective two particle system consisting of a single particle from the group and a center of mass particle. This is reminiscent of "mean field" calculations in statistical mechanics in which the interaction with other particles is replaced with a mean field (in this case, the center of mass acts as the field). In this system, since each particle is coupled to all others, there is no need to make any approximations; the calculation is exact.

The Langevin equations for the evolution of the position of the mth particle in the group, x_m, and the center of mass position are

$$\dot{x}_m = -N\gamma(x_m - \bar{x}) + v_m + \Gamma_m(t), \tag{4.76}$$

$$\dot{\bar{x}} = \bar{v} + \bar{\Gamma}(t) \tag{4.77}$$

where $\bar{\Gamma}(t) \equiv \frac{1}{N}\sum_m \Gamma_m(t)$. We treat this now as a two variable (x_m and $\bar{x}$) system. Care must be taken when constructing the Fokker-Planck equation for this system since the noises Γ_m and $\bar{\Gamma}$ are correlated,

$$\begin{aligned}\langle \Gamma_m(t)\bar{\Gamma}(t')\rangle &= \langle \bar{\Gamma}(t)\Gamma_m(t')\rangle \\ &= \frac{1}{N}\sum_n \langle \Gamma_m(t)\Gamma_n(t')\rangle \\ &= \frac{2D_0}{N}\delta(t-t') \end{aligned} \tag{4.78}$$

where we have used $\langle \Gamma_m(t)\Gamma_n(t')\rangle = 2D_0\delta_{mn}\delta(t-t')$.

Using this, the Fokker-Planck equation for the distribution $W(x_m, \bar{x}, t)$ is

$$\begin{aligned}\frac{\partial W}{\partial t} = &\frac{\partial}{\partial x_m}(N\gamma x_m - N\gamma\bar{x} - v_m)W - \bar{v}\frac{\partial}{\partial \bar{x}}W \\ &+ D_0\frac{\partial^2}{\partial x_m^2}W + \frac{D_0}{N}\frac{\partial^2}{\partial \bar{x}^2}W + \frac{2D_0}{N}\frac{\partial^2}{\partial x_m \partial \bar{x}}W. \end{aligned} \tag{4.79}$$

The mixed partial derivative term is a consequence of the nonzero correlation between Γ_m and $\bar{\Gamma}$. This Fokker-Planck equation can be solved by performing two change of variable transformations. Firstly, we use again our transformation to u_m variables to remove the bias,

$$u_m \equiv x_m - \bar{v}t - \frac{v_m - \bar{v}}{N\gamma}. \tag{4.80}$$

The Langevin equations for u_m and $\bar{u}$ become

$$\dot{u}_m = -N\gamma(u_m - \bar{u}) + \Gamma_m(t), \tag{4.81}$$

$$\dot{\bar{u}} = \bar{\Gamma}(t). \tag{4.82}$$

The transformed Fokker-Planck equation (which again may be obtained either by transforming the partial derivatives in the old Fokker-Planck equation, or constructed directly from the transformed Langevin equations) is

$$\frac{\partial W'}{\partial t} = N\gamma\frac{\partial}{\partial u_m}(u_m - \bar{u})W' + D_0\frac{\partial^2}{\partial u_m^2}W' + \frac{D_0}{N}\frac{\partial^2}{\partial \bar{u}^2}W' + \frac{2D_0}{N}\frac{\partial^2}{\partial u_m \partial \bar{u}}W'. \tag{4.83}$$

The prime is used as a reminder that we have changed to a different set of variables. This is again classified as an Ornstein-Uhlenbeck process, but with only two variables instead of N as before. Although this Fokker-Planck equation can be solved directly using standard methods, it is simpler to perform one further change of variables by introducing the displacement y between u_m and $\bar{u}$,

$$y \equiv u_m - \bar{u} \tag{4.84}$$

which obeys the equation of motion

$$\dot{y} = -N\gamma y + \Gamma_m(t) - \bar{\Gamma}(t). \tag{4.85}$$

The Fokker-Planck equation in y and $\bar{u}$ coordinates is then

$$\frac{\partial W''}{\partial t} = N\gamma \frac{\partial^2}{\partial y^2} y W'' + D_0 \left(1 - \frac{1}{N}\right) \frac{\partial^2}{\partial y^2} W'' + \frac{D_0}{N} \frac{\partial^2}{\partial \bar{u}^2} W'' \tag{4.86}$$

where we have written two primes since we have changed variables twice. This Fokker-Planck equation is much easier to solve, since through the transformations we have removed both the bias and the mixed partial derivative terms. Since the right hand side is a sum of terms which contain only y and $\bar{u}$ separately, the solution can be written as a product. The y part is an ordinary 1D Ornstein-Uhlenbeck process, and the $\bar{u}$ part is simply a Wiener (diffusion) process. The Green's function can be written down from the known solutions for the two processes,

$$G''(y, \bar{u}, y', \bar{u}', t) = \frac{1}{\sqrt{2\pi S_y(t)}} \exp\left[-\frac{(y - y' e^{-N\gamma t})^2}{2S_y(t)}\right] \frac{1}{\sqrt{2\pi S_{\bar{u}}(t)}} \exp\left[-\frac{(\bar{u} - \bar{u}')^2}{2S_{\bar{u}}(t)}\right]. \tag{4.87}$$

where

$$S_y(t) \equiv \frac{D_0(1 - 1/N)(1 - e^{-2N\gamma t})}{N\gamma}, \tag{4.88}$$

$$S_{\bar{u}}(t) \equiv \frac{2D_0 t}{N}. \tag{4.89}$$

Integrating out the y variable and changing from $\bar{u}$ to $\bar{x}$ reproduces the same center of mass distribution as calculated earlier, a Gaussian drifting at velocity $\bar{v}$ with variance $2D_0 t/N$.

To obtain the single particle distribution, we should first return to u_m and $\bar{u}$ coordinates since y depends on $\bar{u}$,

$$G'(u_m, \bar{u}, u'_m, \bar{u}', t) = \frac{1}{\sqrt{2\pi S_y(t)}} \exp\left[-\frac{[u_m - \bar{u} - (u'_m - \bar{u}')e^{-N\gamma t}]^2}{2S_y(t)}\right] \cdot \frac{1}{\sqrt{2\pi S_{\bar{u}}(t)}} \exp\left[-\frac{(\bar{u} - \bar{u}')^2}{2S_{\bar{u}}(t)}\right]. \tag{4.90}$$

Now $\bar{u}$ can be integrated out using a Gaussian integral. The result is

$$\int_{-\infty}^{\infty} G'(u_m, \bar{u}, u'_m, \bar{u}', t) d\bar{u} = \frac{1}{\sqrt{2\pi S(t)}} \exp\left[-\frac{[u_m - u'_m e^{-N\gamma t} + \bar{u}'(1 - e^{-N\gamma t})]^2}{2S(t)}\right] \tag{4.91}$$

with $S(t)$ as defined earlier,

$$S(t) \equiv 2D_0 \left[\frac{t}{N} + (1 - 1/N)\frac{1 - e^{-2N\gamma t}}{2N\gamma}\right]. \tag{4.92}$$

Finally, changing back to x_m coordinates, we obtain the same result as before for the single particle distribution functions,

$$P_m^{(1)}(x, t) = \frac{\exp\left(\frac{-[x_m - x'_m e^{-N\gamma t} - \bar{x}'(1 - e^{-N\gamma t}) - v_m \tau - \bar{v}(t - \tau)]^2}{2S(t)}\right)}{\sqrt{2\pi S(t)}} \tag{4.93}$$

with again $\tau \equiv (1 - e^{-N\gamma t})/(N\gamma)$.

Although we derived again the same results for the center of mass distribution and the single particle distributions in a simpler way, this method does not allow for the calculation of two particle observables, for example $\langle x_m x_n \rangle$. To calculate such observables, one must use the full solution derived in the previous section.

This "mean field" calculation could be used as a starting point for constructing approximate solutions when the full problem cannot be solved exactly, for example when the interactions are more complicated.

4.5 Time Evolution of the Density

Next, we look at another coarse-grained quantity: the density. Like the center of mass distribution and the single particle distributions, the density $\rho(x, t)$ is a continuous

function of space and time. We define the density per particle $\rho(x,t)$ so that the probability to find any particle in a small interval between x and $x+dx$ divided by the total number of particles N is $\rho(x,t)dx$. Defined in this way, the density is simply the average of the single particle distribution functions,

$$\rho(x,t) = \frac{1}{N}\sum_m P_m^{(1)}(x,t) = \frac{1}{N}\sum_m \int \delta(x-x_m)W(\{x\},t)d^N x. \tag{4.94}$$

In order to connect this model with continuum models in the literature, we seek to write a continuum equation of motion for the evolution of the density. One method of doing this is to determine a linear, time independent, idempotent projection operator $\mathcal{P}$ which performs the coarse graining, then apply the Zwanzig projection operator approach described in Chapter 2 to write an equation of motion for the coarse grained quantity $\mathcal{P}W$. Although such a projection operator can be constructed, it remains difficult to calculate explicitly the evolution equation using this method. Instead, we use our full solution to write the density as a function of time, then work backwards to find an equation of motion which it obeys. Before we do this however, we must pause and discuss initial conditions.

4.5.1 Initial Conditions

Since the density per particle $\rho(x,t)$ is a coarse-grained quantity, it should not be surprising that the density at time $t=0$, $\rho(x,0)$ is not enough to uniquely determine the density at all later times $\rho(x,t)$; the full initial distribution $W(\{x\},0)$ must be known. We will see this explicitly by looking at two types of initial distributions $W(\{x\},0)$ which give the same initial density $\rho(x,0)$ but different densities at later times.

What sort of initial condition should we use? We should not give any particular particle special treatment, so the initial condition should be symmetric in every x_m. Furthermore, if we wish to write an evolution equation which is linear, the density as

a function of time must depend linearly on the initial density. We will see that for a particular class of initial conditions, the evolution is indeed linear.

One obvious distribution which is symmetric in every x_m is simply a product:

$$W(\{x\},0) = \prod_m f(x_m) \tag{4.95}$$

where f is a function with unit integral,

$$\int_{-\infty}^{\infty} f(x)dx = 1. \tag{4.96}$$

It is easy to see that the single particle distribution functions are initially $P_m^{(1)}(x,0) = f(x)$, and so the density per particle at time $t = 0$ is also

$$\rho(x,0) = f(x). \tag{4.97}$$

For this type of initial condition, the positions of any two particles are uncorrelated at time $t = 0$ in the sense that

$$\langle x_m x_n \rangle - \langle x_m \rangle \langle x_n \rangle = 0. \tag{4.98}$$

The evolution of the probability distribution for this class of initial conditions is

$$W(\{x\},t) = \int G(\{x\},\{x'\},t) \prod_m f(x_m) d^N x' \tag{4.99}$$

and the density evolves in time as

$$\rho(x,t) = \int g(x,\{x'\},t) \prod_m \rho(x_m,0) d^N x' \tag{4.100}$$

where g depends on x, every x'_m, and time, and is related to the full Green's function G through

$$g(x,\{x'\},t) = \frac{1}{N} \sum_m \int \delta(x - x_m) G(\{x\},\{x'\},t) d^N x. \tag{4.101}$$

For this class of initial condition, we see that the density at later times depends nonlinearly on the initial density. Consequently, it will be impossible to write a linear equation of motion for the density in this case.

We will now look at a different class of initial conditions and show that it does result in the density evolving linearly. Consider initial conditions of the form

$$W(\{x\},0) = f(x_1)\prod_{m=1}^{N-1}\delta(x_{m+1}-x_m) \tag{4.102}$$

where f is again a normalized function. Again, this initial condition gives the same single particle distribution functions at time $t=0$, $P_m^{(1)}(x,t) = f(x)$, and therefore the same initial density

$$\rho(x,0) = f(x). \tag{4.103}$$

How does this differ from the previous case? For this kind of initial distribution, the delta functions ensure that at time 0 if any particle m is found at some position x, *all other particles must be found there as well*, i.e. the particles all exist together in a cluster. The location of the cluster of particles itself is determined by the function f. In this case, the correlation $\langle x_m x_n\rangle - \langle x_m\rangle\langle x_n\rangle$ does *not* vanish at $t=0$.

Let us make this more clear by looking at a specific example for $N=2$ particles. Choose the function f to be simply a sum of two delta functions,

$$f(x) = \frac{1}{2}\delta(x-a) + \frac{1}{2}\delta(x-b). \tag{4.104}$$

For the first kind of initial condition, we have

$$\begin{aligned} W(x_1,x_2,0) = f(x_1)f(x_2) = \frac{1}{4}[&\delta(x_1-a)\delta(x_2-a) + \delta(x_1-a)\delta(x_2-b) \\ &+ \delta(x_1-b)\delta(x_2-a) + \delta(x_1-b)\delta(x_2-b)]. \end{aligned} \tag{4.105}$$

Each of the following have a 1/4 probability to occur:

- Both particles at $x=a$
- Both particles at $x=b$
- Particle 1 at $x=a$ and particle 2 at $x=b$

- Particle 2 at $x = a$ and particle 1 at $x = b$

For the second kind of initial condition with the same f, the initial distribution becomes

$$\begin{aligned} W(x_1, x_2, 0) &= f(x_1)\delta(x_1 - x_2) \\ &= \frac{1}{2}[\delta(x_1 - a)\delta(x_2 - a) + \delta(x_1 - b)\delta(x_2 - b)]. \end{aligned} \tag{4.106}$$

In this case, only two possibilities can occur (each with probability 1/2):

- Both particles at $x = a$
- Both particles at $x = b$

Unlike in the previous case, the particles cannot be found physically separated from each other at time $t = 0$; they must be found together.

We show now that the second kind of initial condition results in the density evolving linearly in time. For the initial condition $W(\{x\}, 0) = f(x_1)\prod_{m=1}^{N-1}\delta(x_{m+1} - x_m)$, the distribution evolves as

$$\frac{\partial W}{\partial t} = \int G(x_1, ..., x_N, x', ..., x', t)f(x')dx', \tag{4.107}$$

and the density as a function of time is

$$\rho(x, t) = \int_{-\infty}^{\infty} \mathcal{G}(x, x', t)\rho(x', 0)dx' \tag{4.108}$$

where the function $\mathcal{G}$ is related to the full Green's function through

$$\mathcal{G}(x, x', t) = \frac{1}{N}\sum_m \int \delta(x - x_m)G(x_1, ..., x_N, x', ..., x', t)d^N x. \tag{4.109}$$

We have found two different classes of initial conditions, both of which give the same density at time $t = 0$, but different densities at later times. The second type results in a linear evolution of the density, equation (4.108). This is not necessarily the only class of initial conditions which gives linear evolution of the density, but it does seem to be the simplest.

4.5.2 Linear Evolution Equations from the Green's Function

Before we proceed to calculate $\mathcal{G}$ for this model, let us first see how a linear evolution equation can be written once the Green's function $\mathcal{G}$ is known. There are two equivalent ways to do this: a *time-dependent* way and *memory* way. The precise meaning of these terms will soon become clear. This discussion is based on work by Kenkre and Sevilla [117].

We assume that the system is translationally invariant, i.e. the entire system can be translated by an arbitrary amount without changing the dynamics. In this case $\mathcal{G}(x, x', t)$ depends only on $x - x'$ and t, and equation (4.108) becomes

$$\rho(x,t) = \int_{-\infty}^{\infty} \mathcal{G}(x - x', t)\rho(x', 0)dx'. \tag{4.110}$$

For a function ρ which depends on x and t and evolves linearly according to equation (4.110), a completely general equation of motion is

$$\frac{\partial}{\partial t}\rho(x,t) = \int_{-\infty}^{\infty} \mathcal{K}(x - x', t)\rho(x', t)dx'. \tag{4.111}$$

This is the *time-dependent* way of writing the evolution. We will prove that this is indeed general by showing that the kernel $\mathcal{K}$ can be expressed in terms of the Green's function $\mathcal{G}$. First, Fourier transform equation (4.110) to obtain

$$\hat{\rho}(k,t) = \hat{\mathcal{G}}(k,t)\hat{\rho}(0) \tag{4.112}$$

where we have used the fact that a convolution in x-space becomes a product in k-space. Taking a time derivative gives

$$\frac{\partial}{\partial t}\hat{\rho}(k,t) = \hat{\rho}(0)\frac{\partial}{\partial t}\hat{\mathcal{G}}(k,t) = \hat{\rho}(k,t)\frac{1}{\hat{\mathcal{G}}(k,t)}\frac{\partial}{\partial t}\hat{\mathcal{G}}(k,t). \tag{4.113}$$

where equation (4.112) has been used to eliminate $\hat{\rho}(k, 0)$. On the other hand, Fourier transforming equation (4.111) gives

$$\frac{\partial}{\partial t}\hat{\rho}(k,t) = \hat{\mathcal{K}}(k,t)\hat{\rho}(k,t). \tag{4.114}$$

Comparing the two, the kernel must be related to the Green's function in the Fourier domain by

$$\hat{\mathcal{K}}(k,t) = \frac{1}{\hat{\mathcal{G}}(k,t)}\frac{\partial}{\partial t}\hat{\mathcal{G}}(k,t) = \frac{\partial}{\partial t}\ln\hat{\mathcal{G}}(k,t). \tag{4.115}$$

In order to connect with existing work in the literature in which an advection-diffusion equation with memory is used as a continuum equation of motion, we have also investigated equations of motion with memory. The most general equation ofw motion with memory when the evolution is linear and translationally invariant is

$$\frac{\partial}{\partial t}\rho(x,t) = \int_0^t \int_{-\infty}^{\infty} \mathcal{M}(x-x',t-t')\rho(x',t')dx'dt'. \tag{4.116}$$

The function $\mathcal{M}$ is a kind of memory as it connects the evolution at time t with the state of the system at previous times. Again, we show that this is indeed completely general by expressing the memory $\mathcal{M}$ in terms of the Green's function $\mathcal{G}$. Fourier and Laplace transforming (4.110) gives

$$\breve{\rho}(k,\epsilon) = \breve{\mathcal{G}}(k,\epsilon)\hat{\rho}(k,0) \tag{4.117}$$

where the breve denotes joint Fourier-Laplace transform. Multiply by ϵ and subtract $\hat{\rho}(k,0)$ to obtain

$$\epsilon\breve{\rho}(k,\epsilon) - \hat{\rho}(k,0) = [\epsilon\breve{\mathcal{G}}(k,\epsilon) - 1]\hat{\rho}(k,0) = \frac{[\epsilon\breve{\mathcal{G}}(k,\epsilon) - 1]}{\breve{\mathcal{G}}(k,\epsilon)}\breve{\rho}(k,\epsilon) \tag{4.118}$$

where equation (4.117) has been used to eliminate $\hat{\rho}(k,0)$ on the right hand side. Now, compare this with the Fourier-Laplace transform of equation (4.116),

$$\epsilon\breve{\rho}(k,\epsilon) - \hat{\rho}(k,0) = \breve{\mathcal{M}}(k,\epsilon)\breve{\rho}(k,\epsilon) \tag{4.119}$$

to see that the memory $\mathcal{M}$ is related to the Green's function $\mathcal{G}$ in the Fourier-Laplace domain by

$$\breve{\mathcal{M}}(k,\epsilon) = \epsilon - \frac{1}{\breve{\mathcal{G}}(k,\epsilon)}. \tag{4.120}$$

We may furthermore relate the time-dependent kernel $\mathcal{K}$ to the memory $\mathcal{M}$ by first solving equation (4.115) for $\hat{\mathcal{G}}$,

$$\hat{\mathcal{G}}(k,t) = \exp\left[\int_0^t \hat{\mathcal{K}}(k,t')dt'\right] \tag{4.121}$$

then Laplace transforming it,

$$\breve{\mathcal{G}}(k,\epsilon) = \int_0^\infty e^{-\epsilon t} \exp\left[\int_0^t \hat{\mathcal{K}}(k,t')dt'\right] dt \tag{4.122}$$

and substituting into equation (4.120),

$$\breve{\mathcal{M}}(k,\epsilon) = \epsilon - \frac{1}{\int_0^\infty e^{-\epsilon t} \exp\left[\int_0^t \hat{\mathcal{K}}(k,t')dt'\right] dt}. \tag{4.123}$$

In both of these cases, the evolution can be expressed in a more familiar form, in terms of x derivatives of ρ, by Fourier transforming and expanding in powers of ik. Doing this for both the time-dependent and memory versions, we have

$$\frac{\partial}{\partial t}\hat{\rho}(k,t) = \sum_{m=0}^\infty \frac{(ik)^m}{m!} \frac{\partial^m \hat{\mathcal{K}}(k,t)}{\partial (ik)^m}\bigg|_{k=0} \hat{\rho}(k,t), \tag{4.124}$$

$$\frac{\partial}{\partial t}\hat{\rho}(k,t) = \int_0^t \sum_{m=0}^\infty \frac{(ik)^m}{m!} \frac{\partial^m \hat{\mathcal{M}}(k,t-t')}{\partial (ik)^m}\bigg|_{k=0} \hat{\rho}(k,t')dt'. \tag{4.125}$$

The Fourier transform can be inverted since

$$\frac{\partial^m}{\partial x^m}\rho(x,t) = \frac{\partial^m}{\partial x^m}\frac{1}{2\pi}\int_{-\infty}^\infty e^{ikx}\hat{\rho}(k,t)dk = \frac{1}{2\pi}\int_{-\infty}^\infty (ik)^m e^{ikx}\hat{\rho}(k,t)dk, \tag{4.126}$$

so we have

$$\frac{\partial}{\partial t}\rho(x,t) = \sum_{m=0}^\infty \frac{1}{m!} \frac{\partial^m \hat{\mathcal{K}}(k,t)}{\partial (ik)^m}\bigg|_{k=0} \frac{\partial^m \rho(x,t')}{\partial x^m}, \tag{4.127}$$

$$\frac{\partial}{\partial t}\rho(x,t) = \int_0^t \sum_{m=0}^\infty \frac{1}{m!} \frac{\partial^m \hat{\mathcal{M}}(k,t-t')}{\partial (ik)^m}\bigg|_{k=0} \frac{\partial^m \rho(x,t')}{\partial x^m}dt'. \tag{4.128}$$

Since the integral of ρ over all space must remain constant in time (because of conservation of probability), the $m = 0$ term must vanish in both cases. We can also express the expansion coefficients in terms of moments with the identity

$$\frac{\partial^m}{\partial (ik)^m}\hat{f}(k)\bigg|_{k=0} = \frac{\partial^m}{\partial (ik)^m}\int_{-\infty}^\infty e^{-ikx} f(x)dx\bigg|_{k=0} = \int_{-\infty}^\infty (-x)^m f(x)dx. \tag{4.129}$$

Using this, the expansion coefficients can be written

$$\left.\frac{\partial^m \hat{\mathcal{K}}(k,t)}{\partial(ik)^m}\right|_{k=0} = \int_{-\infty}^{\infty} (-x)^m \mathcal{K}(x,t)dx, \tag{4.130}$$

$$\left.\frac{\partial^m \hat{\mathcal{M}}(k,t-t')}{\partial(ik)^m}\right|_{k=0} = \int_{-\infty}^{\infty} (-x)^m \mathcal{M}(x,t-t')dx. \tag{4.131}$$

We have succeeded in constructing two different linear equations of motion which can be constructed from the Green's function $\mathcal{G}$. Although both approaches are equally valid and yield equivalent dynamics, one representation may be more convenient, for example if one of the series (4.127) or (4.128) terminates after a finite number of terms. According to the Pawula theorem [118], the series in the time-dependent case, equation (4.127), either terminates after one or two terms or contains infinitely many terms. The author does not know at present whether a similar result exists for the memory evolution, equation (4.128). It was however shown in ref. [117] that except in certain very special cases, if one of the series terminates, the other does not. This can be seen from equation (4.123). One of the representations (the one with a terminating series) may therefore be more convenient depending on the particular system under consideration.

In some cases, as we will see, *neither* series terminates after a finite number of terms. However, *approximate* equations of motion can always be written simply by dropping all terms past the second derivative. In both cases, doing this preserves the first and second moments of ρ, but higher moments can be wrong. This can be seen by formally solving equations (4.111) and (4.116) and showing that the first two moments depend only on the first two expansion coefficients (and higher moments depend on higher order expansion coefficients).

It should be noted that the two truncated series will in general result in different evolution for ρ depending on which version is used. The truncated versions of (4.127) and (4.128) are approximate equations of motion which in general are *not* equivalent, so the two truncated series should therefore be viewed as two completely different

approximations. To determine which approximation reproduces the true distribution more accurately (in some sense which must be made clear), one must investigate the behavior of the third and higher moments.

4.5.3 Evolution of the Density in the Absence of Bias

We will now derive equations of motion for the density per particle $\rho(x,t)$ in the absence of bias (i.e. each v_m is set to zero). We restrict ourselves to the second class of initial conditions discussed in the previous section, equation (4.102), to ensure that the evolution is linear. We will see that this equation of motion is most conveniently written as a diffusion equation with a time-dependent diffusion coefficient.

For an initial condition in which all particles begin at x', the quantity $\mathcal{G}$ appearing in equations (4.108) and (4.109) is (using equation (4.71), the earlier result for the single particle distribution functions)

$$\mathcal{G}(x-x',t) = \frac{1}{\sqrt{2\pi S(t)}} \exp\left(\frac{-[x-x']^2}{2S(t)}\right), \tag{4.132}$$

so using equation (4.108), the evolution of the density is

$$\rho(x,t) = \int_{-\infty}^{\infty} \frac{1}{\sqrt{2\pi S(t)}} \exp\left(\frac{-[x-x']^2}{2S(t)}\right) \rho(x',0)dx'. \tag{4.133}$$

The density $\rho(x,t)$ for a delta function initial condition is plotted in Figure 4.1.

We can now write an equation of motion for the evolution of the density. Since the solution to the diffusion equation

$$\frac{\partial P}{\partial t} = D\frac{\partial P}{\partial x^2} \tag{4.134}$$

is

$$P(x,t) = \int_{-\infty}^{\infty} \frac{1}{\sqrt{4\pi Dt}} \exp\left(\frac{-[x-x']^2}{4Dt}\right) P(x',0)dx', \tag{4.135}$$

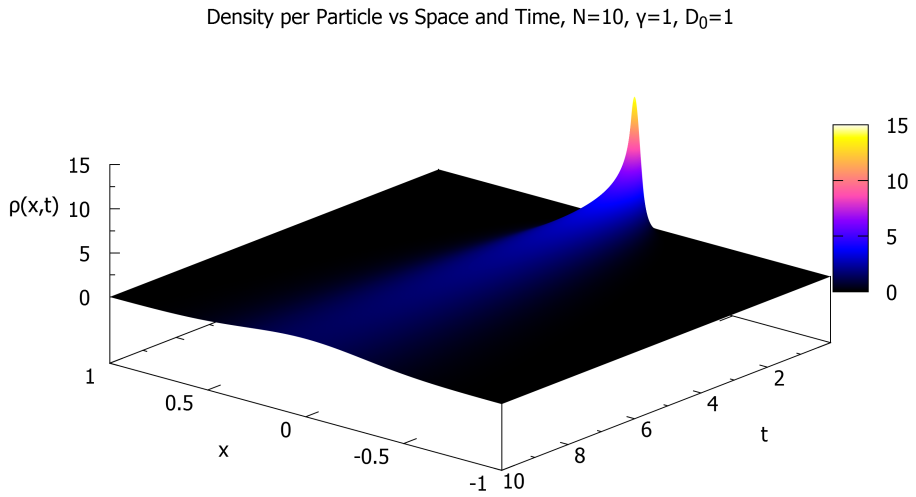

Figure 4.1: Density per particle as a function of time in the simple model of centering without bias for a delta function initial condition.

it is easy to see that the density obeys

$$\frac{\partial \rho}{\partial S} = \frac{1}{2}\frac{\partial^2 \rho}{\partial x^2}. \tag{4.136}$$

Using the chain rule, we can rewrite this as a diffusion equation with a time dependent diffusion coefficient,

$$\frac{\partial \rho}{\partial t} = D_0 \chi(t) \frac{\partial^2 \rho}{\partial x^2} \tag{4.137}$$

with

$$\chi(t) = \frac{1}{2D_0}\frac{dS}{dt} = e^{-2N\gamma t} + \frac{1}{N}(1 - e^{-2N\gamma t}). \tag{4.138}$$

As we saw earlier, at short times the effective diffusion constant is D_0, but at long times the springs counteract the spreading caused by the thermal noise, and the effective diffusion constant is reduced to D_0/N (since the center of mass still diffuses).

We could have derived this in a different way using the expressions obtained in

the previous section. The Fourier transformed Green's function is

$$\hat{\mathcal{G}}(k,t) = \exp\left[-\frac{k^2 S(t)}{2}\right] \tag{4.139}$$

so using equation (4.115), we have

$$\hat{\mathcal{K}}(k,t) = \frac{\partial}{\partial t}\ln\hat{\mathcal{G}}(k,t) = -k^2\frac{1}{2}\frac{dS}{dt}. \tag{4.140}$$

Inserting this into the expansion (4.127) gives again equation (4.137).

In this case, it is more convenient to write the evolution equation as a time-dependent diffusion equation; however, using the results from the previous section we can reformulate the evolution as a memory equation. To do this, we must calculate the joint Fourier-Laplace transform of the Green's function,

$$\begin{aligned}\breve{\mathcal{G}}(k,\epsilon) &= \int_0^\infty e^{-\epsilon t}\hat{\mathcal{G}}(k,t)dt = \int_0^\infty e^{-\epsilon t}\exp\left[-\frac{k^2 S(t)}{2}\right]dt \\ &= \int_0^\infty \exp\left[-\epsilon t - D_0 k^2\left(\frac{t}{N} + (1-1/N)\frac{1-e^{-2N\gamma t}}{2N\gamma}\right)\right]dt.\end{aligned} \tag{4.141}$$

This integral can be written in terms of the incomplete gamma function. First change variables to $\kappa = 2N\gamma t$ to get

$$\breve{\mathcal{G}}(k,\epsilon) = \frac{e^{-\frac{D_0 k^2}{2N\gamma}(1-1/N)}}{2N\gamma}\int_0^t \exp\left[-\left(\frac{\epsilon + \frac{D_0 k^2}{N}}{2N\gamma}\right)\kappa + \frac{D_0 k^2}{2N\gamma}(1-1/N)e^{-\kappa}\right]d\kappa. \tag{4.142}$$

Now consider integrals of the form

$$\int_0^\infty e^{-at}e^{be^{-t}}dt. \tag{4.143}$$

Substitute $u = -be^{-t}$ to get

$$\begin{aligned}\int_0^\infty e^{-at}e^{be^{-t}}dt &= \int_{-b}^0 (-u/b)^a e^{-u}\frac{-du}{u} \\ &= (-b)^{-a}\int_0^{-b} u^{a-1}e^{-u}du \\ &= (-b)^{-a}\gamma_{\text{inc}}(a,-b)\end{aligned} \tag{4.144}$$

where $\gamma_{\text{inc}}(a,x)$ is the lower incomplete gamma function,

$$\gamma_{\text{inc}}(a,x) \equiv \int_0^x t^{a-1}e^{-t}dt. \tag{4.145}$$

Using this, the Fourier-Laplace transformed Green's function is

$$\breve{\mathcal{G}}(k,\epsilon) = \frac{e^{-\mu(k)}}{2N\gamma}\left[-\mu(k)\right]^{-\nu(k,\epsilon)}\gamma_{\text{inc}}\Big(\nu(k,\epsilon),-\mu(k)\Big) \tag{4.146}$$

where we have defined

$$\mu(k) \equiv \frac{D_0k^2}{2N\gamma}(1-1/N), \tag{4.147}$$

$$\nu(k,\epsilon) \equiv \frac{\epsilon+\frac{D_0k^2}{2N\gamma}}{2N\gamma}. \tag{4.148}$$

Using equation (4.120), the memory is

$$\begin{aligned}\breve{\mathcal{M}}(k,\epsilon) &= \epsilon - \frac{1}{\breve{\mathcal{G}}(k,\epsilon)} \\ &= \epsilon - \left\{\frac{e^{-\mu(k)}}{2N\gamma}\left[-\mu(k)\right]^{-\nu(k,\epsilon)}\gamma_{\text{inc}}\Big(\nu(k,\epsilon),-\mu(k)\Big)\right\}^{-1}.\end{aligned} \tag{4.149}$$

We have now explicitly obtained an expression for the memory, at least in the Fourier-Laplace domain.

This completes the calculation of two equivalent equations of motion for the density per particle ρ. The time-dependent evolution equation for ρ is local in space in the sense that the time derivative of $\rho(x,t)$ depends only on the second spatial derivative at x, whereas the memory evolution equation is necessarily *non-local* in space in the sense that the time derivative of $\rho(x,t)$ depends on on $\rho(x,t)$ at points in space away from x.

We end this section with a calculation of an approximate memory evolution equation for ρ using the method described in the previous section. Instead of calculating the expansion coefficients directly from equation (4.149), it is simpler to return to equation (4.120). The $m=0$ term necessarily vanishes due to conservation of probability, and in this case the $m=1$ term vanishes since there is no bias in either

direction. The $m = 2$ term in the Laplace domain is

$$-\frac{1}{2}\frac{\partial^2}{\partial k^2}\breve{\mathcal{M}}(k,\epsilon)\Big|_{k=0} = \frac{1}{2}\frac{\partial^2}{\partial k^2}\frac{1}{\breve{\mathcal{G}}(k,\epsilon)}\Big|_{k=0}$$
$$= \frac{1}{[\breve{\mathcal{G}}(0,\epsilon)]^3}\left[\frac{\partial}{\partial k}\breve{\mathcal{G}}(k,\epsilon)\right]^2\Big|_{k=0} - \frac{1}{2[\breve{\mathcal{G}}(0,\epsilon)]^2}\frac{\partial^2}{\partial k^2}\breve{\mathcal{G}}(k,\epsilon)\Big|_{k=0}. \tag{4.150}$$

Since the distribution is normalized to unity, we have $\hat{\mathcal{G}}(0,t) = 1$ and thus $\breve{\mathcal{G}}(0,\epsilon) = 1/\epsilon$. The first term vanishes since $\mathcal{G}$ is symmetric in x, so we have

$$-\frac{1}{2}\frac{\partial^2}{\partial k^2}\breve{\mathcal{M}}(k,\epsilon)\Big|_{k=0} = -\frac{\epsilon^2}{2}\int_0^\infty e^{-\epsilon t}\frac{\partial^2}{\partial k^2}\hat{\mathcal{G}}(k,t)dt\Big|_{k=0}. \tag{4.151}$$

Using the Fourier transformed Green's function, equation (4.139), this becomes

$$-\frac{1}{2}\frac{\partial^2}{\partial k^2}\breve{\mathcal{M}}(k,\epsilon)\Big|_{k=0} = \frac{\epsilon^2\tilde{S}(\epsilon)}{2}. \tag{4.152}$$

The right hand side may be rewritten as

$$-\frac{1}{2}\frac{\partial^2}{\partial k^2}\breve{\mathcal{M}}(k,\epsilon)\Big|_{k=0} = \frac{\epsilon^2\tilde{S}(\epsilon) - \epsilon S(0) - \dot{S}(0) + \dot{S(0)}}{2} \tag{4.153}$$

since $S(0) = 0$. Inverting the Laplace transform using the identity

$$\mathcal{L}\{\ddot{f}(t)\}(\epsilon) = \epsilon^2\tilde{f}(\epsilon) - \epsilon f(0) - \dot{f}(0) \tag{4.154}$$

gives

$$-\frac{1}{2}\frac{\partial^2}{\partial k^2}\breve{\mathcal{M}}(k,t)\Big|_{k=0} = \frac{1}{2}\ddot{S}(t) + \frac{1}{2}\delta(t)\dot{S}(0). \tag{4.155}$$

Plugging in for $S(t)$ gives explicitly

$$-\frac{1}{2}\frac{\partial^2}{\partial k^2}\breve{\mathcal{M}}(k,t)\Big|_{k=0} = -2D_0\gamma e^{-2N\gamma t}(N-1) + D_0\delta(t). \tag{4.156}$$

Our *approximate* memory equation of motion for the density is therefore

$$\frac{\partial}{\partial t}\rho(x,t) = D_0\frac{\partial}{\partial x^2}\rho(x,t) - 2D_0\gamma(N-1)\int_0^t e^{-2N\gamma(t-t')}\frac{\partial^2}{\partial x^2}\rho(x,t')dt'. \tag{4.157}$$

4.5.4 Evolution of the Density with Bias

Next, we analyze the case when bias v_m is present. For the cluster initial condition described earlier, equation (4.102), the single particle distribution functions evolve as

$$P_m^{(1)}(x,t) = \int_{-\infty}^{\infty} G_m^{(1)}(x-x',t) P_m^{(1)}(x',0) dx \tag{4.158}$$

with $G_m^{(1)}(x-x',t)$ calculated from equation (4.71) by setting $x'_m = x'$ for all m,

$$G_m^{(1)}(x-x',t) = \frac{1}{\sqrt{2\pi S(t)}}.\exp\left(\frac{-[x_m - x' - v_m\tau - \bar{v}(t-\tau)]^2}{2S(t)}\right). \tag{4.159}$$

Fourier transforming, we have

$$\hat{G}_m^{(1)}(k,t) = \exp\left\{-ik[v_m\tau + \bar{v}(t-\tau)] - \frac{k^2 S(t)}{2}\right\}. \tag{4.160}$$

Each individual single particle distribution therefore obeys an advection-diffusion equation with time-dependent coefficients,

$$\frac{\partial}{\partial t}P_m^{(1)}(x,t) = -[v_m e^{-N\gamma t} + \bar{v}(1-e^{-N\gamma t})]\frac{\partial}{\partial x}P_m^{(1)}(x,t) + D_0\chi(t)\frac{\partial^2}{\partial x^2}P_m^{(1)}(x,t) \tag{4.161}$$

where we have used $\dot{\tau}(t) = e^{-N\gamma t}$ and $\dot{S}(t)/2 = D_0\chi(t)$.

The density per particle $\rho(x,t)$, which is the sum of the single particle distribution functions divided by N, obeys neither an advection-diffusion equation with time-dependent coefficients nor an advection diffusion equation with memory unless every v_m is the same. The non-local in space versions, equations (4.111) and (4.116) must be used.

The Green's function for the evolution of the density in this case is

$$\mathcal{G}(x-x',t) = \frac{1}{N}\sum_m \frac{1}{\sqrt{2\pi S(t)}}\exp\left(\frac{-[x - x' - v_m\tau - \bar{v}(t-\tau)]^2}{2S(t)}\right). \tag{4.162}$$

The density per particle as a function of time when the bias is present is plotted in Figure (4.2).

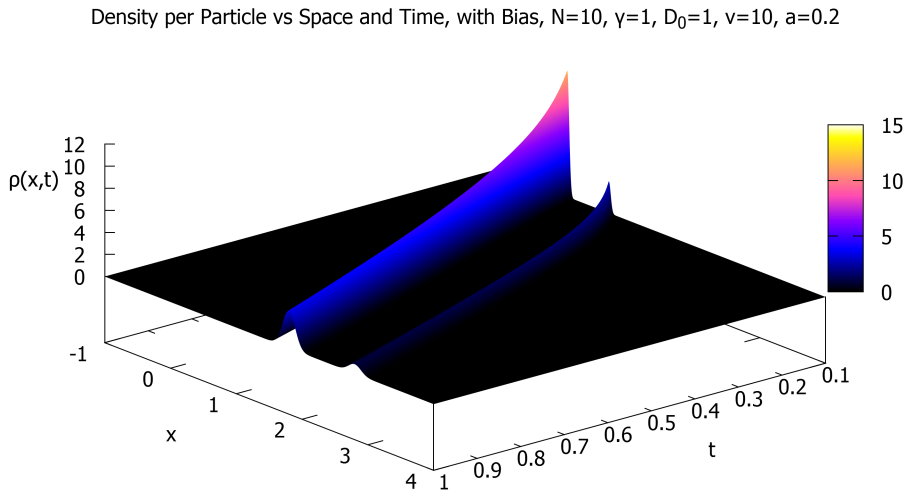

Figure 4.2: Density per particle as a function of time in the simple model of centering when the bias is present for a delta function initial condition. In this case, the individuals are either uninformed $v_m = 0$ or informed $v_m = v$. The concentration of informed individuals is $a = 0.2$.

In general, the neither equation (4.127) nor equation (4.128) terminate after a finite number of terms. The evolution is thus necessarily non-local in space, no matter which formulation, time-dependent or memory, is used to write the equation of motion.

The time-dependent kernel $\mathcal{K}$ may at least be calculated explicitly in the Fourier domain. We will also derive approximate equations of motion in both the time-dependent and memory formulations.

The Fourier transform of the Green's function in equation (4.162) is

$$\hat{\mathcal{G}}(k,t) = \frac{1}{N}\sum_m \exp\left[-ik\left[v_m\tau + \bar{v}(t-\tau)\right] - \frac{k^2 S(t)}{2}\right]. \tag{4.163}$$

Using this in equation (4.115), the time-dependent kernel $\mathcal{K}$ is

$$\hat{\mathcal{K}}(k,t) = \frac{\frac{1}{N}\sum_m \left[-ik[v_m\dot{\tau} + \bar{v}(1-\dot{\tau})] - \frac{k^2\dot{S}(t)}{2}\right]\exp\left[-ik[v_m\tau + \bar{v}(t-\tau)] - \frac{k^2 S(t)}{2}\right]}{\frac{1}{N}\sum_m \exp\left[-ik[v_m\tau + \bar{v}(t-\tau)] - \frac{k^2 S(t)}{2}\right]}. \tag{4.164}$$

We now calculate the expansion coefficients and write approximate equations of motion which are local in space, beginning with the time-dependent formulation. Again the $m = 0$ term vanishes because of conservation of probability. The $m = 1$ term is

$$\begin{aligned}\frac{\partial}{\partial(ik)}\hat{\mathcal{K}}(k,t)\bigg|_{k=0} &= \frac{\partial}{\partial t}\frac{1}{\hat{\mathcal{G}}(k,t)}\frac{\partial}{\partial(ik)}\hat{\mathcal{G}}(k,t)\bigg|_{k=0} \\ &= -\frac{\partial}{\partial t}\frac{1}{N}\sum_m [v_m\tau + \bar{v}(t-\tau)] = -\bar{v}. \end{aligned} \tag{4.165}$$

where we have used $\bar{v} = \frac{1}{N}\sum_m v_m$ and $\hat{\mathcal{G}}(0,t) = 1$. The $m = 2$ term is

$$\begin{aligned}\frac{1}{2}\frac{\partial^2}{\partial(ik)^2}\hat{\mathcal{K}}(k,t)\bigg|_{k=0} &= \frac{1}{2}\frac{\partial}{\partial t}\left[\frac{\partial^2}{\partial(ik)^2}\hat{\mathcal{G}}(k,t)\bigg|_{k=0} - \left(\frac{\partial}{\partial(ik)}\hat{\mathcal{G}}(k,t)\right)^2\bigg|_{k=0}\right] \\ &= \frac{1}{2}\dot{S}(t) + \tau\dot{\tau}\sigma_v^2 \\ &= D_0\chi(t) + e^{-N\gamma t}\tau\sigma_v^2 \end{aligned} \tag{4.166}$$

with χ as defined earlier,

$$\chi(t) = e^{-N\gamma t} + \frac{1}{N}e^{-N\gamma t} \tag{4.167}$$

and where σ_v^2 is related to the spread of the v_ms,

$$\sigma_v^2 \equiv \frac{1}{N}\sum_m v_m^2 - \bar{v}^2. \tag{4.168}$$

Using these results, an *approximate* space-local time-dependent equation of motion for the density is

$$\frac{\partial}{\partial t}\rho(x,t) = -\bar{v}\frac{\partial}{\partial x}\rho(x,t) + [D_0\chi(t) + e^{-N\gamma t}\tau\sigma_v^2]\frac{\partial^2}{\partial x^2}\rho(x,t). \tag{4.169}$$

Next, we calculate an approximate equation of motion with memory. The $m = 1$ expansion coefficient in the Laplace domain is

$$\begin{aligned}\frac{\partial}{\partial(ik)}\breve{\mathcal{M}}(k,\epsilon) &= -\frac{\partial}{\partial(ik)}\frac{1}{\breve{\mathcal{G}}(k,\epsilon)}\bigg|_{k=0} \\ &= \epsilon^2\frac{\partial}{\partial(ik)}\int_0^\infty e^{-\epsilon t}\hat{\mathcal{G}}(k,t)dt\bigg|_{k=0} \\ &= -\bar{v}\epsilon^2\int_0^\infty e^{-\epsilon t}t dt = -\bar{v}. \end{aligned} \tag{4.170}$$

Inverting the Laplace transform, this is

$$\frac{\partial}{\partial(ik)}\hat{\mathcal{M}}(k,t) = -\bar{v}\delta(t). \tag{4.171}$$

The $m = 2$ term in the expansion in the Laplace domain is

$$-\frac{1}{2}\frac{\partial^2}{\partial k^2}\breve{\mathcal{M}}(k,\epsilon)\Big|_{k=0} = \frac{1}{[\breve{\mathcal{G}}(0,\epsilon)]^3}\left[\frac{\partial}{\partial k}\breve{\mathcal{G}}(k,\epsilon)\right]^2\Big|_{k=0} - \frac{1}{2[\breve{\mathcal{G}}(0,\epsilon)]^2}\frac{\partial^2}{\partial k^2}\breve{\mathcal{G}}(k,\epsilon)\Big|_{k=0}. \tag{4.172}$$

We have

$$\begin{aligned}\frac{\partial}{\partial k}\breve{\mathcal{G}}(k,\epsilon)\Big|_{k=0} &= \int_0^\infty e^{-\epsilon t}\frac{\partial}{\partial k}\hat{\mathcal{G}}(k,t)dt\Big|_{k=0} \\ &= -i\bar{v}\int_0^\infty e^{-\epsilon t}t dt = -i\bar{v}\frac{1}{\epsilon^2}\end{aligned} \tag{4.173}$$

and

$$\begin{aligned}\frac{1}{2}\frac{\partial^2}{\partial k^2}\breve{\mathcal{G}}(k,\epsilon)\Big|_{k=0} &= \frac{1}{2}\int_0^\infty e^{-\epsilon t}\frac{\partial^2}{\partial k^2}\hat{\mathcal{G}}(k,t)dt\Big|_{k=0} \\ &= -\frac{1}{2}\int_0^\infty e^{-\epsilon t}\frac{1}{N}\sum_m\left\{S(t) + [v_m\tau + \bar{v}(t-\tau)]^2\right\} \\ &= -\frac{1}{2}\tilde{S}(\epsilon) - \frac{\sigma_v^2}{2}\int_0^\infty e^{-\epsilon t}\tau^2 dt - \frac{\bar{v}^2}{\epsilon^3}\end{aligned} \tag{4.174}$$

Using these along with $\breve{\mathcal{G}}(0,\epsilon) = 1/\epsilon$ we have

$$-\frac{1}{2}\frac{\partial^2}{\partial k^2}\breve{\mathcal{M}}(k,\epsilon)\Big|_{k=0} = \frac{\epsilon^2\tilde{S}(\epsilon) + \sigma_v^2\epsilon^2\int_0^\infty e^{-\epsilon t}\tau^2 dt}{2}. \tag{4.175}$$

Using the definition of τ,

$$\tau^2 = \frac{1}{(N\gamma)^2}(1 - 2e^{-N\gamma t} + e^{-2N\gamma t}) \tag{4.176}$$

so

$$\begin{aligned}\epsilon^2\int_0^\infty e^{-\epsilon t}\tau^2 dt &= \frac{\epsilon^2}{(N\gamma)^2}\left(\frac{1}{\epsilon} - \frac{2}{\epsilon + N\gamma t} + \frac{1}{\epsilon + 2N\gamma t}\right) \\ &= \frac{1}{(N\gamma)^2}\frac{2\epsilon^2(N\gamma)^2}{(\epsilon + N\gamma)(\epsilon + 2N\gamma)} \\ &= \frac{4}{\epsilon + 2N\gamma} - \frac{2}{\epsilon + N\gamma}.\end{aligned} \tag{4.177}$$

where we have performed a partial fraction decomposition in the last step. Inverting the Laplace transform, we have for the $m = 2$ term in the expansion

$$\begin{aligned} -\frac{1}{2}\frac{\partial^2}{\partial k^2}\breve{\mathcal{M}}(k,\epsilon)\Big|_{k=0} &= \frac{1}{2}\ddot{S}(t) + \frac{1}{2}\delta(t)\dot{S}(0) + \sigma_v^2[2e^{-2N\gamma t} - e^{-N\gamma t}] \\ &= -2D_0\gamma e^{-2N\gamma t}(N-1) + D_0\delta(t) + \sigma_v^2[2e^{-2N\gamma t} - e^{-N\gamma t}]. \end{aligned} \tag{4.178}$$

The *approximate* memory equation of motion for the density is finally

$$\begin{aligned} \frac{\partial}{\partial t}\rho(x,t) = &-\bar{v}\frac{\partial}{\partial x}\rho(x,t) + D_0\frac{\partial}{\partial x^2}\rho(x,t) \\ &- \int_0^t [2D_0\gamma(N-1) - \sigma_v^2(2 - e^{N\gamma(t-t')})]e^{-2N\gamma(t-t')}\frac{\partial^2}{\partial x^2}\rho(x,t')dt'. \end{aligned} \tag{4.179}$$

4.6 Remarks

Let us summarize what we have found in this chapter. We have calculated exactly the probability distribution as a function of time for a simple model of flocking consisting only of a centering interaction, noise, and a bias. In the absence of noise, each particle moves at the same speed but is displaced from the center of mass by an amount which depends on the strength of the bias the particle feels. The noisy dynamics, analyzed with a Fokker-Planck equation, are similar, but there is a spread in the particles positions. At long times the distribution spreads more slowly due to the spring forces counteracting the thermal noise. We saw also how a "mean-field" calculation could be used to calculate the center of mass and single particle distribution functions in a simpler way.

Next, we calculated another coarse-grained quantity: the density. It was shown that for a certain class of initial conditions in which the particles are found clustered together that the evolution of the density is linear, and we wrote continuum equations of motion for the evolution of the density.

We saw that in the absence of bias, the evolution of the density is naturally described by a diffusion equation with a time-dependent diffusion constant. We then showed that the evolution equation can be recast as a memory equation, but in doing so we found that the memory must be non-local in space as well as time.

In the presence of bias, it was shown that the density does not obey simply an advection-diffusion equation with time-dependent coefficients (although the single particle distributions themselves do). Instead, the density obeys time-dependent evolution equation which is non-local in space. An equivalent memory equation, also non-local in space, was found as well.

This simple model has proven to be amenable to analytic calculations, and we were successfully able to write continuum equations of motion for coarse-grained quantities starting from a dynamical description of the motion of each individual particle.

Chapter 5

Collective Motion of Macroscopic Objects: A Model with Alignment

In the previous chapter, we constructed a simple model of collective motion which consisted of a centering interaction, noise, and a bias. Although the model could be exactly solved, it lacks an important feature present in many models of collective motion: self-propulsion.

In this chapter, we construct and analyze another simple model of collective motion with a slightly different set of ingredients: self-propulsion, an alignment interaction, and noise.

A heavily cited model in the literature with self-propulsion, alignment, and noise is the model by Vicsek et al. [85]. Their model is rule-based with the following single rule:

> at each time step a given particle driven with a constant absolute velocity assumes the average direction of motion of the particles in its neighborhood of radius r with some random perturbation added.

The model discussed in this chapter is based on Vicsek's central idea. However, we will treat it in a simplified form and, to allow for analytic calculations to be done, we will make a crucial assumption: we will take the alignment interaction have infinite range. We begin with the known single-particle version of the model and generalize first to two-particles, then to many particles.

The one- and two-particle versions can be solved exactly, and we calculate the first two moments and write equations of motion for some coarse-grained continuous quantities. The many-particle version cannot be solved exactly, but we do calculate the first two moments.

5.1 Single-Particle Model

First, consider a single particle which moves in one dimension at a constant speed c, but which changes directions at random. Suppose that the probability per unit time for the particle to flip is a constant, which we will call F. One possible path of such a particle is illustrated in Figure 5.1. This simple model is already known in the literature, see for example refs. [117, 119–122]. We will reproduce here the main results from the single-particle model, then generalize the model to more than one-particle and introduce an interaction.

The complete state of the particle can be described by two functions of space and time which we will call $Q_+(x,t)$ and $Q_-(x,t)$. We define Q_+ so that $Q_+(x,t)dx$ is the probability to find the particle moving to the right in a small interval between x and $x+dx$ at time t. Similarly, $Q_-(x,t)dx$ is the probability to find the particle moving to the left in a small interval between x and $x+dx$ at time t.

What equations of motion do Q_+ and Q_- obey? If the particle did not flip ($F=0$)

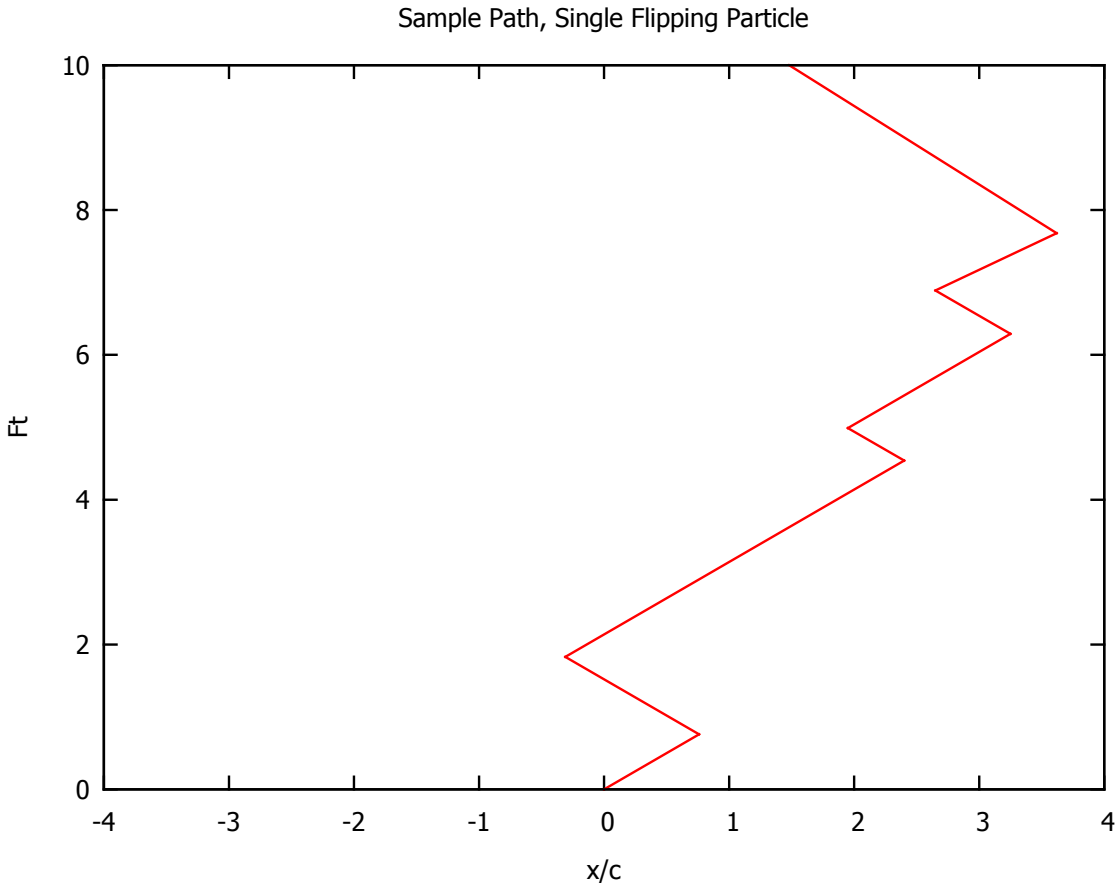

Figure 5.1: Sample path of a particle moving at speed c which flips directions at random.

then the equations of motion would simply be advection equations,

$$\frac{\partial}{\partial t}Q_+ = -c\frac{\partial}{\partial x}Q_+, \tag{5.1}$$

$$\frac{\partial}{\partial t}Q_- = +c\frac{\partial}{\partial x}Q_-. \tag{5.2}$$

On the other hand, if the particles were stationary, then the equations of motion would simply resemble the Master equation for a two-state system,

$$\frac{\partial}{\partial t}Q_+ = F[Q_- - Q_+], \tag{5.3}$$

$$\frac{\partial}{\partial t}Q_- = F[Q_+ - Q_-]. \tag{5.4}$$

Combining these, when the particle is not stationary and does flip, the equations of motion are

$$\frac{\partial}{\partial t}Q_+ = -c\frac{\partial}{\partial x}Q_+ + F[Q_- - Q_+], \tag{5.5}$$

$$\frac{\partial}{\partial t}Q_- = +c\frac{\partial}{\partial x}Q_- + F[Q_- - Q_+]. \tag{5.6}$$

This set of equations can be solved by Fourier and Laplace transforming and solving the resulting system of linear equations. We again define the Fourier transform of a function f which depends on space as

$$\hat{f}(k) \equiv \int_{-\infty}^{\infty} f(x)e^{-ikx}dx \tag{5.7}$$

and the Laplace transform of a function g which depends on time as

$$\tilde{g}(\epsilon) \equiv \int_{0}^{\infty} g(t)e^{-\epsilon t}dt. \tag{5.8}$$

The joint Fourier-Laplace transform of a function h which depends on both space and time, which we label with a breve, is

$$\breve{h}(k,\epsilon) = \int_{0}^{\infty}\int_{-\infty}^{\infty} h(x,t)e^{-ikx}e^{-\epsilon t}dxdt. \tag{5.9}$$

We have for the joint Fourier-Laplace transform of the equations of motion (5.5) and (5.6)

$$\epsilon\breve{Q}_+(k,\epsilon) - \hat{Q}_+(k,0) = -ikc\breve{Q}_+(k,\epsilon) + F[\breve{Q}_-(k,\epsilon) - \breve{Q}_+(k,\epsilon)], \tag{5.10}$$

$$\epsilon\breve{Q}_-(k,\epsilon) - \hat{Q}_-(k,0) = ikc\breve{Q}_-(k,\epsilon) + F[\breve{Q}_+(k,\epsilon) - \breve{Q}_-(k,\epsilon)]. \tag{5.11}$$

Rearranging and rewriting as a matrix equation, this becomes

$$\begin{pmatrix} \epsilon + F + ikc & -F \\ -F & \epsilon + F - ikc \end{pmatrix} \begin{pmatrix} \breve{Q}_+(k,\epsilon) \\ \breve{Q}_-(k,\epsilon) \end{pmatrix} = \begin{pmatrix} \hat{Q}_+(k,0) \\ \hat{Q}_-(k,0) \end{pmatrix}. \tag{5.12}$$

Inverting the matrix on the left hand side then gives the solution as

$$\begin{pmatrix} \breve{Q}_+(k,\epsilon) \\ \breve{Q}_-(k,\epsilon) \end{pmatrix} = \frac{1}{\epsilon^2 + 2F\epsilon + k^2} \begin{pmatrix} \epsilon + F - ikc & F \\ F & \epsilon + F + ikc \end{pmatrix} \begin{pmatrix} \hat{Q}_+(k,0) \\ \hat{Q}_-(k,0) \end{pmatrix}. \tag{5.13}$$

We will see later that the solution in real space and time can be written in terms of modified Bessel functions.

For now we will calculate some coarse-grained quantities. The total probability to find the particle pointing to the right, which we will call P_+, can be obtained simply by integrating Q_+ over all space,

$$P_+(t) = \int_{-\infty}^{\infty} Q_+(x,t)dx = \hat{Q}(0,t). \tag{5.14}$$

Similarly, the probability to find the particle pointing to the left, P_-, is found by integrating Q_- over all space. We have constructed the model so that the flipping occurs independently of where the particle is located, so P_+ and P_- obey the Master equation

$$\frac{d}{dt}P_+ = F[P_- - P_+], \tag{5.15}$$

$$\frac{d}{dt}P_- = F[P_+ - P_-]. \tag{5.16}$$

This can be seen explicitly by integrating the equations of motion for Q_+ and Q_- over all space.

Using $P_+ + P_- = 1$, the solution is

$$P_+(t) = P_+(0)e^{-2Ft} + \frac{1}{2}(1 - e^{-2Ft}), \tag{5.17}$$

$$P_-(t) = P_-(0)e^{-2Ft} + \frac{1}{2}(1 - e^{-2Ft}), \tag{5.18}$$

so at times $t \gg 1/(2F)$, it is equally likely to find the particle pointing in either direction. The evolution of P_+ and P_- for a particle initially pointing to the right is plotted in Figure 5.2.

Now let us calculate the average position $\langle x \rangle$. Define Q to be the sum of Q_+ and Q_-;

$$Q(x,t) \equiv Q_+(x,t) + Q_-(x,t). \tag{5.19}$$

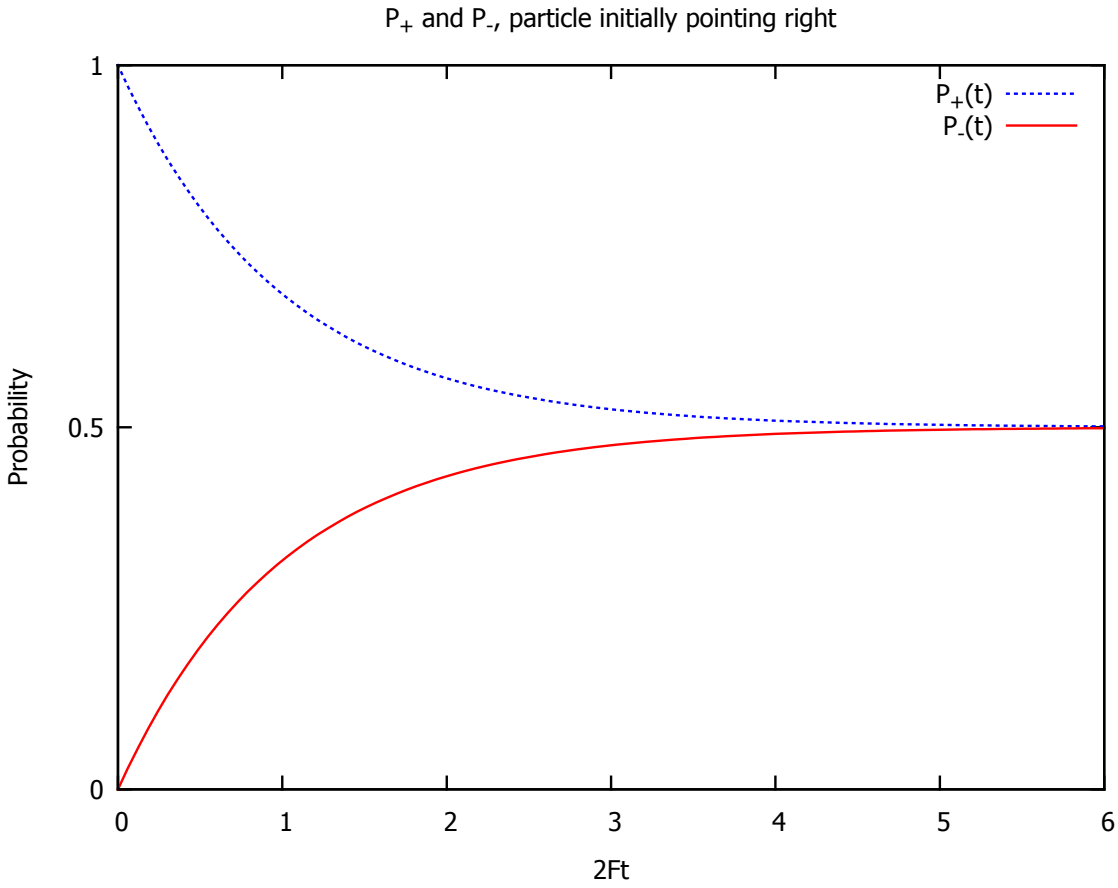

Figure 5.2: Probability to find a randomly flipping particle pointing to the left or right as a function of time, given that the particle was initially pointing to the right.

The probability to find the particle in a small interval between x and $x+dx$ going in either direction at time t is then $Q(x,t)dx$. The average position is then

$$\langle x \rangle = \int_{-\infty}^{\infty} xQ(x,t)dx = \int_{-\infty}^{\infty} x[Q_+(x,t) + Q_-(x,t)]dx. \tag{5.20}$$

Fourier transforming equations (5.5) and (5.6) gives

$$\frac{\partial}{\partial t}\hat{Q}_+ = -c(ik)\hat{Q}_+ + F[\hat{Q}_- - \hat{Q}_+], \tag{5.21}$$

$$\frac{\partial}{\partial t}\hat{Q}_- = +c(ik)\hat{Q}_+ + F[\hat{Q}_+ - \hat{Q}_-]. \tag{5.22}$$

Adding these, we have

$$\frac{\partial}{\partial t}\hat{Q} = -c(ik)[\hat{Q}_+ - \hat{Q}_-]. \tag{5.23}$$

Since the Fourier transform of Q is given by $\hat{Q}(k,t) \equiv \int e^{-ikx}Q(x,t)dx$, the nth moment can be computed by taking k-space derivatives of $\hat{Q}$;

$$\langle x^n \rangle \equiv \int_{-\infty}^{\infty} x^n Q(x,t)dx = \left.\frac{\partial^n \hat{Q}}{\partial(-ik)^n}\right|_{k=0}, \tag{5.24}$$

so using this in equation (5.23) gives the evolution of $\langle x \rangle$,

$$\frac{d}{dt}\langle x(t)\rangle = c[P_+(t) - P_-(t)]. \tag{5.25}$$

The quantity $P_+(t) - P_-(t)$ is *the average direction the particle is pointing in at time t*. This can be seen by defining a stochastic variable $\sigma(t)$ which represents the direction of the particle and can take on only the values -1 or $+1$. Then the average direction is

$$\langle \sigma(t)\rangle = \sum_{\sigma=-1,+1} \sigma P_\sigma(t) = P_+(t) - P_-(t). \tag{5.26}$$

We can therefore write the evolution of the first moment as

$$\frac{d}{dt}\langle x(t)\rangle = c\langle \sigma(t)\rangle. \tag{5.27}$$

In words, this equation states simply that *the time derivative of the average position is the speed c times the average direction*. From equations (5.17) and (5.18), the average direction decays exponentially from its initial value,

$$\langle \sigma(t)\rangle = \langle \sigma(0)\rangle e^{-2Ft}. \tag{5.28}$$

Substituting this into equation (5.27) and integrating gives the average position as

$$\langle x(t)\rangle = \langle x(0)\rangle + c\langle \sigma(0)\rangle \frac{1 - e^{-2Ft}}{2F}. \tag{5.29}$$

For short times, $t \ll 1/(2F)$, the particle simply drifts at speed c in whichever direction it is initially pointing in,

$$\langle x(t)\rangle \approx \langle x(0)\rangle + c\langle \sigma(0)\rangle t. \tag{5.30}$$

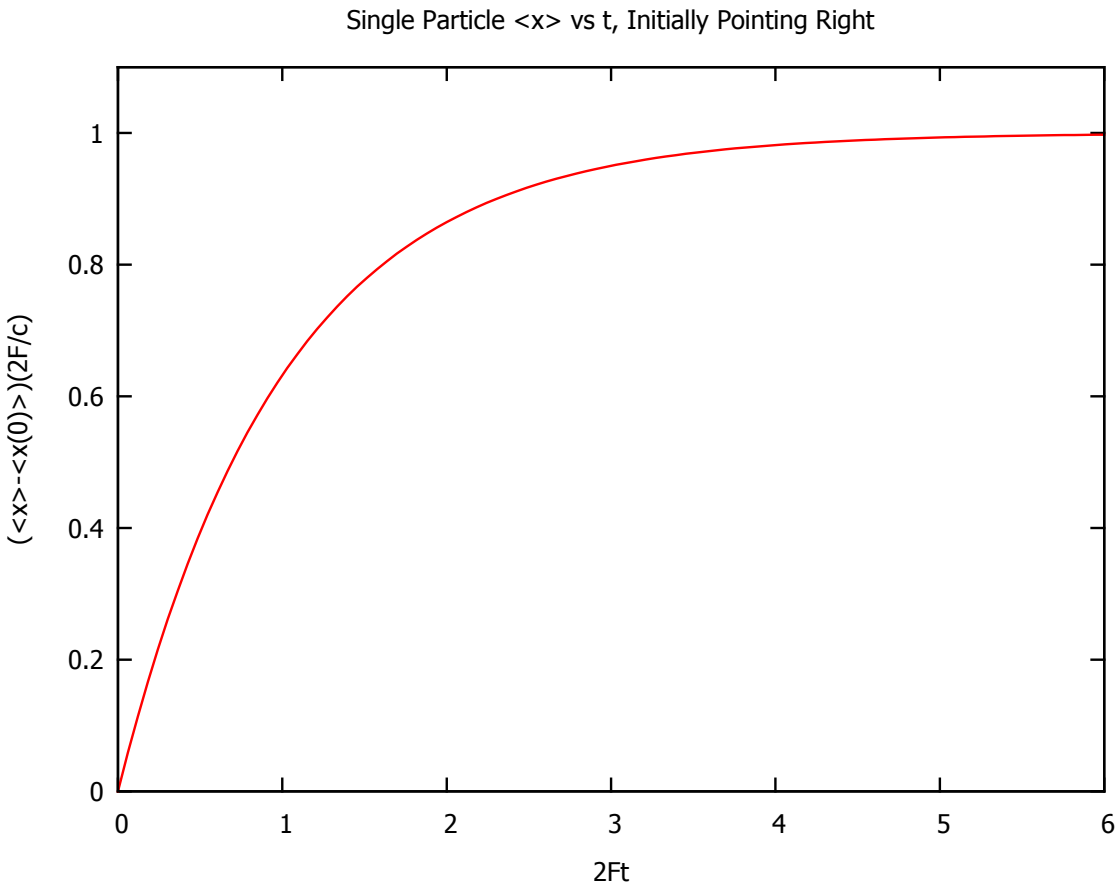

Figure 5.3: The average position versus time of a randomly flipping particle moving at speed c, given that the particle was initially pointing to the right.

At long times, $t \gg 1/(2F)$, the probability to find the particle pointing to the left is equal to the probability to find the particle pointing to the right, so the average direction is zero and the first moment becomes a constant,

$$\langle x(t)\rangle \approx \langle x(0)\rangle + c\langle\sigma(0)\rangle\frac{1}{2F}. \tag{5.31}$$

The average position for an initial condition in which the particle is pointing to the right is displayed in Figure 5.3.

Now let us calculate the second moment. Using equation (5.23), we have

$$\frac{d}{dt}\langle x^2\rangle = \frac{d}{dt}\frac{\partial^2}{\partial(-ik)^2}\hat{Q}\bigg|_{k=0} = 2c\left[\frac{\partial}{\partial(-ik)}\hat{Q}_+\bigg|_{k=0} - \frac{\partial}{\partial(-ik)}\hat{Q}_+\bigg|_{k=0}\right]. \tag{5.32}$$

Define

$$\langle x_+\rangle = \frac{\partial}{\partial(-ik)}\hat{Q}_+\bigg|_{k=0}, \tag{5.33}$$

$$\langle x_-\rangle = \frac{\partial}{\partial(-ik)}\hat{Q}_-\bigg|_{k=0}. \tag{5.34}$$

From the equations of motion for Q_+ and Q_-, we have

$$\frac{d}{dt}[\langle x_+\rangle - \langle x_-\rangle] = c[\hat{Q}_+(0,t) + \hat{Q}_-(0,t)] - 2F[\langle x_+\rangle - \langle x_-\rangle]. \tag{5.35}$$

Because of normalization, $\hat{Q}(0,t) = \hat{Q}_+(0,t) + \hat{Q}_-(0,t) = 1$ so

$$\langle x_+(t)\rangle - \langle x_-(t)\rangle = [\langle x_+(0)\rangle - \langle x_-(0)\rangle]e^{-2Ft} + \frac{c}{2F}(1 - e^{-2Ft}). \tag{5.36}$$

Substituting,

$$\frac{\partial}{\partial t}\langle x^2\rangle = 2c^2\frac{(1 - e^{-2Ft})}{2F} + 2ce^{-2Ft}[\langle x_+(0)\rangle - \langle x_-(0)\rangle]. \tag{5.37}$$

Integrating,

$$\langle x^2(t)\rangle - \langle x^2(0)\rangle = 2c^2\frac{2Ft - (1 - e^{-2Ft})}{(2F)^2} + 2c\frac{1 - e^{-2Ft}}{2F}[\langle x_+(0)\rangle - \langle x_-(0)\rangle]. \tag{5.38}$$

To see what happens for a simple initial condition, suppose that at time $t = 0$ the particle is located at $x = 0$ and has a random direction. In terms of the Qs, this means

$$Q_+(x,0) = Q_-(x,0) = \frac{1}{2}\delta(x). \tag{5.39}$$

We then have $\langle x_+(0)\rangle = \langle x_-(0)\rangle = 0$, $\langle x^2(0)\rangle = 0$, and $\langle x(t)\rangle = 0$, and the second moment is

$$\langle x^2(t)\rangle = 2c^2\frac{2Ft - (1 - e^{-2Ft})}{(2F)^2}. \tag{5.40}$$

At short times, $t \ll 1/(2F)$, the second moment is proportional to t^2, and the motion is said to be *ballistic*,

$$\langle x^2(t)\rangle \approx (ct)^2. \tag{5.41}$$

At long times, $t \gg 1/(2F)$, the second moment is proportional to t, and the motion is said to be *diffusive*,

$$\langle x^2(t)\rangle \approx 2\frac{c^2}{2F}t - \frac{2c^2}{(2F)^2}. \tag{5.42}$$

The effective diffusion constant, which can be defined as

$$D_{\text{eff}} = \frac{1}{2}\frac{d}{dt}\left(\langle x^2(t)\rangle - \langle x(t)\rangle^2\right), \tag{5.43}$$

is

$$D_{\text{eff}} = \frac{c^2}{2F}. \tag{5.44}$$

The second moment as a function of time is illustrated in Figure 5.4.

Now let us look at continuous coarse-grained quantities. Since there is only one particle, the density, center of mass distribution, and single particle distribution are all the same:

$$\rho(x,t) = Q_{\text{cm}}(x,t) = Q(x,t) = Q_+(x,t) + Q_-(x,t). \tag{5.45}$$

What equation of motion does Q obey? We could follow our procedure as discussed in the previous chapter for constructing equations of motion from the Green's function, but it is simpler to use the following procedure as described in ref. [122]. First, take the sum and difference of the equations of motion for Q_+ and Q_-, equations (5.5) and (5.6), to obtain

$$\frac{\partial}{\partial t}Q = -c\frac{\partial}{\partial x}R \tag{5.46}$$

$$\frac{\partial}{\partial t}R = -c\frac{\partial}{\partial x}Q - 2FR. \tag{5.47}$$

where R is defined to be

$$R(x,t) \equiv Q_+(x,t) - Q_-(x,t). \tag{5.48}$$

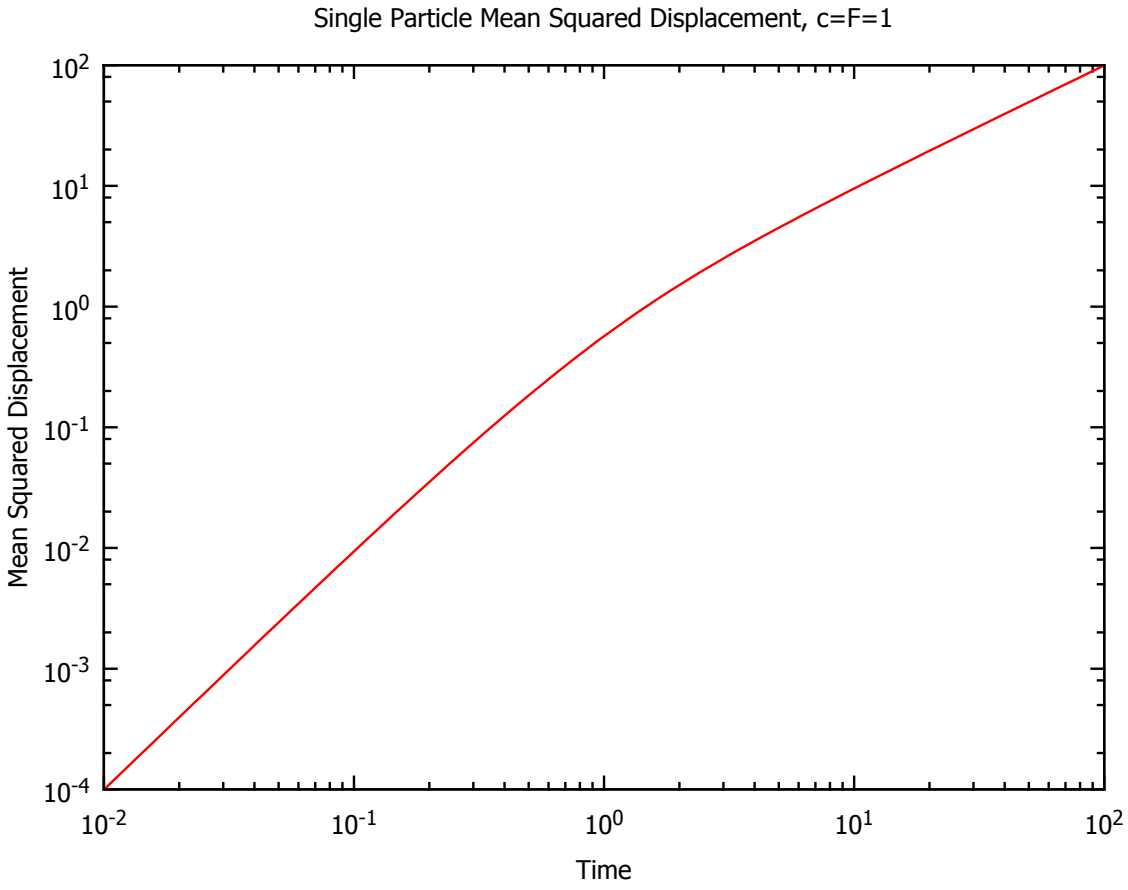

Figure 5.4: Mean square displacement versus time of a randomly flipping particle which moves at constant speed c on a log-log scale to illustrate the change from t^2 growth to t growth.

Take a time derivative of the first and substitute the second in the right hand side to obtain

$$\frac{\partial^2}{\partial t^2}Q = -c\frac{\partial}{\partial x}\frac{\partial}{\partial t}R = c^2\frac{\partial^2}{\partial x^2}Q + 2Fc\frac{\partial}{\partial x}R. \tag{5.49}$$

Finally, eliminate R from the right hand side using again equation (5.46) to obtain a closed equation for Q,

$$\frac{\partial^2}{\partial t^2}Q + 2F\frac{\partial}{\partial t}Q = c^2\frac{\partial^2}{\partial x^2}Q. \tag{5.50}$$

This partial differential equation, which is second order in time, is known as the

telegrapher's equation. If there were no flipping, $F = 0$, Q would obey simply the wave equation. On the other hand, if the first term were not present, Q would obey a diffusion equation with diffusion constant $D = c^2/(2F)$.

Since this is a second order in time equation, both Q and $\dot{Q}$ must be specified at time $t = 0$. Using the definition of Q, we have simply

$$Q(x,0) = Q_+(x,0) + Q_-(x,0), \tag{5.51}$$

and using equation (5.46), $\dot{Q}(x,0)$ is

$$\dot{Q}(x,0) = -c\frac{\partial}{\partial x}\left[Q_+(x,0) - Q_-(x,0)\right]. \tag{5.52}$$

The solution to the telegrapher's equation (5.50) can be obtained by standard techniques (see for example ref. [123]), and has been applied in diverse areas ranging from particle transport to stress distribution in granular compacts [124–126]. For an initial condition $Q(x,0) = \delta(x)$, $\dot{Q}(x,0) = 0$ (i.e. the particle starts at $x = 0$ with a random direction), the solution is

$$Q(x,t) = e^{-Ft}\frac{\delta(x-ct)+\delta(x+ct)}{2} + \frac{F}{2c}e^{-Ft}H(ct-|x|)\left[I_0(\Lambda) + \frac{Ft}{\Lambda}I_1(\Lambda)\right] \tag{5.53}$$

where H is the unit step function, the Is are modified Bessel functions, and

$$\Lambda \equiv \frac{F}{c}\sqrt{c^2t^2 - x^2}. \tag{5.54}$$

How does Q evolve in time? The distribution $Q(x,t)$ is zero for $|x| > ct$ due to the fact that the particle moves at a constant speed c, so it cannot be found anywhere with $|x| > ct$ (since it would have to move faster than c to get there). The delta functions in the first term represent the motion of the particle if it has not flipped. They are multiplied by a factor e^{-Ft} because the probability that the particle has not flipped decays exponentially in time. The second term is nonzero in the interior region $|x| < ct$ and is a result of the flipping. Using the asymptotic properties of the modified Bessel

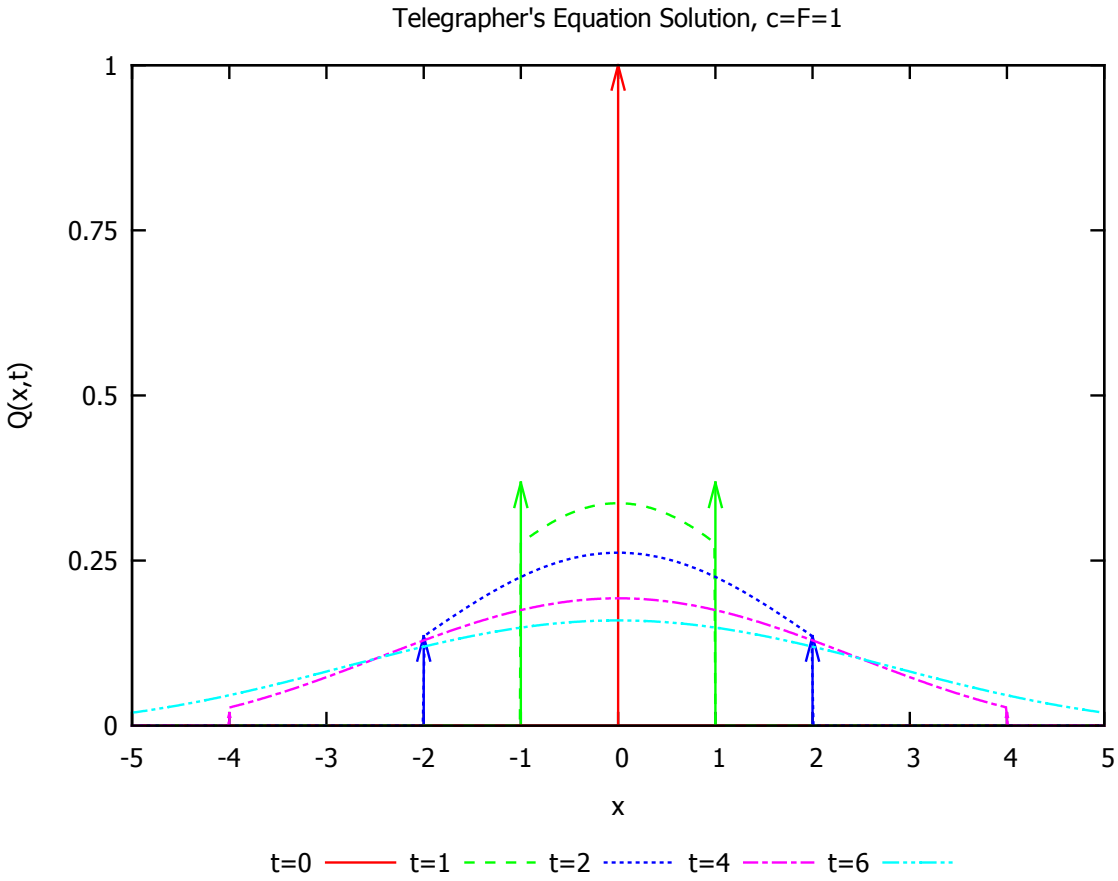

Figure 5.5: The solution to the telegrapher's equation for different times for a delta function initial condition. The vertical arrows represent delta functions, with the length of the arrow representing the amplitude of the delta function.

functions it can be shown that at long times, Q becomes approximately a Gaussian [122]. The solution is illustrated in Figure 5.5.

Instead of a second order in time partial differential equation, the evolution of Q may also be written as a first order in time partial differential equation with a memory [117]. Formally solving equation (5.47) for R in terms of Q gives

$$R(x,t) = e^{-2Ft}R(x,0) - c\int_0^t e^{-2F(t-t')}\frac{\partial}{\partial x}Q(x,t')dt'. \tag{5.55}$$

Substituting into (5.46) gives an equation which is closed in Q except for a term which

depends on R at time $t = 0$,

$$\frac{\partial}{\partial t}Q(x,t) = -ce^{-2Ft}\frac{\partial}{\partial x}R(x,0) + c^2\int_0^t e^{-2F(t-t')}\frac{\partial^2}{\partial x^2}Q(x,t')dt'. \tag{5.56}$$

5.2 Two-Particle Model

Next, we generalize the model constructed in the previous section to two interacting particles. The particles still flip randomly, but we construct the flipping rates so that the particles tend to point in the same direction. This is a kind of *alignment* interaction. An important simplification we will use is to make the interaction infinite ranged, in the sense that the strength of the alignment interaction is independent of the distance between the particles.

Since there are four total configurations, the state of the system may be described by four functions of two spatial variables (the positions of each of the two-particles) and time which we will denote Q_{++}, Q_{+-}, Q_{-+} and Q_{--}. Define Q_{++} so that the probability to find both particles pointing to the right with the first particle in a small interval between x_1 and $x_1 + dx_1$ and the second particle in a small interval between x_2 and $x_2 + dx_2$ is

$$Q_{++}(x_1, x_2, t)dx_1dx_2. \tag{5.57}$$

Similarly define Q_{+-} (except with the first particle pointing to the right and the second to the left), Q_{-+} (first pointing to the left, second to the right), and Q_{--} (both particles pointing to the left).

Before we construct the equations of motion for the Qs, let us first construct equations of motion for the probabilities to find the particles in a given configuration, which we will denote P_{++}, P_{+-}, P_{-+}, and P_{--}. The quantity $P_{++}(t)$ is the total probability to find both particles pointing to the right at time t, and is related to

Q_{++} by integrating over the positions of the two-particles,

$$P_{++}(t) = \int_{-\infty}^{\infty}\int_{-\infty}^{\infty} Q_{++}(x_1, x_2, t)dx_1dx_2. \tag{5.58}$$

The remaining quantities P_{+-}, P_{-+}, and P_{--} are similarly related to Q_{+-}, Q_{-+}, and Q_{--}.

Since we have assumed that the strength of the alignment interaction does not depend on the relative distance between the two-particles, the directions of the particles evolve independently of the positions and closed equations of motion can be written for the Ps. We assume that their evolution can be described by a Master equation, and we introduce alignment by constructing the rates in such a way that the aligned states are favored. More precisely, let F by the probability per unit time for the system to change from an unaligned state to an aligned state (e.g. $-+$ to $++$ or $-+$ to $--$), and let $f < F$ be the probability per unit time to flip from an aligned state to an unaligned state. The situation is illustrated in Figure 5.6. The Master equation for the evolution of the Ps is

$$\frac{dP_{++}}{dt} = F[P_{+-} + P_{-+}] - 2fP_{++}, \tag{5.59}$$

$$\frac{dP_{--}}{dt} = F[P_{+-} + P_{-+}] - 2fP_{--}, \tag{5.60}$$

$$\frac{dP_{+-}}{dt} = f[P_{++} + P_{--}] - 2FP_{+-}, \tag{5.61}$$

$$\frac{dP_{-+}}{dt} = f[P_{++} + P_{--}] - 2FP_{-+}. \tag{5.62}$$

This system of equations can be solved in the following way. This procedure is equivalent to diagonalizing the interaction matrix. Adding all four equations together, we have simply conservation of total probability:

$$\frac{d}{dt}[P_{++} + P_{--} + P_{+-} + P_{-+}] = 0. \tag{5.63}$$

Subtracting the second from the first and the fourth from the third,

$$\frac{d}{dt}[P_{++} - P_{--}] = -2f[P_{++} - P_{--}], \tag{5.64}$$

$$\frac{d}{dt}[P_{+-} - P_{-+}] = -2F[P_{+-} - P_{-+}], \tag{5.65}$$

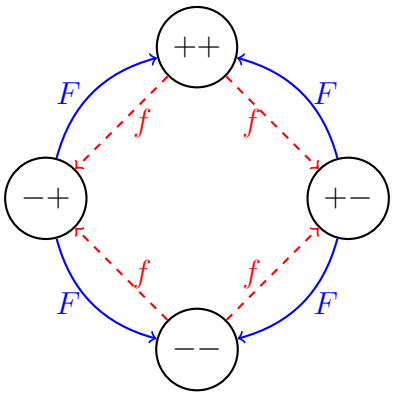

Figure 5.6: Illustration of the flipping rates for the two-particle alignment model.

which can be solved as

$$[P_{++}(t) - P_{--}(t)] = e^{-2ft}[P_{++}(0) - P_{--}(0)], \tag{5.66}$$

$$[P_{+-}(t) - P_{-+}(t)] = e^{-2Ft}[P_{+-}(0) - P_{-+}(0)]. \tag{5.67}$$

Finally, combining all four equations we also have

$$\frac{d}{dt}[2f(P_{++}+P_{--})-2F(P_{+-}+P_{-+})] = -(2f+2F)[2f(P_{++}+P_{--})-2F(P_{+-}+P_{-+})] \tag{5.68}$$

which can be solved as

$$\begin{aligned} &2f[P_{++}(t) + P_{--}(t)] - 2F[P_{+-}(t) + P_{-+}(t)] \\ &\quad = e^{-(2f+2F)t}\{2f[P_{++}(0) + P_{--}(0)] - 2F[P_{+-}(0) + P_{-+}(0)]\}. \end{aligned} \tag{5.69}$$

If we now solve for $P_{++}, P_{--}, P_{+-}, P_{-+}$, we have

$$\begin{aligned} P_{++}(t) &= \frac{1}{2}e^{-2ft}[P_{++}(0) - P_{--}(0)] \\ &\quad + \frac{1}{2}e^{-2(F+f)t}[P_{++}(0) + P_{--}(0)] + \frac{1}{2}\frac{F}{F+f}(1 - e^{-2(F+f)t}) \qquad (5.70) \\ P_{--}(t) &= \frac{1}{2}e^{-2ft}[P_{--}(0) - P_{++}(0)] \\ &\quad + \frac{1}{2}e^{-2(F+f)t}[P_{++}(0) + P_{--}(0)] + \frac{1}{2}\frac{F}{F+f}(1 - e^{-2(F+f)t}) \qquad (5.71) \\ P_{+-}(t) &= \frac{1}{2}e^{-2Ft}[P_{+-}(0) - P_{-+}(0)] \\ &\quad + \frac{1}{2}e^{-2(F+f)t}[P_{+-}(0) + P_{-+}(0)] + \frac{1}{2}\frac{f}{F+f}(1 - e^{-2(F+f)t}) \qquad (5.72) \\ P_{-+}(t) &= \frac{1}{2}e^{-2Ft}[P_{-+}(0) - P_{+-}(0)] \\ &\quad + \frac{1}{2}e^{-2(F+f)t}[P_{+-}(0) + P_{-+}(0)] + \frac{1}{2}\frac{f}{F+f}(1 - e^{-2(F+f)t}) \qquad (5.73) \end{aligned}$$

In the steady state, the probabilities become

$$P_{++} = P_{--} = \frac{1}{2}\frac{F}{F+f}, \qquad (5.74)$$

$$P_{+-} = P_{-+} = \frac{1}{2}\frac{f}{F+f}. \qquad (5.75)$$

Since we have chosen $F > f$, the probability to find the particles in the aligned states $++$ and $--$ is larger than the probability to find them in the unaligned states $+-$ and $-+$.

We now construct equations of motion for the four Qs. We do this simply by keeping the flipping terms the same (again, since we have made the simplification that the interaction does not depend on the separation between the particles) and

adding drift terms,

$$\frac{\partial Q_{++}}{\partial t} = -c\frac{\partial Q_{++}}{\partial x_1} - c\frac{\partial Q_{++}}{\partial x_2} + F[Q_{+-} + Q_{-+}] - 2f[Q_{++}], \tag{5.76}$$

$$\frac{\partial Q_{--}}{\partial t} = +c\frac{\partial Q_{--}}{\partial x_1} + c\frac{\partial Q_{--}}{\partial x_2} + F[Q_{+-} + Q_{-+}] - 2f[Q_{--}], \tag{5.77}$$

$$\frac{\partial Q_{+-}}{\partial t} = -c\frac{\partial Q_{+-}}{\partial x_1} + c\frac{\partial Q_{+-}}{\partial x_2} + f[Q_{++} + Q_{--}] - 2F[Q_{+-}], \tag{5.78}$$

$$\frac{\partial Q_{-+}}{\partial t} = +c\frac{\partial Q_{-+}}{\partial x_1} - c\frac{\partial Q_{-+}}{\partial x_2} + f[Q_{++} + Q_{--}] - 2F[Q_{-+}]. \tag{5.79}$$

It is possible to solve the equations of motion exactly by Fourier transforming and solving the resulting set of linear ordinary differential equations by diagonalizing a 4x4 matrix, i.e. write

$$\frac{\partial}{\partial t}\hat{\mathbf{Q}}(k_1, k_2, t) = -\mathbf{A}(k_1, k_2)\hat{\mathbf{Q}}(k_1, k_2, t) \tag{5.80}$$

where $\hat{\mathbf{Q}}(k_1, k_2, t)$ is a vector which contains the Fourier transformed distributions,

$$\hat{\mathbf{Q}}(k_1, k_2, t) \equiv \begin{pmatrix} \hat{Q}_{++}(k_1, k_2, t) \\ \hat{Q}_{--}(k_1, k_2, t) \\ \hat{Q}_{+-}(k_1, k_2, t) \\ \hat{Q}_{-+}(k_1, k_2, t) \end{pmatrix} \tag{5.81}$$

and the matrix $\mathbf{A}(k_1, k_2)$ is

$$\mathbf{A}(k_1, k_2) = \begin{pmatrix} ic(k_1 + k_2) + 2f & 0 & -F & -F \\ 0 & -ic(k_1 + k_2) + 2f & -F & -F \\ -f & -f & ic(k_1 - k_2) + 2F & 0 \\ -f & -f & 0 & ic(k_2 - k_1) + 2F \end{pmatrix}. \tag{5.82}$$

The solution can be formally written as

$$\hat{\mathbf{Q}}(k_1, k_2, t) = \exp[-\mathbf{A}(k_1, k_2)t]\hat{\mathbf{Q}}(k_1, k_2, 0), \tag{5.83}$$

or in the Laplace domain as

$$\breve{\mathbf{Q}}(k_1, k_2, \epsilon) = [\epsilon\mathbf{I} + \mathbf{A}(k_1, k_2)]^{-1}\hat{\mathbf{Q}}(k_1, k_2, 0). \tag{5.84}$$

Explicit expressions can be found by diagonalizing the 4x4 matrix $\mathbf{A}$ to calculate the exponential (in the time domain), or inverting $\epsilon\mathbf{I}+\mathbf{A}$ (in the Laplace domain). These operations can be performed in computer algebra systems, but the resulting expression are too large to reproduce here. Instead, we calculate the first two moments, and some continuous coarse-grained quantities.

One way to calculate the first two moments is to follow the same procedure as in the single-particle case: Fourier transform the equations of motion for the Qs and take k-space derivatives to obtain equations of motion for the moments. A simpler method which we will apply here is to write stochastic differential equations for the positions of the two-particles, and calculate the moments from them by ensemble averaging. The velocity of the mth particle is simply the speed c times the direction the particle is moving in σ_m,

$$\dot{x}_m(t) = c\sigma_m(t). \tag{5.85}$$

Since σ_m is a stochastic variable (and therefore x_m is as well), these are stochastic differential equations, but not necessarily Langevin equations since σ_m does not represent Gaussian white noise. However, since the interaction strength does not depend on the positions, the statistical properties of the directions are defined simply through the Master equation (5.59)–(5.62). Ensemble averaging equation (5.85), we have an equation of motion for the first moment $\langle x_m\rangle$.

$$\frac{d}{dt}\langle x_m(t)\rangle = c\langle\sigma_m(t)\rangle. \tag{5.86}$$

This may also be derived directly from the equations of motion for the Qs.

How does the average direction $\langle\sigma_m(t)\rangle$ evolve in time? The total probability for the first particle to be pointing to the right is $P_{++} + P_{+-}$, and the total probability for the first particle to be pointing to the left is $P_{-+} + P_{--}$, therefore the average direction of the first particle is

$$\langle\sigma_1(t)\rangle = [P_{++}(t) + P_{+-}(t)] - [P_{-+}(t) + P_{--}(t)]. \tag{5.87}$$

Similarly, the average direction of the second particle is

$$\langle \sigma_2(t) \rangle = [P_{++}(t) + P_{-+}(t)] - [P_{+-}(t) + P_{--}(t)]. \tag{5.88}$$

Using equations (5.66) and (5.67) average directions evolve as

$$\langle \sigma_1(t) \rangle = e^{-2ft} \frac{\langle \sigma_1(0) \rangle + \langle \sigma_2(0) \rangle}{2} + e^{-2Ft} \frac{\langle \sigma_1(0) \rangle - \langle \sigma_2(0) \rangle}{2}, \tag{5.89}$$

$$\langle \sigma_2(t) \rangle = e^{-2ft} \frac{\langle \sigma_1(0) \rangle + \langle \sigma_2(0) \rangle}{2} - e^{-2Ft} \frac{\langle \sigma_1(0) \rangle - \langle \sigma_2(0) \rangle}{2}. \tag{5.90}$$

Substituting into equation (5.86) and integrating, the average positions of the first and second particles are

$$\frac{\langle x_1(t) \rangle - \langle x_1(0) \rangle}{c} = \frac{1 - e^{-2ft}}{2f} \frac{\langle \sigma_1(0) \rangle + \langle \sigma_2(0) \rangle}{2} + \frac{1 - e^{-2Ft}}{2F} \frac{\langle \sigma_1(0) \rangle - \langle \sigma_2(0) \rangle}{2}, \tag{5.91}$$

$$\frac{\langle x_2(t) \rangle - \langle x_2(0) \rangle}{c} = \frac{1 - e^{-2ft}}{2f} \frac{\langle \sigma_1(0) \rangle + \langle \sigma_2(0) \rangle}{2} - \frac{1 - e^{-2Ft}}{2F} \frac{\langle \sigma_1(0) \rangle - \langle \sigma_2(0) \rangle}{2}. \tag{5.92}$$

At short times, the particles simply drift in whichever direction they are initially pointing in,

$$\langle x_1(t) \rangle \approx \langle x_1(0) \rangle + c \langle \sigma_1(0) \rangle t, \tag{5.93}$$

$$\langle x_2(t) \rangle \approx \langle x_2(0) \rangle + c \langle \sigma_2(0) \rangle t. \tag{5.94}$$

At long times, both $\langle x_1 \rangle$ and $\langle x_2 \rangle$ go to a constant, since even though the particles tend to align, there is no preferred direction for them to point in (i.e. the $++$ state is just as likely as the $--$ state).

The alignment interaction does affect the average positions at intermediate times. For example, consider the case when at time $t = 0$ the direction of the first particle is random, $\langle \sigma_1(0) \rangle = 0$, but the second particle is pointing to the right, $\langle \sigma_2(0) \rangle = 1$. In this case, we have

$$\langle x_1(t) \rangle = \langle x_1(0) \rangle + \frac{c}{2} \left(\frac{1 - e^{-2ft}}{2f} - \frac{1 - e^{-2Ft}}{2F} \right), \tag{5.95}$$

$$\langle x_2(t) \rangle = \langle x_2(0) \rangle + \frac{c}{2} \left(\frac{1 - e^{-2ft}}{2f} + \frac{1 - e^{-2Ft}}{2F} \right). \tag{5.96}$$

At short times, the first particle is stationary, and the second particle drifts to the right at speed c, but at intermediate times, the first particle also begins to drift to the right due to the alignment interaction.

Now let us calculate the second moments. Again, these may be calculated direction from the equations of motion for the Qs, but instead we calculate starting from the stochastic differential equations for the positions. Integrating equation (5.85), we have

$$x_m(t) = x_m(0) + c\int_0^t \sigma_m(t')dt'. \tag{5.97}$$

Multiplying by $x_n(t)$ and ensemble averaging,

$$\begin{aligned}\langle x_m(t)x_n(t)\rangle = \langle x_m(0)x_n(0)\rangle + c\int_0^t \langle x_m(0)\sigma_n(t')\rangle dt' + c\int_0^t \langle x_n(0)\sigma_m(t')\rangle dt' \\ + c^2\int_0^t\int_0^t \langle \sigma_m(t')\sigma_n(t'')\rangle dt'dt''.\end{aligned} \tag{5.98}$$

The two-time correlation function on the right hand side may be written as [127, 128]

$$\langle \sigma_m(t)\sigma_n(t+t')\rangle = \sum_{\boldsymbol{\sigma}}\sum_{\boldsymbol{\sigma}'} P_{\boldsymbol{\sigma}}(t)\sigma_m P_{\boldsymbol{\sigma}|\boldsymbol{\sigma}'}(t')\sigma'_n \tag{5.99}$$

where $\boldsymbol{\sigma}$ represents an entire configuration (i.e. for this two-particle system $++$, $-+$, $+-$, or $--$), $P_{\boldsymbol{\sigma}}(t)$ is the probability to find the particles in that configuration at time t, and $P_{\boldsymbol{\sigma}|\boldsymbol{\sigma}'}(t')$ is the conditional probability for finding the configuration $\boldsymbol{\sigma}'$ at time t' given that the particles began in a configuration $\boldsymbol{\sigma}$. We have

$$\sum_{\boldsymbol{\sigma}'} P_{\boldsymbol{\sigma}|\boldsymbol{\sigma}'}(\tau)\sigma'_n = \langle \sigma_n(\tau)\rangle_{\boldsymbol{\sigma}} \tag{5.100}$$

where the right hand side means the average value of the nth direction at time τ given that the system began in a configuration $\boldsymbol{\sigma}$. Using equations (5.89) and (5.90), these are

$$\langle \sigma_1(t')\rangle_{\boldsymbol{\sigma}} = \frac{e^{-2ft'}+e^{-2Ft'}}{2}\sigma_1 + \frac{e^{-2ft'}-e^{-2Ft'}}{2}\sigma_2, \tag{5.101}$$

$$\langle \sigma_2(t')\rangle_{\boldsymbol{\sigma}} = \frac{e^{-2ft'}-e^{-2Ft'}}{2}\sigma_1 + \frac{e^{-2ft'}+e^{-2Ft'}}{2}\sigma_2. \tag{5.102}$$

Using $\sigma_1^2 = \sigma_2^2 = 1$, we have

$$\begin{aligned}\langle\sigma_1(t)\sigma_1(t+t')\rangle &= \langle\sigma_2(t)\sigma_2(t+t')\rangle \\ &= \frac{e^{-2ft'}+e^{-2Ft'}}{2} + \frac{e^{-2ft'}-e^{-2Ft'}}{2}\langle\sigma_1(t)\sigma_2(t)\rangle \end{aligned} \tag{5.103}$$

and

$$\begin{aligned}\langle\sigma_1(t)\sigma_2(t+t')\rangle &= \langle\sigma_2(t)\sigma_1(t+t')\rangle \\ &= \frac{e^{-2ft'}-e^{-2Ft'}}{2} + \frac{e^{-2ft'}+e^{-2Ft'}}{2}\langle\sigma_1(t)\sigma_2(t)\rangle. \end{aligned} \tag{5.104}$$

We must now calculate the equal-time pair correlation function $\langle\sigma_1(t)\sigma_2(t)\rangle$. We have

$$\langle\sigma_1(t)\sigma_2(t)\rangle = \sum_{\boldsymbol{\sigma}} \sigma_1\sigma_2 P_{\boldsymbol{\sigma}}(t) = P_{++}(t) + P_{--}(t) - P_{+-}(t) - P_{-+}(t). \tag{5.105}$$

Using equations (5.70) through (5.73), the equal time pair correlation function is

$$\langle\sigma_1(t)\sigma_2(t)\rangle = e^{-2(F+f)t}\langle\sigma_1(0)\sigma_2(0)\rangle + \frac{F-f}{F+f}(1-e^{-2(F+f)t}). \tag{5.106}$$

Now, let us simplify to the case where both particles start at $x = 0$ with random directions. In this case $\langle x_m(0)\sigma_n(t)\rangle = 0$, $\langle x_m(0)x_n(0)\rangle = 0$, $\langle\sigma_1(0)\sigma_2(0)\rangle = 0$, and equation (5.98) reduces to

$$\langle x_m(t)x_n(t)\rangle = c^2\int_0^t\int_0^t \langle\sigma_m(t')\sigma_n(t'')\rangle dt'dt''. \tag{5.107}$$

Rewriting the double integral on the right hand side and using the fact that nothing changes in this system if σ_1 and σ_2 are interchanged,

$$\langle x_m(t)x_n(t)\rangle = 2c^2\int_0^t\int_0^{t-t'} \langle\sigma_m(t')\sigma_n(t'+t'')\rangle dt''dt'. \tag{5.108}$$

Substituting and performing the integration, we have

$$\begin{aligned}\langle x_1^2(t)\rangle = \langle x_2^2(t)\rangle = 2c^2\Bigg[&\left(\frac{1-e^{-2Ft}}{2F} - \frac{1-e^{-2ft}}{2f}\right)\left(\frac{F-f}{4F(F+f)}\right) \\ &- \left(\frac{1-e^{-2(F+f)t}}{2(F+f)}\right)\left(\frac{F^2+f^2}{4Ff(F+f)}\right) \\ &+ \frac{2ft-(1-e^{-2ft})}{(2f)^2}\frac{F}{F+f} + \frac{2Ft-(1-e^{-2Ft})}{(2F)^2}\frac{f}{F+f}\Bigg]. \end{aligned} \tag{5.109}$$

and

$$\langle x_1(t)x_2(t)\rangle = 2c^2\Bigg[\frac{F-f}{8Ff(F+f)}\left(e^{-2Ft}+e^{-2ft}-e^{-2(F+f)t}-1\right) \\ \frac{2ft-(1-e^{-2ft})}{(2f)^2}\frac{F}{F+f}-\frac{2Ft-(1-e^{-2Ft})}{(2F)^2}\frac{f}{F+f}\Bigg] \tag{5.110}$$

At short times, we have $\langle x_1^2(t)\rangle \approx (ct)^2$ (ballistic motion), and at long times the second moment is proportional to time,

$$\langle x_1^2(t)\rangle \approx \text{const} + c^2\frac{F^2+f^2}{Ff(F+f)}t, \tag{5.111}$$

which is characteristic of diffusive motion with an effective diffusion constant

$$D_{\text{eff}} = c^2\frac{F^2+f^2}{2Ff(F+f)} \tag{5.112}$$

This is similar to the one-particle (telegrapher) case. In fact, if we set $f = F$, i.e. both particles flip independently and we get the same effective diffusion constant as in the one-particle case, $D_{\text{eff}} = c^2/(2F)$.

If F and f are switched, then for this initial condition, $\langle x_1^2\rangle$ and $\langle x_2^2\rangle$ do not change, i.e. it does not matter for $\langle x_1^2\rangle$ and $\langle x_2^2\rangle$ if the birds tend to align or antialign because the interaction has infinite range.

To see the effect of the alignment, we must look at two-particle observables such as the mixed moment $\langle x_1x_2\rangle$. This is a measure of how strongly the positions of the two-particles are correlated. At long times the positions are positively correlated so long as $F > f$,

$$\langle x_1x_2\rangle \approx \text{const} + c^2\frac{F^2-f^2}{Ff(F+f)}t. \tag{5.113}$$

For $F = f$, the correlation vanishes for all times since the particles then flip independently of each other.

We now look at coarse-grained continuum quantities, starting with the joint dis-

tribution function defined by

$$Q(x_1, x_2, t) \equiv Q_{++}(x_1, x_2, t) + Q_{+-}(x_1, x_2, t) + Q_{-+}(x_1, x_2, t) + Q_{--}(x_1, x_2, t). \tag{5.114}$$

Defined in this way, $Q(x_1, x_2, t)dx_1dx_2$ is the total probability to find the first particle in a small interval between x_1 and $x_1 + dx_1$ and the second particle in a small interval between x_2 and $x_2 + dx_2$ at time t with either particle pointing in any direction.

We take an initial condition in which the directions of both particles are random, i.e.

$$Q_{++}(x_1, x_2, 0) = Q_{+-}(x_1, x_2, 0) = Q_{-+}(x_1, x_2, 0) = Q_{--}(x_1, x_2, 0) = \tfrac{Q(x_1,x_2,0)}{4} \ . \tag{5.115}$$

Using a computer algebra system to perform coarse-graining on the full solution, the evolution of Q in the Fourier-Laplace domain for this initial condition is

$$\breve{Q}(k_1, k_2, \epsilon) = \frac{1}{\epsilon - \breve{\mathcal{M}}(k_1, k_2, \epsilon)} \hat{Q}(k_1, k_2, 0) \tag{5.116}$$

where the memory $\mathcal{M}$ is, in the transformed domain,

$$\breve{\mathcal{M}}(k_1, k_2, \epsilon) \equiv \tfrac{-c^2[(\epsilon^2+3F\epsilon+4F^2)k_+^2+(3f\epsilon+4f^2)k_-^2+c^2(k_+k_-)^2]}{8Ff(F+f)+4(F^2+f^2)\epsilon+4(F+f)\epsilon^2+12Ff\epsilon+c^2Fk_+^2+c^2fk_-^2+c^2\epsilon(k_+^2+k_-^2)/2+\epsilon^3} \ . \tag{5.117}$$

with

$$k_+ \equiv k_1 + k_2, \tag{5.118}$$

$$k_- \equiv k_1 - k_2. \tag{5.119}$$

Since the series expansion of $\breve{\mathcal{M}}(k_1, k_2, \epsilon)$ in powers of k_1 and k_2 has infinitely many terms, the joint distribution Q obeys an equation of motion which is non-local in both space and time,

$$\frac{\partial}{\partial t} Q(x_1, x_2, t) = \int_{-\infty}^{\infty} \int_{-\infty}^{\infty} \int_0^t \mathcal{M}(x_1 - x_1', x_2 - x_2', t - t') Q(x_1', x_2', t) dt' dx_1' dx_2'. \tag{5.120}$$

From the joint distribution Q, we can coarse-grain further to the single-particle distributions by integrating out one of the position variables,

$$Q_1^{(1)}(x,t) \equiv \int_{-\infty}^{\infty} Q(x,x_2,t)dx_2, \tag{5.121}$$

$$Q_2^{(1)}(x,t) \equiv \int_{-\infty}^{\infty} Q(x_1,x,t)dx_1. \tag{5.122}$$

For the same initial condition, we have

$$\breve{Q}_1^{(1)}(k,\epsilon) = \frac{1}{\epsilon - \breve{\mathcal{M}}_1(k,\epsilon)}\hat{Q}_1^{(1)}(k,0) \tag{5.123}$$

$$\breve{Q}_2^{(1)}(k,\epsilon) = \frac{1}{\epsilon - \breve{\mathcal{M}}_1(k,\epsilon)}\hat{Q}_2^{(1)}(k,0) \tag{5.124}$$

with

$$\begin{aligned}\breve{\mathcal{M}}_1(k,\epsilon) &= \breve{\mathcal{M}}(k,0,\epsilon) = \breve{\mathcal{M}}(0,k,\epsilon) \\ &= \tfrac{-c^2[(4F^2+4f^2+3F\epsilon+3f\epsilon+\epsilon^2+c^2k^2)k^2]}{8Ff(F+f)+4(F^2+f^2)\epsilon+4(F+f)\epsilon^2+12Ff\epsilon+c^2(F+f)k^2+c^2k^2\epsilon+\epsilon^3}\ .\end{aligned} \tag{5.125}$$

The memory $\mathcal{M}_1$ is again non-local in both space and time, and the single-particle distributions obey

$$\frac{\partial}{\partial t}Q^{(1)}(x,t) = \int_{-\infty}^{\infty}\int_0^t \mathcal{M}_1(x-x',t-t')Q^{(1)}(x',t')dt'dx'. \tag{5.126}$$

Finally, we calculate the center of mass distribution. We define $Q_{\rm cm}(x,t)dx$ as the probability to find the center of mass $x_{\rm cm} = (x_1+x_2)/2$ between x and $x+dx$ at time t. This can be obtained from the joint distribution by changing to coordinates

$$x_+ = \frac{x_1+x_2}{2} \tag{5.127}$$

$$x_- = \frac{x_1-x_2}{2} \tag{5.128}$$

and integrating out x_-. For the same initial condition, the evolution of the center of mass distribution in the Fourier-Laplace domain is

$$\breve{Q}_{\rm cm}(k,\epsilon) = \frac{1}{\epsilon - \breve{\mathcal{M}}_{\rm cm}(k,\epsilon)}\hat{Q}_{\rm cm}(k,0) \tag{5.129}$$

with the memory given by

$$\breve{\mathcal{M}}_{\rm cm}(k,\epsilon) = \frac{-c^2k^2(4F+\epsilon)}{8f(F+f)+4\epsilon(F+2f)+c^2k^2+2\epsilon^2}. \tag{5.130}$$

The center of mass distribution again obeys an equation of motion which is non-local in both space in time,

$$\frac{\partial}{\partial t}Q_{\rm cm}(x,t) = \int_{-\infty}^{\infty}\int_0^t \mathcal{M}_{\rm cm}(x-x',t-t')Q_{\rm cm}(x',t')dt'dx' \tag{5.131}$$

Since memory for the center of mass distribution $\mathcal{M}_{\rm cm}$ is relatively simple, let us look at it in more detail.

We can use the methods described in section 4.5.2 to write an approximate evolution equation which is local in space. We have for the first expansion coefficient in the Laplace domain

$$-\frac{1}{2}\frac{\partial^2}{\partial k^2}\breve{\mathcal{M}}_{\rm cm}(k,\epsilon)\bigg|_{k=0} = \frac{c^2(4F+\epsilon)}{8f(F+f)+4\epsilon(F+2f)+2\epsilon^2}. \tag{5.132}$$

The Laplace transform can be inverted with a partial fraction decomposition. The result is

$$-\frac{1}{2}\frac{\partial^2}{\partial k^2}\hat{\mathcal{M}}_{\rm cm}(k,t)\bigg|_{k=0} = \frac{1}{2}c^2e^{-(F+2f)t}\left[\cosh(Ft)+\frac{3F-2f}{F}\sinh(Ft)\right]. \tag{5.133}$$

This is the approximate space local memory. For large t, it decays exponentially like e^{-2ft}, but since the derivative at $t=0$ is $c^2(F-2f)$ it can grow or decay at short times depending on whether f is smaller or larger than $F/2$.

Now let us try to gain some insight into the spatial dependence of the memory. The series expansion of $\mathcal{M}$ in powers of k does not contain any terms of order lower than k^2, so we can rewrite the evolution as

$$\frac{\partial}{\partial t}Q_{\rm cm}(x,t) = \int_{-\infty}^{\infty}\int_0^t \mathcal{D}(x-x',t-t')\frac{\partial^2}{\partial x'^2}Q_{\rm cm}(x',t')dt'dx' \tag{5.134}$$

with $\mathcal{D}$ related to $\mathcal{M}_{\rm cm}$ by

$$\breve{\mathcal{D}}(k,t) = \frac{-1}{k^2}\breve{\mathcal{M}}_{\rm cm}(k,t) = \frac{c^2(4F+\epsilon)}{8f(F+f)+4\epsilon(F+2f)+c^2k^2+2\epsilon^2}. \tag{5.135}$$

The Fourier transform can be inverted by using the fact that the Fourier transform of $e^{-a|x|}$ is

$$\mathcal{F}[e^{-a|x|}](k) = \int_{-\infty}^{\infty} e^{-a|x|}e^{-ikx}dx = \frac{2a}{a^2+k^2}. \tag{5.136}$$

Then in the real space-Laplace domain, we have

$$\tilde{\mathcal{D}}(x,\epsilon) = \frac{c(4F+\epsilon)}{2\sqrt{8f(F+f)+4\epsilon(F+2f)+2\epsilon^2}} \exp\left(-\frac{|x|}{c}\sqrt{8f(F+f)+4\epsilon(F+2f)+2\epsilon^2}\right). \tag{5.137}$$

Although we cannot invert the Laplace transform we can gain some understanding of the long time dynamics by making the so-called Markovian approximation, in which the memory is replaced with a delta function times its integral,

$$\mathcal{D}(x,t) \approx \delta(t)\int_0^{\infty} \mathcal{D}(x,t')dt'. \tag{5.138}$$

Using equation (5.137) gives for the integral on the right hand side

$$\int_0^{\infty} \mathcal{D}(x,t')dt' = \tilde{\mathcal{D}}(x,0) = \frac{cF}{\sqrt{2f(F+f)}} \exp\left(-\frac{|x|}{c}\sqrt{8f(F+f)}\right). \tag{5.139}$$

In this limit, the memory decays exponentially with distance at rate which depends on the speed c and the flipping rates F and f.

What about the short time dynamics? Suppose that we have an initial condition where both particles start at $x = 0$ with random directions. At short times, before the particles have had a chance to flip, there is probability $1/2$ to have one particle pointing right and one particle pointing left. Therefore the center of mass does not move. Otherwise, with probability $1/4$ each, we have both particles pointing to the right (in which case the center of mass moves to the right at speed c) or both particles pointing to the left (in which case the center of mass moves to the left at speed c). The Green's function for the center of mass at short times is thus

$$G_{\text{cm}}(x,0,t) \approx \frac{1}{2}\delta(x) + \frac{1}{4}\delta(x-ct) + \frac{1}{4}\delta(x+ct). \tag{5.140}$$

Using the formalism developed in Section 4.5.2, the memory is approximately

$$\breve{\mathcal{M}}_{cm}(k,\epsilon) = \epsilon - \frac{1}{\breve{\mathcal{G}}(k,\epsilon)} \approx -(ck)^2\frac{\epsilon}{2\epsilon^2+(ck)^2} \tag{5.141}$$

in which case $\mathcal{D}$ is approximately

$$\breve{\mathcal{D}}(k,\epsilon) \approx c^2 \frac{\epsilon}{2\epsilon^2 + (ck)^2}. \tag{5.142}$$

Inverting both the Laplace and Fourier transforms gives the short time memory as

$$\mathcal{D}(x,t) \approx \frac{c^2}{4}\left[\delta\left(x - \frac{ct}{\sqrt{2}}\right) + \delta\left(x - \frac{ct}{\sqrt{2}}\right)\right]. \tag{5.143}$$

The memory at short times thus connects the evolution of distribution at a point x at time t only to the distribution at different positions within the range $|x| < ct/\sqrt{2}$. This is entirely expected and represents ballistic motion at short times.

5.3 Generalization to Many Particles

We now generalize the model to N particles. Again, the particles move in one dimension at a constant speed c, but with directions that change randomly, with the flipping rates constructed so that there is an alignment effect. We will make use of an existing model, Glauber dynamics for the Ising model, to construct the rates. The interaction will again be infinite ranged in the sense that the tendency for particles to align is not affected by the relative distance between them.

We will describe the complete state of the system using 2^N functions which depend on N spatial variables (the positions of the particles) and time. Generalizing our earlier notation, we denote these by $Q_{\boldsymbol{\sigma}}(\mathbf{x},t)$. The quantity $\boldsymbol{\sigma}$ represents a complete set of directions, i.e. it is a quantity with N components with the nth component, σ_n, representing the direction of the nth particle (either -1 or $+1$). The quantity $\mathbf{x}$ is an N dimensional vector with the nth component x_n representing the position of the nth particle. Let $Q_{\boldsymbol{\sigma}}(\mathbf{x},t)d^N x$ be the probability to find the system in a state with directions given by $\boldsymbol{\sigma}$ and particle 1 between x_1 and $x_1 + dx_1$, particle 2 between x_2 and $x_2 + dx_2$ et cetera at time t.

For the evolution of $Q_{\boldsymbol{\sigma}}(\mathbf{x},t)$ we take the general form

$$\frac{\partial}{\partial t}Q_{\boldsymbol{\sigma}}(\mathbf{x},t) = -c\sum_n \sigma_n \frac{\partial}{\partial x_n}Q_{\boldsymbol{\sigma}}(\mathbf{x},t) + \sum_{\boldsymbol{\sigma}'}\left[w_{\boldsymbol{\sigma},\boldsymbol{\sigma}'}Q_{\boldsymbol{\sigma}'}(\mathbf{x},t) - w_{\boldsymbol{\sigma}',\boldsymbol{\sigma}}Q_{\boldsymbol{\sigma}}(\mathbf{x},t)\right] \quad (5.144)$$

where the sum over $\boldsymbol{\sigma}'$ means to sum on all possible configurations $\boldsymbol{\sigma}'$, i.e. sum over $\sigma_1' = -1, +1$, $\sigma_2' = -1, +1$ et cetera, and $w_{\boldsymbol{\sigma},\boldsymbol{\sigma}'}$ is the probability per unit time to flip from a configuration $\boldsymbol{\sigma}'$ to a configuration $\boldsymbol{\sigma}$.

The first term on the right hand side represents the motion of the particles at speed c in the directions specified by $\boldsymbol{\sigma}$, and the next two terms represent the directional flipping.

The probabilities $P_{\boldsymbol{\sigma}}$ to find the particles in with a set of directions $\boldsymbol{\sigma}$ no matter where they are located are obtained by integrating out the positions,

$$P_{\boldsymbol{\sigma}}(t) = \int Q_{\boldsymbol{\sigma}}(\mathbf{x},t)d^N x = \hat{Q}_{\boldsymbol{\sigma}}(\mathbf{k}=0,t). \quad (5.145)$$

These evolve in time simply as

$$\frac{d}{dt}P_{\boldsymbol{\sigma}}(t) = \sum_{\boldsymbol{\sigma}'}\left[w_{\boldsymbol{\sigma},\boldsymbol{\sigma}'}P_{\boldsymbol{\sigma}'}(t) - w_{\boldsymbol{\sigma}',\boldsymbol{\sigma}}P_{\boldsymbol{\sigma}}(t)\right]. \quad (5.146)$$

Again, we can see explicitly that since the interaction is infinite ranted, the direction flipping dynamics is completely independent of the positions of the particles.

We will now construct the flipping rates $w_{\boldsymbol{\sigma}',\boldsymbol{\sigma}}$. The directions of the particles are similar to spins in an Ising model [129] in the sense that each spin or direction can take on only two values. Discussion of the Ising model can be found in many introductory textbooks on statistical physics, see for example refs. [130, 131].

In a ferromagnetic Ising model, aligning two interacting spins lowers the interaction energy between those two spins, but the Ising model itself has no intrinsic dynamics so gives us no insight into how to construct the flipping rates. There are however ways to add dynamics to the Ising model. The approach applicable to this system, due to Glauber [127], is to construct equations of motion for the probabilities

to find the system in a given spin configuration, the quantities which we have here written as $P_{\boldsymbol{\sigma}}$.

We construct the rates following Glauber's procedure. The procedure will only be outlined here, more detail can be found in the papers by Glauber [127] and Suzuki and Kubo [128]. First we take an Ising model Hamiltonian (with no field),

$$H(\boldsymbol{\sigma}) = -\sum_{m<n} J_{mn}\sigma_m\sigma_n \tag{5.147}$$

where the interaction matrix J_{mn} determines which particles interact with each other and how strongly. We suppose that the system is in contact with a heat bath at temperature T which causes the particles to flip directions stochastically. We only allow only one-particle to flip at a time, so that $w_{\boldsymbol{\sigma}',\boldsymbol{\sigma}}$ is zero unless the initial configuration $\boldsymbol{\sigma}$ and the final configuration $\boldsymbol{\sigma}'$ differ by a only single direction flip. In the steady state, the probabilities $P_{\boldsymbol{\sigma}}(t)$ to form a Boltzmann distribution,

$$P_{\boldsymbol{\sigma}}(t) \to \frac{1}{Z}e^{-\beta H(\boldsymbol{\sigma})} \tag{5.148}$$

where Z is the partition function,

$$Z = \sum_{\boldsymbol{\sigma}} e^{-\beta H(\boldsymbol{\sigma})}. \tag{5.149}$$

In the steady state, we must also have

$$\frac{d}{dt}P_{\boldsymbol{\sigma}}(t) = 0 = \sum_{\boldsymbol{\sigma}'}\left[w_{\boldsymbol{\sigma},\boldsymbol{\sigma}'}P_{\boldsymbol{\sigma}'}(t) - w_{\boldsymbol{\sigma}',\boldsymbol{\sigma}}P_{\boldsymbol{\sigma}}(t)\right]. \tag{5.150}$$

Knowing the $P_{\boldsymbol{\sigma}}$s in the steady state is still not enough to determine the rates uniquely. To determine them uniquely, we make the assumption of *detailed balance*, i.e. that every term in the sum in equation (5.150) vanishes. We then have in the steady state

$$0 = w_{\boldsymbol{\sigma},\boldsymbol{\sigma}'}P_{\boldsymbol{\sigma}'}(t) - w_{\boldsymbol{\sigma}',\boldsymbol{\sigma}}P_{\boldsymbol{\sigma}}(t) \tag{5.151}$$

and thus

$$\frac{w_{\boldsymbol{\sigma},\boldsymbol{\sigma}'}}{w_{\boldsymbol{\sigma}',\boldsymbol{\sigma}}} = \frac{P_{\boldsymbol{\sigma}}(t)}{P_{\boldsymbol{\sigma}'}(t)} = \frac{e^{-\beta H(\boldsymbol{\sigma})}}{e^{-\beta H(\boldsymbol{\sigma}')}} \tag{5.152}$$

(provided that $\boldsymbol{\sigma}'$ and $\boldsymbol{\sigma}$ differ only by a single spin flip). In the literature some authors use the notation $w_m(\sigma_m)$ to mean the probability per unit time that the mth particle flips from σ_m to $-\sigma_m$. Although we write this as a function of σ_m, this quantity really depends on the configuration of the rest of the particles as well. Similarly, $w_m(-\sigma_m)$ is the probability per time that the mth particle flips back from $-\sigma_m$ to σ_m. Using this notation, we have

$$\frac{w(\sigma_m)}{w(-\sigma_m)} = \frac{e^{-\beta E_m \sigma_m}}{e^{\beta E_m \sigma_m}} = \frac{1 - \sigma_m \tanh(\beta E_m)}{1 + \sigma_m \tanh(\beta E_m)} \tag{5.153}$$

with

$$E_m \equiv \sum_n J_{mn} \sigma_n. \tag{5.154}$$

We then choose

$$w_m(\sigma_m) = \frac{1}{2\tau}[1 - \sigma_m \tanh(\beta E_m)] \tag{5.155}$$

where τ is a constant with dimensions of time and determines the timescale of the dynamics.

We must now decide on the form of the interaction matrix J_{mn}. There are two situations in which it is possible to obtain analytic results. The first is the case analyzed by Glauber [127] where the interactions between particles form a one-dimensional lattice, i.e. the nth particle only interacts with the $(n+1)$th and $(n-1)$th particles.

The second case where analytic results can be obtained is the "mean field" or "molecular field" limit of a large number of particles with each particle interacting with all others. The dynamics near the critical point are analyzed by Suzuki and Kubo [128].

The second case is more applicable to this system since because the particles are allowed to move, so the particles may not be found in order according to their labels. For example, the $n = 3$ particle may be found in between the $n = 1$ and

$n = 2$ particles. Thus, in this simplified case when the interaction does not depend on distance, it makes more sense to have all particles interacting with all others.

As it does not matter what the diagonal elements of the interaction matrix are, we simply set them to zero. Let all the off diagonal elements have the same strength $J_0 z/(N-1)$ where J_0 is a constant. We have modulated the strength of the interaction by a factor $z/(N-1)$ where z is an effective number of other particles each particle is interacting with (and $N-1$ is the actual number). This interaction matrix can be written

$$J_{mn} = (1 - \delta_{mn}) J_0 \frac{z}{N-1}. \tag{5.156}$$

To summarize, we have a set of Ising spins which all interact with each other with equal strengths. The spins evolve in time from some initial configuration to a Boltzmann distribution via Glauber dynamics. The timescale of the flipping dynamics is determined by a single parameter τ. The other parameters relevant to the flipping dynamics are the inverse temperature β and the effective interaction strength $J_0 z$. What we call temperature here does not necessarily mean temperature in the thermodynamic sense; it should be thought of simply as a parameter which controls the strength of the noise. In addition, the particles all move at a constant speed c (as such, they are self-propelled) in the positive x direction for "spin" +1, or in the negative x direction for spin -1.

5.3.1 Average Positions

Although we cannot solve for $Q_{\boldsymbol{\sigma}}(\mathbf{x}, t)$ exactly for systems larger than $N = 2$, it is possible to calculate at least the first two moments. We apply the same procedure used for calculating the moments. Using equation (5.86), the average value of the position of the nth particle, $\langle x_n \rangle$, is related to the average direction of the nth particle by

$$\langle x_n(t) \rangle - \langle x_n(0) \rangle = c \int_0^t \langle \sigma_n(t') \rangle dt'. \tag{5.157}$$

Multiplying the equation for the evolution of the $P_{\boldsymbol{\sigma}}$s, equation (5.146), by σ_n and summing over all configurations $\boldsymbol{\sigma}$, the evolution of the average direction of the nth particle when the rates are given by equation (5.155) can be shown to be [127, 128]

$$\frac{d}{dt}\langle\sigma_n(t)\rangle = \frac{d}{dt}\sum_{\boldsymbol{\sigma}}\sigma_n P_{\boldsymbol{\sigma}}(t) = \frac{1}{\tau}\left[-\langle\sigma_m\rangle + \langle\tanh(\beta E_m)\rangle\right] \tag{5.158}$$

with

$$\langle\tanh(\beta E_m)\rangle \equiv \sum_{\boldsymbol{\sigma}}\tanh(\beta E_m)P_{\boldsymbol{\sigma}}(t). \tag{5.159}$$

We proceed to analyze the dynamics near the critical point following Suzuki and Kubo [128]. In the mean field limit we move the ensemble average inside the hyperbolic tangent,

$$\langle\tanh(\beta E_m)\rangle \approx \tanh(\beta\langle E_m\rangle) \tag{5.160}$$

and furthermore we make the approximation that all the average directions are the same, i.e. that $\langle\sigma_m\rangle = \langle\sigma\rangle$. Then using $J_{mn} = (1-\delta_{mn})J_0 z/(N-1)$, we have

$$\tau\frac{d}{dt}\langle\sigma\rangle = -\langle\sigma\rangle + \tanh(\beta J_0 z\langle\sigma\rangle). \tag{5.161}$$

In the steady state, we have the familiar mean field equation

$$\langle\sigma\rangle = \tanh(\beta J_0 z\langle\sigma\rangle). \tag{5.162}$$

The solutions are plotted in Figure 5.7. There is a phase transition at $\beta J_0 z = 1$. When $\beta J_0 z < 1$ there is only one solution, $\langle\sigma\rangle = 0$, which is stable in the sense that perturbations away from zero will decay. For $\beta J_0 z > 1$, zero is still a solution, but it becomes unstable in the sense that perturbations will grow. Furthermore, two additional nonzero solutions with opposite signs appear for $\beta J_0 z > 1$, and they are stable. These nonzero solutions correspond to phases with magnetic ordering.

Near the critical temperature, the argument of the hyperbolic tangent in equation (5.161) is small, so we expand it in a power series and keep terms up to $\langle\sigma\rangle^3$,

$$\tau\frac{d}{dt}\langle\sigma\rangle = -\langle\sigma\rangle + \beta J_0 z\langle\sigma\rangle - \frac{1}{3}(\beta J_0 z\langle\sigma\rangle)^3. \tag{5.163}$$

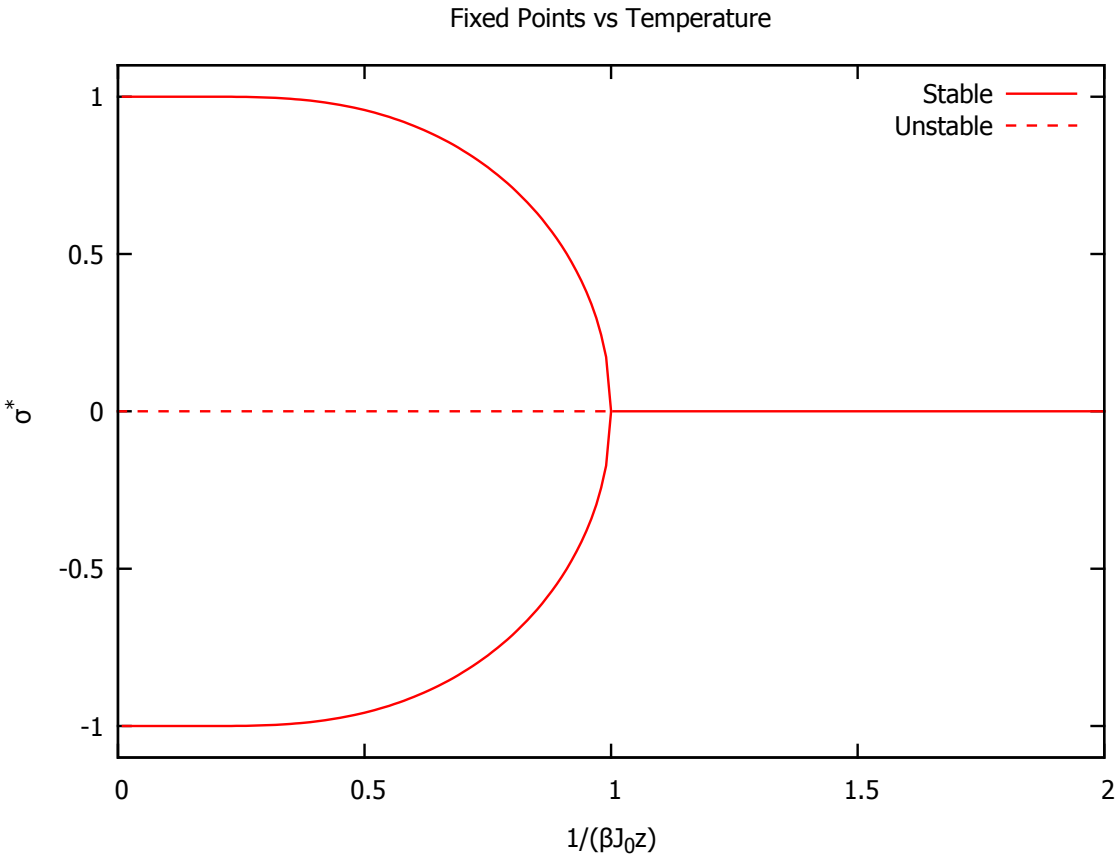

Figure 5.7: Solutions of $\sigma^* = \tanh(\beta J_0 z \sigma^*)$ versus $1/(\beta J_0 z)$.

This differential equation can be solved exactly (it is a Bernoulli differential equation). Away from the critical temperature, the solution is [128]

$$\langle \sigma(t) \rangle = \pm \left[\left(\frac{1}{\langle \sigma(0) \rangle^2} + \frac{\eta}{\kappa} \right) e^{2\kappa t/\tau} - \frac{\eta}{\kappa} \right]^{-1/2} \tag{5.164}$$

with

$$\kappa \equiv 1 - \beta J_0 z, \tag{5.165}$$

$$\eta \equiv \frac{1}{3}(\beta J z)^3. \tag{5.166}$$

The sign must be taken to be the same as the sign of $\langle \sigma(0) \rangle$, i.e. if $\langle \sigma(0) \rangle$ is positive, the positive sign is correct, otherwise the negative sign is correct.

Above the critical temperature ($\beta J_0 z < 1$), $\langle\sigma\rangle$ decays from its initial value to zero. This means that the average positions, $\langle x_m\rangle$ can increase or decrease at short times but eventually saturate to a constant value, as in the two-particle case.

Below the critical temperature ($\beta J_0 z > 1$), if $\langle\sigma\rangle$ starts at zero, then it remains at zero. However since zero is unstable, if the system is perturbed it will go to one of the stable solutions, $\langle\sigma\rangle = \pm\sqrt{-\kappa/\eta}$.

At the critical point, $\beta J_0 z = 1$, the solution becomes [128]

$$\langle\sigma(t)\rangle = \left[\frac{1}{\langle\sigma(0)\rangle^2} + \frac{2\eta t}{\tau}\right]^{-1/2}. \tag{5.167}$$

The average direction decays from its initial value to zero at long times, but it does so much slower (like $1/\sqrt{t}$) than it does away from the critical point.

For the mean position at the critical point, we have

$$\langle x(t)\rangle - \langle x(0)\rangle = \frac{c\tau}{\eta\langle\sigma(0)\rangle}\left[\sqrt{1 + \frac{2\eta\langle\sigma(0)\rangle^2}{\tau}t} - 1\right] \tag{5.168}$$

which surprisingly still increases at long times like $\sqrt{t}$ if $\langle\sigma(0)\rangle$ is nonzero.

5.3.2 Second Moments

We now calculate the second moments $\langle x_m^2\rangle$ and the mixed moments $\langle x_m x_n\rangle$. For an initial condition in which all particles start at $x = 0$ we have again

$$\langle x_m(t)x_n(t)\rangle = 2c^2\int_0^t\int_0^{t-t'}\langle\sigma_m(t')\sigma_n(t'+t'')\rangle dt''dt'. \tag{5.169}$$

We analyze separately the dynamics in the disordered and ordered phases.

Disordered Phase, $\beta J_0 z < 1$

We can calculate the two time spin correlation function following the procedure described by Glauber [127] and Suzuki and Kubo [128]. We have again

$$\langle \sigma_m(t)\sigma_n(t+t')\rangle = \sum_{\boldsymbol{\sigma},\boldsymbol{\sigma}'} \sigma_m \sigma_n' P_{\boldsymbol{\sigma}}(t) P_{\boldsymbol{\sigma}|\boldsymbol{\sigma}'}(t') \tag{5.170}$$

where $P_{\boldsymbol{\sigma}|\boldsymbol{\sigma}'}(t')$ is the conditional probability to find the spins in a configuration $\boldsymbol{\sigma}'$ at time t' given that they began at a configuration $\boldsymbol{\sigma}$. We can write

$$\sum_{\boldsymbol{\sigma}'} \sigma_n' P_{\boldsymbol{\sigma}|\boldsymbol{\sigma}'}(t') = \langle \sigma_n(t')\rangle_{\boldsymbol{\sigma}} \tag{5.171}$$

where $\langle \sigma_n(t')\rangle_{\boldsymbol{\sigma}}$ means the average value of σ_n at time t' given that the spins began in a configuration $\boldsymbol{\sigma}$. In the mean field, we have again for the evolution of the average directions

$$\tau \frac{d}{dt}\langle \sigma_n\rangle = -\langle \sigma_n\rangle + \tanh(\beta \langle E_n\rangle). \tag{5.172}$$

We do not assume here that all the average directions are the same. Above the critical temperature, we expect the argument of the tanh to be small, so we expand the right hand side and this time only keep the linear term,

$$\tau \frac{d}{dt}\langle \sigma_n\rangle = -\langle \sigma_n\rangle + \beta J_{nl} \sum_l \langle \sigma_l\rangle = -\langle \sigma_n\rangle + \beta J_0 z \frac{1}{N-1} \sum_{l\neq n} \langle \sigma_l\rangle. \tag{5.173}$$

For large N, the right hand side can be rewritten approximately as

$$\tau \frac{d}{dt}\langle \sigma_n\rangle = -\langle \sigma_n\rangle + \beta J_0 z \frac{1}{N} \sum_l \langle \sigma_l\rangle. \tag{5.174}$$

The solution for an initial condition $\boldsymbol{\sigma}$ is

$$\langle \sigma_n(t)\rangle_{\boldsymbol{\sigma}} = \sum_l \Pi_{nl}(t)\sigma_l \tag{5.175}$$

with

$$\Pi_{nl}(t) = \left(\delta_{nl} - \frac{1}{N}\right) e^{-t/\tau} + \frac{1}{N} e^{-\kappa t/\tau} \tag{5.176}$$

with $\kappa = (1 - \beta J_0 z)$ as defined earlier.

We now have

$$\langle \sigma_m(t)\sigma_n(t+t')\rangle = \sum_l \Pi_{nl}(t') \sum_{\boldsymbol{\sigma}} \sigma_m \sigma_l P_{\boldsymbol{\sigma}}(t) = \sum_l \Pi_{nl}(t')\langle \sigma_m(t)\sigma_l(t)\rangle \quad (5.177)$$

so we have related the spin correlation function at unequal times to the spin correlation function at equal times.

We now calculate the equal time pair correlation function $\langle \sigma_m(t)\sigma_n(t)\rangle$ in the mean field limit, following once again Suzuki and Kubo [128]. The pair correlation function obeys (this can be derived from the evolution equation of the $P_{\boldsymbol{\sigma}}$s),

$$\tau \frac{d}{dt}\langle \sigma_m \sigma_n\rangle = -2\langle \sigma_m\sigma_n\rangle + \langle \sigma_m \tanh \beta E_n\rangle + \langle \sigma_n \tanh \beta E_m\rangle. \quad (5.178)$$

Since σ_m and σ_n can only be ± 1, they can be brought inside the tanh. Next, the ensemble average is brought inside the tanh in the mean field approximation,

$$\tau \frac{d}{dt}\langle \sigma_m \sigma_n\rangle = -2\langle \sigma_m\sigma_n\rangle + \tanh\langle \beta\sigma_m E_n\rangle + \tanh\langle \beta\sigma_n E_m\rangle. \quad (5.179)$$

For $m = n$, $\langle \sigma_m^2\rangle = 1$, and for $m \neq n$ linearize the right hand side around zero to find

$$\tau \frac{d}{dt}\langle \sigma_m \sigma_n\rangle = -2\langle \sigma_m\sigma_n\rangle + \beta \sum_l J_{nl}\langle \sigma_m\sigma_l\rangle + \beta \sum_l J_{ml}\langle \sigma_n\sigma_l\rangle. \quad (5.180)$$

Next, define $G_{ml} = \langle \sigma_m\sigma_n\rangle$ for $m \neq n$, then

$$\tau \frac{d}{dt} G_{mn} = -2G_{mn} + \beta \sum_{l\neq n} J_{nl}G_{ln} + \beta \sum_{l\neq m} J_{ml}G_{ln} + 2\beta J_{mn}. \quad (5.181)$$

For an initial condition in which is translationally invariant (i.e. $G_{mn}(0)$ only depends on $|m-n|$), G_{mn} remains translationally invariant for all time (since the interaction matrix we have chosen is also translationally invariant). We can then discrete Fourier transform to get

$$\tau \frac{d}{dt} G^q = -2G^q + 2\beta J^q G^q + 2\beta J^q \quad (5.182)$$

where

$$G^q \equiv \sum_{n\neq l} G_{nl} e^{iq(n-l)}, \qquad J^q \equiv \sum_{n\neq l} J_{nl} e^{iq(n-l)}. \tag{5.183}$$

The solution is

$$G^q(t) = G^q(0) e^{-2(1-\beta J^q)t/\tau} + \frac{\beta J^q}{1-\beta J^q}\left[1 - e^{-2(1-\beta J^q)t/\tau}\right]. \tag{5.184}$$

For an initial condition where the directions are random, $G^q(0) = 0$. For the interaction matrix defined earlier, we have

$$J^q = \sum_{n\neq l} J_{nl} e^{iq(n-l)} = \frac{J_0 z}{N-1} \sum_{n\neq l} e^{iq(n-l)} = J_0 z \delta_{q,0} \tag{5.185}$$

so

$$G^q(t) = \delta_{q,0} \frac{1-\kappa}{\kappa}\left[1 - e^{-2\kappa t/\tau}\right]. \tag{5.186}$$

Inverting the discrete Fourier transform then gives

$$G_{mn}(t) = \frac{1}{(N-1)} \frac{1-\kappa}{\kappa}\left[1 - e^{-2\kappa t/\tau}\right]. \tag{5.187}$$

We then have

$$\begin{aligned}\int_0^{t-t'} \langle \sigma_m(t')\sigma_n(t'+t'')\rangle dt'' &= \sum_l \langle \sigma_m(t')\sigma_l(t')\rangle \int_0^{t-t'} \Pi_{nl}(t'')dt'' \\ &= \tau \sum_l \langle \sigma_m(t')\sigma_l(t')\rangle \left[\left(\delta_{nl} - \frac{1}{N}\right)\left[1 - e^{-(t-t')/\tau}\right] + \frac{1}{N}\frac{1 - e^{-\kappa(t-t')/\tau}}{\kappa}\right].\end{aligned} \tag{5.188}$$

Using $\sum_l \langle \sigma_m(t')\sigma_l(t')\rangle = 1 + G^{q=0}$, this becomes

$$\begin{aligned}\int_0^{t-t'} \langle \sigma_m(t')\sigma_n(t'+t'')\rangle dt'' = \tau \langle \sigma_m(t')\sigma_n(t')\rangle [1 - e^{-(t-t')/\tau}] \\ + \frac{\tau}{N}\left[\frac{1 - e^{-\kappa(t-t')/\tau}}{\kappa} - [1 - e^{-(t-t')/\tau}]\right] \\ \cdot \left[1 + \frac{1-\kappa}{\kappa}[1 - e^{-2\kappa t'/\tau}]\right].\end{aligned} \tag{5.189}$$

To find the second moments, we need to integrate this expression over t' from 0 to t. Let us focus on the long time behavior. At long times, the integrals of the exponential terms become constants, and for $m = n$, we have

$$\langle x_m^2(t)\rangle \approx 2c^2\tau t\left[1 + \frac{1}{N}\frac{1-\kappa}{\kappa^2}\right] + \text{constant} \tag{5.190}$$

and for $m \neq n$,

$$\begin{aligned}\langle x_m(t)x_n(t)\rangle &\approx 2c^2\tau t\frac{1-\kappa}{\kappa}\left[\frac{1}{N-1} + \frac{1}{N}\frac{1}{\kappa}\right] + \text{constant} \\ &\approx 2c^2\tau t\frac{1-\kappa^2}{N\kappa^2} + \text{constant}\end{aligned} \tag{5.191}$$

for large N.

The second moments $\langle x_m^2(t)\rangle$ scale like t in the disordered phase, characteristic of diffusive motion. The effective diffusion constant is

$$D_{\text{eff}} = c^2\tau\left(1 + \frac{1}{N}\frac{1-\kappa}{\kappa^2}\right). \tag{5.192}$$

For large N and away from the critical point at $\kappa = 0$, the second term is small compared to the first term, so $D_{\text{eff}} \approx c^2\tau$.

As in the two-particle case, the correlations $\langle x_m x_n\rangle$ scale with time; however, the rate of growth scales like $1/N$ and is therefore very small away from the critical point.

Ordered Phase, $\beta J_0 z > 1$

We can also do a linear mean field analysis below the critical temperature. We have again in the mean field

$$\tau\frac{d}{dt}\langle\sigma_n\rangle = -\langle\sigma_n\rangle + \tanh(\beta\langle E_n\rangle). \tag{5.193}$$

Above the critical point, we proceeded by linearizing the tanh around zero. Below the critical point, we linearize the tanh around one of the stable fixed points σ^*. Since there is no preferred direction, $-\sigma^*$ is also a stable fixed point. We assume here the

system is perturbed from the unstable fixed point so that it moves toward the positive fixed point σ^*. The fixed point σ^* satisfies

$$0 = -\sigma^* + \tanh(\beta J_0 z \sigma^*) \tag{5.194}$$

so we have

$$\begin{aligned}\tau \frac{d}{dt}\langle\sigma_n\rangle &= -\langle\sigma_n\rangle + \tanh\left(\frac{\beta J_0 z}{N-1}\sum_{l\neq n}\langle\sigma_l\rangle\right) \\ &\approx -\langle\sigma_n\rangle + \sigma^* + \beta J_0 z\left(\frac{1}{N-1}\sum_{l\neq n}\langle\sigma_l\rangle - \sigma^*\right)[1-(\sigma^*)^2]\end{aligned} \tag{5.195}$$

using $\mathrm{sech}^2(\beta J_0 z\sigma^*) = 1 - \tanh^2(\beta J_0 z\sigma^*) = 1-(\sigma^*)^2$. For large N, we the sum can be rewritten approximately as

$$\frac{1}{N-1}\sum_{l\neq n}\langle\sigma_l\rangle \approx \frac{1}{N}\sum_{l}\langle\sigma_l\rangle. \tag{5.196}$$

The solution for an initial condition $\boldsymbol{\sigma}$ is

$$\langle\sigma_n(t)\rangle_{\boldsymbol{\sigma}} = \sigma_n e^{-t/\tau} + \sigma^*(1-e^{-t/\tau}) + \left(\frac{1}{N}\sum_l \sigma_l - \sigma^*\right)[e^{-\lambda t/\tau} - e^{-t/\tau}] \tag{5.197}$$

with

$$\lambda \equiv 1 - \beta J_0 z[1-(\sigma^*)^2]. \tag{5.198}$$

At zero temperature ($\beta = \infty$) λ goes to one, and at the critical point ($\beta J_0 z = 1$) λ vanishes. The two-time correlation function is

$$\begin{aligned}\langle\sigma_m(t)\sigma_n(t+t')\rangle &= \langle\sigma_m(t)\sigma_n(t)\rangle e^{-t'/\tau} + \langle\sigma_m(t)\rangle\sigma^*(1-e^{-t'/\tau}) \\ &+ \left(\frac{1}{N}\sum_l\langle\sigma_m(t)\sigma_l(t)\rangle - \langle\sigma_m(t)\rangle\sigma^*\right)[e^{-\lambda t'/\tau} - e^{-t'/\tau}].\end{aligned} \tag{5.199}$$

Now we need to calculate the equal time correlation function $\langle\sigma_m(t)\sigma_n(t)\rangle$. If we are only interested in the long time behavior, we only need calculate the steady state

value. For $m = n$ we have always $\langle \sigma_m^2 \rangle = 1$, and in the steady state, in the mean field we have for $m \neq n$,

$$0 = -2G_{mn} + 2\tanh\left(\frac{\beta J_0 z}{N-1}\sum_{l\neq n} G_{ln} + \frac{\beta J_0 z}{N-1}\right) \tag{5.200}$$

where again $G_{mn} \equiv \langle \sigma_m \sigma_n \rangle$ for $m \neq n$. In the global coupling case, we should expect G_{mn} to equal some G^* independent of m and n. Then

$$0 = -2G^* + 2\tanh\left(\beta J_0 z G^* + \frac{\beta J_0 z}{N-1}\right). \tag{5.201}$$

For large N the second term inside the tanh is small, so we have approximately

$$G^* \approx \sigma^*. \tag{5.202}$$

Except for the second term in equation (5.199), $\langle \sigma_m \rangle$ and $\langle \sigma_m \sigma_l \rangle$ can be replaced with their steady state values in the long time limit, so we have

$$\begin{aligned}\langle \sigma_m(t')\sigma_n(t'+t'')\rangle &= e^{-t''/\tau} + (\sigma^*)^2(1-e^{-\lambda t'/\tau})(1-e^{-t''/\tau}) \\ &\quad + \left[\sigma^* - (\sigma^*)^2\right][e^{-\lambda t''/\tau} - e^{-t''/\tau}].\end{aligned} \tag{5.203}$$

Integrating over t'', this is

$$\begin{aligned}\int_0^{t-t'} \langle \sigma_m(t')\sigma_n(t'+t'')\rangle dt'' &= \tau(1-e^{-(t-t')/\tau}) \\ &\quad + (\sigma^*)^2(1-e^{-\lambda t'/\tau})[t-t'-\tau(1-e^{-(t-t')/\tau})] \\ &\quad + \tau\left[\sigma^* - (\sigma^*)^2\right]\left[\frac{1-e^{-\lambda(t-t')/\tau}}{\lambda} - (1-e^{-(t-t')/\tau})\right].\end{aligned} \tag{5.204}$$

Integrating over t' and taking the limit of large t we finally have

$$\langle x_m^2 \rangle = (c\sigma^* t)^2 + 2c^2\tau t\left(1 - \sigma^* + \frac{\sigma^* - 2(\sigma^*)^2}{\lambda}\right) + \text{constant}. \tag{5.205}$$

A similar calculation for $m \neq n$ gives at long times

$$\langle x_m x_n \rangle = (c\sigma^* t)^2 + 2c^2\tau t\left(\frac{\sigma^* - 2(\sigma^*)^2}{\lambda}\right) + \text{constant}. \tag{5.206}$$

Even though these grow like t^2, we must remember to subtract the first moments since they are not constant at long times. Assuming all particles started at zero with random directions, the first moments at long times are

$$\langle x_m \rangle = c\sigma^* \left(t - \frac{\tau}{\lambda} \right) \tag{5.207}$$

so the *centered* second moments at long times are proportional only to t

$$\langle x_m^2 \rangle - \langle x_m \rangle^2 = 2c^2 \tau t \left(1 - \sigma^*\right) \left(1 + \frac{\sigma^*}{\lambda} \right) \tag{5.208}$$

and the *covariances* are

$$\langle x_m x_n \rangle - \langle x_m \rangle \langle x_n \rangle = 2c^2 \tau t \left(1 - \sigma^*\right) \frac{\sigma^*}{\lambda}. \tag{5.209}$$

Since the centered second moments are only proportional to time, the motion is diffusive with effective diffusion constant

$$D_{\text{eff}} = c^2 \tau \left(1 - \sigma^*\right) \left(1 + \frac{\sigma^*}{\lambda} \right). \tag{5.210}$$

The effective diffusion constant D_{eff} is displayed in Figure 5.8. Since λ goes to zero as $\beta J_0 z$ goes to one, the effective diffusion constant diverges at the critical point. At low temperatures, the effective diffusion constant goes to zero, and the motion becomes purely advective.

The covariances $\langle x_m x_n \rangle - \langle x_m \rangle \langle x_n \rangle$, which measure how strongly correlated the positions of the mth and nth particles are, grow proportional to t at long times as in the disordered phase, but the rate of growth is much faster in the ordered phase since it is not scaled by $1/N$.

5.4 Remarks

We have analyzed in this chapter a simple model of self-propelled particles in one dimension with a long-range alignment interaction.

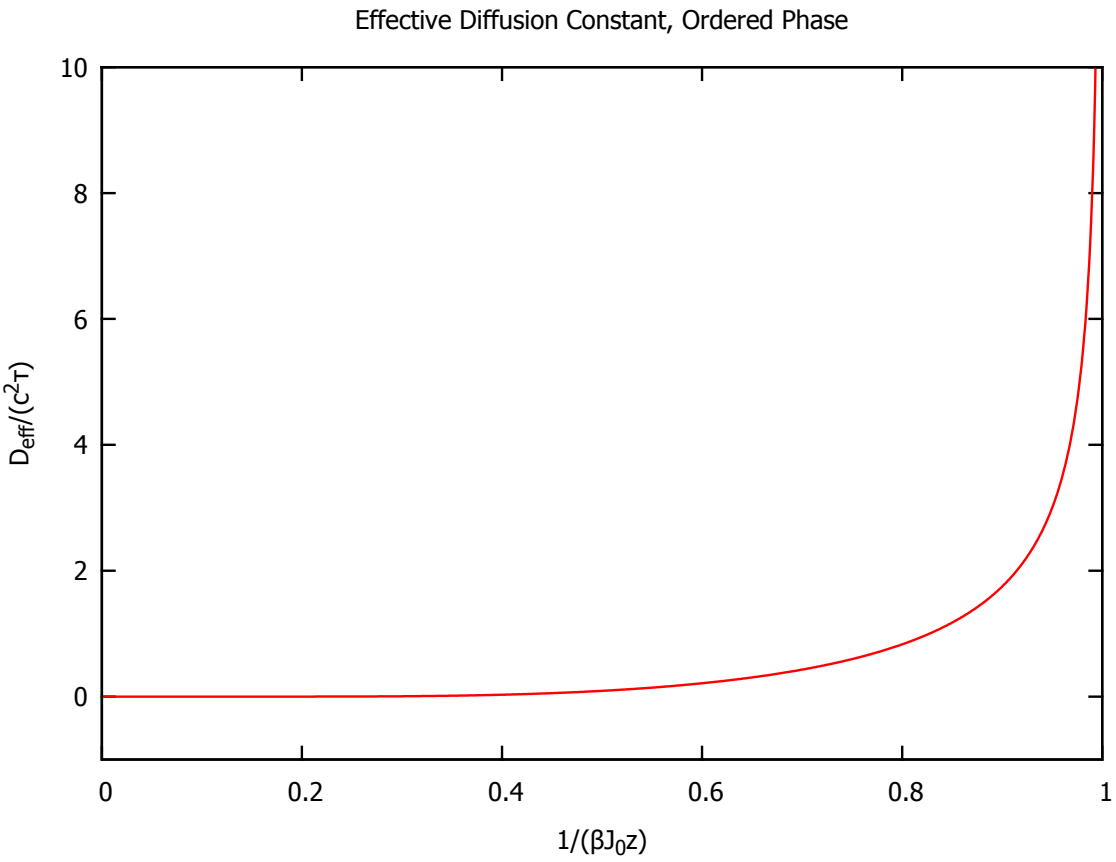

Figure 5.8: The effective diffusion constant versus temperature in the ordered phase for the N particle alignment model.

The single-particle version of this model is known in the literature. At short times, the motion is ballistic (mean squared displacement proportional to t^2), but changes to diffusive (mean squared displacement proportional to t) at long times. We saw that the the density obeys the evolution equation (5.56) which is local in space, but non-local in time with an exponential memory.

We generalized the analysis to two particles by constructing flipping rates which cause the particles to align on average. By calculating the mean squared displacement, given by equation (5.109), we found that the motion is again ballistic at short times but diffusive at long times. The positions of the two-particles were found

to be correlated, as a result of the alignment. We also calculated some continuous coarse-grained quantities and saw that, unlike in the single-particle case, the evolution equations (5.120), (5.126), and (5.130) are non-local in space.

Finally, we generalized the analysis further to many particles by building upon Glauber dynamics. Although the model could not be solved exactly, in sections 5.3.1 and 5.3.2 we were able to calculate the first two moments in the mean field limit. The many-particle model exhibits a phase transition from a disordered phase to an ordered phase at a particular strength of the noise. In the ordered phase, the particles can experience a net drift to left or right at long times, with the direction chosen depending on initial conditions, an effect which did not happen in the one and two-particle versions. The mean squared displacement given by equations (5.190) and (5.208) grows proportional to t at long times in both phases, indicative of diffusive motion. We found in both phases that the positions of any two particles are correlated, and the correlation in the ordered phase, equation (5.209), is independent of the number of particles N while the correlation in the disordered phase, equation (5.191), scales like $1/N$.

Chapter 6

Miscellaneous Topics and Conclusions

The study of two additional problems in transport theory related only incidentally to the investigations described in the preceding chapters were undertaken in the course of this thesis work. The first of these is motion in disordered one-dimensional lattices, and the second is a magnetic model of flocking. We will give a brief description of our work on these two problems and then close with some final comments.

6.1 Transport in Disordered Lattices and Effective Medium Theory

Consider a one-dimensional disordered system which obeys a Master equation of the form

$$\frac{dP_m}{dt} = F_{m+1}[P_{m+1} - P_m] + F_m[P_{m-1} - P_m] \tag{6.1}$$

where P_m is the probability to be in the mth state and the F_ms are transfer rates. We have chosen the rates to be nearest-neighbor, i.e. the mth site is only connected

to the $(m-1)$th and $(m-1)$th sites, and symmetric (the rate to go from m to $m+1$ is the same as the rate to go from $m+1$ back to m). Disorder can be introduced by choosing the rates F_m from some distribution $\rho(F)$; this is known as *bond disorder*. The Master equation (6.1) can be solved in the ordered case using the discrete Fourier transform, but the presence of disorder often makes exact solution impossible as one is left with the problem of diagonalizing a large matrix with random entries.

One method of analyzing such problems is to replace the disordered system, such as the one described by equation (6.1), with an ordered one which has memory,

$$\frac{d}{dt}P_m(t) = \int_0^t \mathcal{F}(t-t')[P_{m+1}(t') + P_{m-1}(t') - 2P_m(t')]dt' \tag{6.2}$$

where the memory $\mathcal{F}$ is chosen self-consistently and depends on the distribution of rates $\rho(F)$. This is the basic idea behind *effective medium theory* (also known as the coherent potential approximation in quantum mechanics) [56, 132–161].

The resulting expression for the memory $\mathcal{F}$ is evidently approximate, and questions about when the effective medium approximation is good and when it is bad are left largely unanswered except in a few investigations such as by Kenkre et al. [161].

We can try to answer some of these questions by writing an exact expression for the memory and comparing the result with the effective medium expression. We do this following the treatment in ref. [161]. First we rewrite the Master equation (6.1) in the more general form

$$\frac{dP_m}{dt} = -\sum_n A_{mn}P_n. \tag{6.3}$$

We wish to replace the disordered lattice with an ordered one plus a memory, i.e.

$$\frac{dP_m}{dt} = -\sum_n \int_0^t B_{m-n}(t-t')P_n(t')dt' \tag{6.4}$$

where the memory B must be somehow determined from rate matrix A. By ordered, we mean that the quantity B depends only on $|m-n|$ so that equation (6.4) can be solved with a discrete Fourier transform.

The formal solution to (6.3) in the Laplace domain is

$$\tilde{P}_m(\epsilon) = \sum_n \{[\epsilon \mathbf{I} + \mathbf{A}]^{-1}\}_{mn} P_n(0) \tag{6.5}$$

where $\{[\epsilon \mathbf{I} + \mathbf{A}]^{-1}\}_{mn}$ means the m, n element of the matrix $[\epsilon \mathbf{I} + \mathbf{A}]^{-1}$. Discrete Fourier transforming,

$$\tilde{P}^k(\epsilon) = \sum_m \sum_n \{[\epsilon \mathbf{I} + \mathbf{A}]^{-1}\}_{mn} P_n(0) e^{ikm} \tag{6.6}$$

where $P^k \equiv \sum_m P_m e^{ikm}$. A similar calculation gives the solution to (6.4) as

$$\tilde{P}^k(\epsilon) = \frac{P^k(0)}{\epsilon + \tilde{B}^k(\epsilon)}. \tag{6.7}$$

Solving for $\tilde{B}^k$ and plugging in $\tilde{P}^k(\epsilon)$ from (6.6) we have now a formula for B in terms of A in the transformed domain

$$\tilde{B}^k(\epsilon) = \frac{P^k(0)}{\sum_m \sum_n \{[\epsilon \mathbf{I} + \mathbf{A}]^{-1}\}_{mn} P_n(0) e^{ikm}} - \epsilon. \tag{6.8}$$

Note that this expression has the rather undesirable property that the memory B depends on the initial conditions $P_m(0)$.

The dependence on initial conditions can be removed in the following way. Suppose that we have an *ensemble* of disordered lattices with different realizations of the disorder. For an ensemble member labeled ξ, let ${}^{\xi}P_m$ be the probability to find the system in a state m in that ensemble member, and let ${}^{\xi}\mathbf{A}$ be the rate matrix for the particular realization of the disorder in that ensemble member.

For each ensemble member we have

$${}^{\xi}\tilde{P}_m(\epsilon) = \sum_n [\epsilon \mathbf{I} + {}^{\xi}\mathbf{A}]^{-1}_{mn} {}^{\xi}P_n(0). \tag{6.9}$$

Next, define define the ensemble average over realizations of the disorder $\langle f \rangle$ of any quantity ${}^{\xi}f$ as

$$\langle f \rangle \equiv \sum_{\xi} {}^{\xi}f P(\xi) \tag{6.10}$$

where $P(\xi)$ is the probability of generating the ensemble member ξ. Ensemble averaging equation (6.9) and assuming that each ensemble member starts with the same initial condition ${}^{\xi}P_m(0) = P_m(0)$ gives

$$\langle \tilde{P}_m(\epsilon) \rangle = \sum_n \langle [\epsilon \mathbf{I} + \mathbf{A}]^{-1} \rangle_{mn} P_n(0). \tag{6.11}$$

For bond disorder as described earlier, the ensemble averaged propagator $\langle [\epsilon \mathbf{I} + \mathbf{A}]^{-1} \rangle$ becomes translationally invariant even though the propagators for individual ensemble members are not. We can then discrete Fourier transform to find

$$\langle \tilde{P}^k(\epsilon) \rangle = \langle [\epsilon \mathbf{I} + \mathbf{A}]^{-1} \rangle^k P^k(0) \tag{6.12}$$

with

$$\langle [\epsilon \mathbf{I} + \mathbf{A}]^{-1} \rangle^k = \sum_m \langle [\epsilon \mathbf{I} + \mathbf{A}]^{-1} \rangle_{mn} e^{ik(m-n)}. \tag{6.13}$$

Using equation (6.8), the ensemble averaged probabilities $\langle P_m \rangle$ therefore obey

$$\frac{d\langle P_m \rangle}{dt} = -\sum_n \int_0^t \mathcal{B}_{m-n}(t - t') \langle P_n(t') \rangle dt' \tag{6.14}$$

with a memory which is now independent of the initial conditions,

$$\tilde{\mathcal{B}}^k(\epsilon) = \frac{1}{\langle [\epsilon \mathbf{I} + \mathbf{A}]^{-1} \rangle^k} - \epsilon. \tag{6.15}$$

This expression for the memory is exact, but it requires the computation of the propagator of each disordered lattice in the ensemble: exactly the task the effective medium theory seeks to avoid. We can however glean a few insights from this expression. Firstly, we note there is no guarantee that the memory $\mathcal{B}$ will be nearest-neighbor even if the rates in every ensemble member are nearest neighbor, a fact pointed out already in ref. [161]. Secondly, we can compute the exact memory for small (i.e. $N = 3$, $N = 4$ et cetera) lattices. The exact memory can then be compared to the approximate one obtained through effective medium theory.

We will perform here the calculation of the exact memory for a 4 site chain with random nearest neighbor rates all drawn from some distribution $\rho(F)$. In general, the rate matrix for a 4 site chain with nearest neighbor rates is

$$\mathbf{A} = \begin{pmatrix} F_1 + F_2 & -F_2 & 0 & -F_1 \\ -F_2 & F_2 + F_3 & -F_3 & 0 \\ 0 & -F_3 & F_3 + F_4 & -F_4 \\ -F_1 & 0 & -F_4 & F_4 + F_1 \end{pmatrix}. \tag{6.16}$$

The discrete Fourier transformed ensemble averaged propagator in the Laplace domain is (a computer algebra system is useful for this computation)

$$\left\langle [\epsilon \mathbf{I} + \mathbf{A}]^{-1} \right\rangle^{k=0} = \frac{1}{\epsilon}, \tag{6.17}$$

$$\left\langle [\epsilon \mathbf{I} + \mathbf{A}]^{-1} \right\rangle^{k=\pi/2} = \left\langle \frac{\epsilon^2 + 4F_1\epsilon + 4F_1F_2 + 4F_1F_3}{\Delta(\epsilon)} \right\rangle = \left\langle [\epsilon \mathbf{I} + \mathbf{A}]^{-1} \right\rangle^{k=3\pi/2}, \tag{6.18}$$

$$\left\langle [\epsilon \mathbf{I} + \mathbf{A}]^{-1} \right\rangle^{k=\pi} = \left\langle \frac{\epsilon^2 + 4F_1\epsilon + 4F_1F_2}{\Delta(\epsilon)} \right\rangle. \tag{6.19}$$

with

$$\begin{aligned} \Delta(\epsilon) \equiv \epsilon^3 &+ 2\epsilon^2(F_1 + F_2 + F_3 + F_4) \\ &+ \epsilon[3(F_1F_2 + F_2F_3 + F_3F_4 + F_4F_1) + 4(F_1F_3 + F_2F_4)] \\ &+ 4[F_1F_2F_3 + F_2F_3F_4 + F_3F_4F_1 + F_4F_1F_2]. \end{aligned} \tag{6.20}$$

Simplifications have been made using the fact that all the rates (F_1, F_2, F_3 and F_4) are chosen from the same distribution $\rho(F)$ so we can permute labels inside the ensemble averages.

Using equation (6.15) we have for the discrete Fourier transformed memory in the

Laplace domain

$$\tilde{\mathcal{B}}^{k=0}(\epsilon) = 0, \tag{6.21}$$

$$\tilde{\mathcal{B}}^{k=\pi/2}(\epsilon) = \frac{1}{\left\langle \frac{\epsilon^2+4F_1\epsilon+4F_1F_2+4F_1F_3}{\Delta(\epsilon)} \right\rangle} - \epsilon = \tilde{B}^{k=3\pi/2}(\epsilon), \tag{6.22}$$

$$\tilde{\mathcal{B}}^{k=\pi}(\epsilon) = \frac{1}{\left\langle \frac{\epsilon^2+4F_1\epsilon+4F_1F_2}{\Delta(\epsilon)} \right\rangle} - \epsilon. \tag{6.23}$$

What does this tell us? The $k = 0$ part is simply a result of conservation of probability. Is the exact memory nearest-neighbor? A nearest-neighbor memory would have the form $\tilde{\mathcal{B}}^k(\epsilon) = 2\mathcal{F}(\epsilon)(1 - \cos k)$, but in general the computed $\tilde{\mathcal{B}}^k(\epsilon)$ does not have this form.

To compare with effective medium theory, we now take the Markovian limit, i.e. replace the memory with its integral times a delta function,

$$\mathcal{B}_{m-n}(t) \approx \delta(t) \int_0^\infty \mathcal{B}_{m-n}(t')dt' = \delta(t)\tilde{B}_{m-n}(0). \tag{6.24}$$

In this limit we have

$$\tilde{\mathcal{B}}^{k=0}(0) = 0, \tag{6.25}$$

$$\tilde{\mathcal{B}}^{k=\pi/2}(0) = \frac{1}{\left\langle \frac{8F_1F_2}{\Delta(0)} \right\rangle} = \tilde{B}^{k=3\pi/2}(0), \tag{6.26}$$

$$\tilde{\mathcal{B}}^{k=\pi}(0) = \frac{1}{\left\langle \frac{4F_1F_2}{\Delta(0)} \right\rangle} - \epsilon \tag{6.27}$$

where we have used the fact that $\langle F_1F_3/\Delta(0)\rangle$ is equal to $\langle F_1F_2/\Delta(0)\rangle$ since again we can freely permute indices inside the ensemble average. This is of the nearest-neighbor form with the effective nearest-neighbor hopping rate

$$F_{\text{eff}}^{\text{exact}} = \left[4 \left\langle \frac{F_1F_2}{F_1F_2F_3 + F_2F_3F_4 + F_3F_4F_1 + F_4F_1F_2} \right\rangle \right]^{-1}. \tag{6.28}$$

How does this compare to the effective medium result? For a finite lattice, the effective nearest-neighbor hopping rate $F_{\text{eff}}^{\text{emt}}$ is given implicitly by [161]

$$\frac{1}{F_{\text{eff}}^{\text{emt}}} = \frac{N}{N-1} \int_0^\infty \frac{\rho(F)}{F + \frac{F_{\text{eff}}^{\text{emt}}}{N-1}} dF. \tag{6.29}$$

To compare the two, a particular distribution of the rates $\rho(F)$ must be chosen. We will not proceed any further here, but suffice it to say that even in the Markovian limit the effective hopping rate given by effective medium theory, equation (6.29), does indeed differ from the exact result (6.28) for nontrivial distributions.

6.2 A Magnetic Model of Flocking

In Chapter 4, we discussed collective motion the idea of information transfer from informed to uninformed individuals (see refs. [90, 92, 110, 111]). In this section we will briefly analyze a simple magnetic model of the same phenomenon. In this model we will have only static ingredients, i.e. there will be no motion undergone by the elements.

As in the model discussed in Chapter 5, we will again treat the members of the flock as Ising spins, but we now apply a field. The strength of the field is not uniform: we designate a certain fraction a of individuals as "informed" which feel a magnetic field of strength h, and the remaining fraction as "uninformed" which do not feel a magnetic field. We reiterate that here the particles do not move, unlike the particles in Chapter 5. We study only the equilibrium properties of the magnetic system.

The standard Ising model Hamiltonian is:

$$H = -\sum_{i<j} J_{ij}\sigma_i\sigma_j - \sum_i h_i\sigma_i \tag{6.30}$$

where the σ_is are a set of N spin variables which can either be -1 or -1, the J_{ij}'s are exchange energies, and h_i is the magnetic field on the ith site.

The partition function in the one-dimensional case can likely be solved exactly with transfer matrices, but the system in one dimension does not exhibit a phase transition. Exact calculations are prohibitively difficult in higher dimensions, so we simply perform a mean field analysis. The standard set of N mean field equations

are

$$\langle \sigma_i \rangle = \tanh\left(\beta \sum_j J_{ij} \langle \sigma_j \rangle + \beta h_i\right) \tag{6.31}$$

where $\beta \equiv 1/kT$ is the inverse temperature. If the dimensionality of the lattice is very large, then we may assume that $\sum_j J_{ij}\langle \sigma_j \rangle$ is independent of i, and replace it with $J_0 z m$ where J_0 is the pair exchange energy, z is the configuration number of the lattice, and m is the magnetization per spin of the entire system,

$$m \equiv \frac{1}{N} \sum_j \langle \sigma_j \rangle. \tag{6.32}$$

We are now left with only two equations:

$$\langle \sigma_i \rangle = \tanh\left(\beta J_0 z m\right) \tag{6.33}$$

if there is no magnetic field on site i, or

$$\langle \sigma_i \rangle = \tanh\left(\beta J_0 z m + \beta h\right) \tag{6.34}$$

if there is a magnetic field on site i. We can now obtain a single self consistent mean field equation for the magnetization m:

$$m = \frac{1}{N} \sum_j \langle \sigma_j \rangle = (1-a)\tanh(\beta J_0 z m) + a \tanh(\beta J_0 z m + \beta h) \tag{6.35}$$

where a is again the fraction of spins affected by the field. Note that the spatial configuration of spins which are affected by the magnetic field does not matter in the mean field analysis. It is convenient to introduce the dimensionless quantities $b \equiv \beta J_0 z$ and $c \equiv \beta h$, so that the equation for m can be written more simply as

$$m = (1-a)\tanh(bm) + a\tanh(bm + c). \tag{6.36}$$

It can be seen graphically that equation (6.36) can have between one and five solutions. The left and right hand sides for a particular choice of a, b, and c are plotted in Figure 6.1.

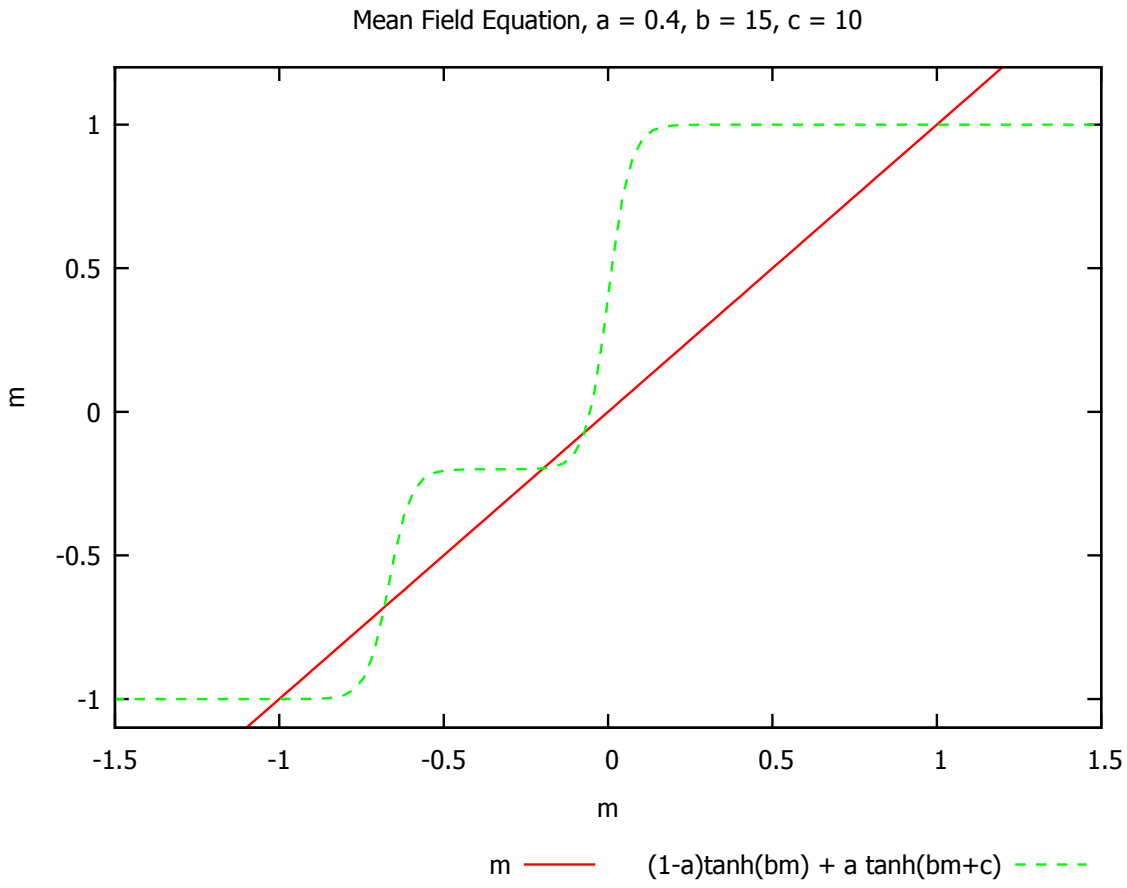

Figure 6.1: Left and right hand sides of the mean field equation $m = (1-a)\tanh(bm)+ a\tanh(bm+c)$f for $a = 0.4$, $b = 15$, $c = 10$. The intersections of the two curves represent are solutions of the mean field equation.

First let us analyze the solutions at very low temperature ($b \gg 1$). At low temperatures the hyperbolic tangents become step-like and the mean field equation is approximately

$$m \approx \begin{cases} +1 & m > 0 \\ 2a-1 & -c/b < m < 0 \\ -1 & m < -c/b \end{cases} . \tag{6.37}$$

The three stable (or at least metastable) solutions for $h > 0$ are

- $m = +1$: all spins aligned in the direction of the field.
- $m = -1$: all spins aligned opposite the direction of the field. Only a solution for sufficiently weak field, $c < b$.
- $m = 2a - 1$: informed spins aligned with the field; uninformed spins aligned opposite the field. Only a solution for certain fractions of informed spins $\frac{1-c/b}{2} < a < \frac{1}{2}$.

For certain ranges of parameters, we have solutions where all the particles ignore the field or where only uninformed spins ignore the field.

What about at nonzero temperatures? To gain some insight we can make several kinds of plots. One kind of plot that can be made is that of magnetization (found numerically) versus temperature at fixed field, for different fractions of informed birds. One such plot is shown in Figure 6.2.

Alternatively, the magnetization versus field at fixed temperature and concentration can be plotted. One such plot is given in Figure 6.3.

Another kind of diagram that can be made is called a *stability diagram* (see ref. [162]) and shows how many solutions there are in different regions of parameter space. These can be made by noting that the number of solutions to (6.36) changes exactly when m is tangent to $(1-a)\tanh(bm) + a\tanh(bm+c)$. Setting their slopes equal, we obtain

$$1 = (1-a)b\,\mathrm{sech}^2(bm) + ab\,\mathrm{sech}^2(bm+c). \tag{6.38}$$

This, together with equation (6.36) form a system of two coupled equations which for fixed a and b can be solved for the values of m and c where a change in the number of solutions occurs. This can be done numerically, and the results for different values of a are shown in 6.4.

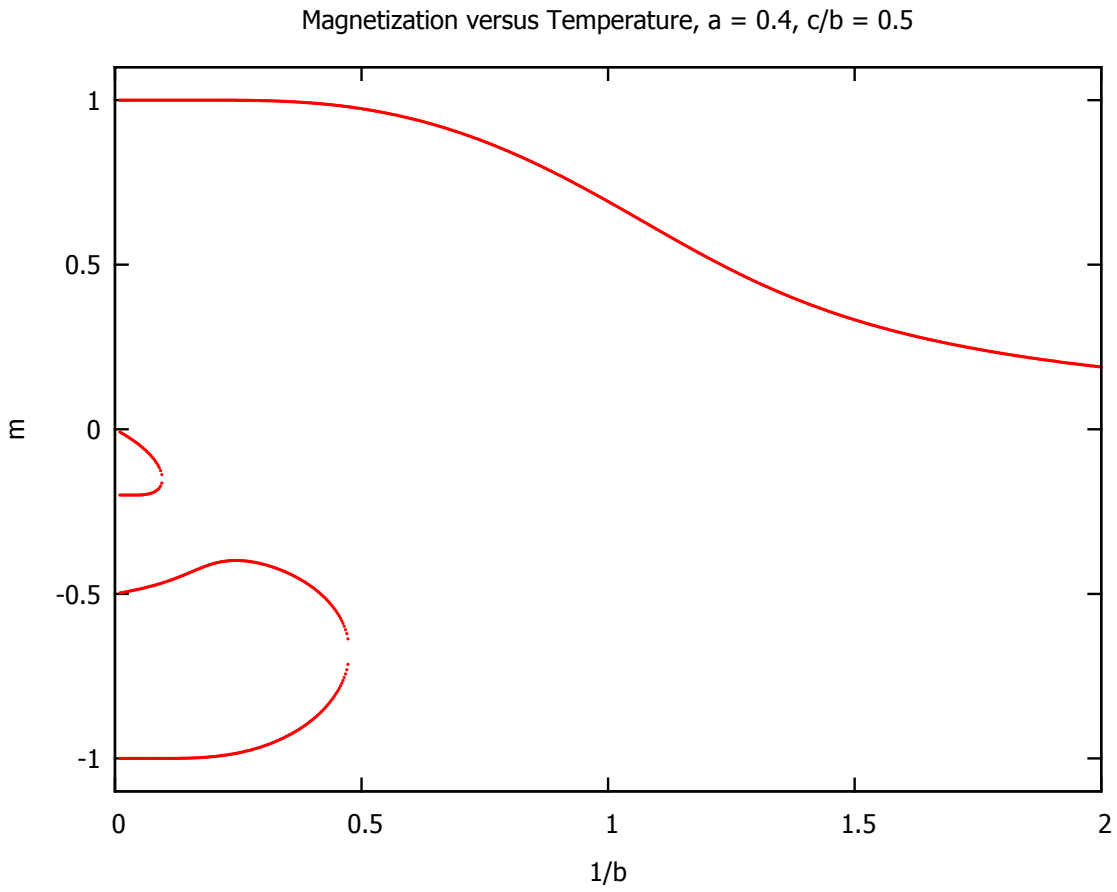

Figure 6.2: Magnetization (both stable and unstable solutions) versus temperature at fixed field $c/b = 0.5$ and fixed concentration of informed spins $a = 0.4$.

For $a > 1/2$, the behavior is qualitatively similar to the ordinary Ising model and there can be only one or three solutions. Only for $a < 1/2$ can five solutions appear.

6.3 Closing Remarks

The two main problems studied in this thesis, electrons moving in mesoscopic devices and macroscopic biological entities such as birds moving collectively, are certainly quite different from each other, but despite the vast difference in scale, we did en-

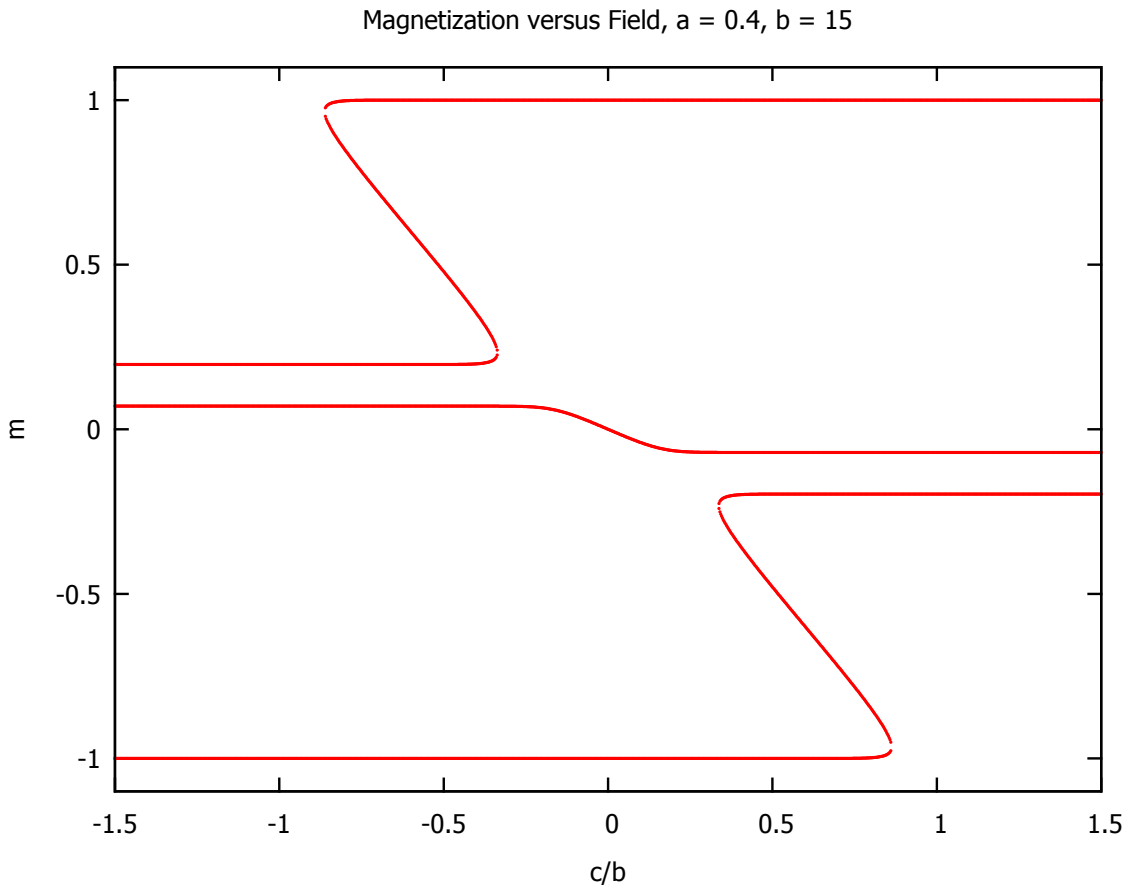

Figure 6.3: Magnetization (both stable and unstable solutions) versus field at fixed inverse temperature $b = 15$ and fixed concentration of informed spins $a = 0.4$.

counter certain similarities. Remarkably, some of the same tools from statistical physics can be used to analyze both kinds of systems. In Section 2.4 we saw how a Master equation can be used to describe electronic transport, and in Chapter 4, a Fokker-Planck equation was used to describe transport of macroscopic biological objects. A Fokker-Planck equation can be viewed as a continuous space version of the Master equation. Furthermore, for both systems, we made use of powerful tools of general applicability such as integral transforms and Green's functions

In our discussions of microscopic as well as macroscopic objects we encountered non-locality in both space and time. The Zwanzig-Nakajima projection formalism

shows how coarse-graining results in non-locality in time, but the projection formalism does not make clear that coarse-graining can also give rise to non-locality in space. In the macroscopic systems described in Chapters 4 and 5, we saw explicitly several coarse-grained quantities which obey equations of motion which are non-local in space. In Section 6.1 we saw in a microscopic system how a different kind of coarse-graining, ensemble averaging over different realizations of disorder, also produces spatially long-range effects. A few other examples of spatially long-range memories can be found in the literature, in particular see refs. [69, 163].

The models of microscopic and macroscopic transport discussed in this thesis were quite simple from a mathematical standpoint. These simple models certainly do not capture all the details of the real systems, but they are amenable to analytic calculations. The author hopes the analyses presented here can thereby provide a better understanding of certain aspects of the difficult problems in transport theory.

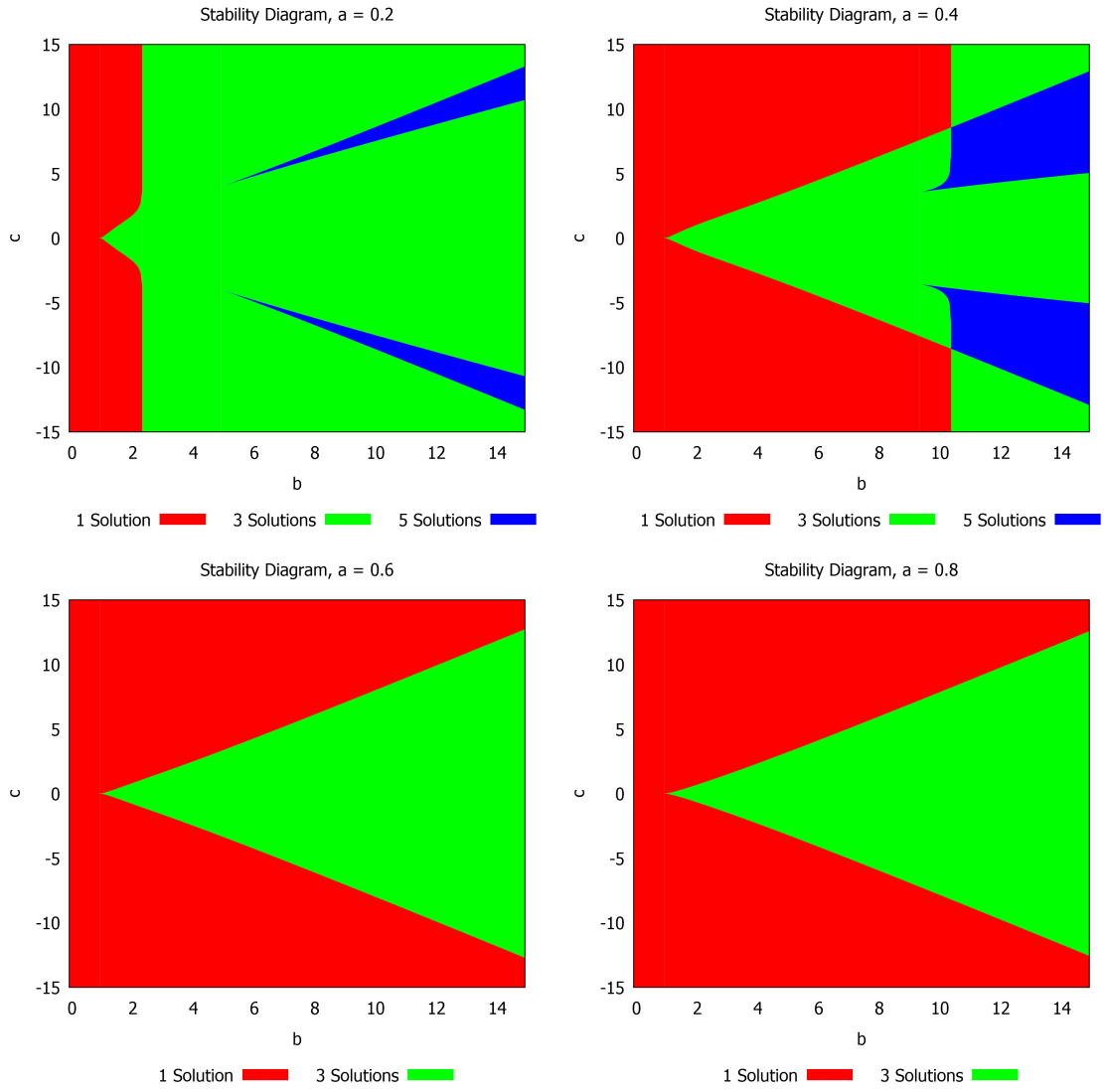

Figure 6.4: Stability diagrams showing the total number of solutions in different regions of parameter space.

References

[1] Neil W. Ashcroft and N. David Mermin. *Solid state physics*. Holt, Rinehart and Winston, 1976.

[2] D. A. Wharam, T. J. Thornton, R. Newbury, M. Pepper, H. Ahmed, J. E. F. Frost, D. G. Hasko, D. C. Peacock, D. A. Ritchie, and G. A. C. Jones. One-dimensional transport and the quantisation of the ballistic resistance. *Journal of Physics C: Solid State Physics*, 21(8):L209–L214, March 1988.

[3] B. J. van Wees, L. P. Kouwenhoven, H. van Houten, C. W. J. Beenakker, J. E. Mooij, C. T. Foxon, and J. J. Harris. Quantized conductance of magnetoelectric subbands in ballistic point contacts. *Physical Review B*, 38(5):3625–3627, 1988.

[4] B. J. van Wees, H. van Houten, C. W. J. Beenakker, J. G. Williamson, L. P. Kouwenhoven, D. van der Marel, and C. T. Foxon. Quantized conductance of point contacts in a two-dimensional electron gas. *Physical Review Letters*, 60(9):848–850, February 1988.

[5] Theodosius Dobzhansky, Jeffery R. Powell, Charles E. Taylor, and Michael Andregg. Ecological variables affecting the dispersal behavior of drosophila pseudoobscura and its relatives. *The American Naturalist*, 114(3):325–334, September 1979.

[6] Hiroshi Fujikawa and Mitsugu Matsushita. Fractal growth of bacillus subtilis on agar plates. *Journal of the Physical Society of Japan*, 58(11):3875–3878, 1989.

[7] Eshel Ben-Jacob, Adam Tenenbaum, Ofer Shochet, and Orna Avidan. Holotransformations of bacterial colonies and genome cybernetics. *Physica A: Statistical Mechanics and its Applications*, 202(1–2):1–47, January 1994.

[8] Eshel Ben-Jacob, Ofer Schochet, Adam Tenenbaum, Inon Cohen, Andras Czirók, and Tamas Vicsek. Generic modelling of cooperative growth patterns in bacterial colonies. *Nature*, 368(6466):46–49, March 1994.

[9] Eshel Ben-Jacob, Inon Cohen, Ofer Shochet, Adam Tenenbaum, András Czirók, and Tamás Vicsek. Cooperative formation of chiral patterns during growth of bacterial colonies. *Physical Review Letters*, 75(15):2899–2902, October 1995.

[10] András Czirók, Eshel Ben-Jacob, Inon Cohen, and Tamás Vicsek. Formation of complex bacterial colonies via self-generated vortices. *Physical Review E*, 54(2):1791–1801, August 1996.

[11] M. Ballerini, N. Cabibbo, R. Candelier, A. Cavagna, E. Cisbani, I. Giardina, V. Lecomte, A. Orlandi, G. Parisi, A. Procaccini, M. Viale, and V. Zdravkovic. Interaction ruling animal collective behavior depends on topological rather than metric distance: Evidence from a field study. *Proceedings of the National Academy of Sciences*, 105(4):1232 –1237, January 2008.

[12] Michele Ballerini, Nicola Cabibbo, Raphael Candelier, Andrea Cavagna, Evaristo Cisbani, Irene Giardina, Alberto Orlandi, Giorgio Parisi, Andrea Procaccini, Massimiliano Viale, and Vladimir Zdravkovic. Empirical investigation of starling flocks: a benchmark study in collective animal behaviour. *Animal Behaviour*, 76(1):201–215, July 2008.

[13] Andrea Cavagna, Alessio Cimarelli, Irene Giardina, Giorgio Parisi, Raffaele Santagati, Fabio Stefanini, and Massimiliano Viale. Scale-free correlations in starling flocks. *Proceedings of the National Academy of Sciences*, 107(26):11865–11870, June 2010.

[14] Andrea Cavagna, Alessio Cimarelli, Irene Giardina, Giorgio Parisi, Raffaele Santagati, Fabio Stefanini, and Raffaele Tavarone. From empirical data to inter-individual interactions: unveiling the rules of collective animal behavior. *Mathematical Models and Methods in Applied Sciences*, 20:1491–1510, September 2010.

[15] William Bialek, Andrea Cavagna, Irene Giardina, Thierry Mora, Edmondo Silvestri, Massimiliano Viale, and Aleksandra M. Walczak. Statistical mechanics for natural flocks of birds. *Proceedings of the National Academy of Sciences*, 109(13):4786–4791, March 2012.

[16] D. P. O'Brien. Analysis of the internal arrangement of individuals within crustacean aggregations (Euphausiacea, mysidacea). *Journal of Experimental Marine Biology and Ecology*, 128(1):1–30, June 1989.

[17] Andreas Huth and Christian Wissel. The simulation of the movement of fish schools. *Journal of Theoretical Biology*, 156(3):365–385, June 1992.

[18] Andreas Huth and Christian Wissel. The simulation of fish schools in comparison with experimental data. *Ecological Modelling*, 75–76:135–146, September 1994.

[19] Yael Katz, Kolbjørn Tunstrøm, Christos C. Ioannou, Cristián Huepe, and Iain D. Couzin. Inferring the structure and dynamics of interactions in schooling fish. *Proceedings of the National Academy of Sciences*, 108(46):18720–18725, November 2011.

[20] Wolfgang Alt. Elements of a systematic search in animal behavior and model simulations. *Biosystems*, 34(1–3):11–26, 1995.

[21] J. Buhl, D. J. T. Sumpter, I. D. Couzin, J. J. Hale, E. Despland, E. R. Miller, and S. J. Simpson. From disorder to order in marching locusts. *Science*, 312(5778):1402 –1406, June 2006.

[22] Dirk Helbing, Joachim Keltsch, and Péter Molnár. Modelling the evolution of human trail systems. *Nature*, 388(6637):47–50, July 1997.

[23] Dirk Helbing, Frank Schweitzer, Joachim Keltsch, and Péter Molnár. Active walker model for the formation of human and animal trail systems. *Physical Review E*, 56(3):2527–2539, September 1997.

[24] Alexander S. Mikhailov and Damián H. Zanette. Noise-induced breakdown of coherent collective motion in swarms. *Physical Review E*, 60(4):4571–4575, October 1999.

[25] R. Landauer. Spatial variation of currents and fields due to localized scatterers in metallic conduction. *IBM Journal of Research and Development*, 1(3):223–231, July 1957.

[26] Rolf Landauer. Electrical resistance of disordered one-dimensional lattices. *Philosophical Magazine*, 21(172):863–867, 1970.

[27] R. Landauer. Electrical transport in open and closed systems. *Zeitschrift für Physik B Condensed Matter*, 68(2):217–228, 1987.

[28] M. Büttiker, Y. Imry, R. Landauer, and S. Pinhas. Generalized many-channel conductance formula with application to small rings. *Physical Review B*, 31(10):6207–6215, May 1985.

[29] Yoseph Imry. Physics of mesoscopic systems. In Geoffrey Grinstein and Gene Mazenko, editors, *Directions in condensed matter physics: memorial volume in honor of Prof. S.K. Ma*. World Scientific, 1986.

[30] M. Büttiker. Role of quantum coherence in series resistors. *Physical Review B*, 33(5):3020–3026, March 1986.

[31] Supriyo Datta. *Electronic Transport in Mesoscopic Systems*. Cambridge University Press, May 1997.

[32] E. Wigner. On the quantum correction for thermodynamic equilibrium. *Physical Review*, 40(5):749–759, June 1932.

[33] Umberto Ravaioli, Mohamed A. Osman, Walter Pötz, Norman Kluksdahl, and David K. Ferry. Investigation of ballistic transport through resonant-tunnelling quantum wells using Wigner function approach. *Physica B+C*, 134(1–3):36–40, November 1985.

[34] N. Kluksdahl, W. Pötz, U. Ravaioli, and D.K. Ferry. Wigner function study of a double quantum barrier resonant tunnelling diode. *Superlattices and Microstructures*, 3(1):41–45, 1987.

[35] William R. Frensley. Wigner-function model of a resonant-tunneling semiconductor device. *Physical Review B*, 36(3):1570–1580, July 1987.

[36] A. M. Kriman, N. C. Kluksdahl, and D. K. Ferry. Scattering states and distribution functions for microstructures. *Physical Review B*, 36(11):5953–5959, October 1987.

[37] N. C. Kluksdahl, A. M. Kriman, D. K. Ferry, and C. Ringhofer. Self-consistent study of the resonant-tunneling diode. *Physical Review B*, 39(11):7720–7735, April 1989.

[38] V. M. Kenkre, F. Biscarini, and C. Bustamante. Theoretical framework for the interpretation of STM images of adsorbates. *Ultramicroscopy*, 42–44, Part 1:122–127, July 1992.

[39] Fabio Biscarini. *Theory of Electron Transport in Scanning Tunneling Microscopy and Applications to the Simulation of Images of Metal Surfaces and Adsorbed Molecules.* PhD thesis, University of Oregon, 1993.

[40] F. Biscarini, C. Bustamante, and V. M. Kenkre. Cluster models for the simulation of STM images of adsorbates: Origin of non-topographical features. *ICEM*, 13:581, 1994.

[41] V. M. Kenkre, F. Biscarini, and C. Bustamante. Scanning tunneling microscopy. I. Theoretical framework and coherence effects. *Physical Review B*, 51(16):11074–11088, April 1995.

[42] F. Biscarini, C. Bustamante, and V. M. Kenkre. Scanning tunneling microscopy. II. Calculation of images of atomic and molecular adsorbates. *Physical Review B*, 51(16):11089–11102, April 1995.

[43] F. Biscarini and V.M. Kenkre. Quantum coherence effects in the scanning tunneling microscope: a simple interpretation of contact resistance experiments. *Surface Science*, 426(3):336–344, May 1999.

[44] S. K. Lyo and Danhong Huang. Multisublevel magnetoquantum conductance in single and coupled double quantum wires. *Physical Review B*, 64(11):115320, 2001.

[45] S. K. Lyo and Danhong Huang. Magnetoquantum oscillations of thermoelectric power in multisublevel quantum wires. *Physical Review B*, 66(15):155307, October 2002.

[46] S. K. Lyo and Danhong Huang. Temperature-dependent magnetoconductance in quantum wires: Effect of phonon scattering. *Physical Review B*, 68(11):115317, 2003.

[47] S. K. Lyo and Danhong Huang. Effect of electron-electron scattering on the conductance of a quantum wire studied with the boltzman transport equation. *Physical Review B*, 73(20):205336, May 2006.

[48] R Landauer. Conductance determined by transmission: probes and quantised constriction resistance. *Journal of Physics: Condensed Matter*, 1(43):8099–8110, October 1989.

[49] Henk van Houten and Carlo Beenakker. Quantum point contacts. *Physics Today*, 49(7):22–27, 1996.

[50] Yoseph Imry and Rolf Landauer. Conductance viewed as transmission. *Reviews of Modern Physics*, 71(2):S306–S312, March 1999.

[51] David K. Ferry and Stephen M. Goodnick. *Transport in Nanostructures*. Cambridge University Press, 1997.

[52] Yoseph Imry. *Introduction to Mesoscopic Physics*. Oxford University Press, February 2002.

[53] Supriyo Datta. *Quantum Transport: Atom To Transistor*. Cambridge University Press, June 2005.

[54] Albert Messiah. *Quantum Mechanics*. Dover Publications, July 1999.

[55] L. Shubnikov and W. J. de Haas. Magnetische widerstandsvergrosserung in einkristallen von wismut bei tiefen temperaturen. *Communications from the Physical Laboratory at the University of Leiden*, 207a, 1930.

[56] Eleftherios N. Economou. *Green's Functions in Quantum Physics*. Springer, 3rd edition, February 2010.

[57] Daniel S. Fisher and Patrick A. Lee. Relation between conductivity and transmission matrix. *Physical Review B*, 23(12):6851–6854, June 1981.

[58] L. V. Keldysh. Diagram technique for non-equilibrium processes. *Soviet Physics JETP*, 20:1018, 1965.

[59] Leo P. Kadanoff and Gordon Baym. *Quantum statistical mechanics: Green's function methods in equilibrium and nonequilibrium problems*. W.A. Benjamin, 1962.

[60] John Snygg. Use of operator wave functions to construct a refined correspondence principle via the quantum mechanics of Wigner and Moyal. *American Journal of Physics*, 48(11):964, 1980.

[61] M. Hillery, R.F. O'Connell, M.O. Scully, and E.P. Wigner. Distribution functions in physics: Fundamentals. *Physics Reports*, 106(3):121–167, April 1984.

[62] N.L. Balazs and B.K. Jennings. Wigner's function and other distribution functions in mock phase spaces. *Physics Reports*, 104(6):347–391, February 1984.

[63] Hai-Woong Lee. Theory and application of the quantum phase-space distribution functions. *Physics Reports*, 259(3):147–211, August 1995.

[64] William B. Case. Wigner functions and Weyl transforms for pedestrians. *American Journal of Physics*, 76(10):937, 2008.

[65] John M. Ziman. *Principles of the Theory of Solids*. Cambridge University Press, November 1979.

[66] J. E. Moyal. Quantum mechanics as a statistical theory. *Mathematical Proceedings of the Cambridge Philosophical Society*, 45(01):99–124, 1949.

[67] M. Belloni, M. A. Doncheski, and R. W. Robinett. Wigner quasi-probability distribution for the infinite square well: Energy eigenstates and time-dependent wave packets. *American Journal of Physics*, 72(9):1183, 2004.

[68] V. M. Kenkre and Peter Reineker. *Exciton dynamics in molecular crystals and aggregates*. Springer-Verlag, 1982.

[69] V.M. Kenkre and S.M. Phatak. Exact probability propagators for motion with arbitrary degree of transport coherence. *Physics Letters A*, 100(2):101–104, January 1984.

[70] V. M. Kenkre and D. W. Brown. Exact solution of the stochastic Liouville equation and application to an evaluation of the neutron scattering function. *Physical Review B*, 31(4):2479–2487, February 1985.

[71] V. M. Kenkre. Mathematical methods for the description of energy transfer. In B. DiBartolo, editor, *Proceedings of the NATO Advance Study Institute on Energy Transfer, Erice, Italy*. Plenum, New York, 1984.

[72] V. M. Kenkre and Katja Lindenberg. *Modern challenges in statistical mechanics: patterns, noise, and the interplay of nonlinearity and complexity : Pan American Advanced Studies Institute, Bariloche, Argentina, 2-15 June, 2002*. American Institute of Physics, March 2003.

[73] V. M. Kenkre. Generalization to spatially extended systems of the relation between stochastic Liouville equations and generalized master equations. *Physics Letters A*, 65(5–6):391–392, April 1978.

[74] P. Avakian, V. Ern, R. E. Merrifield, and A. Suna. Spectroscopic approach to triplet exciton dynamics in anthracene. *Physical Review*, 165(3):974–980, January 1968.

[75] Yu Kagan and M. I. Klinger. Theory of quantum diffusion of atoms in crystals. *Journal of Physics C: Solid State Physics*, 7(16):2791–2807, August 1974.

[76] Sadao Nakajima. On quantum theory of transport phenomena. *Progress of Theoretical Physics*, 20(6):948–959, 1958.

[77] Robert Zwanzig. Ensemble method in the theory of irreversibility. *The Journal of Chemical Physics*, 33(5):1338–1341, November 1960.

[78] Robert Zwanzig. On the identity of three generalized master equations. *Physica*, 30(6):1109–1123, June 1964.

[79] P. Sautet and C. Joachim. Electronic transmission coefficient for the single-impurity problem in the scattering-matrix approach. *Physical Review B*, 38(17):12238–12247, December 1988.

[80] Herbert Levine, Wouter-Jan Rappel, and Inon Cohen. Self-organization in systems of self-propelled particles. *Physical Review E*, 63(1):017101, December 2000.

[81] Udo Erdmann, Werner Ebeling, and Alexander S. Mikhailov. Noise-induced transition from translational to rotational motion of swarms. *Physical Review E*, 71(5):051904, May 2005.

[82] V. Dossetti, F. J. Sevilla, and V. M. Kenkre. Phase transitions induced by complex nonlinear noise in a system of self-propelled agents. *Physical Review E*, 79(5):051115, May 2009.

[83] Craig W. Reynolds. Flocks, herds and schools: A distributed behavioral model. In *Proceedings of the 14th annual conference on Computer graphics and interactive techniques*, SIGGRAPH '87, page 25–34, New York, NY, USA, 1987. ACM.

[84] G. Bard Ermentrout and Leah Edelstein-Keshet. Cellular automata approaches to biological modeling. *Journal of Theoretical Biology*, 160(1):97–133, January 1993.

[85] Tamás Vicsek, András Czirók, Eshel Ben-Jacob, Inon Cohen, and Ofer Shochet. Novel type of phase transition in a system of self-driven particles. *Physical Review Letters*, 75(6):1226–1229, 1995.

[86] J Hemmingsson. Modellization of self-propelling particles with a coupled map lattice model. *Journal of Physics A: Mathematical and General*, 28(15):4245–4250, August 1995.

[87] Y. Limon Duparcmeur, H. Herrmann, and J. P. Troadec. Spontaneous formation of vortex in a system of self motorised particles. *Journal de Physique I*, 5(9):1119–1128, September 1995.

[88] Zoltán Csahók and Tamás Vicsek. Lattice-gas model for collective biological motion. *Physical Review E*, 52(5):5297–5303, November 1995.

[89] András Czirók, H. Eugene Stanley, and Tamás Vicsek. Spontaneously ordered motion of self-propelled particles. *Journal of Physics A: Mathematical and General*, 30(5):1375–1385, March 1997.

[90] Iain D. Couzin, Jens Krause, Richard James, Graeme D. Ruxton, and Nigel R. Franks. Collective memory and spatial sorting in animal groups. *Journal of Theoretical Biology*, 218(1):1–11, September 2002.

[91] Guillaume Grégoire and Hugues Chaté. Onset of collective and cohesive motion. *Physical Review Letters*, 92(2):025702, January 2004.

[92] Iain D. Couzin, Jens Krause, Nigel R. Franks, and Simon A. Levin. Effective leadership and decision-making in animal groups on the move. *Nature*, 433(7025):513–516, February 2005.

[93] M. Aldana, V. Dossetti, C. Huepe, V. M. Kenkre, and H. Larralde. Phase transitions in systems of self-propelled agents and related network models. *Physical Review Letters*, 98(9):095702, March 2007.

[94] Akira Okubo. Dynamical aspects of animal grouping: Swarms, schools, flocks, and herds. *Advances in Biophysics*, 22:1–94, 1986.

[95] John Toner and Yuhai Tu. Long-range order in a two-dimensional dynamical XY model: How birds fly together. *Physical Review Letters*, 75(23):4326–4329, December 1995.

[96] John Toner and Yuhai Tu. Flocks, herds, and schools: A quantitative theory of flocking. *Physical Review E*, 58(4):4828–4858, October 1998.

[97] András Czirók, Albert-László Barabási, and Tamás Vicsek. Collective motion of self-propelled particles: Kinetic phase transition in one dimension. *Physical Review Letters*, 82(1):209–212, January 1999.

[98] Alexander Mogilner and Leah Edelstein-Keshet. A non-local model for a swarm. *Journal of Mathematical Biology*, 38(6):534–570, June 1999.

[99] John Toner, Yuhai Tu, and Sriram Ramaswamy. Hydrodynamics and phases of flocks. *Annals of Physics*, 318(1):170–244, July 2005.

[100] Chad M. Topaz, Andrea L. Bertozzi, and Mark A. Lewis. A nonlocal continuum model for biological aggregation. *Bulletin of Mathematical Biology*, 68(7):1601–1623, July 2006.

[101] C. William Gear. Equation-free, coarse-grained multiscale computation: Enabling microscopic simulators to perform system-level analysis. *Communications in Mathematical Sciences*, 1(4):715–762, December 2003.

[102] Radek Erban, Ioannis G. Kevrekidis, and Hans G. Othmer. An equation-free computational approach for extracting population-level behavior from individual-based models of biological dispersal. *Physica D: Nonlinear Phenomena*, 215(1):1–24, March 2006.

[103] Allison Kolpas, Jeff Moehlis, and Ioannis G. Kevrekidis. Coarse-grained analysis of stochasticity-induced switching between collective motion states. *Proceedings of the National Academy of Sciences*, 104(14):5931–5935, April 2007.

[104] Sung Joon Moon, B. Nabet, Naomi E. Leonard, Simon A. Levin, and I. G. Kevrekidis. Heterogeneous animal group models and their group-level alignment dynamics: An equation-free approach. *Journal of Theoretical Biology*, 246(1):100–112, May 2007.

[105] Daniel Grünbaum, Karen Chan, Elizabeth Tobin, and Michael T. Nishizaki. Non-linear advection–diffusion equations approximate swarming but not schooling populations. *Mathematical Biosciences*, 214(1–2):38–48, July 2008.

[106] R. R. Coifman, I. G. Kevrekidis, S. Lafon, M. Maggioni, and B. Nadler. Diffusion maps, reduction coordinates and low dimensional representation of stochastic systems. *Multiscale Modeling and Simulation*, 7(2):842–864, 2008.

[107] Christian A. Yates, Radek Erban, Carlos Escudero, Iain D. Couzin, Jerome Buhl, Ioannis G. Kevrekidis, Philip K. Maini, and David J. T. Sumpter. Inherent noise can facilitate coherence in collective swarm motion. *Proceedings of the National Academy of Sciences*, 106(14):5464–5469, April 2009.

[108] M. Raghib, S. A. Levin, and I. G. Kevrekidis. Multiscale analysis of collective motion and decision-making in swarms: An advection–diffusion equation with memory approach. *Journal of Theoretical Biology*, 264(3):893–913, June 2010.

[109] Thomas A. Frewen, Iain D. Couzin, Allison Kolpas, Jeff Moehlis, Ronald Coifman, and Ioannis G. Kevrekidis. Coarse collective dynamics of animal groups. In Alexander N. Gorban and Dirk Roose, editors, *Coping with Complexity: Model Reduction and Data Analysis*, volume 75, pages 299–309. Springer Berlin Heidelberg, Berlin, Heidelberg, 2011.

[110] Iain D. Couzin, Christos C. Ioannou, Güven Demirel, Thilo Gross, Colin J. Torney, Andrew Hartnett, Larissa Conradt, Simon A. Levin, and Naomi E. Leonard. Uninformed individuals promote democratic consensus in animal groups. *Science*, 334(6062):1578–1580, December 2011.

[111] Naomi E. Leonard, Tian Shen, Benjamin Nabet, Luca Scardovi, Iain D. Couzin, and Simon A. Levin. Decision versus compromise for animal groups in motion. *Proceedings of the National Academy of Sciences*, 109(1):227–232, January 2012.

[112] A. D. Fokker. Die mittlere energie rotierender elektrischer dipole im strahlungsfeld. *Annalen der Physik*, 348(5):810–820, 1914.

[113] M. Planck. *Sitzungsberichte der Preussischen Akademie der Wissenschaften*, page 324, 1917.

[114] Hannes Risken. *The Fokker-Planck equation: methods of solution and applications*. Springer, 1996.

[115] G. E. Uhlenbeck and L. S. Ornstein. On the theory of the Brownian motion. *Physical Review*, 36(5):823–841, 1930.

[116] Ming Chen Wang and G. E. Uhlenbeck. On the theory of the Brownian motion II. *Reviews of Modern Physics*, 17(2-3):323–342, April 1945.

[117] V. M. Kenkre and F. Sevilla. Thoughts about anomalous diffusion: Time-dependent coefficients versus memory functions. In T. S. Ali and K. B. Sinha, editors, *Contributions to Mathematical Physics: a Tribute to Gerard G. Emch*, pages 147–160. Hindustan Book Agency, New Delhi, October 2007.

[118] R. F. Pawula. Approximation of the linear Boltzmann equation by the Fokker-Planck equation. *Physical Review*, 162(1):186–188, October 1967.

[119] G. I. Taylor. Diffusion by continuous movements. *Proceedings of the London Mathematical Society*, s2-20(1):196–212, January 1922.

[120] S. Goldstein. On diffusion by discontinuous movements, and on the telegraph equation. *The Quarterly Journal of Mechanics and Applied Mathematics*, 4(2):129–156, January 1951.

[121] Mark Kac. A stochastic model related to the telegrapher's equation. *Rocky Mountain Journal of Mathematics*, 4(3):497–510, September 1974.

[122] H. G. Othmer, S. R. Dunbar, and W. Alt. Models of dispersal in biological systems. *Journal of Mathematical Biology*, 26(3):263–298, June 1988.

[123] Philip McCord Morse and Herman Feshbach. *Methods of Theoretical Physics, Part I*. McGraw-Hill Science/Engineering/Math, June 1953.

[124] J. E. Scott, V. M. Kenkre, E. A. Pease, and A. J. Hurd. Compaction stress in fine powders. *MRS Online Proceedings Library*, 520, 1998.

[125] V. M. Kenkre, J. E. Scott, E. A. Pease, and A. J. Hurd. Nonlocal approach to the analysis of the stress distribution in granular systems. I. Theoretical framework. *Physical Review E*, 57(5):5841–5849, May 1998.

[126] J. E. Scott, V. M. Kenkre, and A. J. Hurd. Nonlocal approach to the analysis of the stress distribution in granular systems. II. application to experiment. *Physical Review E*, 57(5):5850–5857, May 1998.

[127] Roy J. Glauber. Time-Dependent statistics of the Ising model. *Journal of Mathematical Physics*, 4(2):294–307, February 1963.

[128] Masuo Suzuki and Ryogo Kubo. Dynamics of the Ising model near the critical point. I. *Journal of the Physical Society of Japan*, 24(1):51–60, 1968.

[129] Ernst Ising. Beitrag zur theorie des ferromagnetismus. *Zeitschrift für Physik*, 31(1):253–258, February 1925.

[130] Ralph Baierlein. *Thermal Physics*. Cambridge University Press, July 1999.

[131] Daniel V. Schroeder. *An Introduction to Thermal Physics*. Addison Wesley, 1 edition, August 1999.

[132] D. A. G. Bruggeman. Berechnung verschiedener physikalischer konstanten von heterogenen substanzen. I. Dielektrizitätskonstanten und leitfähigkeiten der mischkörper aus isotropen substanzen. *Annalen der Physik*, 416(7):636–664, 1935.

[133] D. A. G. Bruggeman. Berechnung verschiedener physikalischer konstanten von heterogenen substanzen. II. dielektrizitätskonstanten und leitfähigkeiten von vielkristallen der nichtregulären systeme. *Annalen der Physik*, 417(7):645–672, 1936.

[134] D. A. G. Bruggeman. Berechnung verschiedener physikalischer konstanten von heterogenen substanzen. III. die elastischen konstanten der quasiisotropen mischkörper aus isotropen substanzen. *Annalen der Physik*, 421(2):160–178, 1937.

[135] Paul Soven. Coherent-potential model of substitutional disordered alloys. *Physical Review*, 156(3):809–813, April 1967.

[136] D. W. Taylor. Vibrational properties of imperfect crystals with large defect concentrations. *Physical Review*, 156(3):1017–1029, April 1967.

[137] P. L. Leath. Self-consistent-field approximations in disordered alloys. *Physical Review*, 171(3):725–727, July 1968.

[138] R. N. Aiyer, R. J. Elliott, J. A. Krumhansl, and P. L. Leath. Pair effects and self-consistent corrections in disordered alloys. *Physical Review*, 181(3):1006–1014, May 1969.

[139] Scott Kirkpatrick. Classical transport in disordered media: Scaling and effective-medium theories. *Physical Review Letters*, 27(25):1722–1725, December 1971.

[140] Fumiko Yonezawa and Kazuo Morigaki. Coherent potential approximation. *Progress of Theoretical Physics Supplement*, 53:1–76, 1973.

[141] Scott Kirkpatrick. Percolation and conduction. *Reviews of Modern Physics*, 45(4):574–588, October 1973.

[142] J. Bernasconi. Conduction in anisotropic disordered systems: Effective-medium theory. *Physical Review B*, 9(10):4575–4579, May 1974.

[143] R. J. Elliott, J. A. Krumhansl, and P. L. Leath. The theory and properties of randomly disordered crystals and related physical systems. *Reviews of Modern Physics*, 46(3):465–543, July 1974.

[144] Motoo Hori and Fumiko Yonezawa. Statistical theory of effective electrical, thermal, and magnetic properties of random heterogeneous materials. IV. effective-medium theory and cumulant expansion method. *Journal of Mathematical Physics*, 16(2):352–364, February 1975.

[145] J. Bernasconi and H. J. Wiesmann. Effective-medium theories for site-disordered resistance networks. *Physical Review B*, 13(3):1131–1139, February 1976.

[146] C. T. White and E. N. Economou. Self-consistent approach to alloys exhibiting partial order. *Physical Review B*, 15(8):3742–3758, April 1977.

[147] Rolf Landauer. Electrical conductivity in inhomogeneous media. *AIP Conference Proceedings*, 40(1):2–45, April 1978.

[148] James G. Berryman. Long-wavelength propagation in composite elastic media I. Spherical inclusions. *The Journal of the Acoustical Society of America*, 68(6):1809–1819, 1980.

[149] S. Alexander, J. Bernasconi, W. R. Schneider, and R. Orbach. Excitation dynamics in random one-dimensional systems. *Reviews of Modern Physics*, 53(2):175–198, April 1981.

[150] T. Odagaki and M. Lax. Coherent-medium approximation in the stochastic transport theory of random media. *Physical Review B*, 24(9):5284–5294, November 1981.

[151] Itzhak Webman. Effective-medium approximation for diffusion on a random lattice. *Physical Review Letters*, 47(21):1496–1499, November 1981.

[152] Joseph W. Haus, Klaus W. Kehr, and Kazuo Kitahara. Long-time tail effects on particle diffusion in a disordered system. *Physical Review B*, 25(7):4918–4921, April 1982.

[153] Muhammad Sahimi, Barry D. Hughes, L. E. Scriven, and H. Ted Davis. Real-space renormalization and effective-medium approximation to the percolation conduction problem. *Physical Review B*, 28(1):307–311, July 1983.

[154] T. Odagaki, M. Lax, and A. Puri. Hopping conduction in the d-dimensional lattice bond-percolation problem. *Physical Review B*, 28(5):2755–2765, September 1983.

[155] P. E. Parris. Site-diagonal t-matrix expansion for anisotropic transport and percolation on bond-disordered lattices. *Physical Review B*, 36(10):5437–5445, October 1987.

[156] K. R. McCall, D. L. Johnson, and R. A. Guyer. Magnetization evolution in connected pore systems. *Physical Review B*, 44(14):7344–7355, October 1991.

[157] David J. Bergman and David Stroud. Physical properties of macroscopically inhomogeneous media. In *Solid State Physics*, volume 46, pages 147–269. Academic Press, 1992.

[158] Jeppe C. Dyre and Thomas B. Schrøder. Universality of ac conduction in disordered solids. *Reviews of Modern Physics*, 72(3):873–892, July 2000.

[159] V. M. Kenkre. Spatial memories and correlation functions in the theory of stress distribution in granular materials. *Granular Matter*, 3(1-2):23–28, January 2001.

[160] Z. Kalay, P. E. Parris, and V. M. Kenkre. Effects of disorder in location and size of fence barriers on molecular motion in cell membranes. *Journal of Physics: Condensed Matter*, 20(24):245105, June 2008.

[161] V. M. Kenkre, Z. Kalay, and P. E. Parris. Extensions of effective-medium theory of transport in disordered systems. *Physical Review E*, 79(1):011114, January 2009.

[162] Steven H. Strogatz. *Nonlinear Dynamics And Chaos: With Applications To Physics, Biology, Chemistry, And Engineering*. Da Capo Press, January 2001.

[163] V. M. Kenkre. Theory of exciton transport in the limit of strong intersite coupling. I. Emergence of long-range transfer rates. *Physical Review B*, 18(8):4064–4076, October 1978.